Doctoral theses at NTNU, 2019:158

Hans Olaf Hågenvik

Analysis of active and passive metamaterials

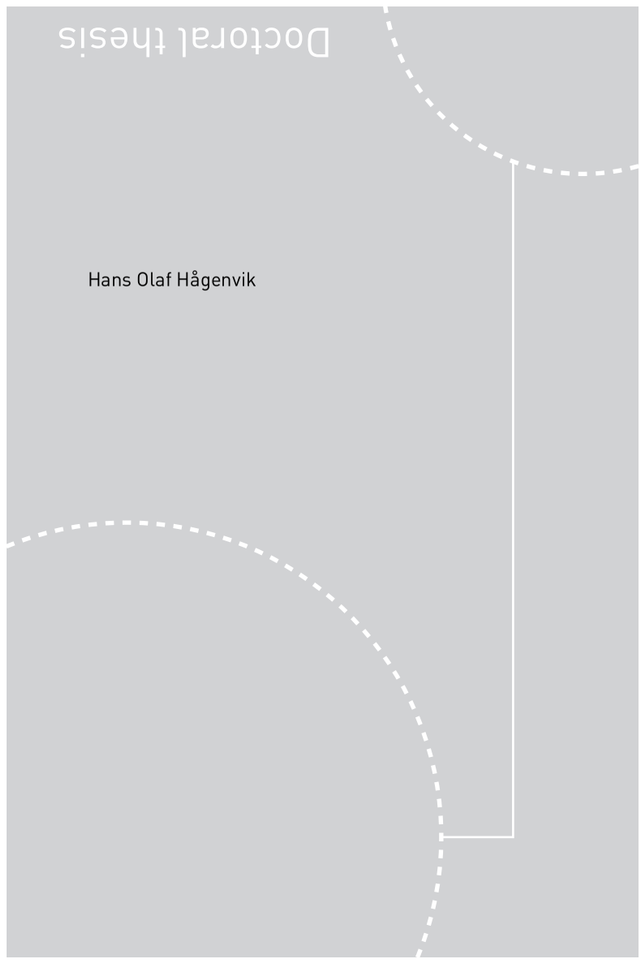

ISBN 978-82-326-3914-4 (printed ver.)
ISBN 978-82-326-3915-1 (electronic ver.)
ISSN 1503-8181

NTNU
Norwegian University of
Science and Technology

NTNU
Norwegian University of Science and Technology
Thesis for the Degree of
Philosophiae Doctor
Faculty of Information Technology and Electrical
Engineering
Department of Electronic Systems

Doctoral theses at NTNU, 2019:158

NTNU
Norwegian University of
Science and Technology

Hans Olaf Hågenvik

Analysis of active and passive metamaterials

Thesis for the Degree of Philosophiae Doctor

Trondheim, June 2019

Norwegian University of Science and Technology
Faculty of Information Technology and Electrical Engineering
Department of Electronic Systems

NTNU
Norwegian University of
Science and Technology

NTNU
Norwegian University of Science and Technology

Thesis for the Degree of Philosophiae Doctor

Faculty of Information Technology and Electrical Engineering
Department of Electronic Systems

ISBN 978-82-326-3914-4 (printed ver.)
ISBN 978-82-326-3915-1 (electronic ver.)
ISSN 1503-8181

Doctoral theses at NTNU, 2019:158

Printed by NTNU Grafisk senter

Abstract

Metamaterials are composite materials acting as effectively continuous media, which are capable of realizing entirely new phenomena such as negative refraction and transformation optics. This class of new materials may therefore in principle make available concepts such as the perfect lens and invisibility cloaks. These materials are thus promised to achieve electromagnetic properties which most certainly go beyond materials found in nature, or ever encountered before, except from perhaps in science fiction. Such media may in general be built up of both active and passive components.

New physical phenomena may require new physical models. A thorough investigation should therefore be made regarding the well established mathematical models from earlier research on electromagnetic properties of continuous, as well as structured media. This thesis contributes in various ways to the development of a solid theoretical framework, which can be used in the analysis of such novel materials. Two lines of inquiry are followed.

The first part of the thesis considers isotropic, possibly active media, which are described by given material parameters; a permittivity $\epsilon(\omega)$ and a permeability $\mu(\omega)$. A mathematical framework based on Fourier-Laplace analysis is introduced for representing the response from such media in terms of (possibly complex) frequency- and transversal wavenumber components. The idealization of monochromatic plane waves may for active systems be dangerous due to the presence of growing waves, and the possibility of approaching this limit is investigated by deforming the integration surface in complex frequency-complex wavenumber space. We also give the most general criterion for absolute instabilities. The general theory is used to analyze example media with weak or strong gain. In particular it is used to show the existence of isotropic media which in principle exhibit simultaneous refraction, meaning they refract positively and negatively at the same time.

In the second part, the importance of spatial dispersion in metamaterials consisting of passive components is considered. We discuss the importance of higher order multipole terms in homogenization theories for metamaterials. While it is common to include polarization, magnetic dipole and perhaps electric quadrupole

terms, it is shown that certain higher order terms are generally significant when second order spatially dispersive effects (e.g. magnetism) are concerned. Based on this notion it is not necessarily clear how the magnetic permeability should be defined. We therefore state and compare four different definitions of the permeability, and analyze their properties in general. As a further investigation of their physical relevance we compare how well the parameters predict the reflection from semi-infinite periodic metamaterial structures. The predictions are based on the Fresnel equation using these four permeabilities. It is found that the Fresnel equation gives accurate results for 2D metamaterials which mimic natural magnetism, in a frequency range where the magnetic moment dominates the $\mathcal{O}(k^2)$ part of the total Landau-Lifshitz permittivity. For a 1D layered structure, or for large frequencies, the correspondece is poor.

Acknowledgements

Throughout my life it has been my accomplishments in school and university which have been most noticed. I have always found learning and developing an understanding of advanced problems exciting, and I must be humble to say that this is also where I have one of my biggest strengths. In my first and only job after finishing my master studies I have been employed as a PhD candidate at the Department of Electronic systems at NTNU. This means my working days mainly have consisted of doing what I enjoy the most, and at the same time I am quite good at: learning new things, and trying to understand advanced problems. For this I am truly grateful. The job has been very exciting, however, from time to time it has also been challenging to find the motivation necessary for working towards a goal which at that time always seemed to be *far into the future*. Now, my 4,5 years as a PhD student are suddenly moving towards the end. I would, however, never have made it to this point all by myself. I must therefore express my appreciation of those people whom have helped me along the road.

First, to Professor Johannes Skaar, who has now been my supervisor for 5,5 years, both during my master thesis as well as my PhD. Thank you so much for your excellent support and guidance, and for our fruitful collaboration. You have from our very first meeting always treated my as an equal, and listened to my inputs and suggestions as if I knew what I was talking about (sometimes perhaps more than I really did). One of the few drawbacks of my time as a PhD student has been not to share my permanent working location with you. I would probably have been able to stay even more focused and efficient if we daily were able to meet down the hallway. Your unbelievable accessibility through email and phone has however made it work out quite well after all. Despite the time-wise lack of progress, in the end I must say I am really proud of what we have accomplished together.

A special thanks is also sent to Professors Astrid Aksnes and Thomas Tybell, for your endless queries of how I am doing, when I must have looked like an orphan strolling down the corridors of the department. Despite my never ending rejections of your inquires, I must now say I am truly grateful. It means a lot to know that I am being seen and looked after.

I must also thank my fellow PhD student Christopher Dirdal for all our discussions; ranging from the importance of higher order terms in metamaterial parameters, through the more or less important topics of what to call *a metamaterial researcher*, to philosophical considerations over the *mysteries of light*. I am truly grateful for your friendship, as well as for getting the opportunity to work with you through our overlapping years as employees at NTNU. I hope we are able to stay in touch also in the years to come as fellow coworkers in SINTEF, despite working in different departments and living in different cities.

Thanks to the master students Erlend, Haakon, Frode and Anders, whom I've had the honor of co-supervising and work together with during their thesis' work. Thanks for all the interesting questions, for which I'm sorry I too often could not provide thoughtful and meaningful answers to. From browsing this thesis I hope that you all recognize that you have made valuable contributions to my strive towards getting a PhD.

Finally, I must send a thanks to all of my family, friends, colleagues; and to God. For sure there is more to life than Maxwell's equations. There's a saying, "never change a winning team". I am very happy and thankful with how life treats me at the moment, so unless you run off on your own, I am not planning to substitute any of you off the pitch of my social and spiritual life.

Being the only one from the metamaterial group with permanent working place in the department, my working days have from time to time been very lonely. I must therefore thank all attendees of the library lunches, for providing me with a working environment. Seeing you all there has definitely been one of the highlights of the days. It has also been encouraging to have something to look forward to after the working days, weeks and semesters are over. I would therefore also like to thank all of you who have prioritized to spend your spare time together with me during my life in Trondheim so far.

To my parents, for always believing in me, and for always supporting my decisions in any aspects of my life. To my *less educated* brothers Christian and Anders, for your persistent pressure of me getting a PhD, but at the same time prioritizing things outside school and work. I would never have made it to where I am today if it weren't for the two of you. I highly appreciate and value your friendship, and always enjoy getting to spend time with you. You are welcome to visit in Trondheim any time, and we highly value how you always set aside time for us when we come home for visits.

To my son Sven Olaf, for the way you always express gratitude and great joy when I finally get home from work. Getting home to your smiles and hugs is a highlight every day, and has certainly given a boost to my concentration and motivation. The last five months I have got to spend 2-3 days a week together with you on parental leave. This has worked out surprisingly well, as I have got to

enjoy the days home with you, and at the same time this has been a big motivation for getting things done the days I go to the office. If you ever read this, I am very proud of you, and always will be.

My biggest support over the last four years has, however, been my beloved wife Anne Oline. You have stayed with me from my very first day as an NTNU employee, until today; and so you will do forever. We have gone through many life changing decisions during our 4,5 years as a couple, e.g. getting married, becoming parents, buying our first apartment, selling our first car, renovating our bathroom and starting a scout troop together, just to mention a few. I am satisfied with all of those decisions, and most of all that I made them together with you. Perhaps besides the *selling the car* part. Thank you so much for your patience with me these last months. I must for certain have been a boring husband, working day and night, and constantly being grumpy. All in all, I do believe that we have had so much fun together. Hopefully things will get even better after the new year when I am finished with my Doctorate and work becomes more structured.

A final thanks goes to my parents in law, Liv Elin and Knut Olaf. Thank you so much for taking such good care of Sven Olaf and Anne Oline those last weeks of my intensive thesis writing. The final product would never have reached the same quality if I at the same time were to follow up my duties of changing diapers, waking up at night and making my wife fancy dinners.

Contents

Chapter 1

Introduction

Optical technologies play an important role in today's society, and they are making a significant impact on everyday life. Wireless and fiber communication as well as cameras, detectors and sensors are all crucial elements present in almost any device, and may be regarded as important factors for societal and individual advancement. Applications range from the basic to the recreational - e.g. from medical devices to high resolution images for social media. To continue the ongoing development of better optical and wireless components, the engineers will eventually need new materials to work with. *Metamaterial* researchers might e.g. provide solutions to problems such as cost, efficiency, sensitivity and size of micro-sensors.

Metamaterials are structured, composite media with tailored optical properties, in particular properties that cannot be found in nature. Negative refraction, optical cloaking and transformation optics are potential effects which may be realized by metamaterials. Such novel properties may be obtained by tailoring the micro structure, so that the macroscopic electromagnetic properties can be described by *effective* material parameters. For this to be the case the unit cell of the micro structure should be much smaller than the wavelength of the electromagnetic wave propagating inside the material.

In the analysis of novel physical phenomena, the well established results from classical physics cannot necessarily be straightforwardly applied. A well known example of this is if one consider an object moving at a velocity close to the speed of light c. Despite the purity and simplicity of the classical solution according to Newton's laws, it has no physical relevance. This is because the classical solution relies on assumptions not valid in this regime of particle velocities. To predict the trajectory of the object accurately one has to resort to the mathematically more advanced model offered by Einstein's special theory of relativity. This thesis considers certain assumptions and simplifications often made in classical electrodynamics, which should be cautiously applied in the analysis of metamaterials.

There are two aspects to the possible necessity of new physical models. As the

above example illustrate, the classical models may predict unphysical results, and thus become irrelevant. In addition, being tied up by the well established theories for *conventional media* might also prevent us from seeing the true possibilities of properties which may be achieved by careful design of metamaterial structures.

The research field of metamaterials is often considered to be started by John Pendry's paper from 1999 [1]. The paper demonstrates how one can achieve a magnetic response from a medium consisting of non-magnetic metallic microstructures. Artificial materials for manipulating electromagnetic waves were, however, not new at that time. Already in 1898 twisted structures were reported to have the potential of field rotation [2], and the effective permittivity of metal inclusions in glass was calculated in 1904 [3]. The calculations rely on the Clausius-Mossotti relation derived in the 19th century.

The split-ring structure proposed in [1] is found to exhibit a negative permeability $\mu < 0$ close to the resonance frequency. A composite medium based on a periodic array of inter-spaced split-ring resonators and continuous wires was then shown to exhibit a frequency region with simultaneous negative permittivity $\epsilon < 0$ *and* a negative permeability $\mu < 0$ [4]. In his paper from 1967 Veselago showed that in such a medium also the refractive index n will be negative [5]. This means the refraction angle at an interface can be negative, and the phase and group velocities of the electromagnetic wave may point in opposite directions. Also negative refraction and negative group velocity had already been studied in the preceding years [6–8]. However, the phenomenon was first experimentally verified for microwaves in 2000 [4]. Recent development in nano structuring techniques and simulation tools has led to the huge progress seen in metamaterial research the last decades.

Veselago argued that a slab of a negative refractive index material in some sense will work as an unconventional lens [5]. Pendry showed that such a slab in fact functions as a *perfect* lens, where the resolution is not limited to the order of a wavelength according to the Abbe diffraction limit. This is because the negative refraction amplifies and restores the evanescent components of the field, so that all Fourier components still are present in the image plane. An actual realization of such a lens will suffer from losses. Along with the fact that negative refraction can only be achieved over a finite bandwidth, these losses cause the perfect lens to become imperfect. The optimal resolution as a function of bandwidth can however still be found [9].

The metamaterial application which attracts the most attention from popular culture is the concept of optical invisibility [10, 11]. Both these papers use coordinate transformations to find the required electromagnetic parameters for obtaining the desired optical ray trajectories. An experimental display of the cloaking mechanism for microwave frequencies was given in [12]. The transformation op-

tics technique in general relies on the theory of differential geometry [13], mostly known from Einstein's general theory of relativity. Also the invisibility cloak turns out to be difficult to realize in practice. Again, this is due to lossy components, and the fundamental limitation that one can only achieve the desired parameters over a narrow bandwidth. These problems will in general be potential obstacles in metamaterial applications. Even another challenge is the difficulty of fabricating the 3D micro- and nano structures. For some applications, the recent development of *metasurfaces* [14,15] may be a potential solution. Metasurfaces are planar metamaterial structures with sub-wavelength thickness.

The papers included in this thesis all contribute to the development of theoretical frameworks which strengthen our understanding of the electromagnetic response from metamaterials. It has been suggested to use optical amplification to overcome the losses in metamaterial structures [16]. In the analysis of such gain media it turns out one should be very careful with approximating the illuminating source as a monochromatic plane wave. The first two papers of this thesis deals with this concern. Paper I presents a mathematical framework which can be used for analyzing the response from a semi-infinite gain medium excited by a physical source, which is causal and has finite size. It turns out that the monochromatic and plane wave limits in general do not commute, due to possible instabilities being present. The general theory is applied in several cases, and is used to predict media with novel properties. Paper II applies the same theory in analyzing the response from a gainy slab made from a conventional weak gain medium. Unphysical results obtained when applying the conventional monochromatic plane wave approximation are first demonstrated, and the theory from Paper I is used to resolve these peculiarities. These two papers consider homogeneous media where the material permittivity $\epsilon(\omega)$ and permeability $\mu(\omega)$ are given parameters. The mathematical framework presented is thus only applicable to media where these given parameters describe the electromagnetic response well for all frequencies. How these parameters may be achieved, e.g. from given metamaterial structures, is not considered.

The remaining included papers (Papers III - VI) consider different topics within metamaterial *homogenization*, i.e. the procedure of obtaining effective parameters from a given microscopic structure. All example structures considered in these papers are periodic. Conventional textbook treatments on electromagnetic wave propagation consider the induced charge and current densities as "bound", and therefore absorb them into a refractive index. In Paper III we consider the possibility of rather treating the medium as vacuum, where all charge and current densities are considered as "free". An explanation of why the wavelength inside the medium still becomes different from that in vacuum is given, along with associated time domain simulations. The paper is meant to demonstrate how different

mathematical descriptions of the same phenomenon always should predict the same physical response.

Papers IV, V and VI consider spatial dispersion in metamaterial homogenization. We argue in Paper IV that in metamaterial structures, higher order multipoles may contribute significantly to the effective medium response; in particular to the magnetic permeability μ. The conventional dipole approximation (the material response is only given by the electric and magnetic dipole moments) is therefore not in general sufficient to describe the response of such media. This leads to the question how to define the magnetic permeability μ in general. In Paper V we compare four different definitions of μ, and discuss the connection between them, and properties in general. The discussed properties include causality, passivity, symmetry, asymptotic behavior, and origin dependence. Finally, Paper VI considers how well these permeabilities predict the reflection from several example structures, when used in the Fresnel reflection coefficient.

Chapter 2

Background

Metamaterial research relies on the assumption that a composite material can be viewed as an *effective medium*. When this is the case the microscopic electromagnetic fields inside the composite can be approximated by macroscopically averaged fields, and these macroscopic fields can be related by *effective material parameters*. Intuitively this may be possible if the constituents of the composite are much smaller than the effective wavelength of the light propagating through the material.

The electromagnetic properties of most natural materials are well described by the permittivity $\epsilon(\omega)$ and possibly also a permeability $\mu(\omega)$, which in general depend on the frequency ω. For brevity, this frequency dependency is sometimes suppressed in the notation. The reflection and transmission of a monochromatic plane wave can often be described in terms of these parameters through Fresnel's equations. In this and the next chapter we will assume that the effective response of the metamaterial similarly can be approximated by an effective permittivity and permeability. The macroscopic fields and effective material parameters must be obtained from a *homogenization method*. Numerous such methods have been developed, which mainly follow two lines: retrieval from scattering parameters [17, 18], or field averaging [1]. Several difficulties and limitations of the different methods have been reported (e.g. branch problems, non-local, non-causal or thickness dependent parameters). Possible improvements and modifications of the methods have been suggested [19–29].

Natural materials are well approximated as continua for a wide range of frequencies. Even natural materials are built up by discrete building blocks (e.g. atoms in a periodic lattice in a crystal or molecules in a liquid or gas). For X-rays this discreteness becomes apparent in the reflection from a crystal structure in terms of Bragg diffraction [30]. This shows that natural media cannot be viewed as continua for all frequencies. Models for the effective parameters of metamaterials will similarly break down for sufficiently high frequencies.

This chapter describes the outline of a classical homogenization procedure used by Russakoff [31] and Jackson [32], where the averaged fields are calculated as a spatial convolution of the microscopic fields by a test function $f(\mathbf{r})$[1]. In Chapter 4 we present a recent homogenization method for infinite periodic structures [33–35], and we use this formalism in the analysis of spatial dispersion in metamaterials.

In all examples in this work where actual homogenization calculations are to be performed and analyzed, we will consider one or two dimensional *periodic structures*. In such media the microscopic structure is given by a unit cell, which is repeated in the given number of dimensions. It is worth mentioning that interesting electromagnetic properties can also be achieved using amorphous structures [36].

2.1 Classical approach

Electromagnetic fields in a medium are governed by Maxwell's equations

$$\epsilon_0 \nabla \cdot \mathbf{e} = \varrho_{\text{ext}} + \varrho, \tag{2.1a}$$

$$\nabla \cdot \mathbf{b} = 0, \tag{2.1b}$$

$$\nabla \times \mathbf{e} = i\omega \mathbf{b}, \tag{2.1c}$$

$$\frac{1}{\mu_0} \nabla \times \mathbf{b} = -i\omega \epsilon_0 \mathbf{e} + \mathbf{j}_{\text{ext}} + \mathbf{j}. \tag{2.1d}$$

Here we have assumed harmonic time dependency $\mathrm{e}^{-i\omega t}$. We will use lower case letters to denote the *microscopic* fields and current densities. These fields will depend on the position inside the unit cell of a periodic structure, e.g. $\mathbf{e} = \mathbf{e}(\mathbf{r})$.

The charge and current densities on the right hand side of (2.1a) and (2.1d) have been split into two contributions: *external* and *induced*. The external charge and current densities, ϱ_{ext} and $\mathbf{j}_{\text{ext}}$, are given or known quantities, independent of the local fields. The induced charge and current densities, ϱ and $\mathbf{j}$, are on the other hand functions of the fundamental electromagnetic fields $\mathbf{e}$ and $\mathbf{b}$ [37].

We will now consider an electromagnetic wave propagating in vacuum. By combining the two Maxwell curl equations we obtain the wave equation for the electric field in vacuum, where there are no charge or current densities:

$$\nabla^2 \mathbf{e} + \frac{\omega^2}{c^2} \mathbf{e} = 0, \tag{2.2}$$

[1] The method was initially derived for natural materials consisting of atoms or molecules, but can straightforwardly be applied to metamaterials by replacing these fundamental building blocks by the structured inclusions.

where $c = 1/\sqrt{\epsilon_0\mu_0}$ is the speed of light in vacuum. The solutions to this equation are plane waves, i.e.

$$\mathbf{e}(\mathbf{r}) = \mathbf{e}_0 \mathrm{e}^{i\mathbf{k}\cdot\mathbf{r}}. \tag{2.3}$$

Here $|\mathbf{k}| = \omega/c$, and $\mathbf{e}_0$ is some complex vector amplitude. Such a plane wave in vacuum would have to be excited by some external current density $\mathbf{j}_{\text{ext}}$, which would determine the amplitude and direction of $\mathbf{e}_0$, as well as the propagation direction of the plane wave $\mathbf{k}/|\mathbf{k}|$.

When materials are present, the solution (2.3) will be altered due to induced charge and current densities. We will consider metamaterials consisting of components made of linear, isotropic and time-shift invariant materials. Microscopically the induced charge density may then be expressed

$$\mathbf{j}(\mathbf{r}) = -i\omega\mathbf{p}(\mathbf{r}) + \nabla \times \mathbf{m}(\mathbf{r}), \tag{2.4}$$

where

$$\mathbf{p}(\mathbf{r}) = \epsilon_0[\varepsilon(\mathbf{r}) - 1]\mathbf{e}(\mathbf{r}), \tag{2.5a}$$

$$\mathbf{m}(\mathbf{r}) = \frac{1}{\mu_0}\Big(1 - \frac{1}{\mu(\mathbf{r})}\Big)\mathbf{b}(\mathbf{r}). \tag{2.5b}$$

The introduced parameters $\varepsilon(\mathbf{r})$ and $\mu(\mathbf{r})$ are the microscopic *relative* permittivity and permeability, which describe the material present at a given position $\mathbf{r}$. We will in the following leave out the word "relative" when refering to the material parameters. Note that there has already happened a homogenization from the level of atoms and molecules, in order to describe the materials of the different constituents in terms of their material parameters. I will later homogenize the fields and materials parameters to the next level. These *macroscopic* fields will be denoted by calligraphic capital letters, and the composite media will be described in terms of *effective* material parameters.

For a homogeneous medium with constant $\varepsilon(\mathbf{r}) = \varepsilon$ and $\mu(\mathbf{r}) = 1$ the wave equation takes a similar form as (2.2):

$$\nabla^2\mathbf{e} + \frac{[n\cdot\omega]^2}{c^2}\mathbf{e} = 0. \tag{2.6}$$

Also here the solution is given by the plane wave (2.3), but now $|\mathbf{k}| = n\cdot\omega/c$. Here we have introduced the refractive index $n = \omega\sqrt{\varepsilon}/c$. The refractive index predicts how the wavelength and phase velocity of the electromagnetic wave will change inside the homogeneous medium compared to in vacuum. Equation (2.6) may be found by insertion of (2.4)-(2.5) into (2.1d), before combining it with (2.1c) to eliminate $\mathbf{b}$. This is the conventional method used to show that the wavelength of

an electromagnetic wave inside an homogeneous medium will be given by

$$\lambda = \frac{2\pi}{|\mathbf{k}|} = \frac{2\pi c}{n \cdot \omega} = \frac{\lambda_0}{n}, \tag{2.7}$$

where λ_0 is the wavelength a plane wave at a frequency ω would have had in vacuum.

No matter how we choose to describe $\mathbf{j}$, the fundamental fields $\mathbf{e}$ and $\mathbf{b}$, as well as the relation between $\mathbf{j}$ and these fields will remain the same. Paper III of this thesis serves as an example of this, where rather than using the decomposition (2.4), we consider $\mathbf{j}$ inside a dielectric as a superposition of current sheets situated in a vacuum. A current sheet in vacuum will emit electromagnetic waves with the vacuum wavelength. The total electric field inside the dielectric will then be given as a superposition of the incident wave and the waves produced by the "current sheets". All these waves have the vacuum wavelength. The paper provides an explanation of how this superposition still will add up to a wave with wavelength λ_0/n inside the dielectric. As an attempt to visualize these "current sheets in vacuum" we present finite difference time domain (FDTD) simulations [38] of a plane wave propagating through a layered structure where we essentially have compressed the induced currents into thin current sheets surrounded by vacuum. It is worth mentioning that even though we consider the medium as source charge and current densities, these sources depend on the electric field and should therefore be characterized as *induced* charges and currents [37].

A similar analysis using perturbation theory was done by James and Griffiths [39]. Their analysis is however somewhat complicated, and does not explain the physical mechanism for the altered wavelength in terms of a z-dependent set of sources. After Paper III was published we were made aware of another paper which deals with the same subject in more general terms, and use an identical technique to solve the fundamental integral (10) of our paper [40].

We will now consider 1D propagation through the same periodic, layered structure of alternating permittivities $\varepsilon_1 = 31$ and $\varepsilon_2 = 1$ to visualize the classical homogenization procedure from Russakoff-Jackson [31, 32]. The resulting electric field from the FDTD simulation is shown in Fig. 2.1. Considering the structure as a metamaterial we expect it to behave approximately as a continuum with effective permittivity given as a weighted averaged of the two permittivities [41]:

$$\epsilon = \frac{\varepsilon_1 d_1 + \varepsilon_2 d_2}{d_1 + d_2} = 4. \tag{2.8}$$

Here $d_1 = 0.1a$ and $d_2 = 0.9a$ are the thicknesses of the two alternating layers expressed in terms of the lattice parameter a. In the FDTD simulation Fig. 2.1 we used the excitation frequency $\omega_1 = 0.1c/a$. As everything scales with the lattice

parameter, and we consider non-dispersive components (permittivity independent on frequency), the parameter a can be chosen arbitrarily.

From the figure it is clear that $\mathbf{e}(z)$ effectively propagates with a wavelength $\lambda \approx \lambda_0/2$, where λ_0 is the wavelength outside of the metamaterial slab. This is in good agreement with (2.7), where $n = \sqrt{\epsilon} = 2$. The field profile is however jagged due to the rapid fluctuation of the microscopic permittivity. The macroscopic field behavior may be found by homogenization. The macroscopic field should be a smooth profile approximating the behavior of the microscopic field $\mathbf{e}(z)$. We will denote such macroscopic (averaged) fields by calligraphic capital letters, e.g. $\boldsymbol{\mathcal{E}}$ for the macroscopic electric field. The Russakoff-Jackson homogenization procedure [31, 32] calculates such an average by using a test function $f(\mathbf{r})$:

$$\boldsymbol{\mathcal{E}}(\mathbf{r}) = \int f(\mathbf{r}')\mathbf{e}(\mathbf{r} - \mathbf{r}')\mathrm{d}\mathbf{r}', \tag{2.9}$$

where $f(\mathbf{r})$ is real, non-zero in some neighborhood of $\mathbf{r} = 0$, and it's integral is normalized to unity over all space. In the calculation of the macroscopic field at position $\mathbf{r}$ the test function weights the microscopic field at the surrounding points differently. The macroscopic magnetic field $\boldsymbol{\mathcal{B}}$ and the induced charge and current densities $\rho, \rho_{\text{ext}}, \boldsymbol{\mathcal{J}}$ and $\boldsymbol{\mathcal{J}}_{\text{ext}}$ are defined similarly from their microscopic counterparts $\mathbf{b}$, ϱ, $\varrho_{\text{ext}}, \mathbf{j}$ and $\mathbf{j}_{\text{ext}}$.

It can be shown that the average operation (2.9) commutes with the operations of spatial differentiation. This gives the macroscopic Maxwell equations

$$\epsilon_0 \nabla \cdot \boldsymbol{\mathcal{E}} = \rho_{\text{ext}} + \rho, \tag{2.10a}$$

$$\nabla \cdot \boldsymbol{\mathcal{B}} = 0, \tag{2.10b}$$

$$\nabla \times \boldsymbol{\mathcal{E}} = i\omega \boldsymbol{\mathcal{B}}, \tag{2.10c}$$

$$\frac{1}{\mu_0} \nabla \times \boldsymbol{\mathcal{B}} = -i\omega\epsilon_0 \boldsymbol{\mathcal{E}} + \boldsymbol{\mathcal{J}}_{\text{ext}} + \boldsymbol{\mathcal{J}}. \tag{2.10d}$$

These equations can be used to describe macroscopic wave phenomena in periodic metamaterials. To be able to do so, we do however need a relation between $\boldsymbol{\mathcal{J}}$ and the macroscopic fields $\boldsymbol{\mathcal{E}}, \boldsymbol{\mathcal{B}}$.

For the microscopic fields the material parameters enter (2.1d) by insertion of the known relations (2.4)-(2.5). To obtain effective material parameters from the macroscopic fields and current densities in (2.10) we should thus find similar constitutive relations between the macroscopic induced current density $\boldsymbol{\mathcal{J}}$ and the macroscopic electromagnetic fields $\boldsymbol{\mathcal{E}}$ and $\boldsymbol{\mathcal{B}}$. In the Russakoff-Jackson formalism such relations are found by approximating the macroscopic induced current density by a macroscopic multipole expansion [32, 42]. If only the macroscopic electric and magnetic dipole moments contribute significantly in this expansion we get

$$\boldsymbol{\mathcal{J}}(\mathbf{r}) = -i\omega\boldsymbol{\mathcal{P}} + \nabla \times \boldsymbol{\mathcal{M}}. \tag{2.11}$$

The macroscopic electric and magnetic dipole moments are given by

$$\boldsymbol{\mathcal{P}}(\mathbf{r}) = \int f(\mathbf{r}')\mathbf{p}(\mathbf{r}-\mathbf{r}')\mathrm{d}\mathbf{r}', \tag{2.12}$$

and

$$\boldsymbol{\mathcal{M}}(\mathbf{r}) = \int f(\mathbf{r}')\Big[\mathbf{m}(\mathbf{r}-\mathbf{r}') + \frac{(\mathbf{r}-\mathbf{r}')\times\mathbf{p}(\mathbf{r}-\mathbf{r}')}{2}\Big]\mathrm{d}\mathbf{r}'. \tag{2.13}$$

In (2.12) the macroscopic electric dipole moment is expressed in terms of an average of the microscopic electric dipole moment. The macroscopic magnetic dipole moment on the other hand is expressed in (2.13) in terms of the average of the sum of the microscopic magnetization density $\mathbf{m}$ and the microscopic magnetic dipole moment $(\mathbf{r}\times\mathbf{p})/2$.

In our application of the Russakoff-Jackson method to homogenization of metamaterials the microscopic magnetization density $\mathbf{m}$ denotes the intrinsic magnetic moment of the constitutes, while the term $(\mathbf{r}\times\mathbf{p})/2$ takes into account the additional magnetic moment due to potential induced currents circulating around an origin of the unit cell. In the original Russakoff-Jackson derivation of the macroscopic Maxwell equations the term $\mathbf{m}$ similarly denotes the intrinsic magnetic moments of each charge in a molecule, while the term $(\mathbf{r}\times\mathbf{p})/2$ takes into account the *molecular magnetic moment* due to the charges' movement around an origin of the molecule.

Inspired by (2.5), effective macroscopic material parameters may be defined by relating the macroscopic dipole moments $\boldsymbol{\mathcal{P}}, \boldsymbol{\mathcal{M}}$ to the macroscopic electromagnetic fields $\boldsymbol{\mathcal{E}}, \boldsymbol{\mathcal{B}}$:

$$\boldsymbol{\mathcal{P}}(\mathbf{r}) = \epsilon_0\Big[\epsilon - 1\Big]\boldsymbol{\mathcal{E}}(\mathbf{r}), \tag{2.14a}$$

$$\boldsymbol{\mathcal{M}}(\mathbf{r}) = \frac{1}{\mu_0}\Big[1 - \frac{1}{\mu}\Big]\boldsymbol{\mathcal{B}}(\mathbf{r}). \tag{2.14b}$$

For simplicity, we here consider media where the macroscopic response may be described in terms of *isotropic* material parameters; the relative permittivity ϵ, and the relative permeability μ. Again, we will leave out the word "relative" when refering to the material parameters. The anisotropic case is considered in Chapter 4, and in Paper V of this thesis. Note that the permeability μ in (2.14) is a different parameter than the microscopic permeability in (2.5).

From (2.13) it becomes apparent that it is possible to obtain a magnetic response $\mu \neq 1$ in a metamaterial consisting of non-magnetic components, where $\mathbf{m}(\mathbf{r}) = 0$ for all $\mathbf{r}$. This is referred to as *artificial magnetism*, and is an important

reason to why metamaterials can be used to obtain novel scattering properties. In metamaterials, not only the permittivity $\epsilon(\omega)$, but also the permeability $\mu(\omega)$ can contribute significantly to the electromagnetic response, also for quite high frequencies where the magnetic response of all natural materials is absent.

Macroscopic Maxwell equations which can be used to predict wave phenomena in metamaterials may now be found by insertion of (2.11) into (2.10d). With the relations (2.14) it is convenient to introduce auxiliary fields $\boldsymbol{\mathcal{D}} = \epsilon_0 \epsilon \boldsymbol{\mathcal{E}}$ and $\boldsymbol{\mathcal{H}} = \boldsymbol{\mathcal{B}}/(\mu_0 \mu)$. This gives the macroscopic Maxwell equations

$$\nabla \cdot \boldsymbol{\mathcal{D}} = \rho_{\text{ext}}, \tag{2.15a}$$
$$\nabla \cdot \boldsymbol{\mathcal{B}} = 0, \tag{2.15b}$$
$$\nabla \times \boldsymbol{\mathcal{E}} = i\omega \boldsymbol{\mathcal{B}}, \tag{2.15c}$$
$$\nabla \times \boldsymbol{\mathcal{H}} = -i\omega \boldsymbol{\mathcal{D}} + \boldsymbol{\mathcal{J}}_{\text{ext}}. \tag{2.15d}$$

In the remaining of this and the next chapter, we will assume that effective parameters $\epsilon(\omega)$ and $\mu(\omega)$ for a metamaterial are given, and rather consider the electromagnetic response from a homogeneous medium with these parameters. The given parameters may for instance be obtained through an analytical model, or through a numerical implementation of a given homogenization theory. In Chapter 4 we will consider the homogenization of actual periodic structures in more detail.

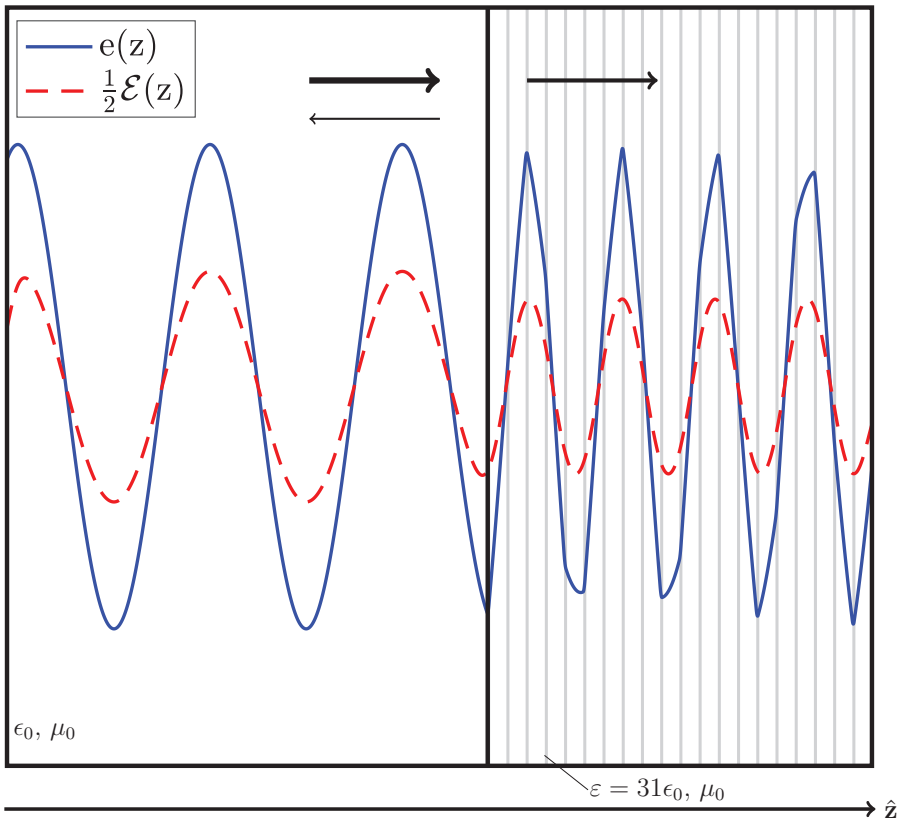

Figure 2.1: The microscopic electric field profile of a plane wave incident from vacuum on the left-hand side, upon a layered dielectric structure on the-right hand side. The figure also shows the macroscopic field calculated according to a one dimensional variant of (2.9), with $f(z)$ being a Gaussian with a full width of half maximum approximately equal to the lattice parameter of the layered structure a. The macroscopic field has been scaled with a factor 0.5, to make the two graphs distinguishable. It is seen that $\mathcal{E}(z)$ is a smoothened version of $e(z)$. The arrows indicate the phase velocity of the wave at that given z. The two arrows for $z < 0$ indicates that in this area the field is a sum of the incident and reflected wave. The difference in thickness of the arrows roughly describe the amplitude ratios between the three different modes of the macroscopic electric field (incident, reflected, transmitted). Note that the axes in the plot has been left out. This is because neither the magnitude of the field, nor numerical values for the position z are used in any of our interpretations of the plot. Including axes with numerical values (in arbitrary units) will thus only disturb the points the figure is meant to illustrate. The axes will, for the same reason, be left out in all similar figures in this thesis.

2.2 Negative refraction in a medium with $\epsilon < 0$ and $\mu < 0$

We now consider *negative refraction*, as an example of a novel property which can be attained in a metamaterial. In his paper from 1968 Veselago suggested that negative refraction will occur at an interface between vacuum and a medium with simultaneous negative permittivity and permeability [5]. By inserting plane wave solutions $\boldsymbol{\mathcal{E}} = \mathbf{E}_0 \mathrm{e}^{i\mathbf{k}\cdot\mathbf{r}-i\omega t}$ and $\boldsymbol{\mathcal{H}} = \mathbf{H}_0 \mathrm{e}^{i\mathbf{k}\cdot\mathbf{r}-i\omega t}$ in the curl equations in (2.15), with the constitutive relations (2.14) we get

$$\mathbf{k} \times \mathbf{E}_0 = i\omega\mu\mathbf{H}_0, \tag{2.16a}$$

$$\mathbf{k} \times \mathbf{H}_0 = -i\omega\epsilon\mathbf{E}_0. \tag{2.16b}$$

Since ϵ and μ are real, we can without loss of generality assume that $\mathbf{E}_0$ and $\mathbf{H}_0$ are real vector amplitudes. If ϵ and μ are negative, the vectors $(\boldsymbol{\mathcal{E}}, \boldsymbol{\mathcal{H}}, \mathbf{k})$ form a left-handed set. Media with negative ϵ and μ are therefore often referred to as left-handed media.

The energy flow in the medium is described by the Poynting vector

$$\boldsymbol{\mathcal{S}} = \frac{1}{2}\mathbf{E}_0 \times \mathbf{H}_0, \tag{2.17}$$

so $\boldsymbol{\mathcal{S}}$ and $\mathbf{k}$ are anti-parallel in a medium with negative ϵ and μ. This is demonstrated in Fig. 2.2. We note that the definition of "left handed" and "right handed" that is based on the set formed by the vectors $(\boldsymbol{\mathcal{E}}, \boldsymbol{\mathcal{H}}, \mathbf{k})$ is not rigorous, since the permittivity $\epsilon(\omega)$ and permeability $\mu(\omega)$ generally are complex quantities. It is therefore common to adopt the following definition: A medium is said to be left handed at the frequency ω if the associated, time-averaged Poynting vector and the phase velocity point in opposite directions. If they point in the same direction, the medium is right handed.

The electron gas in a metal approximately behaves as a plasma:

$$\epsilon(\omega) = 1 - \frac{\omega_\mathrm{p}^2}{\omega^2}. \tag{2.18}$$

In a metal the permittivity is therefore negative below the plasma frequency ω_p, which typically is in the ultraviolet region. A metamaterial consisting of parallel metal wires, as shown in Fig. 2.3a, will therefore exhibit a negative effective permittivity ϵ, where the plasma frequency can be tuned by the thickness of the wires [43, 44].

A negative permeability may be obtained in a medium where the effective permeability $\mu(\omega)$ is given by the Lorentz oscillator model [41, p. 176] $\mu(\omega) = f(\omega)$, where

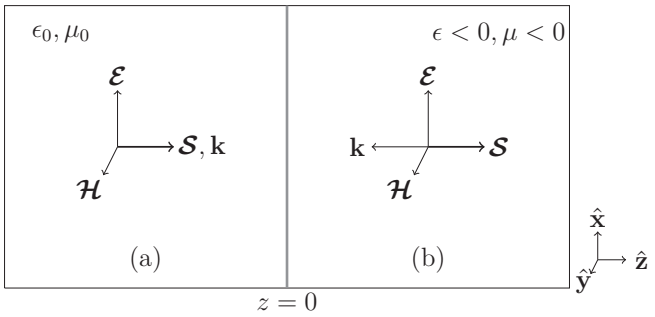

Figure 2.2: An electromagnetic plane wave propagating from vacuum (figure a) upon a medium with $\epsilon < 0$ and $\mu < 0$ (figure b). In vacuum (a) $\boldsymbol{\mathcal{S}}$ and $\mathbf{k}$ are parallel, while inside the medium (b) they are anti-parallel.

$$f(\omega) = 1 + \frac{F\omega_0^2}{\omega_0^2 - \omega^2 - i\Gamma\omega}. \tag{2.19}$$

Here the parameter F is the strength of the response, ω_0 is the resonance frequency, and Γ is the damping rate, which also describes the bandwidth of the resonant frequency response. Provided the resonance is strong enough, the real part of μ will be negative for frequencies above the resonance ω_0. A magnetic response $\mu(\omega)$ given by (2.19) may be approximated by a medium consisting of periodically placed split-ring resonators [1], shown in Fig. 2.3b. Assuming a uniform time varying magnetic field across the unit cell, an expression similar to (2.19) may be derived for this structure using the field averaging approach from [1]. The parameters F, ω_0 and Γ are then expressed in terms of geometric sizes from the split-ring structure.

By combining the split-ring and wire structures into a single composite effective medium, and carefully choosing the parameters of the structures, we may thus achieve negative refraction. Both structures in Fig. 2.3 are clearly anisotropic. The negative effective permittivity of the wire medium will only be experienced by the electric field component pointing along the metal wire. Similarly the magnetic response from the split-ring structure will only affect the magnetic field component normal to the split-ring cross section. In the combined structure the wires should therefore be placed in a plane parallel to the split-ring cross section. A similar structure has been experimentally verified to experience negative refraction [45].

Figure 2.4 shows the propagation of a plane wave normally incident to a medium where $\epsilon(\omega) = \mu(\omega)$ are both given by the same Lorentz response given in (2.19). Close to the medium boundary the backward wave is established. Further inside the medium the Brillouin and Sommerfeld precursors can be seen.

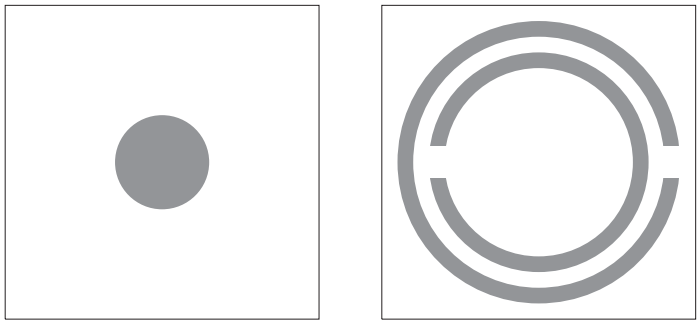

(a) (b)

Figure 2.3: Unit cell cross sections of a wire medium (a) and a split-ring resonator medium (b). Combined, these structures may result in a negative refracting medium.

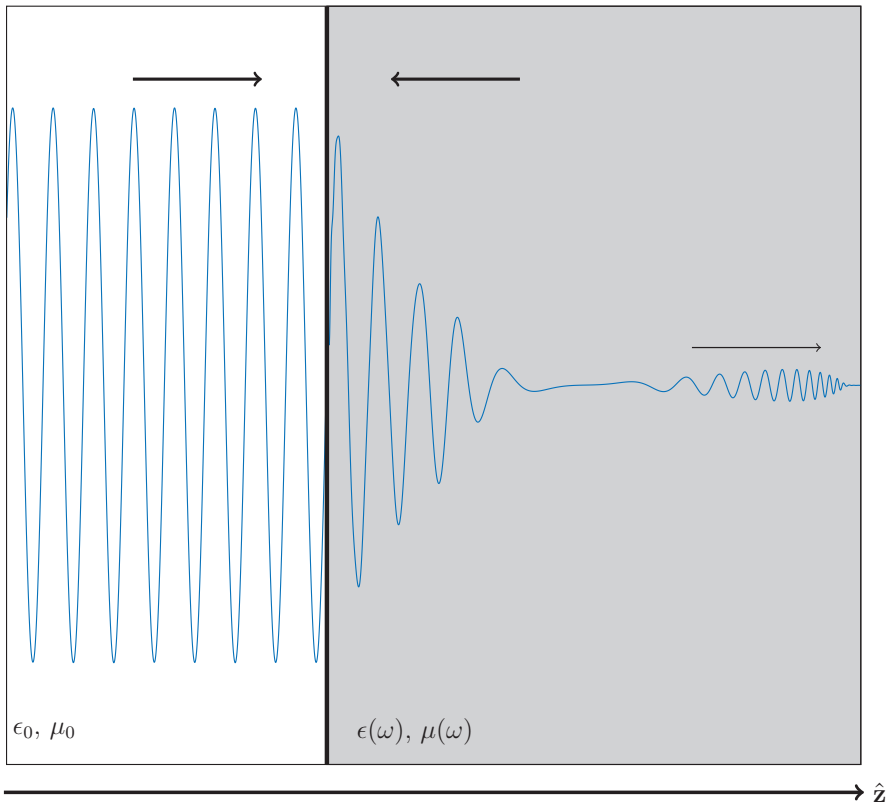

Figure 2.4: A FDTD simulation of a plane wave propagating from vacuum incident to a medium with $\epsilon = \mu$ given by (2.19). The boundary surface at $z = 0$ is indicated by the thick vertical line, and close to the boundary a backward wave is established. The parameters $F = 20$, $\Gamma = 0.1\omega_0$, and the excitation frequency $\omega_1 = \omega_0\sqrt{11}$ were used in the simulation. Here ω_0 is the resonance frequency of the permittivity and permeability. Again, note that axes has been left out, as the numerical values are not relevant for our interpretations of the plot. Also here, and in the remaining plots, the arrows display the direction of phase velocity at different z.

2.2.1 Obtaining desired ϵ and μ

Inspired by transmission line metamaterials [46] one possible route to finding the required microstructure for given desired effective parameters ϵ and μ is through combining circuit elements in a specific manner [1,4,47,48]. The circuit equivalent for the split-ring will be a RLC-circuit, where R is the internal resistance of the ring, L is the self-inductance of the ring, and C is the capacitance from the gap. An oscillating magnetic field through the split-ring will induce a current, and the RLC-circuit equations can be used to show that the magnetic response μ of this medium in fact is approximated by a Lorentz function. A more general method for finding the necessary combination of circuit elements for a desired response is the procedure of Brune synthesis [49].

The experimental verification of negative refraction in a combined split-ring and wire medium suggests that even more sophisticated responses may be obtained by combination of several known metamaterial building blocks. A magnetic response $\mu(\omega)$ with multiple resonances may for instance be obtained in a unit cell with multiple split-ring resonators of different geometry. Assuming the inclusions contribute to the response independent of each other is of course a simplification. In general the inclusions will interact with each other, and the actual homogenized parameters may be tedious to find. One should also note that even if a given structure is predicted to achieve your desired response, the given structure may be difficult to fabricate. The model may also be based on assumptions which are not valid for the frequency range of interest.

From a theoretical perspective a natural question arises: given any desired response how close can a metamaterial approach this response, while obeying the fundamental principle of causality?

2.2.2 Kramers-Kronig relations

To obtain desired responses such as negative refraction, some metamaterials make use of material resonances. A resonant response is often associated with high losses. Imperfectness in production may lead to additional loss. This means the permittivity and permeability, and therefore also the refractive index, will in general be complex quantities, as appears from e.g. (2.19). As an example, consider the perfect lens which requires a real refractive index $n = -1$ [50]. As already mentioned, fundamental limitations prohibit such a lossless response over a finite bandwidth of frequencies [9].

Despite the fact that the loss is undesirable, it may in fact be a requirement for negative refraction to occur in a passive medium. The Kramers-Kronig relations relates the real and imaginary parts of a function that is analytic in the upper half plane $\mathrm{Im}\,(\omega) > 0$. We here consider media where the Kramers-Kronig relations for

$n(\omega)$ are valid. For the refractive index $n(\omega)$ the relations in question are

$$\mathrm{Re}\, n(\omega_1) = 1 + \frac{2}{\pi}\mathcal{P}\int_0^\infty \frac{\omega \mathrm{Im}\, n(\omega)}{\omega^2 - \omega_1^2}\mathrm{d}\omega, \tag{2.20a}$$

$$\mathrm{Im}\, n(\omega_1) = -\frac{2\omega_1}{\pi}\mathcal{P}\int_0^\infty \frac{\omega \mathrm{Re}\, n(\omega)}{\omega^2 - \omega_1^2}\mathrm{d}\omega. \tag{2.20b}$$

Here $\mathcal{P}$ means the principal value. The Kramers-Kronig relations in the form (2.20) rely on the fact that $\mathrm{Im}\, n(\omega)$ is an odd function.

We note that the factor $\omega/(\omega^2 - \omega_1^2)$ in (2.20a) is positive for $\omega > \omega_1$ and negative for $\omega < \omega_1$. To obtain $\mathrm{Re}\, n(\omega_1) < 0$ we must thus have either $\mathrm{Im}\, n(\omega) < 0$ for $\omega > \omega_1$ and/or $\mathrm{Im}\, n(\omega) > 0$ for $\omega < \omega_1$. It is also worth noting that $\mathrm{Im}\, n(\omega)$ at the frequencies close to ω_1 is weighted the most, as the denominator gets small. It is therefore possible to obtain a negative $\mathrm{Re}\, n(\omega_1)$ with $\mathrm{Im}\, n(\omega_1) \approx 0$ at an observation frequency ω_1, if there is a steep drop in $\mathrm{Im}\, n(\omega)$ just above this frequency [51]. It is similarly possible to achieve a negative refractive index $n = \sqrt{\epsilon\mu}$ at arbitrarily low gain through a steep drop in $\mathrm{Im}\, n(\omega)$ just above the observation frequency.

The relations (2.20) will be valid if the same relations are separately satisfied for $\epsilon(\omega)$ and $\mu(\omega)$. We now consider how such relations for these parameters may be established.

The conventional derivation of the Kramers-Kronig relations for $\epsilon(\omega)$ is based on Titchmarsh's theorem [52, 53]. This theorem states that if a function $\chi(\omega)$ is square integrable over the real ω-axis, then any of the following implies the other two:

1. Causality: The inverse Fourier transform $\chi(t) = F_\omega[\chi(\omega)]$ is zero for $t < 0$.

2. Analyticity: The function $\chi(\omega)$ is analytic for $\mathrm{Im}\,\omega > 0$. Furthermore, $\chi(\omega)$ is uniformly square integrable along a line parallel to the real axis in the upper half-plane: $\int_{-\infty+i\gamma}^{\infty+i\gamma} |\chi(\omega)|^2 \mathrm{d}\omega < k$ for some number $k > 0$ and all $\gamma > 0$.

3. Kramers-Kronig: The real and imaginary parts of $\chi(\omega)$ (where ω is real) are Hilbert transforms of each other.

That the susceptibility $\chi(\omega) = \epsilon(\omega) - 1$ is integrable over the real ω-axis must either be assumed, or verified for a given homogenized permittivity $\epsilon(\omega)$. For media where this is the case, it follows from Titchmarsh's theorem that the relations (2.20) will be valid for $\epsilon(\omega)$, provided $\chi(t)$ is zero for $t < 0$. This is usually considered to follow from causality. A causality argument requires an input-output relation, where the output response cannot precede the onset of the input. In case of the susceptibility $\chi(t)$, the electric field $\boldsymbol{\mathcal{E}}(t)$ is considered the input, and $\boldsymbol{\mathcal{P}}(t)$

the output. As $\chi(t)$ describes how the polarization density depends on the electric field at earlier times, it should therefore be zero for $t < 0$. It can be argued that this is not a rigorous formulation, as the polarization density $\boldsymbol{\mathcal{P}}$ and field $\boldsymbol{\mathcal{E}}$ both should be considered as the output from a source current density $\boldsymbol{\mathcal{J}}_{\text{ext}}$ [54] (see Appendix C of Paper V for a more detailed discussion).

According to Landau-Lifshitz' textbook [55] the permeability $\mu(\omega)$ ceases to be physically meaningful for relatively low frequencies. Modified Kramers-Kronig relations are therefore suggested for $\mu(\omega)$. We note that these arguments are made for natural materials and not metamaterials [56]. For metamaterials it has been argued that the Kramers-Kronig relations for $\mu(\omega)$ should be even further modified [57].

In Paper V of this thesis we present our interpretation of the Landau-Lifshitz permeability argument. We also consider different definitions of magnetic permeability which in principle can be used for all frequencies, and discuss whether Kramers-Kronig relations for these permeabilities can be established.

2.3 Non-magnetic negative refraction

The discussion in Sec. 2.2 shows that when ϵ and μ are simultaneously negative, the refractive index also becomes negative. For such media the negative sign of the square root must chosen in the calculation $n(\omega) = \sqrt{\epsilon(\omega)\mu(\omega)}$. In passive media, where losses are present, it is sufficient to choose the sign such that $\operatorname{Im} n(\omega) > 0$. For active media, however, one must be careful when identifying the sign of the refractive index.

This is seen by writing the permittivity and permeability in polar form, giving

$$n(\omega) = \sqrt{|\epsilon||\mu|}\mathrm{e}^{i(\theta_\epsilon+\theta_\mu)/2}, \tag{2.21}$$

where θ_ϵ and θ_μ are the complex phases of ϵ and μ respectively. Adding a phase 2π to either ϵ or μ will not change the value of these parameters, but will flip the sign of n. For the refractive index to describe something physical it cannot depend on such mathematical manipulations. Assuming $\epsilon(\omega)$ and $\mu(\omega)$ are analytic and zero-free functions in the upper frequency plane it is possible to retain a physical interpretation of $n(\omega)$ by considering the global properties of these analytic functions [58]. We define $n(\omega)$ for $\operatorname{Im}\omega > 0$ as the analytic branch of $\sqrt{\epsilon(\omega)\mu(\omega)}$ that tends to $+1$ as $\operatorname{Re}\omega \to \infty$.

It is seen from (2.21) that a negative refractive index may be obtained even in a non-magnetic medium, provided that sufficiently amount of phase is accumulated in ϵ as we reduce ω from ∞ down to a certain observation frequency ω_1. If the accumulated phase in ϵ is $\theta_\epsilon(\omega_1) = 2\pi$ we indeed get $n(\omega_1) = -1$. In this medium

both $\epsilon(\omega_1)$ and $\mu(\omega_1)$ are positive, which shows that negative refraction is also possible in right handed media.

One way of obtaining a right-handed, non-magnetic negative refracting medium is to use a permittivity function which is a sum of a passive and active Lorentz function [59]. It has been suggested that such a medium can be physically realized using Bose-Einstein condensates [60]. The propagation of a plane wave incident from vacuum to such a medium is shown in Fig. 2.5. As in Fig. 2.3 a backward wave is established close to the boundary. It is seen that the electric field decays very fast with z inside the medium. This is due to the large positive value $\operatorname{Im} n(\omega_1)$. Since the backward wave reaches a larger magnitude than the incident wave (due to the gain), the excess energy leaves the medium, and appears as an amplified reflection. By examining the time evolution as the incoming wave hits the boundary surface it is found that the reflection grows in magnitude for a while, before it stabilizes at a maximum amplitude of around 4.5 times the amplitude of the incident field. This gives a reflection coefficient of 3.5, which corresponds to a power reflection coefficient larger than 10.

It is worth noting that the gain of this medium is relatively high. For other media, this high gain may have lead to rapidly growing fields, which again leads to artificial reflections destroying the validity of the simulation. The reason this does not happen for this medium is that the frequencies for which the medium has gain are refracted negatively. The gain is therefore working towards the boundary, so the fields don't propagate a long distance, and thus never grow very large.

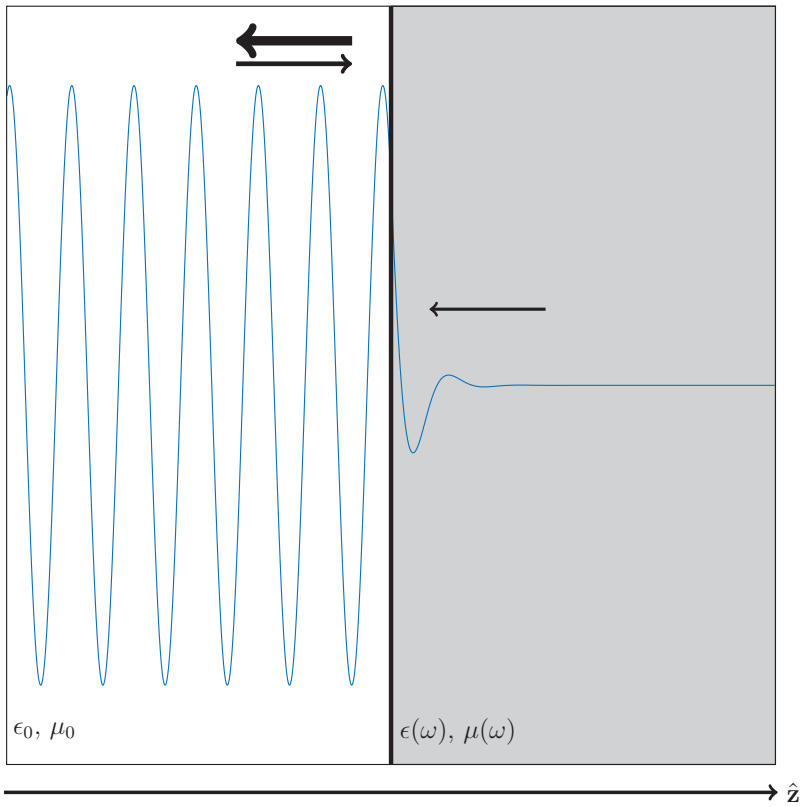

Figure 2.5: A FDTD simulation of a plane wave propagating from vacuum incident to a right handed negative index medium similar to the one suggested by [59]. The boundary surface at $z = 0$ is indicated by the thick vertical line, and close to the boundary a backward wave is established. The arrows display the direction of phase velocity at different z. The arrows in both directions for $z < 0$ indicate that the total field is a sum of the incident field and its reflection here. The arrow in the negative z-direction is thicker to indicate that the reflection has a larger amplitude than the incident field, due to gain. The permittivity $\epsilon(\omega)$ is given as as sum of to Lorentzian terms with $F_1 = 2.44$, $\Gamma_1 = 0.0572\omega_{01}$, and $F_2 = -0.14$, $\omega_{02} = 1.428\omega_{01}$, $\Gamma_2 = 0.0572\omega_{01}$, with the observation frequency $\omega_1 = 1.4708\omega_{01}$. Here ω_{01} is the resonance frequency of the first Lorentzian term of $\epsilon(\omega)$. The medium is non-magnetic, i.e. $\mu = 1$ for all frequencies.

Chapter 3

Active media

To overcome the undesirable losses in metamaterials it has been suggested to introduce gain in the design of these media [16, 61–65]. For example, introducing gain may improve the performance of actual realizations of the "perfect" lens, where finite loss cuts off the finer details of the image [16,66]. The introduction of gain may also enable properties not achievable in passive systems, such as negative refraction in a right-handed medium (Sec. 2.3). Waves propagating inside gain media will be amplified, and instabilities may therefore be present. Due to the possibility of instabilities and novel properties, the well established theory for passive media should be applied with care. In this chapter we consider certain potential pitfalls in the analysis of wave propagation in gainy media, and discuss how they may be resolved.

The idealization of monochromatic plane waves may for active systems be dangerous, due to the presence of growing waves. This problem is the topic of Papers I and II of this thesis. In general it turns out to be necessary to involve complex frequencies ω and/or complex transversal wavenumbers k_x, even for the case with a weakly amplifying slab that does not lase [67]. The framework from these papers is reviewed here, and we present two examples where the framework is applied to analyze novel phenomena which may occur in certain gain media. In Paper II a gainy slab of finite width in the longitudinal direction is analyzed. We will here only consider the semi-infinite case.

We restrict the analysis to linear, time-shift invariant, isotropic, homogeneous media without spatial dispersion. Moreover, we assume the following asymptotic behavior for the product of relative permittivity ϵ and relative permeability μ, as $\omega \to \infty$ [55]: $\epsilon(\omega)\mu(\omega) = 1 + \mathcal{O}(\omega^{-2})$. Finally, we assume that the medium does not support super-exponential instabilities [51], meaning that any field solution should not grow faster with time than an exponential. For simplicity, we limit the discussion to propagation in two dimensions x and z and transversal electric (TE) fields.

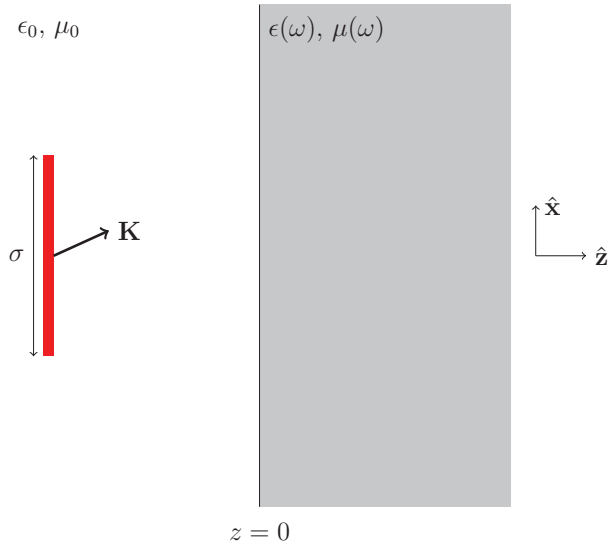

Figure 3.1: A semi-infinite active medium, described by parameters $\epsilon(\omega)$ and $\mu(\omega)$ covers the region $z > 0$. For $z < 0$ there is vacuum. The active medium is illuminated by a TE polarized source of finite width σ, located somewhere to the left of the boundary. The source is indicated by the solid red line, and the vector $\mathbf{K} = K_x\hat{\mathbf{x}} + K_{1z}\hat{\mathbf{z}}$ indicates the propagation direction of the main plane wave component of the source. Here $K_{1z} = \sqrt{\omega_1^2/c^2 - K_x^2}$, and ω_1 and K_x are input parameters of the source.

In the analysis we consider a semi-infinite medium which is illuminated by a realistic incident beam, which both is causal and has finite width. A schematic of the setup considered is shown in Fig. 3.1.

We will here consider an excitation in the form $u(x)v(t)$, where

$$u(x) = \text{beam}(x/\sigma)\exp(iK_x x), \tag{3.1a}$$
$$v(t) = H(t)\exp(-i\omega_1 t). \tag{3.1b}$$

Here $\text{beam}(x/\sigma)$ stands for a function which vanishes for $|x| > \sigma$, is smooth for $|x| < \sigma$, and $\text{beam}(0) = 1$. This represents a beam of thickness $\sim \sigma$, and a bundle of transversal wavenumbers around the central transversal wavenumber K_x. The envelope function $H(t)$ in (3.1b) will in most of our examples be a unit step function, i.e. $H(t) = 0$ for $t < 0$, and $H(t) = 1$ for $t > 0$. This sharp onset will cause all frequencies ω to be excited to some extent. We will also consider two examples where $H(t)$ is a truncated Gaussian function. This will be referred to as

a Gaussian pulse in time. Note that the excitation $u(x)v(t)$ is complex, and will thus produce complex electromagnetic fields. The corresponding physical fields and current densities are given as the real values of these complex quantities.

Considering semi-infinite media helps us understand the electromagnetic response given solely by the media's properties; effects related to e.g. reflections from the back side of a slab have been ruled out. Of course, there are no semi-infinite gain media in practice. However, as long as the smallest distance from an observation point to the boundary of the medium is larger than $ct_{\max}$, where $t_{\max}$ is the maximum duration of the experiment, the size does not matter and we may as well assume it is infinite. To approach steady state (or the monochromatic limit) we must require $t_{\max}$ to be large. Then, we must have in mind that the dimensions of the gain medium must be accordingly large.

In reality the active media will be restricted by gain saturation, which will make the optical response non-linear. This problem is dealt with by assuming that the excitation is sufficiently weak, so that the magnitude of the fields always are below the saturation limit.

3.1 Instabilities

Wave propagation in semi-infinite gain media may involve instabilities. The waves are allowed to travel an infinitely large distance, picking up gain as they propagate, and may thus result in infinite fields. Active systems are well understood from the research on plasma physics [68], where instabilities are classified in terms of two main categories which we will adopt here.

Diverging fields due to an infinite traveled distance, and which does not grow with time for a fixed point in space are called *convective instabilities* - the diverging fields are convected away. This means the electric field at a given point (x_0, z_0) will remain finite for all times, i.e. $\lim_{t\to\infty} \mathcal{E}(x_0, z_0, t) < \infty$.

In certain cases the fields may also grow with time at a fixed point in space. This means $\lim_{t\to\infty} \mathcal{E}(x_0, z_0, t) = \infty$. Such instabilities are referred to as *absolute instabilities*. The two types of instabilities are illustrated in terms of FDTD simulations in Figs. 3.2-3.3.

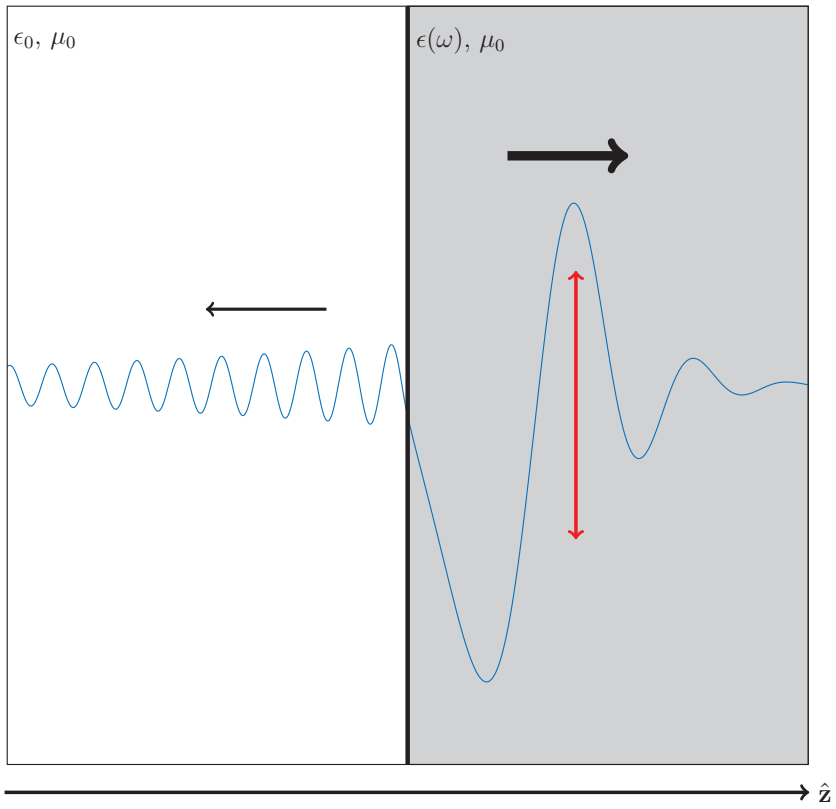

Figure 3.2: A Gaussian pulse in time has propagated from vacuum towards the interface of a semi-infinite active medium. The active medium is described by a permittivity $\epsilon(\omega)$ which has a pole in the upper half plane $\operatorname{Im}\omega > 0$. The image shows the electric field profile at a time frame long after the pulse was reflected at the boundary. Even after the reflected pulse has traveled out through the left edge of the image, there is still produced a constant reflection at the interface. Inside the active medium the electric field grows exponentially in time, with a growth rate consistent with $\operatorname{Im}\omega$ for the pole of $\epsilon(\omega)$. The black arrows indicate the phase velocity of the wave at different z. The vertical red double arrow indicates that the field grows with time inside this medium.

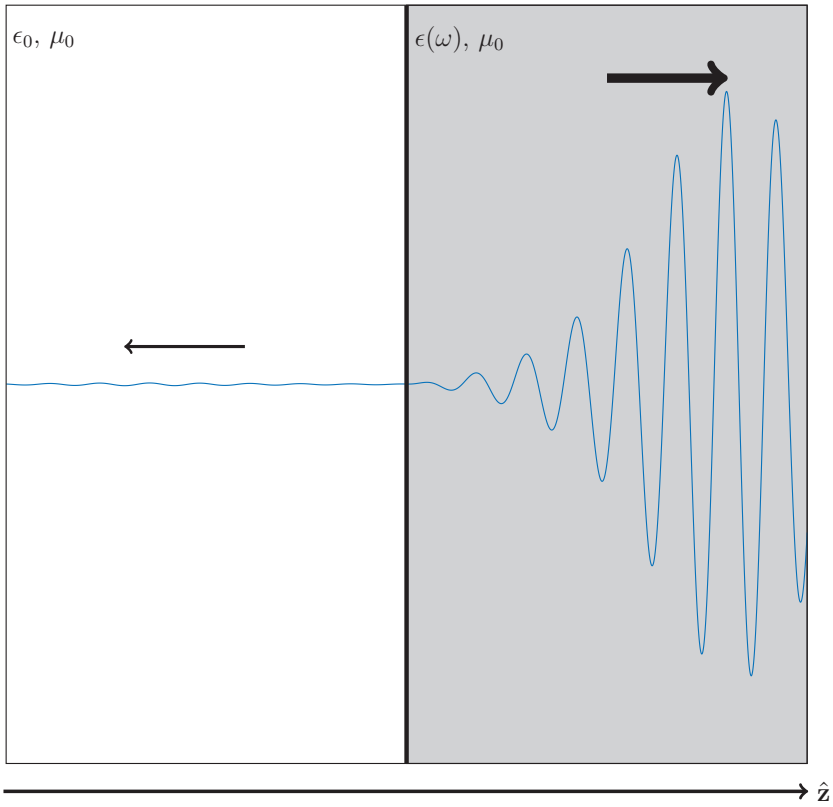

Figure 3.3: A Gaussian pulse in time has propagated from vacuum towards the interface of a semi-infinite conventional weak gain medium. The image shows the electric field profile at a time frame right after the pulse crossed the interface. The pulse will grow without bounds as it propagates towards positive z. For each z the electric field will, however, eventually die out to zero. The instability is thus "convected away". The arrows indicate the phase velocity of the wave at different z. The reflection to the left is small, as we consider a weak gain medium where $\epsilon(\omega) \approx 1$.

3.2 Fourier and Laplace transforms

Due to the possible occurence of instabilities, the analysis of wave propagation cannot necessarily be done by considering a single real frequency and a single plane-wave component, as is usually done in linear, passive media. We must have in mind that real physics happens in the time-spatial domain; the monochromatic and plane-wave limits can never be realized in practice. The monochromatic limit is approached by turning on the excitation at some time $t = 0$, and waiting a sufficiently long time until the transients have died out. The plane-wave limit is approached by letting the width of the excitation σ be sufficiently large. If instabilities are present, the Fourier transform does not necessarily exist.

A remedy is to use the Laplace transform, decomposing the time-domain fields into exponentially increasing functions $\mathrm{e}^{-i\omega t}$ for $\mathrm{Im}\,\omega = \gamma$ for some real $\gamma > 0$ [51]. The excitation in time starts at time $t = 0$, so all fields are equal to 0 for $t < 0$. We here consider the physical electric field in the time-spatial domain, which is denoted $\boldsymbol{\mathcal{E}}(x, z, t) = \mathcal{E}(x, z, t)\hat{\mathbf{y}}$. The Laplace transform is given by

$$\mathcal{E}(x, z, \omega) = \int_0^\infty \mathcal{E}(x, z, t)\mathrm{e}^{i\omega t}\mathrm{d}t, \tag{3.2}$$

where the standard transformation variable s has been substituted with $-i\omega$. The calligraphic capital letter is kept for the Laplace transformed field, to get consistency with the notation in Chapter 2. Explicitly stating the arguments are therefore required to distinguish between $\mathcal{E}(x, z, t)$ and $\mathcal{E}(x, z, \omega)$. For the Laplace transform to exist we must require that the signal does not grow faster than as an exponential with time, so it is assumed that

$$|\mathcal{E}(x, z, t)| < E_0\mathrm{e}^{\gamma t} \tag{3.3}$$

for some positive, finite E_0 and γ. This requires $\mathrm{Im}\,\omega > \gamma$ (i.e. $\mathrm{Re}\,s > \gamma$).

In reality the width of the source cannot be infinitely large, so the signal will also contain different plane wave components. This decomposition can be done using the Fourier transform

$$E(k_x, z, \omega) = \int_{-\infty}^\infty \mathcal{E}(x, z, \omega)\mathrm{e}^{-ik_x x}\mathrm{d}x, \tag{3.4}$$

where all the k_x's are real. For the Fourier-Laplace transformed field $E(k_x, z, \omega)$ we have here used a regular capital letter, to make it easy to distinguish from the physical field $\mathcal{E}(x, z, t)$.

By comparing the transforms in (3.2) and (3.4) it can be seen that the Laplace transform is just a Fourier transform with a possibly complex argument[1]. The

[1] In the Laplace transform the integral is taken from $t = 0$ to ∞, but since the electric field is 0 for $t < 0$, it wouldn't make any difference to change the lower limit to $-\infty$.

signs of the transformation variables are opposite for the transformation in space and time. This convention is chosen because this gives a wave propagating in the positive x-direction for positive k_x and $\mathrm{Re}\,\omega$.

The inverse Fourier transform is taken by performing a similar integral as the forward transform, but where the sign in the exponent has switched, and with an extra factor of $1/(2\pi)$. The convenience of the substitution of the Laplace transformation variable now becomes apparent, as the inverse Laplace transform becomes an inverse Fourier transform taken along the line $\mathrm{Im}\,\omega = \gamma$. The actual electric field in the temporal and spatial domain is thus given by

$$\mathcal{E}(x,z,t) = \frac{1}{(2\pi)^2}\int_{i\gamma-\infty}^{i\gamma+\infty}\int_{-\infty}^{\infty} E(k_x,z,\omega)\mathrm{e}^{ik_x x - i\omega t}\mathrm{d}k_x\mathrm{d}\omega. \tag{3.5}$$

From this equation we see that the line $\mathrm{Im}\,\omega = \gamma$ must lie above all singularities of $E(k_x,z,\omega)$, to ensure $\mathcal{E}(x,z,t) = 0$ for $t < 0$[2]. The ω and k_x integration paths are for clarity shown in Fig. 3.4.

In Paper I of this thesis we show that for a wide range of active media of interest it is possible to deform the inverse Laplace transform contour (Bromwich path) down to the real ω-axis[3]. When this is possible, no absolute instability is present, and the monochromatic limit may be reached by waiting a sufficiently long time until the transients have died out. This may however come at the expense of deforming the paths for each ω [68]; i.e. the fields may have to be described as a sum of complex plane wave components, meaning the fields grow in the $\pm x$-directions. This corresponds to a convective instability.

If the Bromwich path in the ω domain cannot be moved down to the real ω-axis for all $\mathrm{Re}\,\omega$, the electric field *must* be described in terms of complex frequency components $\mathrm{e}^{-i\omega t}$. This means the field grows with time even at a fixed point in space. Thus we have an absolute instability. It is shown in the paper that this happens if $\epsilon\mu$ is not analytic or zero-free in the upper half plane $\mathrm{Im}\,\omega > \gamma$.

When no absolute instabilities are present we get

$$\mathcal{E}(x,z,t) = \frac{1}{(2\pi)^2}\int_{-\infty}^{\infty}\int_{\kappa(\omega)} E(k_x,z,\omega)\mathrm{e}^{ik_x x - i\omega t}\mathrm{d}k_x\mathrm{d}\omega, \tag{3.6}$$

where the paths $\kappa(\omega)$ are found by tracing the singular points of $E(k_x,z,\omega)$ in the complex k_x-plane as we reduce $\mathrm{Im}\,\omega$ from γ to 0 for each ω along the Bromwich path.

[2]This is seen by closing the integration path along an infinite semi-circle in the upper half plane. If there are no singularities for $\mathrm{Im}\,\omega > \gamma$ the integral along the closed path is zero from Cauchy's integral theorem [69].

[3]The deformation theory is explained in detail in Paper I. The application of Fubini's theorem requires the source $u(x)v(t)$ to be sufficiently smooth. These requirements are specified in Appendix B in the paper.

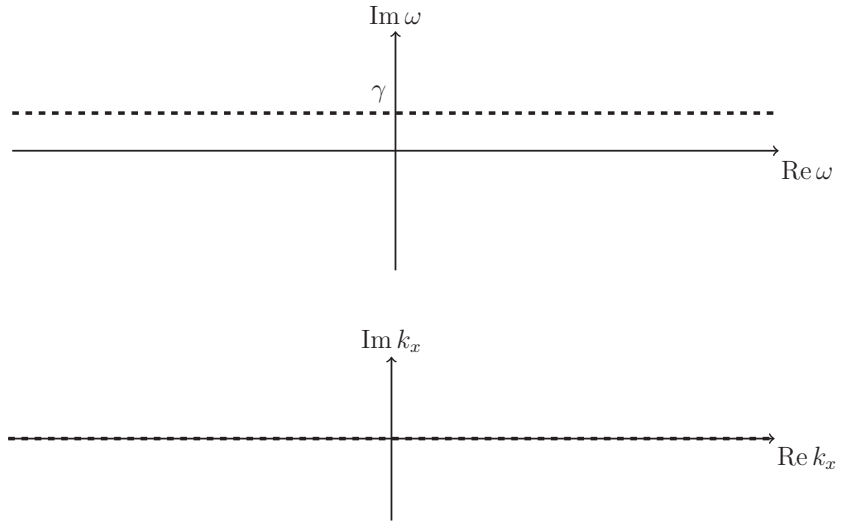

Figure 3.4: (a) The initial ω-integration path (black, dashed line) in (3.5). (b) For each $\omega = \mathrm{Re}\,\omega + i\gamma$, the integration over transversal wavenumbers is taken along the real k_x-axis. We consider the possibility of deforming the ω-integration path in (a) down to the real ω-axis. To do this, we may have to deform the integration path in the complex k_x domain, to avoid singularities of the integrand in (3.5). The resulting deformed k_x-path $\kappa(\omega)$ may in general be different for each frequency ω.

Even though the monochromatic limit exists, it may for certain gain media take a long time for the transients to die out. This will be the case if the gain is very strong in a frequency region Ω_g, while the structure is excited at a frequency ω_1 outside of Ω_g. Due to the causal onset of the source, all frequencies will be excited at some extent. Since the gain is very large for $\omega \in \Omega_\mathrm{g}$ these frequency components will be amplified strongly, and may therefore dominate the field propagation even for relatively long times. The excitation of frequencies away from the observation frequency ω_1 can be reduced by turning on the source smoothly. To completely remove unwanted frequency content a long onset-time is however required, which will increase the necessary simulation time or experiment duration. In media with strong gain numerical errors or physical imperfections may then invalidate the results from a simulation or actual experiment before the monochromatic response at ω_1 can be observed.

By examining the monochromatic and plane wave limits, we find that the limits do not in general commute. Whether the fields tend to ∞ or not may also depend on which excitation is used to approach the plane wave limit (see Paper I for details). The plane wave limit $\sigma \to \infty$ can in some cases cause instabilities to

occur. This may be explained in terms of side waves, which will propagate the infinite distance from $x = \pm\infty$ picking up gain, and thus leading to diverging fields. In other cases the limit $\sigma \to \infty$ can prevent instabilities from occurring, by limiting the excitation of the k_x's associated with the instabilities.

Papers I and II of this thesis demonstrate that monochromatic plane wave analysis of gain media may be dangerous in general, and may lead to unphysical results. Several publications had pointed this out earlier [51, 70–72]. However, Kolokolov only considered the special case with weak or no dispersion, while Refs. [51, 71, 72] only considered a single plane wave component at the time. The Fourier-Laplace formalism from Ref. [68] applied in Papers I and II provides a robust framework of analyzing active systems. This includes determining how the correct monochromatic limit and/or plane-wave limits can be taken, and predicting the presence of convective and/or absolute instabilities.

3.2.1 Sign of the longitudinal wavenumber k_{2z}

Equation (3.5) express the physical electric field as a superposition of frequency-wavenumber components $E(k_x, z, \omega)\mathrm{e}^{ik_x x - i\omega t}$. Note that we start out with (3.5), and in this subsection thus consider some upper half plane of frequencies $\operatorname{Im}\omega > \gamma$. The linearity of Maxwell's equations (2.10) gives that these equations must be satisfied for each component $E(k_x, z, \omega)\mathrm{e}^{ik_x x - i\omega t}$ separately. This means that $E(k_x, z, \omega)$ must obey the Helmholtz equation for each (k_x, ω):

$$\Big[\frac{\mathrm{d}^2}{\mathrm{d}z^2} - k_x^2 + \epsilon\mu\omega^2/c^2\Big]E(k_x, z, \omega) = 0. \tag{3.7}$$

The general solution to this equation is

$$E(k_x, z, \omega) = A(k_x, \omega)\mathrm{e}^{ik_{2z}z} + B(k_x, \omega)\mathrm{e}^{-ik_{2z}z}, \tag{3.8}$$

where

$$k_{2z}^2 = \epsilon\mu\omega^2/c^2 - k_x^2. \tag{3.9}$$

Since k_{2z} must be found by taking the square root of (3.9) we must choose a sign convention. For a passive medium only one of the terms in (3.8) may be present, as an imaginary part of k_{2z} would give diverging fields for $z \to \infty$ from one of the two terms. The common approach is to set $B(k_x, \omega) = 0$, and choose the sign of k_{2z} such that $\operatorname{Im} k_{2z} > 0$ for all ω.

Since we here consider potentially active media, we cannot use such a principle. The problem of determining the sign of k_{2z} in active media is far from trivial. It has been discussed in the context of total internal reflection from a weakly amplifying medium [70, 71, 73–86], and more recently in the context of the wave

vector refractive index of more advanced media such as metamaterials [58, 59, 87–96].

There now seems to be agreement that the sign of the wave vector should be determined such that for a fixed k_x:

$$\begin{aligned} &k_{2z}(k_x,\omega) \text{ is analytic for } \operatorname{Im}\omega > \gamma, \text{ and} \\ &k_{2z}(k_x,\omega) \to +\omega/c \text{ as } \omega \to \infty \text{ in the region } \operatorname{Im}\omega > \gamma. \end{aligned} \tag{3.10}$$

In the region $\operatorname{Im}\omega > \gamma$ the principle of causality may be applied to show that $B(k_x,\omega) = 0$, when the sign of k_{2z} is chosen according to (3.10) (see Appendix C in Paper I for details). This result is only valid in the region $\operatorname{Im}\omega > \gamma$. In fact, it turns out there (at least in principle) exist isotropic gain media where both signs of k_{2z} are excited at the same time when interpreted at a real observation frequency ω_1 [97].

3.3 Application of the Fourier-Laplace framework

We now consider two examples where the general path deformation theory from Paper I is applied. First the case of total internal reflection from a conventional weak gain medium is considered. We then consider the exotic possibility of simultaneous refraction from an isotropic medium.

3.3.1 Evanescent gain

Total internal reflection occurs for large angles of incidence, when light is incident from a high-refractive-index medium onto a low-index medium. If the low-index medium is active, *evanescent gain* is possible [71]. By evanescent gain we mean that the evanescent field picks up gain, resulting in a reflectivity exceeding unity.

For concreteness we consider a dielectric medium with $\epsilon_1 = 4.7$ for $z < 0$. For $z > 0$ there is a weak Lorentzian gain medium, where $\epsilon_2(\omega)$ is given by (2.19) with $F = -0.05$, $\Gamma = 0.1\omega_0$, and ω_0 is the resonance frequency. This permittivity is analytic and zero-free for $\operatorname{Im}\omega > 0$, so the medium does not support absolute instabilities, and the monochromatic limit may be reached.

For an excitation of finite transversal width, and with frequency $\omega_1 = \omega_0$, we thus get for $z > 0$ and sufficiently large time

$$\mathcal{E}(x,z,t) = \frac{\mathrm{e}^{-i\omega_1 t}}{2\pi} \int_{\kappa(\omega_1)} A(k_x,\omega_1)\mathrm{e}^{ik_x x + ik_{2z} z}\mathrm{d}k_x. \tag{3.11}$$

Here $A(k_x, \omega)$ is determined by the transversal profile of the source (3.1a) and the Fresnel transmission coefficient [55]. A schematic of the k_x integration path $\kappa(\omega_1)$ is shown in Fig. 3.5.

Note that the resulting integration path $\kappa(\omega_1)$ contains vertical detours with complex k_x, which means exponentially growing side waves with $k_{2z} = 0$ will be present. The plane wave limit $\sigma \to \infty$ will therefore lead to diverging fields. It may be tempting to simply overlook the vertical detours, so that the inverse Fourier transform is taken along the real k_x-axis, as it would be for a passive medium. However, this is not possible due to the branch cuts from the zeros of k_{2z}, which cross the real k_x-axis.

We now consider the possibility of evanescent gain. The sign of k_{2z} will flip at the branch cuts at $\operatorname{Re} k_x \approx \pm\sqrt{\epsilon_2(\omega)}\omega/c$. It turns out that (see Paper I for details) for k_x above the branch cut, the real part of k_{2z} is negative, while $\operatorname{Im} k_{2z}$ is positive. This means, for sufficiently large incident angles[4] the "phase velocity" of the evanescent wave is directed towards the boundary. The wave will be amplified as it "propagates" in this direction, which means evanescent gain may be possible.

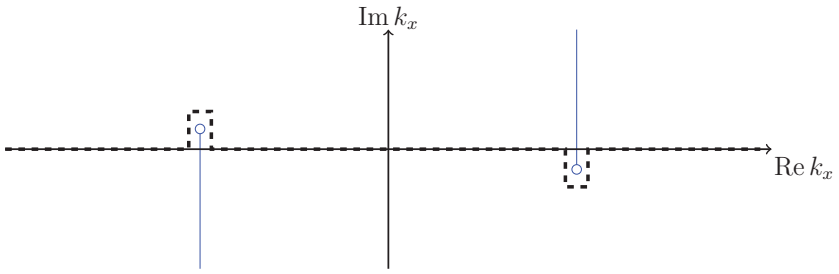

Figure 3.5: The resulting path $\kappa(\omega_1)$ (black, dashed line) after the ω-integration path has been moved down to the real axis. We here consider a weak Lorentzian gain medium, where $\epsilon_2(\omega)$ is given by (2.19), with $F = -0.05$, $\Gamma = 0.1\omega_0$ and ω_0 is the resonance frequency. The k_x integration must detour around the branch points $k_{2z} = 0$ located at $k_x = \pm\sqrt{\epsilon_2(\omega_1)}\omega_1/c$, marked with open blue circles. From the branch points there goes branch cuts (blue lines) towards infinity, through which k_{2z} flips sign.

If we on the other hand take the plane wave limit $\sigma \to \infty$ first, while keeping the Bromwich integration path at $\operatorname{Im}\omega = \gamma$, the plane wave limit of a single K_x is reached. However, then the ω-integration path cannot be moved all the way down to the real axis, due to branch points close to $\omega = K_x c$. Thus, now the system supports absolute instabilities, even though the permittivity $\epsilon_2(\omega)$ is analytic and zero-free in the upper half plane $\operatorname{Im}\omega > 0$. The monochromatic limit can therefore not be reached.

[4]That is, above the critical angle given by $k_x \approx |\sqrt{\epsilon_2(\omega)}\omega/c|$.

The resulting ω-integration path after deforming it as close to the real axis as possible is shown in Fig. 3.6. As argued in Ref. [71] we can interpret the field as "quasi-monochromatic" up to a certain time, provided the excitation frequency is far away from $K_x c$. For sufficiently large times the side waves with $k_{2z} = 0$ corresponding to the frequency obeying $\omega\sqrt{\epsilon_2(\omega)} = K_x c$ will dominate, and eventually result in a diverging field.

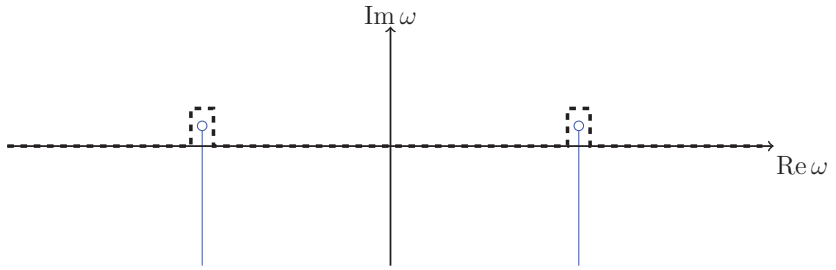

Figure 3.6: If the plane wave limit is taken first, this is the resulting ω-integration path (black, dashed line) one obtain after deforming it down as close to the real axis as possible. The path must take detours around the branch cuts (blue lines) from the branch points close to $\omega = \pm K_x c$ towards $\pm K_x c - i\infty$, and the electric field will therefore eventually grow with time. If the excitation frequency is far from $K_x c$, the field may still be considered as quasi-monochromatic up to a certain time, when the field eventually starts to diverge.

Figure 3.7 shows a FDTD simulation of a plane wave with $K_x = 1.5\omega_0/c$ incident from the high index medium with $\epsilon_1 = 4.7$ upon the weak Lorentzian gain medium. The field is plotted for $x = 0$ and $t = 800/\omega_0$. The arrows for $z < 0$ indicate that the field is a sum of the incident and reflected fields in this region. The power reflection coefficient is found to be larger than unity. By considering the time evolution it is seen that a partially standing wave is established. Since the reflection coefficient is larger than unity, this "standing wave" partially propagates towards the left.

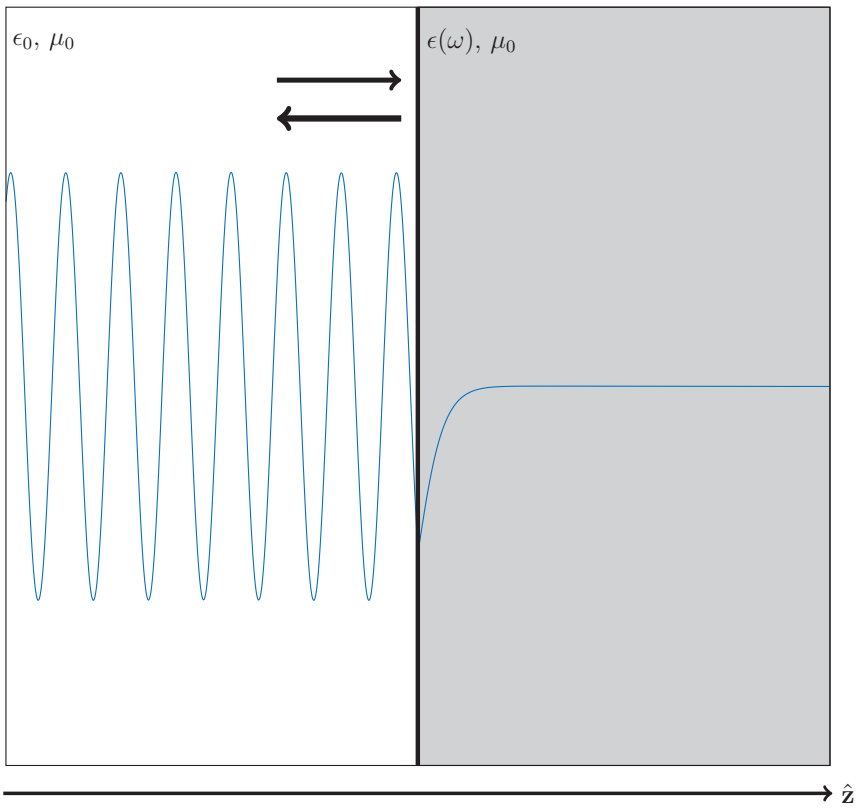

Figure 3.7: A plane wave is incident from a high index medium with $\epsilon_1 = 4.7$ to the left, upon a weak Lorentzian gain medium. The incident plane wave has a transverse plane wave component $K_x = 1.5\omega_0/c$, where ω_0 is the resonance frequency of the gain medium. The permittivity of this gain medium is given by the Lorentz function (2.19), with $F = -0.05$, $\Gamma = 0.1\omega_0$ and ω_0 is the resonance frequency. The excitation frequency of the incident plane wave is $\omega_1 = \omega_0$.

3.3.2 Simultaneous refraction

We now consider an active medium where the refractive index $n(\omega)$ is given by (2.19), with the parameters $F = -0.5$, $\Gamma = 0.05\omega_0$ and ω_0 is the resonance frequency. In the following we consider a nonmagnetic realization of this refractive index, i.e. $\epsilon(\omega) = [n(\omega)]^2$. The medium is placed at $z > 0$, and for $z < 0$ we let there be vacuum. We first consider a causal beam of finite width σ illuminating the medium. We will in this section only consider a normally incident beam, i.e. we set $K_x = 0$.

At the excitation frequency $\omega_1 = 0.853\omega_0$ it turns out that the k_x integration path $\kappa(\omega_1)$ must be deformed as shown in Fig. 3.8, to avoid the branch cuts from $k_{2z}(k_x, \omega) = 0$ (see Paper I for details). The medium under consideration does not support absolute instabilities, as $\epsilon\mu$ is analytic and zero-free for $\operatorname{Im}\omega > 0$. This means the monochromatic limit can be reached. In this limit the field is given by (3.11), where $\kappa(\omega_1)$ is as shown in Fig. 3.8. Also this path contains complex k_x, from the integration around the branch points at $k_x = \pm n(\omega_1)\omega_1/c$. Thus, also in this example the plane wave limit $\sigma \to \infty$ will lead to diverging fields. We therefore instead consider a large, but finite σ.

We argue in the paper that in the monochromatic limit the electric field can be approximated by

$$\mathcal{E}(x, z, t) = \Big(\frac{4k_{1z}\mathrm{e}^{ik_{2z}z}}{k_{1z} + k_{2z}} - \frac{2k_{1z}\mathrm{e}^{-ik_{2z}z}}{k_{1z} - k_{2z}}\Big)\mathrm{e}^{-i\omega_1 t}. \tag{3.12}$$

The isotropic gain medium here considered thus support waves propagating with both signs of k_{2z}, which we refer to as *simultaneous refraction*.

For (3.12) to approximate the field behavior in the monochromatic limit well, the integration around the vertical detours in Fig. 3.8 should be negligible compared to the horizontal integrations through $k_x = 0$. For a beam of finite support the plane wave components in $\kappa(\omega_1)$ with $\operatorname{Im} k_x \neq 0$ will in fact be more and more excited as σ increases. For (3.12) to provide a good approximation of the actual field (given by (3.11)) in a simulation or experiment, the source width σ should therefore be chosen with care; σ should be small enough so that the integration over real k_x's dominate over the vertical detours, while at the same time large enough that $k_x = 0$ dominates over all other $\operatorname{Re} k_x$'s.

If we on the other hand take the limit $\sigma \to \infty$ first, and then approach the monochromatic limit[5], we get

$$\mathcal{E}(x, z, t) = \frac{2k_{1z}}{k_{1z} + k_{2z}}\mathrm{e}^{ik_{2z}z - i\omega_1 t}. \tag{3.13}$$

[5]This can be done here, since we consider a normally incident plane wave.

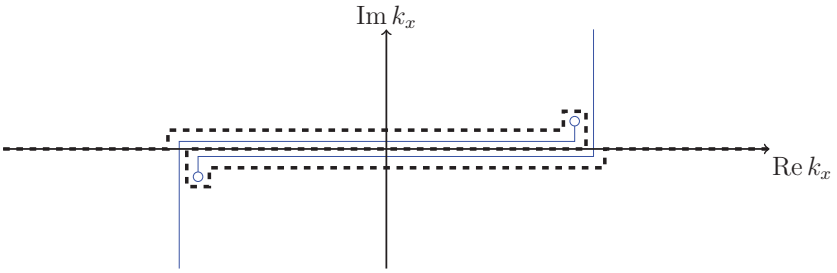

Figure 3.8: The resulting path $\kappa(\omega_1)$ (black, dashed line) at the frequency $\omega_1 = 0.853\omega_0$ for the simultaneous refracting medium. The k_x integration must detour around the branch points $k_{2z} = 0$ located at $k_x = \pm\sqrt{\epsilon_2(\omega_1)}\omega_1/c$, marked with open blue circles. To avoid the branch cuts (blue lines) the integration path becomes zig-zag in the complex k_x domain.

Here only the positive sign of k_{2z} is present[6]. This means, if the plane wave limit $\sigma \to \infty$ ($K_x = 0$) is taken before the monochromatic limit, simultaneous refraction does not occur. Equations (3.12)-(3.13) thus exemplifies the result from Paper I that the two orders of the monochromatic and plane wave limits may yield different results.

From this it is understood that simultaneous refraction is a two-dimensional effect. In the case of a finite σ there will always be oblique waves with $k_x \neq 0$ excited, no matter how large σ is. After a sufficiently long time t these oblique waves will somehow establish waves along the z-direction with both signs for k_{2z}. However, if $\sigma \to \infty$ is taken first, there will be no oblique waves excited. The simultaneous refracting waves can thus not be established. This latter situation is one-dimensional, as the transverse excitation profile is constant for all x, and $K_x = 0$.

The suggested medium has a very large gain at resonance, so the frequencies of the transients close to resonance will be strongly amplified as they propagate into the medium. This medium will thus suffer from the problem mentioned in Sec. 3.2, that it will take a long time before the transients have died out. Media with such a large gain are not suited for FDTD simulations or physical realization. A method which may be used to find simultaneous refracting media with low gain at all ω may be found in Chapter 8 of the Author's Master thesis [98]. The method is based on the discussion on how to obtain a negative refractive index at low loss/gain done by [99]. Even though the maximum gain was drastically reduced, the gain was still too large for this medium to be suited for FDTD simulations.

[6]This corresponds to a *negatively* refracted plane wave, as $\mathrm{Re}\, n(\omega)$ is negative at our observation frequency ω_1.

Chapter 4

Spatial dispersion in metamaterials

We now leave the discussion of active media, and turn to the topic of homogenization of media consisting of *passive* constituents. Up until now we have considered media where the macroscopic electromagnetic response can be described by two frequency dependent parameters; the permittivity $\epsilon(\omega)$ and the permeability $\mu(\omega)$. For most metamaterial structures these two parameters are not sufficient to give an accurate description. As already mentioned in Chapter 2 the unit cells are often anisotropic, which means the response must be described by *tensors* $\boldsymbol{\epsilon}(\omega)$ and $\boldsymbol{\mu}(\omega)$. Secondly, if the microscopic susceptibility $\varepsilon(\mathbf{r})-1$ and/or the frequency ω is large, the assumption of small ka[1] is not necessarily valid. When this is the case, *spatial dispersion* becomes important.

In Chapter 2 we considered *temporal dispersion*, that is the material parameter's dependency on the frequency ω. In the time domain this means the material response, e.g. the polarization density $\boldsymbol{\mathcal{P}}(\mathbf{r},t)$ at a given point $\mathbf{r}$ and time t will depend on the electric field $\boldsymbol{\mathcal{E}}(\mathbf{r},t')$ at the same point at all previous times $t'<t$. If a medium in addition is *spatially dispersive*, then $\boldsymbol{\mathcal{P}}(\mathbf{r},t)$ also depends on the electric field at surrounding points $\mathbf{r}'\neq\mathbf{r}$. In the wavenumber space this leads to material parameters depending on the wavenumber $\mathbf{k}$, as well as the frequency ω.

The effects of spatial dispersion have previously been studied in crystal optics [100] and continuous media [55], and the importance of spatial dispersion in metamaterials has also been known for quite some time [101–103]. The emergence of spatial dispersion may possibly explain the strange and apparently unphysical behavior of certain metamaterial parameters [19–29, 104], and makes the analysis more difficult. Homogenization of such non-local media becomes more complicated and the boundary conditions for the macroscopic electromagnetic fields may have

[1] I.e. if the unit cells are small compared to the effective wavelength inside the medium.

to be modified. In addition, such media may allow the propagation of additional modes. The latter result means that even *additional* boundary conditions for the electromagnetic fields may be required [105–109], which is covered in Chapter 5 of this thesis.

Possible routes have been suggested for achieving artificial magnetism without spatial dispersion [110–113]. Such an approach would avoid having to deal with the obstacles mentioned above. As many common metamaterial realizations turns out to be (weakly or strongly) spatially dispersive [101,102,114–117], it is however crucial to develop theoretical framework for analysis and development of such media. The strong spatial dispersion due to structural inhomogenity in layered media [116] has recently been reported as the intrinsic property which makes such structures suitable for obtaining frequency-independent anti-reflection for a wide range of incident angles [118, 119]. Despite the large amount of research already done on the topic, many possibilities and limitations caused by spatial dispersion, with implications for metamaterial applications, probably still remains to be discovered.

In this chapter we present a homogenization method suitable for analyzing media with spatial dispersion, based on the analysis in Refs. [33–35]. It is shown how artificial magnetism may be viewed as a second order spatially dispersive effect, that is the magnetic permeability may be described by $\mathcal{O}(k^2)$-term in the Taylor expansion of the total Landau-Lifshitz permittivity $\boldsymbol{\epsilon}(\omega, \mathbf{k})$. Based on a multipole expansion of the induced current density it is argued that the electric quadrupole moment [120], but also even higher order multipole moments [121] (Paper IV) may equally contribute to the $\mathcal{O}(k^2)$-term of $\boldsymbol{\epsilon}(\omega, \mathbf{k})$. Based on this observation, we state and compare four different definitions of magnetic permeability for periodic, artificial media, or metamaterials [122] (Paper V).

4.1 Homogenization procedure

We consider an *infinite* periodic structure, which is excited by a source. The periodic structure consists of cubic unit cells with lattice parameter a, which contains linear, isotropic, time-shift invariant, non-magnetic, spatially non-dispersive but potentially temporally dispersive constituents, described by a microscopic permittivity $\varepsilon(\mathbf{r})$. We consider a single frequency component $\mathrm{e}^{-i\omega t}$, which is always possible for passive media [97]. It is convenient to also look at a single spatial Fourier component of the source,

$$\boldsymbol{\mathcal{J}}_{\text{ext}}(\mathbf{r}) = \mathbf{J}_{\text{ext}} \mathrm{e}^{i\mathbf{k}\cdot\mathbf{r}}, \tag{4.1}$$

to enable the use of Floquet theory. Here $\mathbf{J}_{\text{ext}}$ is independent on $\mathbf{r}$, and $\mathbf{k}$ is a fixed parameter, in general unrelated to the frequency ω.

The resulting microscopic electric field $\mathbf{e}(\mathbf{r})$ is found from the microscopic Maxwell equations (2.1). For special cases (e.g. a layered structure) these equations may be solved analytically, but in general a numerical method must be used. In our case we use the finite difference frequency domain (FDFD) method [121,123]. From the microscopic electric field the microscopic induced current density is found from (2.4) and (2.5) (since we consider non-magnetic constituents, we have $\mathbf{m} = 0$):

$$\mathbf{j}(\mathbf{r}) = -i\omega[\varepsilon(\mathbf{r}) - 1]\mathbf{e}(\mathbf{r}). \tag{4.2}$$

The spatial dependency $\mathrm{e}^{i\mathbf{k}\cdot\mathbf{r}}$ of the source will cause the microscopic field to be Bloch-periodic with Bloch-vector equal to $\mathbf{k}$:

$$\mathbf{e}(\mathbf{r}) = \mathbf{u}_\mathbf{e}(\mathbf{r})\mathrm{e}^{i\mathbf{k}\cdot\mathbf{r}}. \tag{4.3}$$

Here $\mathbf{u}_\mathbf{e}(\mathbf{r})$ is a periodic function with the same periodicity as the lattice. The other microscopic fields are expressed similarly. Let V be the unit cell containing the origin. We now define the macroscopic fields as the fundamental Floquet mode, expressed from the averaged Bloch function [33]. For the electric field we then get

$$\boldsymbol{\mathcal{E}}(\mathbf{r}) = \frac{\mathrm{e}^{i\mathbf{k}\cdot\mathbf{r}}}{V}\int_V \mathbf{e}(\mathbf{r})\mathrm{e}^{-i\mathbf{k}\cdot\mathbf{r}}\mathrm{d}^3r, \tag{4.4}$$

and the macroscopic magnetic field $\boldsymbol{\mathcal{B}}(\mathbf{r})$ and the macroscopic induced current $\boldsymbol{\mathcal{J}}(\mathbf{r})$ are defined similarly. The definition of the macroscopic fields according to (4.4) may be shown to be a special case of (2.9), with a specific choice of the test function $f(\mathbf{r}')$ [123].

Since the average operation (4.4) commutes with the operations of spatial differentiation, the two macroscopic Maxwell curl equations given by (2.10c) and (2.10d) are still valid with the definition (4.4) of the macroscopic fields. Since the only spatial dependency of these macroscopic fields is the exponential factor $\mathrm{e}^{i\mathbf{k}\cdot\mathbf{r}}$, the curl equations may be written

$$i\mathbf{k}\times\mathbf{E} = i\omega\mathbf{B}, \tag{4.5a}$$

$$\frac{1}{\mu_0}i\mathbf{k}\times\mathbf{B} = -i\omega\epsilon_0\mathbf{E} + \mathbf{J}_\mathrm{ext} + \mathbf{J}. \tag{4.5b}$$

Here we have multiplied both equations by the factor $\mathrm{e}^{-i\mathbf{k}\cdot\mathbf{r}}$, and all capital (regular) letters denote the amplitudes of the corresponding macroscopic fields or current densities (e.g. $\mathbf{E} = \boldsymbol{\mathcal{E}}\mathrm{e}^{-i\mathbf{k}\cdot\mathbf{r}}$). This is done to obtain Maxwell equations for fields only depending on $\mathbf{k}$ and ω. This dependency is suppressed in the notation for brevity. The next step of the homogenization procedure is to find material parameters relating $\mathbf{J}$ to the fundamental fields $\mathbf{E}$ and $\mathbf{B}$.

We will here consider four approaches appearing in literature. In the Landau-Lifshitz approach [55,100] a single parameter, that is the Landau-Lifshitz (relative) permittivity tensor $\boldsymbol{\epsilon}(\omega, \mathbf{k})$, is used to describe the entire electromagnetic response of the infinite periodic medium. The second approach decomposes the induced current into two terms; that is a longitudinal and transversal component. In the third approach $\mathbf{J}$ is approximated by a multipole expansion. The fourth approach write $\mathbf{J}$ in terms of modified electric and magnetic polarization densities, based on an exact decomposition of the microscopic current into three terms [124]. These four decompositions are considered in detail in Paper V of this thesis. In particular, properties of the corresponding permeabilities, as well as the parameter $\boldsymbol{\epsilon}(\omega, \mathbf{k})$, are discussed, including causality, passivity, symmetry, asymptotic behavior and origin dependence.

The homogenization method presented here relies on the assumption that we can consider a single spatial Fourier component of the source at the time. This approach has faced some opposition, and should therefore be justified. It has been argued that such a plane wave source is not physically realizable [125, 126], as the external source necessarily overlaps with the *infinite* medium. Inside the volume occupied by the source, which in a physical realization has to be finite, constitutive relations characteristic of the medium no longer hold. We note that in the homogenization method the source is only introduced to produce fields from which the constitutive parameters may be extracted. The method highly relies on numerical calculations, where an infinite plane wave source, which is unaffected by the local fields, is straightforward to implement, despite the possible challenges related to physically realizing such a source.

A valid point made in Refs. [125,126] is, however, that surface currents at the media boundaries cannot be determined by considering infinite media. Considering infinite media helps us understand the electromagnetic response given solely by the medium's properties; effects related to interactions with surrounding media have been ruled out. After the material parameters are extracted, one often desires to use them to predict the response of finite objects. Whether the material parameters obtained from any homogenization method are useful in such situations, can be determined by comparing predictions based on these material parameters to analytical solutions or e.g. time domain simulations. The topics of surface currents and modified boundary conditions are covered in Chapter 5.

4.1.1 Landau-Lifshitz approach

In their famous textbook Landau, Lifshitz and Pitaevskii describe all induced current in terms of an electric polarization density $\mathbf{P}_{\text{ll}}$:

$$\mathbf{J} = -i\omega \mathbf{P}_{\text{ll}}. \tag{4.6}$$

This means that the magnetization is zero ($\mathbf{M}_{\text{ll}} = 0$), and the permeability is trivial, $\boldsymbol{\mu}_{\text{ll}} = \mathbf{I}$, where $\mathbf{I}$ is the identity. The auxiliary magnetic field is thus given by $\mathbf{H}_{\text{ll}} = \mathbf{B}/\mu_0$. In a linear medium there is a linear relationship between the displacement vector $\mathbf{D}_{\text{ll}}$ and $\mathbf{E}$:

$$\mathbf{D}_{\text{ll}} = \epsilon_0 \mathbf{E} + \mathbf{P}_{\text{ll}} = \epsilon_0 \boldsymbol{\epsilon}(\omega, \mathbf{k}) \cdot \mathbf{E}. \tag{4.7}$$

Considering terms up to second order in k, the single constitutive parameter $\boldsymbol{\epsilon}(\omega, \mathbf{k})$ becomes

$$\epsilon_{ij}(\omega, \mathbf{k}) - \delta_{ij} = \chi_{ij} + \alpha_{ikj} k_k/\epsilon_0 + \beta_{iklj} k_k k_l c^2/\omega^2, \tag{4.8}$$

for some tensors $\chi_{ij}, \alpha_{ikj}, \beta_{iklj}$ independent of $\mathbf{k}$. Media where (4.8) gives an accurate description of the macroscopic response we classify as *weakly* spatially dispersive. If the spatial dispersion is strong, where higher order terms are not negligible, we let the $\beta_{iklj} k_k k_l c^2/\omega^2$ term absorb the remainder. For such media the β_{iklj} tensor gets dependent on $\mathbf{k}$.

By eliminating $\mathbf{B}$, and inserting (4.6) in (4.5) we obtain using (4.7):

$$\left(k^2 \mathbf{I}_\perp - \frac{\omega^2}{c^2} \boldsymbol{\epsilon}(\omega, \mathbf{k})\right) \cdot \mathbf{E} = i\omega\mu_0 \mathbf{J}_{\text{ext}}, \tag{4.9}$$

with $\mathbf{I}_\perp = \mathbf{I} - \mathbf{k}\mathbf{k}/k^2$. The matrix in the brackets in (4.9) may be inverted to obtain an input-output relation

$$\mathbf{E} = \mathbf{G}(\omega, \mathbf{k}) \mathbf{J}_{\text{ext}}, \tag{4.10}$$

where $\mathbf{G}(\omega, \mathbf{k})$ is a (matrix) response function given by

$$\mathbf{G}(\omega, \mathbf{k})^{-1} = (i\omega\mu_0)^{-1} \left(k^2 \mathbf{I}_\perp - \frac{\omega^2}{c^2} \boldsymbol{\epsilon}(\omega, \mathbf{k})\right). \tag{4.11}$$

In Paper V of this thesis we prove in Appendix C that $\mathbf{G}(\omega, \mathbf{k})^{-1}$ is analytic in the upper half-plane $\operatorname{Im}\omega > 0$, and from (4.11) thus so is $\epsilon(\omega, \mathbf{k})$. In the limit $\omega \to \infty$ the microscopic susceptibility $\varepsilon(\mathbf{r}) - 1$ will tend to unity [55], and we thus have $\boldsymbol{\epsilon}(\omega, \mathbf{k}) \to \mathbf{I}$ in this limit. It may then be showed that the function

$$\boldsymbol{\chi}(\omega, \mathbf{k}) = \boldsymbol{\epsilon}(\omega, \mathbf{k}) - \mathbf{I} \tag{4.12}$$

satisfies Kramers-Kronig relations for a fixed $\mathbf{k}$ [27, 122]. These relations are valid provided $\boldsymbol{\chi}(\omega, \mathbf{k}) \to 0$ sufficiently fast as $|\omega| \to \infty$, and that $\boldsymbol{\chi}(\omega, \mathbf{k})$ does not have singularities for real frequencies. It may further be shown [35] that for reciprocal metamaterial inclusions $\boldsymbol{\epsilon}(\omega, \mathbf{k})$ satisfies the symmetry relation

$$\boldsymbol{\epsilon}^{\text{T}}(\omega, -\mathbf{k}) = \boldsymbol{\epsilon}(\omega, \mathbf{k}). \tag{4.13}$$

For non-gyrotropic media the first order term in (4.8) will vanish, and the relation above becomes

$$\boldsymbol{\epsilon}(\omega, -\mathbf{k}) = \boldsymbol{\epsilon}(\omega, \mathbf{k}). \tag{4.14}$$

This will be the case if there is a center of symmetry in the periodic structure.

Source free propagation inside the infinite periodic structure is described by (4.5) if we set $\mathbf{J}_{\text{ext}} = 0$. Equation (4.9) then gives the dispersion relation for the plane wave modes in a generic spatially dispersive material [33, 100]:

$$\det(\mathbf{G}(\omega, \mathbf{k})^{-1}) = 0. \tag{4.15}$$

For weakly spatially dispersive media, i.e. when the approximation (4.8) holds, the equation above in general has 6 solutions[2] $\mathbf{k}(\omega)$. In the case of a semi-infinite *passive* periodic structure excited by an incident plane wave with frequency ω, three of these modes may be disregarded by requiring the fields to vanish in the limit $z \to \infty$. For structures with certain symmetries some of the coefficients β_{iklj} in (4.8) will become zero, which may lead to a fewer number of modes being allowed to propagate. For instance in a layered structure, only a single Bloch mode $\mathbf{k}(\omega)$ is excited.

In this work we consider spatial dispersion to be present if $\boldsymbol{\epsilon}(\omega, \mathbf{k})$ is dependent on $\mathbf{k}$. Based on this definition, we now demonstrate how a magnetic response may be considered as a second order spatially dispersive effect. In certain situations, e.g. when the dispersion equation (4.15) is to be solved to find the allowed propagating modes $\mathbf{k}(\omega)$, it is convenient to have a single parameter $\epsilon(\omega, \mathbf{k})$ describing the entire macroscopic electromagnetic response of the infinite structure. In metamaterial structures designed to possess artificial magnetism it is, however, often desirable to express the magnetic response more explicitly by introducing a permeability tensor, related to the second order term in (4.8) [33, 55, 128].

We now show how the parameter $\boldsymbol{\epsilon}(\omega, \mathbf{k})$ can be converted into two such parameters $\hat{\boldsymbol{\epsilon}}$ and $\hat{\boldsymbol{\mu}}$. We start by observing that the macroscopic quantities $\mathbf{E}$ and $\mathbf{B}$ in (4.5) are left invariant upon the transformation

$$\mathbf{J} \to -i\omega\hat{\mathbf{P}} + i\mathbf{k} \times \hat{\mathbf{M}}, \tag{4.16}$$

where the quantities $\hat{\mathbf{P}}$ and $\hat{\mathbf{M}}$ are arbitrarily chosen. The left hand side may be expressed in terms of the non-local tensor $\epsilon(\omega, \mathbf{k})$ by (4.7), and the right hand side in terms of two new tensors $\hat{\boldsymbol{\epsilon}}$ and $(\mathbf{I} - \hat{\boldsymbol{\mu}}^{-1})$, in order to obtain [33, 121]

$$\boldsymbol{\epsilon}(\omega, \mathbf{k}) = \hat{\boldsymbol{\epsilon}} - \frac{c^2}{\omega^2}\mathbf{k} \times [\mathbf{I} - \hat{\boldsymbol{\mu}}^{-1}] \times \mathbf{k}. \tag{4.17}$$

[2]Each component of the matrix $\mathbf{G}(\omega, \mathbf{k}\ ^{1})$ may contain terms up to second order in k. Equation (4.15) thus can contain terms up to sixth order in k, which gives (at most) 6 solutions in general [127].

This division into two terms is inspired by (2.14), as the two new parameters $\hat{\boldsymbol{\epsilon}}$ and $\hat{\boldsymbol{\mu}}$ will relate $\hat{\mathbf{P}}$ and $\hat{\mathbf{M}}$ to the fundamental fields $\mathbf{E}$ and $\mathbf{B}$ according to

$$\hat{\mathbf{P}} = \epsilon_0[\hat{\boldsymbol{\epsilon}} - \mathbf{I}]\mathbf{E}, \tag{4.18a}$$

$$\hat{\mathbf{M}} = \mu_0^{-1}[\mathbf{I} - \hat{\boldsymbol{\mu}}^{-1}]\mathbf{B}. \tag{4.18b}$$

In general both $\hat{\boldsymbol{\epsilon}}$ and $\hat{\boldsymbol{\mu}}$ will depend on both ω and $\mathbf{k}$.

For weakly spatially dispersive media only terms up to second order in $\mathbf{k}$ contribute to $\boldsymbol{\epsilon}(\omega, \mathbf{k})$. From (4.17) we see that $\hat{\boldsymbol{\mu}}$ in that case becomes $\mathbf{k}$-independent. For media with certain symmetries it is further possible to define the magnetization $\hat{\mathbf{M}}$ such that both $\hat{\boldsymbol{\epsilon}}$ and $\hat{\boldsymbol{\mu}}$ becomes independent on $\mathbf{k}$.

In the following subsections we consider three different definitions of $\hat{\boldsymbol{\mu}}$, which lead to corresponding permittivities $\hat{\boldsymbol{\epsilon}}$ through (4.17). These parameters will further correspond to polarization and magnetization vectors (4.18), from which (4.16) may be used to relate the induced current density $\mathbf{J}$ to the fundamental fields through the defined two constitutive tensors $\hat{\boldsymbol{\epsilon}}$ and $\hat{\boldsymbol{\mu}}$. We do, however, note that the defined polarization and magnetization vectors in the different decompositions not necessarily correspond to $\hat{\mathbf{P}}$ and $\hat{\mathbf{M}}$ from (4.18). This is because, in certain formulations, the way the magnetization is defined implies that it may be induced by the electric field $\mathbf{E}$ as well as the magnetic field $\mathbf{B}$ through a magneto-electric coupling.

Contributions from the *transversal* component of $\mathbf{E}$ to the specific magnetization may be included in the permeability $\hat{\boldsymbol{\mu}}$ through a suitable transformation. If the structure allows the *longitudinal* component of $\mathbf{E}$ to induce the magnetization, this contribution *must*, however, be described by the permittivity $\hat{\boldsymbol{\epsilon}}$ in the division (4.17). This is because the longitudinal component of $\mathbf{E}$ cannot be expressed explicitly in terms of $\mathbf{B}$ from Faraday's law $\mathbf{B} = \mathbf{k} \times \mathbf{E}/\omega$.

4.1.2 Transversal - longitudinal (tl) decomposition

First we consider the decomposition used in Refs. [33, 55], which is generalized in Paper V of this thesis. In this approach the induced current $\mathbf{J}$ is decomposed in a transversal and a longitudinal part, where the transversal part of the $\mathbf{k}$-dependent part of $\mathbf{J}$ is taken care of by the term $i\mathbf{k} \times \mathbf{M}_{\text{tl}}$. The remainder of $\mathbf{J}$ is described by the term $-i\omega\mathbf{P}_{\text{tl}}$. This strategy puts "as much as possible" of the $\mathbf{k}$-dependent induced current into the magnetization (and therefore the permeability).

In an arbitrary coordinate system the permeability $\boldsymbol{\mu}_{\text{tl}}$ corresponding to $\mathbf{M}_{\text{tl}}$ is given by (see Paper V for details)

$$[\mathbf{I} - \boldsymbol{\mu}_{\text{tl}}^{-1}]_{mn} = \varepsilon_{mip}\varepsilon_{njq}\frac{k_k k_l k_p k_q}{k^4}\beta_{iklj}. \tag{4.19}$$

The permittivity $\boldsymbol{\epsilon}_{\text{tl}}$ then describes the remainder of $\boldsymbol{\epsilon}(\omega, \mathbf{k})$, i.e.

$$\boldsymbol{\epsilon}_{\text{tl}} = \boldsymbol{\epsilon}(\omega, \mathbf{k}) + \frac{c^2}{\omega^2}\mathbf{k} \times [\mathbf{I} - \boldsymbol{\mu}_{\text{tl}}^{-1}] \times \mathbf{k}. \tag{4.20}$$

Provided the *entire* second order term of $\boldsymbol{\epsilon}(\omega, \mathbf{k})$ be described in terms of a permeability, this permeability will be given by $\boldsymbol{\mu}_{\text{tl}}$. For a weakly dispersive, non-gyrotropic medium (i.e. the first order term of $\boldsymbol{\epsilon}(\omega, \mathbf{k})$ is zero), both parameters $\boldsymbol{\epsilon}_{\text{tl}}$ and $\boldsymbol{\mu}_{\text{tl}}$ then will become $\mathbf{k}$-independent, and the macroscopic response may thus be considered as *local*.

4.1.3 Multipole decomposition

We now consider the traditional way of decomposing the induced current by a multipole expansion [31, 32, 34, 42, 121, 129, 130]. The amplitude $\mathbf{J}$ of the macroscopic induced current density may be expressed similarly to (4.4):

$$\boldsymbol{\mathcal{J}}(\mathbf{r}) = \frac{1}{V}\int_V \mathbf{j}(\mathbf{r})\mathrm{e}^{-i\mathbf{k}\cdot\mathbf{r}}\mathrm{d}^3 r, \tag{4.21}$$

where $\mathbf{j}$ is given by (4.2). By Taylor expansion of the exponential $\mathrm{e}^{-i\mathbf{k}\cdot\mathbf{r}}$ to second order in $\mathbf{k}$ we obtain [34, 121, 129]

$$\mathbf{J} \approx \frac{1}{V}\int_V [1 - i\mathbf{k}\cdot\mathbf{r} - \frac{1}{2}(\mathbf{k}\cdot\mathbf{r})(\mathbf{k}\cdot\mathbf{r})]\mathbf{j}(\mathbf{r})\mathrm{d}^3 r \tag{4.22a}$$

$$= -i\omega\Big[\mathbf{P}^{\text{e}} - \frac{\mathbf{k}\times\mathbf{M}^{\text{mm}}}{\omega} - i\mathbf{k}\cdot\mathbf{Q}^{\text{e}}/2 + \mathbf{R}\Big], \tag{4.22b}$$

where we have defined

$$\mathbf{P}^{\text{e}} = \frac{1}{-i\omega V}\int_V \mathbf{j}(\mathbf{r'})\mathrm{d}^3 r' \tag{4.23a}$$

$$\mathbf{M}^{\text{mm}} = \frac{1}{2V}\int_V \mathbf{r}'\times\mathbf{j}(\mathbf{r'})\mathrm{d}^3 r' \tag{4.23b}$$

$$\mathbf{Q}^{\text{e}} = \frac{1}{-i\omega V}\int_V \Big[\mathbf{r}'\mathbf{j}(\mathbf{r}') + \mathbf{j}(\mathbf{r}')\mathbf{r}'\Big]\mathrm{d}^3 r' \tag{4.23c}$$

$$\mathbf{R} = \frac{1}{2i\omega V}\int_V (\mathbf{k}\cdot\mathbf{r}')^2\mathbf{j}(\mathbf{r'})\mathrm{d}^3 r'. \tag{4.23d}$$

To improve the accuracy of the approximation in (4.22) even higher order multipoles could be included. Expressions for the higher order terms similar to (4.23) are found by expanding $\exp(-i\mathbf{k}\cdot\mathbf{r})$ to terms of third or even higher order in $\mathbf{k}$. Alternatively we could let $\mathbf{R}$ include all higher order terms. For weakly spatially dispersive media a second order expansion is sufficient, and both definitions would give approximately the same $\mathbf{R}$.

From (4.23) explicit material parameters may be assigned to relate each multipole term to the fundamental fields $\mathbf{E}$ and $\mathbf{B}$. Also here we consider the decomposition (4.17), where we first define a permeability $\boldsymbol{\mu}_{\rm mm}$ according to

$$(\mathbf{I} - \boldsymbol{\mu}_{\rm mm}^{-1})_{im} = \varepsilon_{mkj}\frac{k_k k_l}{k^2}\nu_{ilj}, \tag{4.24}$$

where ε_{mkj} is the Levi-Civita symbol, and ν_{ilj} will be defined shortly.

The definition (4.24) is based on the discussion in Subsec. III B of Paper V . It relies on the following constitutive relation between the magnetization (4.23b) and $\mathbf{E}$:

$$M_i^{\rm mm} = \omega\zeta_{ij}E_j + \nu_{ilj}k_l E_j/(\mu_0\omega). \tag{4.25}$$

Here ζ_{ij} is a pseudo-tensor describing a magneto-electric coupling. The first order term in $\mathbf{k}$ is included to ensure that contribution $i\mathbf{k}\times\mathbf{M}^{\rm mm}$ gives a contribution up to second order in $\mathbf{k}$ to the induced current. Any dependency of $\mathbf{M}^{\rm mm}$ on $\mathbf{B}$ is described by this term, through Faraday's law $\mathbf{B} = \mathbf{k}\times\mathbf{E}/\omega$. The components of the pseudo-tensor ν_{ilj} which describe such a relation, are included in the permeability definition (4.24).

From (4.17) and (4.24) we find the corresponding permittivity function to be given by

$$\boldsymbol{\epsilon}_{\rm mm} = \boldsymbol{\epsilon}(\omega,\mathbf{k}) + \frac{c^2}{\omega^2}\mathbf{k}\times[\mathbf{I} - \boldsymbol{\mu}_{\rm mm}^{-1}]\times\mathbf{k}. \tag{4.26}$$

Note that this permittivity only becomes $\mathbf{k}$-independent if the magnetic moment density $\mathbf{M}^{\rm mm}$ in loose terms dominates the second order term of $\boldsymbol{\epsilon}(\omega,\mathbf{k})$. This permittivity also describes possible gyrotropic effects, due to a non-zero first order term in $\boldsymbol{\epsilon}(\omega,\mathbf{k})$.

In obtaining (4.22b) we have split the term $(\mathbf{k}\cdot\mathbf{r})\mathbf{j}$ from (4.22a) into a symmetric and anti-symmetric part. This gives the three first terms in the multipole decomposition (4.22b) a clear physical interpretation; as an electric polarization vector $\mathbf{P}^{\rm e}$, an electric quadrupole tensor $\mathbf{Q}^{\rm e}$, and a magnetization vector $\mathbf{M}^{\rm mm}$. In particular, $\mathbf{M}^{\rm mm}$ quantifies the amount of circulating, induced currents. The higher order term $\mathbf{R}$ could further be split into an electric octupole and a magnetic quadrupole term [34, 131][3]. The magnetic quadrupole moment could in that case be included in the magnetization $\mathbf{M}^{\rm mm}$, leading to different material parameters $\boldsymbol{\epsilon}_{\rm mm}$ and $\boldsymbol{\mu}_{\rm mm}$.

4.1.4 Vinogradov-Yaghjian (vy) decomposition

In Ref. [35] Yaghjian, Alù and Silveirinha decompose $\mathbf{J}$ into *modified* electric and magnetic polarization densities. This decomposition is based on the following *exact*

[3]Note that the magnetic quadrupole moment then could be defined in various ways [132,133], where the electric octupole moment must describe the remainder of $\mathbf{R}$.

decomposition of the microscopic induced current density into three terms [124]:

$$\mathbf{j} = -\mathbf{r}\nabla\cdot\mathbf{j} + \frac{1}{2}\nabla\times(\mathbf{r}\times\mathbf{j}) + \frac{1}{2}\nabla\cdot(\mathbf{r}\mathbf{j}+\mathbf{j}\mathbf{r}). \tag{4.27}$$

Inserting this into (4.21) we obtain

$$\mathbf{J} = -i\omega[\mathbf{P}^{\mathrm{vy}} - \frac{\mathbf{k}\times\mathbf{M}^{\mathrm{vy}}}{\omega} + i\mathbf{k}\cdot\bar{\mathbf{Q}}^{\mathrm{vy}}/2], \tag{4.28}$$

where

$$\mathbf{P}^{\mathrm{vy}} = \frac{1}{i\omega V}\int_V [\nabla\cdot\mathbf{j}(\mathbf{r}')]\mathbf{r}'\mathrm{e}^{-i\mathbf{k}\cdot\mathbf{r}'}\mathrm{d}^3r' \tag{4.29a}$$

$$\mathbf{M}^{\mathrm{vy}} = \frac{1}{2V}\int_V \mathbf{r}'\times\mathbf{j}(\mathbf{r}')\mathrm{e}^{-i\mathbf{k}\cdot\mathbf{r}'}\mathrm{d}^3r' \tag{4.29b}$$

$$\bar{\mathbf{Q}}^{\mathrm{vy}} = \frac{1}{-i\omega V}\int_V [\mathbf{r}'\mathbf{j}(\mathbf{r}') + \mathbf{j}(\mathbf{r}')\mathbf{r}']\mathrm{e}^{-i\mathbf{k}\cdot\mathbf{r}'}\mathrm{d}^3r' \tag{4.29c}$$

$$\tag{4.29d}$$

Equations (4.28) and (4.29) are similar to the corresponding expressions in the multipole expansion, i.e. (4.22b) and (4.23). There are, however, certain differences. The generalized multipoles in (4.29) contain the factor $\mathrm{e}^{-i\mathbf{k}\cdot\mathbf{r}}$ in the integrands. Also, note that the sign of the generalized quadrupole term in (4.28) is opposite of that in the conventional expansion (4.22b).

A permeability relating $\mathbf{M}^{\mathrm{vy}}$ to $\mathbf{B}$ may be defined exactly as in Subsec. 4.1.3. Similar to (4.25) we may write a constitutive relation between $\mathbf{M}^{\mathrm{vy}}$ and $\mathbf{E}$:

$$M_i^{\mathrm{vy}} = \omega\zeta_{ij}^{\mathrm{vy}}E_j + \nu_{ilj}^{\mathrm{vy}}k_lE_j/(\mu_0\omega). \tag{4.30}$$

From this relation we again define the permeability as the components of ν_{ilj}^{vy} which may relate $\mathbf{M}^{\mathrm{vy}}$ to $\mathbf{B}$:

$$(\mathbf{I} - \boldsymbol{\mu}_{\mathrm{vy}}^{-1})_{im} = \varepsilon_{mkj}\frac{k_kk_l}{k^2}\nu_{ilj}^{\mathrm{vy}}. \tag{4.31}$$

The corresponding permittivity function is again given by

$$\boldsymbol{\epsilon}_{\mathrm{vy}} = \boldsymbol{\epsilon}(\omega,\mathbf{k}) + \frac{c^2}{\omega^2}\mathbf{k}\times[\mathbf{I} - \boldsymbol{\mu}_{\mathrm{vy}}^{-1}]\times\mathbf{k}. \tag{4.32}$$

Similar to $\boldsymbol{\epsilon}_{\mathrm{mm}}$, this permittivity becomes independent of $\mathbf{k}$ if the modified magnetic moment density $\mathbf{M}^{\mathrm{vy}}$ dominates the second order term of $\boldsymbol{\epsilon}(\omega,\mathbf{k})$. Also in this decomposition the permittivity alone describes possible gyrotropic effects.

We note that in general $\boldsymbol{\mu}_{\mathrm{vy}}$ does not equal $\boldsymbol{\mu}_{\mathrm{mm}}$, due to the factor $\mathrm{e}^{-i\mathbf{k}\cdot\mathbf{r}}$ in (4.29b). For instance, it may be showed that $\boldsymbol{\mu}_{\mathrm{vy}}\to\mathbf{I}$ as $\omega\to\infty$, but in general $\boldsymbol{\mu}_{\mathrm{mm}}$ may approach a constant (which is not necessarily $\mathbf{I}$). The relation between

the terms may be further investigated by expanding the exponential inside the integral in (4.29b). To first order we get

$$\mathbf{M}^{\mathrm{vy}} = \mathbf{M}^{\mathrm{mm}} - \frac{i\mathbf{k}}{2} \cdot \mathbf{Q}^{\mathrm{m}}, \tag{4.33}$$

where we defined a magnetic quadrupole term

$$\mathbf{Q}^{\mathrm{m}} = \frac{1}{V} \int_V \mathbf{r}'[\mathbf{r}' \times \mathbf{j}(\mathbf{r}')]\mathrm{d}^3 r'. \tag{4.34}$$

This magnetic quadrupole term differs from the one used in [34]. The expansion of the exponential inside the integral in (4.29b) could in principle be done to any order in $\mathbf{k}$. Based on this expansion higher order magnetic multipoles could be defined similar to (4.34). From this it is seen that $\mathbf{M}^{\mathrm{vy}}$ may be considered as a series of carefully defined magnetic multipole terms.

4.2 Practical implications of spatial dispersion

In the above discussion an infinite periodic structure is characterized as *spatially dispersive* if the Landau-Lifshitz permittivity $\boldsymbol{\epsilon}(\omega, \mathbf{k})$ is dependent on $\mathbf{k}$. The obtained *material parameters* from the different decompositions of $\mathbf{J}$ are also called non-local if they depend on the wave vector $\mathbf{k}$, not only the frequency ω. In the following we will consider a few examples where the theoretical framework from Sec. 4.1 is applied to describe certain possible effects and properties of spatially dispersive media. For concreteness we consider non-gyrotropic media which are weakly spatially dispersive. In this case any of the permeabilities defined in Subsecs. 4.1.2-4.1.4 will be independent on $\mathbf{k}$. Further, the corresponding permittivities will not contain first order terms. They may, however, contain second order terms in $\mathbf{k}$ which are not taken care of by the permeability of the given decomposition. The permeability $\boldsymbol{\mu}_{\mathrm{tl}}$ takes care of "as much as possible" of the second order term.

However, any second order term of $\boldsymbol{\epsilon}(\omega, \mathbf{k})$ which relates $\mathbf{P}_{\mathrm{ll}}$ and *longitudinal* component of $\boldsymbol{\mathcal{E}}$ cannot be included in *any* permeability definition. This is due to the cross products applied to the tensor $\hat{\boldsymbol{\mu}}$ in (4.17), which makes any component parallel to $\mathbf{k}$ vanish. For media where $\boldsymbol{\epsilon}(\omega, \mathbf{k})$ may be decomposed into $\mathbf{k}$-independent parameters $\hat{\boldsymbol{\epsilon}}$ and $\hat{\boldsymbol{\mu}}$, the decomposition seems meaningful. The dispersion relation may for instance in some cases then be described by the well known $k = \pm\sqrt{\epsilon\mu}\omega/c$, where ϵ and μ are certain components of $\hat{\boldsymbol{\epsilon}}$ and $\hat{\boldsymbol{\mu}}$. If, on the other hand, $\hat{\boldsymbol{\epsilon}}$ depends strongly on $\mathbf{k}$, the decompositions (in the author's opinion) have limited use.

4.2.1 Importance of the electric quadrupole, or even higher order terms

In their paper from 2008, Cho et.al consider the scattering from a single unit cell consisting of two parallel metal bars of equal length [120], as shown in Fig. 4.1a. In such a structure the incident electric field can induce symmetric or anti-symmetric electron oscillations, depending on the driving frequency. For the symmetric mode the current in the two wires are parallel, while for the anti-symmetric mode the currents are anti-parallel, as shown in Fig. 4.1 b and c. By analysis of how the different multipole terms contribute to the scattering intensity spectra, they find that the contribution from the electric quadrupole term is actually comparable to that from magnetic dipole term. A schematic indicating how the two terms $\boldsymbol{\mathcal{M}}$ and $\boldsymbol{\mathcal{Q}}^{\mathrm{e}}$ contribute to the anti-symmetric mode is shown in Fig. 4.2. The schematic provides an intuitive understanding of their obtained result that the contribution from $\boldsymbol{\mathcal{Q}}^{\mathrm{e}}$ is comparable to that from $\boldsymbol{\mathcal{M}}$ to the scattering data. To describe the anti-symmetric current in terms of a magnetization $\boldsymbol{\mathcal{M}}$ one may, as the schematic shows, in addition include an electric quadrupole term $\boldsymbol{\mathcal{Q}}^{\mathrm{e}}$.

An anti-symmetric mode could also be excited due to anti-symmetric lengths of the metal bars [134, 135], rather than due to an anti-symmetric excitation as is the case in [120].

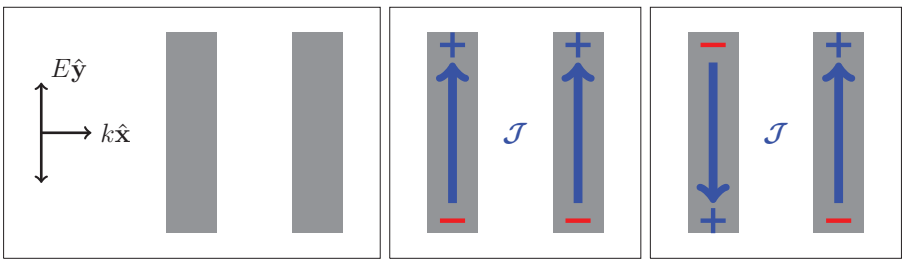

Figure 4.1: (a) An electromagnetic plane wave incident upon a single unit cell consisting of two metal bars. (b) Symmetric mode of the induced current. (c) Anti-symmetric mode of the induced currents

This suggests that for metamaterial structures, the electric quadrupole term should in general not be neglected if effects such as artificial magnetism is included in our medium description. The homogenization method from Sec. 4.1.3 allows us to quite easily include the effects from an arbitrary number of multipoles in our analysis. As we have already seen, the magnetization vector $\mathbf{M}^{\mathrm{mm}}$ in (4.23) may be

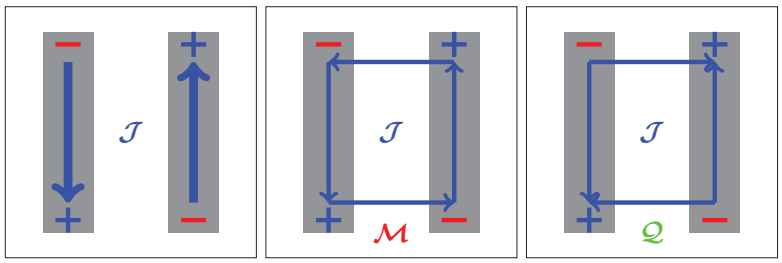

(a) (b) (c)

Figure 4.2: (a) The anti-symmetric mode of the induced currents may be written as an equal contribution from (b) a magnetic dipole and (c) an electric quadrupole. The horizontal currents in (b) and (c) will cancel, while the vertical currents will add up to the current in (a). The arrows refer to currents, and the "+" and "-" signs to the charge distributions.

considered as a second order contribution in $\mathbf{k}$ to the Landau-Lifshitz permittivity $\boldsymbol{\epsilon}(\omega, \mathbf{k})$. In Paper IV of this thesis we use this framework to demonstrate that in general also the electric quadrupole term $\mathbf{Q}^{\mathrm{e}}$, the higher order term $\mathbf{R}$, and even the electric polarization density $\mathbf{P}^{\mathrm{e}}$ all will contribute to the second order term.

To demonstrate this result we consider the response from the two bar structure in Fig. 4.1 a, but where the bars are made of a dielectric with relative permittivity $\epsilon = 16$. The contributions to the second order term from all the multipoles are shown in Fig. 4.3. We observe that the different contributions are of the same order of magnitude, but with different signs. The resulting second order term β is therefore quite small in this case, resulting in a permeability $\boldsymbol{\mu}_{\mathrm{tl}}$ very close to identity.

From the Taylor expansion of $\exp(-i\mathbf{k}\cdot\mathbf{r})$ the multipole decomposition (4.22b) is based upon, the terms with $\mathbf{M}^{\mathrm{mm}}$ and $\mathbf{Q}^{\mathrm{e}}$ are derived from the first order term in $\mathbf{k}$, while the term $\mathbf{R}$, containing the magnetic quadrupole *and* the electric octupole response, comes from the second order term. The reason all these terms still may be equally important is that in a centro-symmetric structure, an anti-symmetric electric field profile throughout the unit cell is required to excite the magnetic dipole - electric quadrupole terms. This means the multipole magnitudes themselves are first order in $\mathbf{k}$, so that the contribution from $i\mathbf{k}\times\mathbf{M}$ and $-i\mathbf{k}\cdot\mathbf{Q}^{\mathrm{e}}$ becomes of second order.

In fact, all the multipole magnitudes in (4.22b) will be $\mathbf{k}$-dependent, even the first term $-i\omega\mathbf{P}^{\mathrm{e}}$. As shown in Fig. 4.3, the second order contribution from $\mathbf{P}^{\mathrm{e}}$ in fact is in the same order of magnitude as from the other terms of the

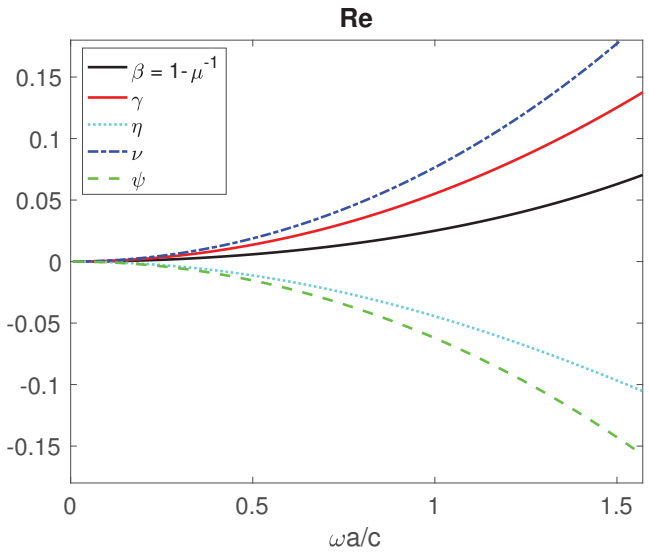

Figure 4.3: The contributions to the second order term β_{1331} of $\boldsymbol{\epsilon}(\omega, \mathbf{k})$ from the different multipoles in (4.22b). The tensor elements η, ν, γ and ψ corresponds to the contributions from $\mathbf{P}^{\mathrm{e}}, \mathbf{M}^{\mathrm{mm}}, \mathbf{Q}^{\mathrm{e}}$ and $\mathbf{R}$, respectively. The tensor element β_{1331} describes the second order contribution to the relation between the $\hat{\mathbf{y}}$-components of the total polarization density $\mathbf{P}_{\mathrm{ll}}$ and the electric field $\mathbf{E}$, when the propagation direction $\mathbf{k}$ of the plane wave is in the z-direction. In our example this is thus the most relevant tensor element of β_{iklj}.

expansion. All these four terms must thus be considered to correctly determine the total second order term in the relation (4.7) between $\mathbf{J} = -i\omega\mathbf{P}_{\mathrm{ll}}$ and $\mathbf{E}$. It was verified numerically that to second order the four terms in (4.22b) sum up to the independent calculation of the second order term in (4.8). The results from Paper IV therefore emphasize that the dipole-dipole approximation, where the $\mathbf{Q}^{\mathrm{e}}$ and $\mathbf{R}$ terms are assumed negligible, should be applied with care in the homogenization of metamaterial structures.

4.2.2 Plane wave modes in a quadrupolar continuum

The potential importance of higher order terms leads to another peculiar feature emerging from the presence of spatial dispersion in metamaterials; the fact that multiple modes may be allowed to propagate, even in an isotropic crystal. As a reference, we first consider an infinite conventional medium, where the dipole-dipole approximation is applicable. The medium is assumed to be isotropic and

passive, and is described by two parameters ϵ and μ. In such a medium the solutions to the dispersion relation are given by $k = \pm\sqrt{\epsilon\mu}\omega/c$. Since the medium is infinite, plane waves with both signs of $k(\omega)$ are allowed to propagate. In the semi-infinite case, one of these solutions must be discarded to ensure non-diverging fields, so only one plane wave mode is allowed in this case. At normal incidence this mode will be *propagating*, provided $\epsilon\mu$ is approximately real and positive.

We then move on to a the case of an infinite, isotropic quadrupolar continuum, that is a medium where all terms except for $-\omega\mathbf{k}\cdot\mathbf{Q}^{\mathrm{e}}/2$ are negligible in the multipole expansion (4.22b). We do not bother here whether such media exist, or how such a medium could be realized practically. This description could, however, work for a medium and frequency range with an electric quadrupolar resonance. In that case, the γ curve in Fig. 4.3 would be much larger than the other curves, and we would have $[1-\mu_{\mathrm{tl}}^{-1}]_{1331} = \beta_{1331} \approx \gamma$, meaning the permeability $\boldsymbol{\mu}_{\mathrm{tl}}$ is solely determined by the quadrupole term.

To describe the possible plane wave solutions which may propagate inside such a medium we need a constitutive relation between

$$\mathbf{J} = -\frac{1}{2}\omega\mathbf{k}\cdot\mathbf{Q}^{\mathrm{e}} \tag{4.35}$$

and $\mathbf{E}$ and/or $\mathbf{B}$, similar to (4.25). Such a relation is suggested in [108, 136]:

$$\mathbf{Q}^{\mathrm{e}} = \frac{\alpha_Q\epsilon_0}{2}i[\mathbf{kE}+\mathbf{Ek}] - \frac{\alpha_Q\epsilon_0}{3}i(\mathbf{k}\cdot\mathbf{E})\mathbf{I}. \tag{4.36}$$

This relation is based upon the point made in Subsec. 4.2.1, that in a symmetric structure (such as this *isotropic* medium) a quadrupolar response must be excited by the asymmetric component of the electric field profile. This suggests that the tensor $\mathbf{Q}^{\mathrm{e}}$ is proportional to the tensor $i\mathbf{kE}$ rather than just some permutations of the components of $\mathbf{E}$. In (4.36) the proportionality constant is chosen as $\alpha_Q\epsilon_0$, where α_Q has the dimensions of m^2, and the vacuum permittivity has been explicitly factored out for later convenience. This parameter is allowed to depend on the frequency ω, but is here assumed to be $\mathbf{k}$ independent. Further, the expression for $\mathbf{Q}^{\mathrm{e}}$ has been made symmetric (in accordance with our definition of $\mathbf{Q}$ in (4.23)) and traceless [32, 108, 136].

By insertion of the above constitutive relation (4.36) into (4.35), we obtain

$$\mathbf{J} = \frac{-i\omega\alpha_Q\epsilon_0}{4}[k^2\mathbf{I}+\frac{1}{3}\mathbf{kk}]\mathbf{E}. \tag{4.37}$$

Recalling that $\mathbf{P}_{\mathrm{ll}} = \mathbf{J}/(-i\omega) = \epsilon_0[\boldsymbol{\epsilon}(\omega,\mathbf{k}) - \mathbf{I}]\mathbf{E}$ the Landau-Lifshitz permittivity may be extracted directly from the above relation, and we obtain

$$\boldsymbol{\epsilon}(\omega,\mathbf{k}) = (1+\frac{\alpha_Q}{4}k^2)\mathbf{I} + \frac{\alpha_Q}{12}\mathbf{kk}. \tag{4.38}$$

Based on the constitutive relation (4.36) we thus obtain a (trivial) zeroth order term, as well as a second order term.

We now continue to find the possible plane wave modes allowed by (4.38). The possible solutions $\mathbf{k}(\omega)$ may be found from the dispersion relation (4.15). In Ref. [108] a different route to the solution is found by observing that $\mathbf{Q}^{\mathrm{e}}$ will be differently excited based on the relative directions of $\mathbf{k}$ and $\mathbf{E}$. For a given direction of $\mathbf{k}$ (could be in *any* direction, as we consider an infinite, isotropic medium), we decompose $\mathbf{E}$ in components parallel and perpendicular to $\mathbf{k}$. We then consider the potential *longitudinal* and *transversal* modes separately. For the longitudinal mode, Faraday's law (4.5a) gives $\mathbf{B}_\parallel = \mathbf{k}_\parallel \times \mathbf{E}_\parallel/\omega = 0$. Ampere's law (4.5b) then gives $\boldsymbol{\epsilon}(\omega, \mathbf{k})\mathbf{E}_\parallel = 0$, and the longitudinal solutions

$$k_\parallel = \pm i\sqrt{\frac{3}{\alpha_Q}} \tag{4.39}$$

are thus found by setting the $\mathbf{kk}$ part of (4.38) equal to 0. Note that for a longitudinal mode, $(\mathbf{k}_\parallel\mathbf{k}_\parallel)\cdot\mathbf{E}_\parallel = k_\parallel^2\mathbf{I}\cdot\mathbf{E}_\parallel$. For an approximately real[4] α_Q this mode is evanescent, and in the case of a semi-infinite medium only the solution with $\operatorname{Im} k_\parallel > 0$ may be excited due to passivity.

The wavenumber $k_\perp$ for the transversal mode on the other hand is found by combining Faraday's and Ampere's law, to obtain the well known wave equation for $\mathbf{E}_\perp$:

$$[\boldsymbol{\epsilon}(\omega, \mathbf{k}_\perp)\frac{\omega^2}{c^2} - k_\perp^2\mathbf{I}]\mathbf{E}_\perp = 0. \tag{4.40}$$

Using $\mathbf{k}_\perp \cdot \mathbf{E}_\perp = 0$ we obtain a scalar equation for $k_\perp$:

$$(1 + \frac{\alpha_Q}{4}k_\perp^2)\frac{\omega^2}{c^2} - k_\perp^2 = 0, \tag{4.41}$$

which gives the solutions

$$k_\perp = \pm\sqrt{\frac{1}{1 - \alpha_Q\omega^2/(4c^2)}}\frac{\omega}{c}. \tag{4.42}$$

For an approximately real α_Q this mode will be propagating for frequencies $\omega < c\sqrt{4/\alpha_Q}$. Again, in the case of a semi-infinite medium only one of the two solution of (4.42) may be excited due to passivity, i.e. the solution with $\operatorname{Im} k_\perp > 0$.

The above discussion shows that in an infinite, isotropic quadrupolar continuum *four modes* with $\mathbf{k} = k\hat{\mathbf{z}}$ are allowed to propagate. In the semi-infinite case the number of allowed modes is two (i.e. the two solutions $k_\parallel$ and $k_\perp$, where $\operatorname{Im} k > 0$

[4] In reality α_Q will always have *some* imaginary part, due to the presence of (potentially small) losses.

for both $k's$). To determine the reflection from such a semi-infinite medium we thus need to match the coefficients of both these modes to the coefficients of the incident and reflected fields. The standard Maxwellian boundary conditions are therefore not sufficient, and an *additional boundary condition* is required.

Boundary conditions for such a medium has been derived in Refs. [107–109,127]. In Ref. [109] these boundary conditions are used to calculate the reflection coefficient from a quadrupolar continuum. It is found that in general the evanescent mode has to be taken into account to correctly determine the reflection coefficient from such a medium. However, for sufficiently small frequencies this mode can be ignored, and the standard Maxwellian boundary conditions should be sufficient. It may be argued that the frequencies from which the evanescent mode becomes important, the quadrupole medium cannot longer be considered a continuum. In other words, for such high frequencies it is likely that terms of higher order than second order in $\mathbf{k}$ should be included in the constitutive relation (4.36), and thus in (4.38).

Whether this particular evanescent mode is physically important or not, this quadrupolar example for sure demonstrate that the possibility of several modes getting excited in weakly spatially dispersive media should be further investigated. The results in Ref. [109] could be independently verified through FDTD simulations [38], but then a method for considering quadrupolar media in such simulations must first be developed. Another possibility is to study[5] the reflection from a given metamaterial structure near a quadrupolar resonance.

4.2.3 Applicability of the obtained parameters

The homogenization method in Sec. 4.1 is appealing as it lets us calculate all constitutive parameters of an infinite periodic structure by only considering a single unit cell. Through our implementation of the FDFD method the parameters of a two dimensional structure may be obtained quite efficiently, for any desired pair of $(\omega, \mathbf{k})$. It has, however, been questioned whether the obtained parameters are of any practical use [125,126]. Some reasonable points are made in these publications, and we agree that the following two aspects therefore should be justified:

- Do the parameters describe the electromagnetic response of an *infinite* structure accurately for the parameter ranges of interest?
- Can these parameters describe the response of a semi-infinite structure accurately?

For the first bullet point it is hard to find independent verification methods, as infinite media do not exist. Some simple checks can, however, still be performed.

[5] This can be done either through time domain simulations, or actual experiments.

In most known applications of the electromagnetic parameters in photonics, electromagnetic fields propagating inside a structure are generated by a source *outside* of the structure. This means we are interested in the response from *eigenmodal* propagation, where the spatial variation of the macroscopic fields are given by the solution to the dispersion relation $\mathbf{k}_{\mathrm{B}} = \mathbf{k}(\omega)$, and not the forced $\mathbf{k}$ of the plane wave source present everywhere in our homogenization method. For the homogenized parameters for a given structure to be of any use, they should therefore be able to describe eigenmodal propagation. To substantiate a potential test for this, we present an example.

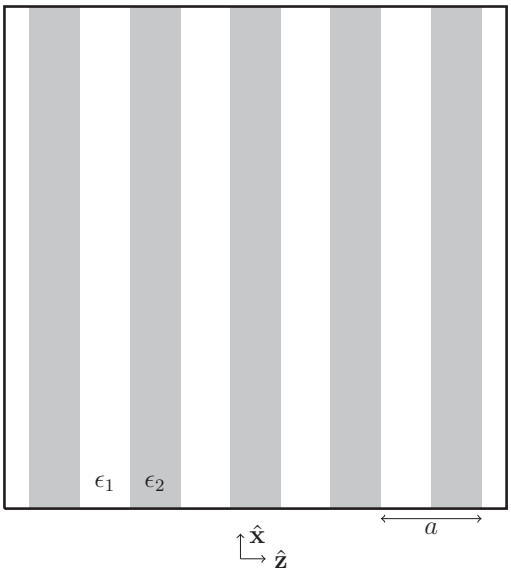

Figure 4.4: An infinite layered structure, consisting of alternating permittivities of $\epsilon_1 = 1$ and $\epsilon_2 = 31$. The thickness of the two repeating layers are $d_1 = d_2 = 0.5a$, where a is the lattice parameter of the unit cell.

For concreteness we again consider a one dimensional layered structure. The structure consists of alternating permittivities of $\epsilon_1 = 1$ and $\epsilon_2 = 31$, as shown in Fig. 4.4. The thickness of the two repeating layers are $d_1 = d_2 = 0.5a$, where a is the lattice parameter of the unit cell. As mentioned, we want to consider eigenmodal propagation inside this infinite structure. For sufficiently small frequencies such a structure may be considered as weakly spatially dispersive, and we expect (4.8) to provide an accurate description. We assume the electric field of the plane wave eigenmode is polarized along the $\hat{\mathbf{x}}$-axis, and propagates along the $\hat{\mathbf{z}}$-axis. The Bloch wavenumber k_{B} may in this simple case be calculated analytically, from

the dispersion relation [126]:

$$\cos(k_{\mathrm{B}}a) = \cos\left[(n_1d_1 + n_2d_2)\omega a/c\right] - \frac{(n_1-n_2)^2}{2n_1n_2}\sin\left(n_1d_1\omega a/c\right)\sin\left(n_2d_2\omega a/c\right). \tag{4.43}$$

To check how the parameters from our homogenization method predict eigenmodal propagation inside an infinite structure, we compare the Bloch wavenumber found from (4.43), to the wavenumbers calculated from the conventional dispersion relation $k = \sqrt{\epsilon\mu}\omega/c$. The relevant permeability tensor element from (4.19) is

$$\mu_{\mathrm{tl}} = \frac{1}{1-\beta_{1331}}. \tag{4.44}$$

The local permittivity ϵ_{11} is defined by $\epsilon_{11} = \lim_{\mathbf{k}\to 0}\boldsymbol{\epsilon}_{11}(\omega,\mathbf{k})$. In Fig. 4.5 we compare the wavenumber $k = \sqrt{\epsilon_{11}\mu_{\mathrm{tl}}}\omega/c$ to the exact solution from (4.43). We also include the corresponding wavenumbers obtained assuming only the magnetic moment term in the multipole expansion, or the generalized magnetization density in the vy-decomposition contribute to the second order term. In addition, we include the wavenumber $k = \sqrt{\epsilon_{11}}\omega/c$, which is obtained by completely ignoring the second order term. All the constitutive parameters are calculated using our FDFD program.

The second bullet point can be answered by considering how well the parameters predict the reflection from a boundary surface. The predictions may be compared to "exact solutions" obtain from e.g. time domain simulations or mode matching techniques. In very simple cases, such as an one dimensional layered structure, even analytical solutions can be found. We note that deviations between the predicted and "exact" solutions may be due to a poorly chosen prediction model, and therefore does not necessarily prove that the homogenized parameters are useless.

In Paper VI of this thesis we insert permittivities and permeabilities obtained from infinite structures in the Fresnel equation, and see how well they predict the reflection from a semi-infinite metamaterial. We consider three example structures: a 1D dielectric layered structure, a 2D metal bar structure and a 2D metallic split-ring medium. The examples show that the Fresnel coefficient predicts the reflection well only in frequency ranges where the magnetic moment density dominates the second order term of $\boldsymbol{\epsilon}(\omega,\mathbf{k})$. When this is the case all three permeabilities defined in Subsecs. 4.1.2-4.1.4 will coincide, and the dipole-dipole approximation valid in conventional media applies to our metamaterial. In this case also the conventional Maxwellian boundary conditions are valid, and all requirements of the derivation of Fresnel's equations are met [55].

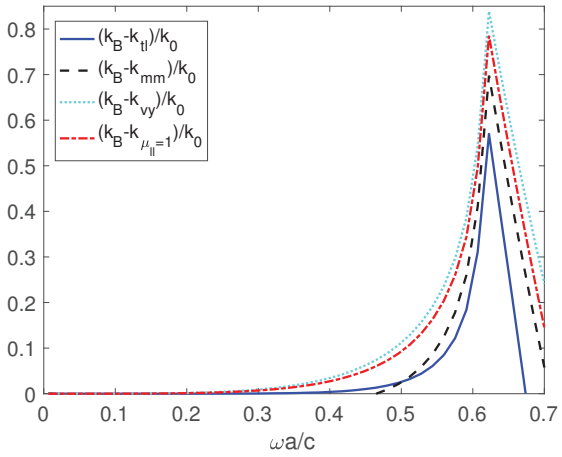

Figure 4.5: The wavenumbers $k = \sqrt{\epsilon_{11}\mu}\omega/c$ calculated using the four different permeabilities from Sec. 4.1 are compared to the actual Bloch wavenumber k_{B} of the structure, calculated from (4.43). This is done by subtracting the different wavenumbers, and dividing by $k_0 = \omega/c$. The parameters which are compared in the plot may thus be viewed as a difference in the refractive index corresponding to the different wavenumbers. It is seen that μ_{tl} gives the best approximation for $\omega a/c < 0.5$, although the deviations are in the same order of magnitude for all the four permeabilities. For $\omega a/c > 0.5$ none of the permeabilities give good match, as the weak spatial dispersion approximation no longer holds for such high frequencies. For small frequencies, $\omega a/c < 0.3$, all the permeabilities give good match, as they all are approximately 1 there.

For media and frequency ranges where the higher order multipole terms significantly contributes to the second order term, several possible explanations exist for the deviation of the reflection curves:

- The boundary conditions should be modified, leading to a different Fresnel reflection coefficient.
- More modes are excited, so even *additional* boundary conditions are required to obtain a correct reflection coefficient.
- The microscopic susceptibility $\varepsilon(\mathbf{r}) - 1$ and/or the considered frequencies are too high, so that the condition of weak spatial dispersion is not met. This means the parameters in (4.8) becomes $\mathbf{k}$-dependent.

Determining which of these points are most significant in each of the three examples in Paper VI may be the topic of a later publication.

The reflection from a semi-infinite periodic structure can always be calculated using only results calculated for an infinite structure [137]. This is done by matching the Bloch modes of the periodic metamaterial to the incident and reflected plane waves. If a modified Fresnel coefficient predics the reflection poorly, this thus means the coefficient is based on a poor selection of constitutive parameters and/or non-accurate boundary conditions.

Chapter 5

Boundary conditions for weakly spatially dispersive media

When an electromagnetic wave is incident from vacuum to a plane boundary, the Fresnel equations can often be used to calculate the reflection and transmission coefficients, provided the medium can be described by a permittivity ϵ and permeability μ. Consider a TM-polarized wave normally incident from vacuum onto a medium with electromagnetic parameters ϵ and μ. The Fresnel reflection coefficient for such a wave is given by [55]

$$r_{\mathrm{TM}} = \frac{\epsilon k_0 - k}{\epsilon k_0 + k}. \tag{5.1}$$

Here r_{TM} is defined as the ratio between the complex amplitudes of reflected and incident magnetic $\mathcal{B}$-field at the boundary. Moreover $k_0 = \omega/c$ and $k = \sqrt{\epsilon\mu}\omega/c$ are the wavenumbers in vacuum and in the medium, respectively.

In Paper VI of this thesis we consider a boundary surface between vacuum and a 2D periodic metamaterial. The metamaterial consists of square unit cells with lattice parameter a, and covers the semi-infinite region $z > 0$, extending infinitely in the x-direction. This medium is illuminated by a normally incident TM-polarized plane wave, using a source located somewhere to the left of the boundary. We are interested in the reflected fields. For simplicity we still assume that the unit cells consist of non-magnetic constituents, and that the metamaterial has a center of symmetry when viewed as an infinite periodic medium.

We consider three different metamaterial structures, and describe them by the permittivity $\epsilon = \lim_{\mathbf{k}\to 0} \boldsymbol{\epsilon}_{xx}(\omega, \mathbf{k})$, and the four permeabilities $\mu_{\mathrm{tl}}, \mu_{\mathrm{mm}}$, μ_{vy} and $\mu_{\mathrm{ll}} = 1$, which are the yy-components of the corresponding permeability tensors from Subsecs. 4.1.1-4.1.4. The examples in this paper demonstrate something important. The permeability μ_{tl} will in general make (4.17) a better approximation than any of the other permeabilities, as it includes as much as possible of the

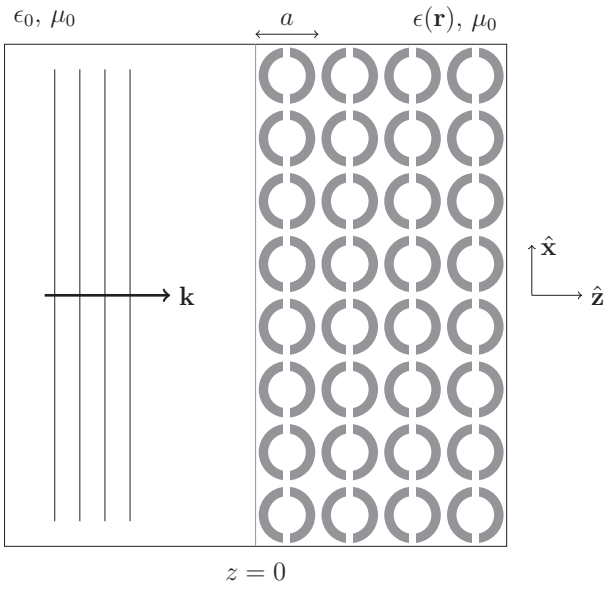

Figure 5.1: A semi-infinite 2D periodic metamaterial covers the region $z > 0$. For $z < 0$ there is vacuum. The structure is illuminated by a TM plane wave source located somewhere to the left of the boundary. The square unit cells of the metamaterial have lattice parameter a.

$\mathcal{O}(k^2)$-term. This permeability thus describes the response from an infinite layered structure the best, as was demonstrated in Subsec. 4.2.3. However, the examples in Paper VI shows that it is only if the magnetic moment density dominates the second order term, i.e. $\mu_{\text{tl}} \approx \mu_{\text{mm}}$, that we can use the Fresnel coefficient (5.1) to accurately predict the reflection from a boundary surface. When $\mu_{\text{tl}} \approx \mu_{\text{mm}}$ the dipole-dipole approximation is valid, and the boundary conditions which the Fresnel coefficient (5.1) is derived from are valid.

The permeabilities μ_{tl} and μ_{mm} will, however, not be equal for structures where any of the multipole terms $\mathbf{P}^{\text{e}}, \mathbf{Q}^{\text{e}}$ or $\mathbf{R}$ significantly contributes to the second order term of $\boldsymbol{\epsilon}(\omega, \mathbf{k})$. In situations where the spatial dispersion is responsible for the appearance of so-called additional electromagnetic waves, the conventional boundary conditions are not even sufficient to find the amplitudes of all the modes. This means an additional boundary condition (ABC) has to be used.

The problem of boundary conditions for spatially dispersive media have a long history [56, 138–141]. In this chapter we review some of the recent attempts at deriving boundary conditions to be used in the analysis of multipolar media or

spatially dispersive metamaterials [42, 107–109, 127].

5.1 Macroscopic derivation of boundary conditions

In this section we consider boundary conditions derived from a macroscopic approach. We first consider a conventional medium, where only the polarization density $\boldsymbol{\mathcal{P}}$ and the magnetization density $\boldsymbol{\mathcal{M}}$ contribute to the macroscopic response of the medium. We then use the same method to derive boundary conditions for multipolar media. In these two subsections the electric and magnetic fields, as well as the multipole terms are allowed to have jump discontinuities, but are assumed to otherwise be free of singularities at the interface. A sharp boundary is assumed, meaning the transition from vacuum ($z < 0$) to the medium under investigation ($z > 0$) happens *exactly* at the interface $z = 0$.

5.1.1 Conventional boundary conditions

As a starting point we choose to describe all charge and current densities explicitly, as was done in (2.10). Following the standard approach of integrating these equations over a pillbox/rectangular loop across the interface $z = 0$ we obtain

$$\epsilon_0(\boldsymbol{\mathcal{E}}_{2\mathrm{n}} - \boldsymbol{\mathcal{E}}_{1\mathrm{n}}) = \rho_{\mathrm{ext,s}} + \rho_{\mathrm{s}}, \tag{5.2a}$$

$$\boldsymbol{\mathcal{B}}_{2\mathrm{n}} - \boldsymbol{\mathcal{B}}_{1\mathrm{n}} = 0, \tag{5.2b}$$

$$\boldsymbol{\mathcal{E}}_{2\mathrm{t}} - \boldsymbol{\mathcal{E}}_{1\mathrm{t}} = 0, \tag{5.2c}$$

$$\frac{1}{\mu_0}(\boldsymbol{\mathcal{B}}_{2\mathrm{t}} - \boldsymbol{\mathcal{B}}_{1\mathrm{t}}) = -\hat{\mathbf{z}} \times [\boldsymbol{\mathcal{J}}_{\mathrm{ext,s}} + \boldsymbol{\mathcal{J}}_{\mathrm{s}}]. \tag{5.2d}$$

Here the subscripts 1 and 2 refer to the fields evaluated just to the left and right of the boundary $z = 0$, respectively. The subscripts "t" and "n" refers to the transversal and longitudinal components of the fields, with respect to the boundary surface at $z = 0$. The surface charge and current densities $\rho_{\mathrm{ext,s}}, \rho_{\mathrm{s}}, \boldsymbol{\mathcal{J}}_{\mathrm{ext,s}}$, and $\boldsymbol{\mathcal{J}}_{\mathrm{s}}$ will be defined in the following.

In obtaining (5.2) we assumed the fields $\boldsymbol{\mathcal{E}}$ and $\boldsymbol{\mathcal{B}}$ to be sectionally continuous, and free of singularities at the interface $z = 0$ [142]. The macroscopic charge and current densities on the other hand are allowed to be singular, represented by the *surface* charge and current densities on the right hand sides of (5.2a) and (5.2d). For later convenience we *define* the induced surface current density as

$$\boldsymbol{\mathcal{J}}_{\mathrm{s}} = \int_0^l \boldsymbol{\mathcal{J}}_0 \mathrm{d}z, \tag{5.3}$$

where $\boldsymbol{\mathcal{J}}_0(z)$ is the induced current density that is valid throughout space. That is, $\boldsymbol{\mathcal{J}}_0 = 0$ for $z < 0$, while $\boldsymbol{\mathcal{J}}_0 = \boldsymbol{\mathcal{J}}$ for $z > 0$.

The upper integration limit l in general is the thickness of a transition layer, which in this sharp medium model may be chosen arbitrarily small. In this and the following subsection the integration $\int_0^h \mathrm{d}z$ may thus be considered as "integration over some infinitesimal small region containing $z = 0$". The surface charge density $\boldsymbol{\mathcal{J}}_{\text{ext,s}}$, and the surface charge densities ρ_{s} and $\rho_{\text{ext,s}}$ are defined similarly.

To obtain the conventional form of the boundary conditions (5.2), these surface charge and current densities are expressed in terms of the multipole densities of the medium inside the half space $z > 0$. Let $\boldsymbol{\mathcal{P}}_0(\mathbf{r})$ and $\boldsymbol{\mathcal{M}}_0(\mathbf{r})$ be the polarization and magnetization densities that are valid throughout all space. We now assume these quantities may be expressed according to

$$\boldsymbol{\mathcal{P}}_0(\mathbf{r}) = u(z)\boldsymbol{\mathcal{P}}, \tag{5.4a}$$
$$\boldsymbol{\mathcal{M}}_0(\mathbf{r}) = u(z)\boldsymbol{\mathcal{M}}, \tag{5.4b}$$

where $u(z)$ is the unit step function, which takes the values 1 for $z > 0$ and 0 for $z < 0$. To the left of the boundary there is vacuum, so $\boldsymbol{\mathcal{P}}_0(\mathbf{r}) = \boldsymbol{\mathcal{M}}_0(\mathbf{r}) = 0$. Inside the medium on the other hand, the polarization and magnetization will take their bulk values $\boldsymbol{\mathcal{P}}$ and $\boldsymbol{\mathcal{M}}$. We assume these quantities are continuous through $z = 0$.

If we insert the two relations from (5.4) in (2.11) we obtain an expression for the induced current density $\boldsymbol{\mathcal{J}}_0(\mathbf{r})$ valid throughout all space:

$$\boldsymbol{\mathcal{J}}_0(\mathbf{r}) = u(z)[-i\omega\boldsymbol{\mathcal{P}} + \nabla \times \boldsymbol{\mathcal{M}}] + \delta(z)\hat{\mathbf{z}} \times \boldsymbol{\mathcal{M}}. \tag{5.5}$$

Here $\delta(z) = u'(z)$ is the Dirac delta function. Note that $\delta(z)$ is a distribution, and not a regular function.

By inserting (5.5) into (5.3) we find $\boldsymbol{\mathcal{J}}_{\text{s}} = \hat{\mathbf{z}} \times \boldsymbol{\mathcal{M}}$. The corresponding induced charge density $\rho_0(\mathbf{r})$ valid throughout all space is found through the law of charge conservation,

$$\rho_0 = \frac{\nabla \cdot \boldsymbol{\mathcal{J}}_0}{i\omega} = -\nabla \cdot \boldsymbol{\mathcal{P}}_0 = -u(z)\nabla \cdot \boldsymbol{\mathcal{P}} - \delta(z)\boldsymbol{\mathcal{P}}_z, \tag{5.6}$$

where $\boldsymbol{\mathcal{P}}_z$ is the z component of the bulk polarization density inside the medium.

Inserting (5.6) into the definition of ρ_{s} corresponding to (5.3) we find $\rho_{\text{s}} = -\boldsymbol{\mathcal{P}}_z$. Insertion of the obtained relations in (5.2) then gives

$$\boldsymbol{\mathcal{D}}_{2\text{n}} - \boldsymbol{\mathcal{D}}_{1\text{n}} = \rho_{\text{ext,s}}, \tag{5.7a}$$
$$\boldsymbol{\mathcal{B}}_{2\text{n}} - \boldsymbol{\mathcal{B}}_{1\text{n}} = 0, \tag{5.7b}$$
$$\boldsymbol{\mathcal{E}}_{2\text{t}} - \boldsymbol{\mathcal{E}}_{1\text{t}} = 0, \tag{5.7c}$$
$$\boldsymbol{\mathcal{H}}_{2\text{t}} - \boldsymbol{\mathcal{H}}_{1\text{t}} = -\hat{\mathbf{z}} \times \boldsymbol{\mathcal{J}}_{\text{ext,s}}, \tag{5.7d}$$

where we have defined the fields $\boldsymbol{\mathcal{D}} = \epsilon_0\boldsymbol{\mathcal{E}} + \boldsymbol{\mathcal{P}}_0$ and $\boldsymbol{\mathcal{H}} = \boldsymbol{\mathcal{B}}/\mu_0 - \boldsymbol{\mathcal{M}}_0$. In obtaining (5.7d) we used $-\hat{\mathbf{z}} \times \hat{\mathbf{z}} \times \boldsymbol{\mathcal{M}} = \boldsymbol{\mathcal{M}}_{2\mathrm{t}}$, where $\boldsymbol{\mathcal{M}}_{2\mathrm{t}}$ is the tangential component of the magnetization density, evaluated just to the right of the boundary at $z = 0$.

This concludes our derivation of the conventional boundary conditions. The above relations state that in the absence of external surface charge and current density at $z = 0$, the normal components of the fields $\boldsymbol{\mathcal{B}}$ and $\boldsymbol{\mathcal{D}}$, as well as the tangential components of the fields $\boldsymbol{\mathcal{E}}$ and $\boldsymbol{\mathcal{H}}$, are continuous across a boundary surface. The conventional Fresnel equations are based upon these two tangential continuity conditions.

5.1.2 Boundary conditions for a multipolar medium, with a sharp boundary model

By including also the electric quadrupole term in our medium model, the bulk induced current density may be expressed similar to (5.5) [42, 107]:

$$\begin{aligned}\boldsymbol{\mathcal{J}}_0 = &-i\omega[\boldsymbol{\mathcal{P}}_0 - \frac{1}{2}\nabla\cdot\boldsymbol{\mathcal{Q}}^{\mathrm{e}}_0] + \nabla\times\boldsymbol{\mathcal{M}}_0 \\ &u(z)[-i\omega\boldsymbol{\mathcal{P}} + \frac{i\omega}{2}\nabla\cdot\boldsymbol{\mathcal{Q}}^{\mathrm{e}} + \nabla\times\boldsymbol{\mathcal{M}}] \\ &+ \delta(z)[\hat{\mathbf{z}}\times\boldsymbol{\mathcal{M}} + \frac{i\omega}{2}\hat{\mathbf{z}}\cdot\boldsymbol{\mathcal{Q}}^{\mathrm{e}}].\end{aligned} \tag{5.8}$$

In comparison to the multipole expansion in Subsec. 4.1.3, the multipoles are here expressed in the spatial domain, and we have assumed the $\boldsymbol{\mathcal{R}}$ term (containing the magnetic quadrupole and electric octupole terms) is negligible. We can now calculate $\boldsymbol{\mathcal{J}}_{\mathrm{s}}$ using (5.3), and we find

$$\boldsymbol{\mathcal{J}}_{\mathrm{s}} = \hat{\mathbf{z}}\times\boldsymbol{\mathcal{M}} + \frac{i\omega}{2}\hat{\mathbf{z}}\cdot\boldsymbol{\mathcal{Q}}^{\mathrm{e}}. \tag{5.9}$$

The induced charge density is then calculated similarly to (5.6):

$$\begin{aligned}\rho_0 = \frac{\nabla\cdot\boldsymbol{\mathcal{J}}_0}{i\omega} = -\nabla\cdot[\boldsymbol{\mathcal{P}}_0 - \frac{1}{2}\nabla\cdot\boldsymbol{\mathcal{Q}}^{\mathrm{e}}_0] = -u(z)[\nabla\cdot\boldsymbol{\mathcal{P}} - \frac{1}{2}\nabla\cdot\nabla\cdot\boldsymbol{\mathcal{Q}}^{\mathrm{e}}] \\ - \delta(z)[\boldsymbol{\mathcal{P}}_z - (\nabla_{\mathrm{t}}\cdot\boldsymbol{\mathcal{Q}}^{\mathrm{e}})_z] + \frac{1}{2}\nabla_z\Big(\nabla_z[u(z)\mathcal{Q}^{\mathrm{e}}_{2,zz}]\Big).\end{aligned} \tag{5.10}$$

The definition (5.3) then gives

$$\rho_{\mathrm{s}} = -\boldsymbol{\mathcal{P}}_z + \nabla_{\mathrm{t}}\cdot(\hat{\mathbf{z}}\cdot\boldsymbol{\mathcal{Q}}^{\mathrm{e}}) + \frac{1}{2}\nabla_z\mathcal{Q}^{\mathrm{e}}_{2,zz}, \tag{5.11}$$

where we used the fundamental theorem of calculus to calculate the integral of the last term in (5.6). Using (5.11) and (5.9) in (5.2) we obtain the boundary conditions for a multipolar medium to electric quadrupole - magnetic dipole order:

$$\boldsymbol{\mathcal{E}}_{2\mathrm{n}} - \boldsymbol{\mathcal{E}}_{1\mathrm{n}} = -\boldsymbol{\mathcal{P}}_{2\mathrm{n}} + \nabla_{\mathrm{t}} \cdot (\hat{\mathbf{z}} \cdot \boldsymbol{\mathcal{Q}}^{\mathrm{e}}) + \frac{1}{2}\nabla_z \mathcal{Q}^{\mathrm{e}}_{2,zz}, \tag{5.12a}$$

$$\boldsymbol{\mathcal{B}}_{2\mathrm{n}} - \boldsymbol{\mathcal{E}}_{1\mathrm{n}} = 0, \tag{5.12b}$$

$$\boldsymbol{\mathcal{E}}_{2\mathrm{t}} - \boldsymbol{\mathcal{E}}_{1\mathrm{t}} = 0, \tag{5.12c}$$

$$\boldsymbol{\mathcal{B}}_{2\mathrm{t}} - \boldsymbol{\mathcal{B}}_{1\mathrm{t}} = -\hat{\mathbf{z}} \times [\hat{\mathbf{z}} \times \boldsymbol{\mathcal{M}} + \frac{i\omega}{2}\hat{\mathbf{z}} \cdot \boldsymbol{\mathcal{Q}}^{\mathrm{e}}]. \tag{5.12d}$$

We have here set $\rho_{\mathrm{ext,s}} = \boldsymbol{\mathcal{J}}_{\mathrm{ext,s}} = 0$, which is often the case in practical situations.

In a quadrupolar medium an additional mode may propagate (see Subsec. 4.2.2), and the above conditions are therefore not sufficient for solving boundary problems. An additional boundary condition is found from insertion of $\boldsymbol{\mathcal{J}}_0$ given by (5.8) as the induced current in Ampere's law (2.10d). Integration of the z component of this equation across the boundary surface gives

$$[\hat{\mathbf{z}} \times \boldsymbol{\mathcal{M}} + \frac{i\omega}{2}\hat{\mathbf{z}} \cdot \boldsymbol{\mathcal{Q}}^{\mathrm{e}}]_z = 0. \tag{5.13}$$

The assumption that none of the fields or multipole densities have singularities at $z = 0$ ensures that the integral of all terms in (5.8) equal zero, except the term containing $\delta(z)$. The first term in (5.8) is zero, since $\hat{\mathbf{z}} \times \boldsymbol{\mathcal{M}}$ is perpendicular to z. We thus arrive at the boundary condition

$$\boldsymbol{\mathcal{Q}}^{\mathrm{e}}_{0,zz} = 0. \tag{5.14}$$

From the assumption of no singularities in $\mathcal{E}_z$ this is essentially the same as (10) in Ref. [143], where $\mathbf{P}^{\delta}$ refers to the potential singular terms in the "total polarization density", which in our case corresponds to $\boldsymbol{\mathcal{P}}_0 - \frac{1}{2}\nabla \cdot \boldsymbol{\mathcal{Q}}^{\mathrm{e}}_0$. The only potential singular term at $z = 0$ is due to the differentiation of the discontinuity of $\boldsymbol{\mathcal{Q}}^{\mathrm{e}}_0$, which is defined similar as $\boldsymbol{\mathcal{P}}_0$ and $\boldsymbol{\mathcal{M}}_0$ in (5.4).

Defining $\boldsymbol{\mathcal{D}} = \epsilon_0\boldsymbol{\mathcal{E}} + \boldsymbol{\mathcal{P}}_0 - \nabla \cdot \boldsymbol{\mathcal{Q}}^{\mathrm{e}}_0/2$ and $\boldsymbol{\mathcal{H}} = \boldsymbol{\mathcal{B}}/\mu_0 - \boldsymbol{\mathcal{M}}_0$, the above conditions may be rewritten as

$$\boldsymbol{\mathcal{D}}_{2\mathrm{n}} - \boldsymbol{\mathcal{D}}_{1\mathrm{n}} = \frac{1}{2}\nabla_{\mathrm{t}} \cdot (\hat{\mathbf{z}} \cdot \boldsymbol{\mathcal{Q}}^{\mathrm{e}}), \tag{5.15a}$$

$$\boldsymbol{\mathcal{B}}_{2\mathrm{n}} - \boldsymbol{\mathcal{B}}_{1\mathrm{n}} = 0, \tag{5.15b}$$

$$\boldsymbol{\mathcal{E}}_{2\mathrm{t}} - \boldsymbol{\mathcal{E}}_{1\mathrm{t}} = 0, \tag{5.15c}$$

$$\boldsymbol{\mathcal{H}}_{2\mathrm{t}} - \boldsymbol{\mathcal{H}}_{1\mathrm{t}} = -\frac{i\omega}{2}\hat{\mathbf{z}} \times [\hat{\mathbf{z}} \cdot \boldsymbol{\mathcal{Q}}^{\mathrm{e}}], \tag{5.15d}$$

$$\mathcal{Q}^{\mathrm{e}}_{2,zz} = 0. \tag{5.15e}$$

The first four boundary conditions above are the same as those found in Ref. [107], and the same conditions were verified in Ref. [108]. In Ref. [108] a transition layer of thickness δ was considered, but the assumption of non-singular fields and multipoles was used in both these publications. In Ref. [108] the additional boundary condition (5.15e) was stated explicitly, although as seen from the above discussion this discussion follows directly from the assumption of fields and multipole densities with potential jump discontinuities, but which are otherwise free of singularities at $z = 0$. We note that in Refs. [107,108] the right hand side of (5.15c) is given as $\frac{1}{2}\nabla_{\mathrm{t}} \cdot \mathcal{Q}^{\mathrm{e}}_{2,zz}$, but after obtaining (5.15e) it is seen that continiuty of $\boldsymbol{\mathcal{E}}_{\mathrm{t}}$ is ensured also in the presence of a quadrupolar response.

The boundary conditions (5.15) were also derived in Refs. [109,127]. In Ref. [127] a completely different approach than the above derivation is used. The derivation relates *transverse* averaged fields to the bulk fields by making use of Green function formalism [144]. Also here the additional boundary condition (5.15e) is found by assuming non-singular fields and multipole densities at the boundary surface.

In Ref. [109] a *transition layer* of thickness l is introduced, where the electromagnetic properties gradually change from those of free space to those of the electric quadrupolar continuum. This is done to get a better understanding of the field behavior at the interface. An explicit expression for the electric quadrupolarization density $\boldsymbol{\mathcal{Q}}^{\mathrm{e}}_0$ is assumed to be valid throughout the transition layer. The electric field is initially assumed to contain singular terms, but it is later shown that under certain assumptions all these singular terms must be zero.

5.2 Fresnel's equations for a quadrupolar continuum

Following the standard procedure, we now derive Fresnel's equations for a TM polarized plane wave incident from vacuum upon a semi-infinite quadrupolar continuum. The procedure below can be straightforwardly modified to be valid for any nongyrotropic, isotropic medium where the second order contribution of $\boldsymbol{\epsilon}(\omega, \mathbf{k})$ may be written on the form $ak^2\mathbf{I}_\perp + b\mathbf{kk}$. For such media the only second order term which may not be described by $(1 - \boldsymbol{\mu}^{-1}_{\mathrm{tl}})$ is the second order contribution to $\boldsymbol{\epsilon}_{zz}(\omega, \mathbf{k})$, in a coordinate system where $\mathbf{k} = k\hat{\mathbf{z}}$ [56].

The electric field in vacuum is a superposition of two plane waves; the incident (i) and reflected (r) waves. Inside the quadrupole continuum, there are also two modes (according to Subsec. 4.2.2): a propagating transmitted (t) wave, and an evanescent (e) longitudinal wave. The electric and magnetic fields of these four modes are given as $\boldsymbol{\mathcal{E}}_m = [\mathcal{E}_{mx}, 0, \mathcal{E}_{mz}]$ for $m =$ i,r,t and e, while the magnetic field is given by $\boldsymbol{\mathcal{B}}_m = \mathcal{B}_m\hat{\mathbf{y}}$ for $m =$ i, r and t. From Faraday's law we get that there

is no evanescent $\boldsymbol{\mathcal{B}}_\mathrm{e}$-field, as $\mathbf{k}_\mathrm{e} \times \boldsymbol{\mathcal{E}}_\mathrm{e} = 0$.

All field components will propagate according to $\mathrm{e}^{i\mathbf{k}\cdot\mathbf{r}}$, but with different wave vectors $\mathbf{k}$. The x component of the wave vector $k_x = \mathbf{k}\cdot\hat{\mathbf{x}}$ will be the same for all waves. The z components of the vacuum waves are given by $k_{\mathrm{i}z} = k_{1z} = \sqrt{\omega^2/c^2 - k_x^2}$ and $k_{\mathrm{r}z} = -k_{1z}$. The z components of the two waves in the quadrupolar continuum are found from Subsec. 4.2.2, where $k_{\mathrm{t}z} = k_{2z}$ is given by (4.42) and $k_{\mathrm{e}z}$ is given by (4.39).

The boundary condition (5.15c) gives that

$$\mathcal{E}_{\mathrm{i}x} + \mathcal{E}_{\mathrm{r}x} = \mathcal{E}_{\mathrm{t}x} + \mathcal{E}_{\mathrm{e}x}. \tag{5.16}$$

Similarly (5.15d) gives

$$\mathcal{B}_\mathrm{t} = \mathcal{B}_\mathrm{i} - \mathcal{B}_\mathrm{r} - \frac{i\omega\mu_0}{2}[\hat{\mathbf{z}} \times (\hat{\mathbf{z}}\cdot\boldsymbol{\mathcal{Q}}_\mathrm{t} + \hat{\mathbf{z}}\cdot\boldsymbol{\mathcal{Q}}_\mathrm{e})]\cdot\hat{\mathbf{y}}, \tag{5.17}$$

since $\boldsymbol{\mathcal{M}} = 0$ in a pure quadrupolar continuum. Here $\boldsymbol{\mathcal{Q}}_\mathrm{t}$ and $\boldsymbol{\mathcal{Q}}_\mathrm{e}$ are the quadrupole density of the transmitted and the evanescent modes, respectively. The additional boundary condition (5.15e) becomes:

$$\hat{\mathbf{z}}\cdot(\boldsymbol{\mathcal{Q}}_\mathrm{t} + \boldsymbol{\mathcal{Q}}_\mathrm{e})\cdot\hat{\mathbf{z}} = 0. \tag{5.18}$$

The different pairs of $\boldsymbol{\mathcal{E}}$- and $\boldsymbol{\mathcal{B}}$-fields must satisfy Maxwell's equations in each medium separately. From Faraday's law we have for the four modes:

$$k_x\mathcal{E}_{\mathrm{i}z} - k_{1z}\mathcal{E}_{\mathrm{i}x} = i\omega\mathcal{B}_\mathrm{i}, \tag{5.19a}$$
$$k_x\mathcal{E}_{\mathrm{r}z} + k_{1z}\mathcal{E}_{\mathrm{r}x} = i\omega\mathcal{B}_\mathrm{r}, \tag{5.19b}$$
$$k_x\mathcal{E}_{\mathrm{t}z} - k_{2z}\mathcal{E}_{\mathrm{t}x} = i\omega\mathcal{B}_\mathrm{t}, \tag{5.19c}$$
$$k_x\mathcal{E}_{\mathrm{e}z} - k_{\mathrm{e}z}\mathcal{E}_{\mathrm{e}x} = 0, \tag{5.19d}$$

Moreover, from Gauss' law for the three propagating modes we have

$$\mathbf{k}_\mathrm{i}\cdot\boldsymbol{\mathcal{E}}_\mathrm{i} = k_x\mathcal{E}_{\mathrm{i}x} + k_{1z}\mathcal{E}_{\mathrm{i}z} = 0, \tag{5.20a}$$
$$\mathbf{k}_\mathrm{r}\cdot\boldsymbol{\mathcal{E}}_\mathrm{r} = k_x\mathcal{E}_{\mathrm{r}x} - k_{1z}\mathcal{E}_{\mathrm{r}z} = 0, \tag{5.20b}$$
$$\mathbf{k}_\mathrm{t}\cdot\boldsymbol{\mathcal{E}}_\mathrm{t} = k_x\mathcal{E}_{\mathrm{t}x} + k_{2z}\mathcal{E}_{\mathrm{t}z} = 0. \tag{5.20c}$$

The boundary condition (5.18), combined with the above equations, relates $\mathcal{E}_{\mathrm{e}x}$ and $\mathcal{E}_{\mathrm{t}z}$:

$$k_{2z}\mathcal{E}_{\mathrm{t}z} + \frac{2}{3}k_{\mathrm{e}z}\mathcal{E}_{\mathrm{e}z} - \frac{1}{3}k_x\mathcal{E}_{\mathrm{e}x} = 0, \tag{5.21}$$

which again may be related to $\mathcal{B}_\mathrm{t}$ through Maxwell's equations.

By combining (5.16), (5.17),(5.19),(5.20) and (5.21) we find two expressions relating $\mathcal{B}_\mathrm{i}, \mathcal{B}_\mathrm{r}$ and $\mathcal{B}_\mathrm{t}$, which allows us to define reflection and transmission coefficients for the $\boldsymbol{\mathcal{B}}$-field:

$$r_\mathcal{B} = \frac{\mathcal{B}_\mathrm{r}}{\mathcal{B}_\mathrm{i}} = \frac{f-g}{f+g}, \tag{5.22}$$

and

$$t_\mathcal{B} = \frac{\mathcal{B}_\mathrm{t}}{\mathcal{B}_\mathrm{i}} = \frac{2}{f+g}. \tag{5.23}$$

We here defined

$$f = \frac{k_{2z}}{k_{1z}} \frac{1-\alpha_Q\omega^2/(4c^2)}{1+\frac{\alpha_Q}{2}k_x^2}, \tag{5.24}$$

and

$$g = \frac{1-\alpha_Q\omega^2/(4c^2)}{1+\alpha_Q k_x^2/2}[1+\frac{1}{2}\alpha_Q k_x^2(2+\frac{1}{2}\alpha_Q\{k_x^2+k_{\mathrm{e}z}k_{2z}\})]. \tag{5.25}$$

Since all components of the $\boldsymbol{\mathcal{E}}$-fields may be expressed through the $\boldsymbol{\mathcal{B}}$-fields, we may also define tensors $\mathbf{r}_E, \mathbf{t}_E$ and $\mathbf{e}_E$, which relate the amplitudes of the reflected, transmitted and evanescent electric field components to the components of the incident electric field.

5.3 Poynting's vector

A natural first check of the validity of the Fresnel equations above is to verify that the normal component of Poynting's vector is continuous across the boundary surface. Poynting's vector, $\boldsymbol{\mathcal{S}}$, inside a spatially dispersive medium is given by (103.15) in [55]:

$$\mathcal{S}_k = \frac{1}{2\mu_0}\mathrm{Re}\,\{\epsilon_{ijk}\mathcal{E}_j^*\mathcal{B}_k\} - \frac{\epsilon_0\omega}{4}\frac{\partial\boldsymbol{\epsilon}_{ij}}{\partial k_k}\mathcal{E}_i^*\mathcal{E}_j, \tag{5.26}$$

where $\boldsymbol{\epsilon}_{ij} = \boldsymbol{\epsilon}_{ij}(\omega, \mathbf{k})$ is the Landau-Lifshitz permittivity function for the given medium. In the quadrupolar continuum this function in given by (4.38). Calculating the derivative wrt. k_k of this function gives

$$\frac{\partial\boldsymbol{\epsilon}_{ij}}{\partial k_k} = \frac{\alpha_Q}{4}[2\delta_{ij}k_l\frac{\partial k_l}{\partial k_k} + \frac{1}{3}(\frac{\partial k_i}{\partial k_k}k_j + k_i\frac{\partial k_j}{\partial k_k})], \tag{5.27}$$

which is a tensor of rank 3. Using the relation $\frac{\partial k_\alpha}{\partial k_\beta} = \delta_{\alpha\beta}$ this becomes

$$\frac{\partial\boldsymbol{\epsilon}_{ij}}{\partial k_k} = \frac{\alpha_Q}{2}[\delta_{ij}k_k + \frac{1}{6}(\delta_{ik}k_j + k_i\delta_{jk})]. \tag{5.28}$$

Only the propagating mode $\boldsymbol{\mathcal{E}}_\mathrm{t}$ will contribute to the Poynting vector. Insertion of expressions for $\boldsymbol{\mathcal{E}}_\mathrm{t}$, $\mathcal{B}_\mathrm{t}$ and (5.28) gives after some algebra

$$\boldsymbol{\mathcal{S}}_{\mathrm{t}} = \frac{c^2}{2\mu_0\omega}\Big(1 - \alpha_Q\omega^2/(4c^2)\Big)^2 |\mathcal{B}_{\mathrm{t}}|^2 \mathbf{k}_{\mathrm{t}}. \tag{5.29}$$

In particular, the normal component is given by

$$\mathcal{S}_{2z} = \frac{c^2}{2\mu_0\omega}\Big(1 - \alpha_Q\omega^2/(4c^2)\Big)^2 |\mathcal{B}_{\mathrm{t}}|^2 k_{2z}. \tag{5.30}$$

For frequencies $\omega^2/c^2 > 4/\alpha_Q$ we have $\boldsymbol{\mathcal{S}}_{\mathrm{t}} = 0$, as $\boldsymbol{\mathcal{E}}_{\mathrm{t}}$ then is evanescent.

A similar expression is found for the normal component of Poynting's vector for $z < 0$, where the contributions from both the incident and reflected waves must be summed up:

$$\mathcal{S}_{1z} = \frac{c^2}{2\mu_0\omega}(1 - |r_{\mathcal{B}}|^2)|\mathcal{B}_{\mathrm{i}}|^2 k_{1z}. \tag{5.31}$$

Due to energy conservation the normal component of Poynting's vector should be continuous. Setting (5.30) equal to (5.31), and using $\mathcal{B}_{\mathrm{t}} = t_{\mathcal{B}}\mathcal{B}_{\mathrm{i}}$ we obtain that the following equation should be satisfied

$$1 - |r_{\mathcal{B}}|^2 = \left[\frac{k_{2z}}{k_{1z}}(1 - \frac{\alpha_Q\omega^2}{4c^2})\right]^2 |t_{\mathcal{B}}|^2. \tag{5.32}$$

It can be checked numerically that this is correct to within computer accuracy.

Chapter 6

Summary and future work

6.1 Summary

Active and passive metamaterials have the potential of exploiting extraordinary electromagnetic properties. It therefore becomes important to develop an accurate theoretical framework which can be used to analyze such media and structures. The papers of this thesis contribute in various ways to do so along the lines of Fourier-Laplace analysis and homogenization theory.

Paper I presents a Fourier-Laplace framework which may be used to describe the response of active media or metamaterials in terms of (possibly complex) frequency and wavenumber components. By considering a causal source of finite width, the paper demonstrates the important fact that a monochromatic plane wave analysis of such media should be applied with care. The monochromatic plane wave limit does not necessarily exist due to the possible presence of instabilities, and it is found that in general the monochromatic limit and plane wave limit do not commute. For example, one order may lead to a diverging field, while the other leads to a finite field. Moreover, the plane-wave limit may be dependent on whether it is realized with a finite-support excitation or a Gaussian excitation, eventually of infinite widths. The framework is used to analyze examples of media with weak and strong gain. In particular it is used to predict the existence of *isotropic* media which in principle exhibit simultaneous refraction, meaning they refract positively and negatively at the same time.

Paper II applies the framework from Paper I in the analysis of a gainy slab. Even for the case with a weakly amplifying slab that does not lase, it is necessary to involve complex frequencies ω and/or complex transversal wavenumbers k_x. We also show that the only possibility to have an absolute instability for a finite width beam is if a normally incident plane wave would experience an instability.

Paper III considers the well known fact that a monochromatic wave propagates

with a different wavelength inside a medium compared to in vacuum. Instead of the standard procedure of describing the induced charge and current as *bound*, and therefore absorb them into a refractive index, we here rather treat the medium as vacuum, but with explicit charge and current densities. However, since the induced waves propagate in vacuum in this picture, it is not straightforward to reconcile that the wavelength becomes different to that in vacuum. Although the main purpose of the paper is educational, the analysis also has relevance in the context of this thesis. It reminds us that in Maxwell's equations the fundamental electromagnetic fields are invariant upon how we chose to describe the induced current.

Papers IV, V and VI are concerned with the consequences of spatial dispersion on the effective parameters. Paper IV demonstrates that certain higher order multipole terms, above the electric quadrupole, are generally as important as the magnetic dipole and electric quadrupole terms when second order spatially dispersive effects are considered. Based on this discovery, Paper V deals with the concern of how one should define the permeability of spatially dispersive media. In particular, four different definitions of the permeability are stated and compared. General properties are discussed, including causality, passivity, symmetry, asymptotic behavior, and origin dependence.

In Paper VI these four permeabilities are paired with a local permittivity defined as the zeroth order contribution to $\boldsymbol{\epsilon}(\omega, \mathbf{k})$, and the predictive power of these four sets of local parameters is tested. This is done by calculating the Fresnel reflection coefficient, and comparing the four predictions with the *true* solution obtained through finite difference time domain simulations. It is found that the Fresnel coefficient predicts the reflection well only in regimes where the three non-trivial permeabilities coincide. One potential explanation is that when considering media where the dipole-dipole approximation does not hold, the boundary conditions should be modified, and the conventional Fresnel's equations are not valid. It may also be that a non-local contribution is lost when we choose describing the medium response by two local parameters. Even another option is that multiple modes are excited, so even additional boundary conditions may be required. Finally, for a sufficiently large microscopic permittivity $\varepsilon(\mathbf{r}) - 1$ and/or frequency ω, the long wavelength limit $ka \ll 1$ will no longer hold, and higher order terms will contribute significantly to $\boldsymbol{\epsilon}(\omega, \mathbf{k})$. Which of these four explanations that dominates the poor reflection predictions is not discussed in the paper. We do however demonstrate another, perhaps even more surprising result. Local constitutive parameters ϵ and μ describing the Landau-Lifshitz permittivity $\boldsymbol{\epsilon}(\omega, \mathbf{k})$ well is not a sufficient condition for the standard Fresnel equation to be valid. This means that the continuity of the tangential components of $\boldsymbol{\mathcal{E}}$ and $\boldsymbol{\mathcal{H}}$ must be violated for the macroscopic fields defined as fundamental Floquet modes. Alternatively

the macroscopic fields may be defined differently, so that they become continuous. There will then be a "transition layer" close to the boundary, with different constitutive behaviour.

6.2 Future work

Based on the discussion of boundary conditions in Chapter 5 it might be necessary to consider the possibility that several modes get excited, even in the case of weak spatial dispersion. For media and frequency regions where other terms than the magnetic moment density have significant contributions to the second order term in $\boldsymbol{\epsilon}(\omega, \mathbf{k})$, it is therefore necessary to obtain boundary conditions valid for such media. Provided the $\boldsymbol{\mathcal{R}}$-term in the multipole expansion is negligible, the boundary conditions in Chapter 5 might be sufficient, but in general new conditions taking also the $\boldsymbol{\mathcal{R}}$-term into account should be derived. It may be that the transverse field approach from Ref. [127] can be used to find such conditions.

If boundary conditions valid for general weakly spatially dispersive media are found, these may be verified through FDTD simulations such as in Paper VI . To verify the boundary conditions obtained for a pure quadrupole continuum in this way, a possibility of considering such media in the FDTD method must, however, first be developed.

It should also be considered whether defining constitutive parameters such as a permeability based on components of $\boldsymbol{\epsilon}(\omega, \mathbf{k})$ actually is an useful approach at all. If one first has to calculate $\boldsymbol{\epsilon}(\omega, \mathbf{k})$, one may find the solutions $\mathbf{k}_n(\omega)$ from (4.15) directly, where $n = 1, ..., N$ for the N possible solutions to the equation. Mode matching techniques [137] may then be used to find the reflected and transmitted fields directly from knowing all potential transmitted modes $\mathbf{k}_n(\omega)$. If the goal is to find the reflection coefficient, going the detour through defining parameters such as the permeability μ may thus be unnecessary complicated. The mode matching techniques will then give the actual discontinuity of the fields directly. This means it might not even be necessary to find new and/or additional boundary conditions.

Another related aspect, which would be interesting to look more into, is how the constitutive relations should be modified inside a transition layer between free space and a general weakly spatially dispersive medium. From FDTD simulations of media where the $\boldsymbol{\mathcal{Q}}$ and $\boldsymbol{\mathcal{R}}$ terms are known to be important, one may calculate the actual multipole densities throughout space according to their spatial domain definitions [32]. In Ref. [109] it was assumed that the quadrupolarizability gradually changes from the value in free space to that of the bulk medium throughout the transition layer. It is natural to expect this to be the case also for a magnetic susceptibility $(\mathbf{I} - \boldsymbol{\mu}^{-1})$. Such intuitive guesses of constitutive relations should however be verified, and it could be that the same transition is valid for all the

second order coefficients β_{iklj} of $\boldsymbol{\epsilon}(\omega, \mathbf{k})$. To the author's best knowledge there has not been any numerical verifications of such transition layer models based on FDTD simulations so far.

From our work with Papers I and II it would be interesting to look further into the possibility of verifying the existence of simultaneous refracting media through e.g. time domain simulations. In this regard I recommend focusing on finding simultaneous refracting media with significantly lower gain than those considered in our work so far. Time domain simulations of media with a very strong gain are challenging, because the transient frequencies might get very strongly amplified, before they eventually are supposed to die out. In any finite difference calculation of wave phenomena artificial reflections will be present, due to the discretization of the physically continuous space. These artificial reflections will grow large due to the strong gain, and eventually destroy the validity of the simulation. Besides searching for simultaneous refracting media with lower gain, there might also be computational workarounds to this problem.

Another potential next step is to perform a similar analysis to that in Paper I to a semi-infinite, potentially active medium described by $\boldsymbol{\epsilon}(\omega, \mathbf{k})$ to second order, rather than the isotropic parameters $\epsilon(\omega)$ and $\mu(\omega)$ used in our paper. To describe a medium boundary, a new set of Fresnel equations based on new boundary conditions are again required. It could be that the dependency of both ω and $\mathbf{k}$ of $\boldsymbol{\epsilon}(\omega, \mathbf{k})$ may lead to some difficulties, but also perhaps some new interesting effects which actually may be made available through some sophisticated metamaterial structure based on active components.

Chapter 7

Publication list

Journal publications

- H.O. Hågenvik, M.E. Malema and J. Skaar, "Fourier theory of linear gain media," Physical Review A **91**, 043826 (2015).
- H.O. Hågenvik and J. Skaar, "Fourier-Laplace analysis and instabilities of a gainy slab," Journal of the Optical Society of America B **32**, 1947-1953 (2015).
- H.O. Hågenvik, K. Bløtekjær and J. Skaar, "Dielectric media considered as vacuum with sources," American Journal of Physics **85**, 830 (2017).
- C.A. Dirdal, H.O. Hågenvik, H.A. Haave and J. Skaar, "Higher order multipoles in metamaterial homogenization," IEEE Trans. Antennas Propag. **66**, 11 (2018).
- J. Skaar, H.O. Hågenvik and C.A. Dirdal, "Four definitions of magnetic permeability for periodic metamaterials," Physical Review B **99**, 064407 (2019).
- H.O. Hågenvik and J. Skaar, "Magnetic permeability in Fresnel's equation," Journal of the Optical Society of America B **36**, 1386-1395 (2019).

Conference contributions

Presenting author in bold.

- **H.O. Hågenvik** and J. Skaar, "Fourier theory of linear gain media," poster at Norwegian Electro Optics Meeting, Fevik, Norway (April 2014).

- **H.O. Hågenvik** and J. Skaar, "Laplace-Fourier analysis and instabilities of an active slab," poster at NANOMETA, Seefeld, Austria (January 2015).
- **C.A. Dirdal**, H.O. Hågenvik and J. Skaar, "Permittivity, permeability, and the significance of the electrical quadrupole in metamaterials," presentation at Norwegian Electro Optics Meeting, Voss, Norway (April 2016).
- **H.O. Hågenvik**, C.A. Dirdal and J. Skaar, "Homogenization of metamaterials: comparison and analysis," presentation at Nano network - 7th annual workshop, Trondheim, Norway (June 2016).
- **C.A. Dirdal**, H.O. Hågenvik and J. Skaar, "Higher order terms and origin dependence in metamaterial homogenization," presentation at The 4th Advanced Electromagnetics Symposium, Torremolinos, Malaga , Spain (July 2016).

Chapter 8

Contributions in papers

This section summarizes my contribution to each of the papers contained in this thesis. The papers are labeled with the same numbers as in this thesis.

Paper I

H.O. Hågenvik, M.E. Malema and J. Skaar "Fourier theory of linear gain media," Physical Review A **91**, 043826 (2015).

My contribution: Significantly contributed to the development of the theory: especially in the establishment of the existence of the involved transforms. Sections III and IV: Choice of excitations, and associated analysis. Subsections V.D and V.E: Choice of medium, analysis, numerical experiments, and discussions. Section VI: Conclusion. I wrote most of Subsec. V.E, and performed the FDTD-simulations which were meant to visualize the effect described in this section. The FDTD-program was also used to verify the responses which are described analytically in the examples V.A-V.C. I was the corresponding author during the lengthy review process.

Paper II

H.O. Hågenvik and J. Skaar, "Fourier-Laplace analysis and instabilities of a gainy slab," Journal of the Optical Society of America B **32**, 9 (2015).

My contribution: Generated all figures, and performed all simulations and analysis. I wrote the paper, with input from Johannes. I suggested the paper topic based on the lengthy review process of Paper I. I came up with the proof in the appendix. I was the corresponding author during the review process.

Paper III

H.O. Hågenvik, K. Bløtekjær and J. Skaar, "Dielectric media considered as vacuum with sources," Am. J. Phys **85**, 11 (2017).

My contribution: I performed the simulations, and contributed to the writing of the paper.

Paper IV

C.A. Dirdal, H.O. Hågenvik, H.A. Haave and J. Skaar, "Higher order multipoles in metamaterial homogenization," IEEE Trans. Antennas Propag. **66**, 11 (2018).

My contribution: Contributed to the development of the theory.

Paper V

J. Skaar, H.O. Hågenvik and C.A. Dirdal, "Four definitions of magnetic permeability for periodic metamaterials," Physical Review B **99**, 064407 (2019).

My contribution: Contributed to the development of the theory.

Paper VI

H.O. Hågenvik and J. Skaar, "Magnetic permeability in Fresnel's equation," Journal of the Optical Society of America B **36**, 1386-1395 (2019).

My contribution: Generated all figures, and performed all simulations and analysis. I wrote the paper, with input from Johannes. I was the corresponding author during the review process.

Bibliography

[1] J. B. Pendry, A. J. Holden, D. J. Robbins, and W. J. Stewart, "Magnetism from conductors and enhanced nonlinear phenomena," IEEE Transactions on Microwave Theory and Techniques **47**, 2075–2084 (1999)

[2] J. C. Bose, "On the rotation of plane of polarisation of electric wave by a twisted structure," Proceedings of the Royal Society of London **63**, 146–152 (1898)

[3] J. C. Maxwell Garnett, "Colours in metal glasses and in metallic films," Philosophical Transactions of the Royal Society of London A: Mathematical, Physical and Engineering Sciences **203**, 385–420 (1904)

[4] D. R. Smith, Willie J. Padilla, D. C. Vier, S. C. Nemat-Nasser, and S. Schultz, "Composite medium with simultaneously negative permeability and permittivity," Phys. Rev. Lett. **84**, 4184–4187 (2000)

[5] V. G. Veselago, "The electrodynamics of substances with simultaneously negative ϵ and μ," Sov. Phys. Usp. **10**, 509 (1968)

[6] H. Lamb, "On group - velocity," Proceedings of the London Mathematical Society **s2-1**, 473–479 (1904)

[7] Schuster A, *An introduction to the theory of optics* (E. Arnold, 1904)

[8] V. M. Agranovich and Y. N. Gartstein, "Spatial dispersion and negative refraction of light," Physics-Uspekhi **49**, 1029 (2006)

[9] Ø. Lind-Johansen, K. Seip, and J. Skaar, "The perfect lens on a finite bandwidth," Journal of Mathematical Physics **50**, 012908 (2009)

[10] U. Leonhardt, "Optical conformal mapping," Science **312**, 1777–1780 (2006)

[11] J. B. Pendry, D. Schurig, and D. R. Smith, "Controlling electromagnetic fields," Science **312**, 1780–1782 (2006)

[12] D. Schurig, J. J. Mock, B. J. Justice, S. A. Cummer, J. B. Pendry, A. F. Starr, and D. R. Smith, "Metamaterial electromagnetic cloak at microwave frequencies," Science **314**, 977–980 (2006)

[13] U. Leonhardt and T. G. Philbin, "Transformation optics and the geometry of light," (Elsevier, 2009) Chap. 2, pp. 69 – 152

[14] C. L. Holloway, A. Dienstfrey, E. F. Kuester, J. F. O'Hara, A. K. Azad, and A. J. Taylor, "A discussion on the interpretation and characterization of metafilms/metasurfaces: The two-dimensional equivalent of metamaterials," Metamaterials **3**, 100 – 112 (2009)

[15] H.-T. Chen, A. J. Taylor, and N. Yu, "A review of metasurfaces: physics and applications," Rep. Prog. Phys. **79** (2016), DOI: 10.1088/0034-4885/79/7/076401

[16] S. A. Ramakrishna and J. B. Pendry, "Removal of absorption and increase in resolution in a near-field lens via optical gain," Phys. Rev. B **67**, 201101 (2003)

[17] D. R. Smith, S. Schultz, P. Markoš, and C. M. Soukoulis, "Determination of effective permittivity and permeability of metamaterials from reflection and transmission coefficients," Phys. Rev. B **65**, 195104 (2002)

[18] X. Chen, B.-I. Wu, J. A. Kong, and T. M. Grzegorczyk, "Retrieval of the effective constitutive parameters of bianisotropic metamaterials," Phys. Rev. E **71**, 046610 (2005)

[19] David R. Smith and John B. Pendry, "Homogenization of metamaterials by field averaging (invited paper)," J. Opt. Soc. Am. B **23**, 391–403 (2006)

[20] Constantin R. Simovski and Sergei A. Tretyakov, "Local constitutive parameters of metamaterials from an effective-medium perspective," Phys. Rev. B **75**, 195111 (2007)

[21] V. A. Markel, "Can the imaginary part of permeability be negative?." Phys. Rev. E **78**, 026608 (2008)

[22] C. Rockstuhl, T. Paul, F. Lederer, T. Pertsch, T. Zentgraf, T. P. Meyrath, and H. Giessen, "Transition from thin-film to bulk properties of metamaterials," Phys. Rev. B **77**, 035126 (2008)

[23] C. R. Simovski, "Material parameters of metamaterials (a review)," Optics and Spectroscopy **107**, 726 (2009)

[24] A. Andryieuski, R. Malureanu, and A. V. Lavrinenko, "Homogenization of metamaterials: Parameters retrieval methods and intrinsic problems," in *2010 12th International Conference on Transparent Optical Networks* (2010) pp. 1–5

[25] C. R. Simovski, "On electromagnetic characterization and homogenization of nanostructured metamaterials," Journal of Optics **13**, 013001 (2011)

[26] A. Alù, "Restoring the physical meaning of metamaterial constitutive parameters," Phys. Rev. B **83**, 081102 (2011)

[27] A. Alù, A. D. Yaghjian, R. A. Shore, and M. G. Silveirinha, "Causality relations in the homogenization of metamaterials," Phys. Rev. B **84**, 054305 (2011)

[28] I. Tsukerman and V. A. Markel, "A non-asymptotic homogenization theory for periodic electromagnetic structures," Proceedings of the Royal Society of London A: Mathematical, Physical and Engineering Sciences **470** (2014), DOI: 10.1098/rspa.2014.0245

[29] I. Tsukerman, "Classical and non-classical effective medium theories: New perspectives," Physics Letters A **381**, 1635 – 1640 (2017)

[30] W. H. Bragg and W. L. Bragg, "The reflection of X-rays by crystals," Proceedings of the Royal Society of London A: Mathematical, Physical and Engineering Sciences **88**, 428–438 (1913)

[31] G. Russakoff, "A derivation of the macroscopic Maxwell equations," Am. J. Phys. **38**, 1188–1195 (1970)

[32] J. D. Jackson, *Classical Electrodynamics* (Wiley, New Jersey, 1999)

[33] M. G. Silveirinha, "Metamaterial homogenization approach with application to the characterization of microstructured composites with negative parameters," Phys. Rev. B **75**, 115104 (2007)

[34] A. Alù, "First-principles homogenization theory for periodic metamaterials," Phys. Rev. B **84**, 075153 (2011)

[35] A. D. Yaghjian, A. Alù, and M. G. Silveirinha, "Homogenization of spatially dispersive metamaterial arrays in terms of generalized electric and magnetic polarizations," Photonics and Nanostructures - Fundamentals and Applications **11**, 374 – 396 (2013)

[36] F. Bilotti and S. Tretyakov, "Amorphous metamaterials and potential nanophotonics applications," in *Amorphous Nanophotonics*, edited by Carsten Rockstuhl and Toralf Scharf (Springer Berlin Heidelberg, Berlin, Heidelberg, 2013) pp. 39–66

[37] V. A. Markel, "External versus induced and free versus bound electric currents and related fundamental questions of the classical electrodynamics of continuous media: discussion," J. Opt. Soc. Am. A **35**, 1663–1673 (2018)

[38] K. S. Yee, "Numerical solution of initial boundary value problems involving Maxwell's equations in isotropic media," IEEE Trans. Antennas Propag. **14**, 302–307 (1966)

[39] M. B. James and D. J. Griffiths, "Why the speed of light is reduced in a transparent medium," American Journal of Physics **60**, 309–313 (1992)

[40] H. M. Lai, Y. P. Lau, and W. H. Wong, "Understanding wave characteristics via linear superposition of retarded fields," American Journal of Physics **70**, 173–179 (2002)

[41] B. E. A. Saleh and M. C. Teich, *Fundamentals of Photonics* (Wiley, New Jersey, 2007)

[42] R. E. Raab and O. L. de Lange, *Mulipole Theory in Electromagnetism: Classical, Quantum, and Symmetry Aspects, with Applications* (Oxford University Press, 2005)

[43] J. B. Pendry, A. J. Holden, W. J. Stewart, and I. Youngs, "Extremely low frequency plasmons in metallic mesostructures," Phys. Rev. Lett. **76**, 4773–4776 (1996)

[44] J. B. Pendry, A. J. Holden, D. J. Robbins, and W. J. Stewart, "Low frequency plasmons in thin-wire structures," Journal of Physics: Condensed Matter **10**, 4785 (1998)

[45] R. A. Shelby, D. R. Smith, and S. Schultz, "Experimental verification of a negative index of refraction," Science **292**, 77–79 (2001)

[46] G. V. Eleftheriades, A. K. Iyer, and P. C. Kremer, "Planar negative refractive index media using periodically L-C loaded transmission lines," Microwave Theory and Techniques, IEEE Transactions on **50**, 2702–2712 (2002)

[47] R. Marqués, J. Martel, F. Mesa, and F. Medina, "Left-handed-media simulation and transmission of em waves in subwavelength split-ring-resonator-loaded metallic waveguides," Phys. Rev. Lett. **89**, 183901 (2002)

[48] J. Martel, R. Marques, F. Falcone, J. D. Baena, F. Medina, F. Martin, and M. Sorolla, "A new LC series element for compact bandpass filter design," IEEE Microwave and Wireless Components Letters **14**, 210–212 (2004)

[49] O. Wing, *Classical Circuit Theory* (Springer US, 2009)

[50] J. B. Pendry, "Negative refraction makes a perfect lens," Phys. Rev. Lett. **85**, 3966–3969 (2000)

[51] B. Nistad and J. Skaar, "Causality and electromagnetic properties of active media," Phys. Rev. E **78**, 036603 (2008)

[52] H. M. Nussenzveig, *Causality and dispersion relations* (Academic Press, New York and London, Chap. 1, 1972)

[53] E. C. Titchmarsh, *Introduction to the theory of Fourier integrals* (Oxford University Press, Oxford,Chapter 5, 1948)

[54] O. V. Dolgov, D. A. Kirzhnits, and E. G. Maksimov, "On an admissible sign of the static dielectric function of matter," Rev. Mod. Phys. **53**, 81–93 (1981)

[55] E. M. Lifshitz L. D. Landau and L. P. Pitaevskii, *Electrodynamics of Continuous Media, 2nd ed., Course of Theoretical Physics, Vol. 8* (Elsevier Butterworth-Heinemann, 2004)

[56] V.M. Agranovich and Y. N. Gartstein, "Electrodynamics of metamaterials and the Landau-Lifshitz approach to the magnetic permeability," Metamaterials **3**, 1 – 9 (2009)

[57] M. G. Silveirinha, "Examining the validity of kramers-kronig relations for the magnetic permeability," Phys. Rev. B **83**, 165119 (2011)

[58] J. Skaar, "On resolving the refractive index and the wave vector," Opt. Lett. **31**, 3372–3374 (2006)

[59] Y.-F. Chen, P. Fischer, and F. W. Wise, "Negative refraction at optical frequencies in nonmagnetic two-component molecular media," Phys. Rev. Lett. **95**, 067402 (2005)

[60] Y. S. Ding and R.-P. Wang, "Possible realization of negative refraction in bose-einstein condensates," Phys. Rev. B **84**, 045107 (2011)

[61] M. A. Noginov, G. Zhu, M. Bahoura, J. Adegoke, C. E. Small, B. A. Ritzo, V. P. Drachev, and V. M. Shalaev, "Enhancement of surface plasmons in an ag aggregate by optical gain in a dielectric medium," Opt. Lett. **31**, 3022–3024 (2006)

[62] A. K. Popov and V. M. Shalaev, "Compensating losses in negative-index metamaterials by optical parametric amplification," Opt. Lett. **31**, 2169–2171 (2006)

[63] V. M. Shalaev, W. Cai, U. K. Chettiar, H. K. Yuan, A. K. Sarychev, V. P. Drachev, and A. V. Kildishev, "Negative index of refraction in optical metamaterials," Opt. Lett. **24**, 3356–3358 (2005)

[64] V. M. Shalaev, "Optical negative-index metamaterials," Nat. Photonics **1**, 41–48 (2007)

[65] A. K. Popov, S. A. Myslivets, T. F. George, and V. M. Shalaev, "Four-wave mixing, quantum control, and compensating losses in doped negative-index photonic metamaterials," Opt. Lett. **32**, 3044–3046 (2007)

[66] M. P. Hatlo Andresen, A. V. Skaldebø, M. W. Haakestad, H. E. Krogstad, and J. Skaar, "Effect of gain saturation in a gain compensated perfect lens," J. Opt. Soc. Am. B **27**, 1610–1616 (2010)

[67] H. O. Hågenvik and J. Skaar, "Fourier-Laplace analysis and instabilities of a gainy slab," J. Opt. Soc. Am. B **32**, 1947–1953 (2015)

[68] R. J. Briggs, *Electron-Stream Interactions with Plasmas* (MIT Press, 1964)

[69] E. Kreyszig, *Advanced Engineering Mathematics, 9th edition* (John Wiley & Sons, Inc., 2006)

[70] A. A. Kolokolov, "Fresnel formulas and the principle of causality," Phys. Usp. **42**, 931–940 (1999)

[71] J. O. Grepstad and J. Skaar, "Total internal reflection and evanescent gain," Opt. Express **19**, 21404–21418 (2011)

[72] A. P. Vinogradov, A. A. Zyablovsky, A. V. Dorofeenko, and A. A. Pukhov, "Total internal reflection in gain medium slab," Applied Physics A **107**, 89–92 (2012)

[73] C. J. Koester, "Laser action by enhanced total internal reflection," IEEE J. Quantum Electron. **2**, 580–584 (1966)

[74] G. N. Romanov and S. S. Shakhidzhanov, "Amplification of electromagnetic field in total internal reflection from a region of inverted population," JETP Lett. **16**, 209–211 (1972)

[75] B. Y. Kogan, V. M. Volkov, and S. A. Lebedev, "Superluminescence and generation of stimulated radiation under internal-reflection conditions," JETP Lett. **16**, 100–101 (1972)

[76] S. A. Lebedev, V. M. Volkov, and B. Ya. Kogan, "Value of the gain for light internally reflected from a medium with inverted population," Opt. Spectrosc. **35**, 565–566 (1973)

[77] A. A. Kolokolov, "Reflection of plane-waves from an amplifying medium," JETP Lett. **21**, 312–313 (1975)

[78] P. R. Callary and C. K. Carniglia, "Internal-reflection from an amplifying layer," J. Opt. Soc. Am. **66**, 775–779 (1976)

[79] W. Lukosz and P. P Herrmann, "Amplification by reflection from an active medium," Opt. Commun. **17**, 192–195 (1976)

[80] R. F. Cybulski and C. K. Carniglia, "Internal-reflection from an exponential amplifying region," J. Opt. Soc. Am. **67**, 1620–1627 (1977)

[81] R. F. Cybulski and M. P. Silverman, "Investigation of light amplification by enhanced internal-reflection. part i. theoretical reflectance and transmittance of an exponentially nonuniform gain region," J. Opt. Soc. Am. **73**, 1732–1738 (1983)

[82] M. P. Silverman and R. F. Cybulski, "Investigation of light amplification by enhanced internal reflection. Part II. Experimental determination of the single-pass reflectance of an optically pumped gain region," J. Opt. Soc. Am. **73**, 1739–1743 (1983)

[83] A. A. Kolokolov, "Determination of the reflection coefficient of a plane monochromatic wave," J. Commun. Technol. Electron. **43**, 837–845 (1998)

[84] J. Fan, A. Dogariu, and L. J. Wang, "Amplified total internal reflection," Opt. Express **11**, 299–308 (2003)

[85] A. Siegman, "Fresnel reflection, Lenserf reflection, and evanescent gain," Opt. Photon. News **21**, 38–45 (2010)

[86] K. J. Willis, J. B. Schneider, and S. C. Hagness, "Amplified total internal reflection: theory, analysis, and demonstration of existence via FDTD," Opt. Express **16**, 1903–1913 (2008)

[87] Tom G. Mackay and Akhlesh Lakhtakia, "Comment on "Negative refraction at optical frequencies in nonmagnetic two-component molecular media"," Phys. Rev. Lett. **96**, 159701 (2006), The authors have corrected the sign of the refractive index in Ref. [96]

[88] S. A. Ramakrishna, "Comment on "Negative refraction at optical frequencies in nonmagnetic two-component molecular media"," Phys. Rev. Lett. **98**, 059701 (2007)

[89] Y.-F. Chen, P. Fischer, and F. W. Wise, "Chen, Fischer, and Wise Reply," Phys. Rev. Lett. **96**, 159702 (2006)

[90] Y.-F. Chen, P. Fischer, and F. W. Wise, "Chen, Fischer, and Wise Reply," Phys. Rev. Lett. **98**, 059702 (2007)

[91] S. A. Ramakrishna and O. J. F. Martin, "Resolving the wave vector in negative refractive index media," Opt. Lett. **30**, 2626–2628 (2005)

[92] V. U. Nazarov and Y.-C. Chang, "Resolving the wave-vector and the refractive index from the coefficient of reflectance," Opt. Lett. **32**, 2939–2941 (2007)

[93] M. Perez-Molina and L. Carretero, "Comment on "Resolving the wave vector and the refractive index from the coefficient of reflectance"," Opt. Lett. **33**, 1828–1828 (2008)

[94] V. U. Nazarov and Y.-C. Chang, "Reply to comment on "Resolving the wave vector and the refractive index from the coefficient of reflectance"," Opt. Lett. **33**, 1829–1829 (2008)

[95] J. Skaar, "Fresnel equations and the refractive index of active media," Phys. Rev. E **73**, 026605 (2006)

[96] J. B. Geddes, III, T. G. Mackay, and A. Lakhtakia, "On the refractive index for a nonmagnetic two-component medium: Resolution of a controversy," Opt. Commun. **280**, 120–125 (2007)

[97] H. O. Hågenvik, M. E. Malema, and J. Skaar, "Fourier theory of linear gain media," Phys. Rev. A **91**, 043826 (2015)

[98] Hans Olaf Hågenvik, *FDTD simulations of novel gain media*, Master's thesis, Norwegian University of Science and Technology. Dept. of Electronic Systems (2014)

[99] C. A. Dirdal and J. Skaar, "Negative refraction in causal media by evaluating polar paths for rational functions," J. Opt. Soc. Am. B **30**, 370–376 (2013)

[100] V. M. Agranovich and V. L. Ginzburg, *Crystal optics with spatial dispersion, and excitons* (Springer Verlag, Berlin, 1984)

[101] A. L. Pokrovsky and A. L. Efros, "Nonlocal electrodynamics of two-dimensional wire mesh photonic crystals," Phys. Rev. B **65**, 045110 (2002)

[102] P. A. Belov, R. Marqués, S. I. Maslovski, I. S. Nefedov, M. Silveirinha, C. R. Simovski, and S. A. Tretyakov, "Strong spatial dispersion in wire media in the very large wavelength limit," Phys. Rev. B **67**, 113103 (2003)

[103] C. R. Simovski and P. A. Belov, "Low-frequency spatial dispersion in wire media," Phys. Rev. E **70**, 046616 (2004)

[104] A. L. Efros, "Comment II on "Resonant and antiresonant frequency dependence of the effective parameters of metamaterials"," Phys. Rev. E **70**, 048602 (2004)

[105] A. A. Golubkov and V. A. Makarov, "Boundary conditions for electromagnetic field on the surface of media with weak spatial dispersion," Physics-Uspekhi **38**, 325 (1995)

[106] M. G. Silveirinha, "Additional boundary conditions for nonconnected wire media," New Journal of Physics **11**, 113016 (2009)

[107] O. L. de Lange and R. E. Raab, "Electromagnetic boundary conditions in multipole theory," Journal of Mathematical Physics **54**, 093513 (2013)

[108] A. D. Yaghjian, "Boundary conditions for electric quadrupolar continua," Radio Science **49**, 1289–1299 (2014)

[109] A. D. Yaghjian and M. G. Silveirinha, "Additional boundary condition for electric quadrupolar continua derived from Maxwell's differential equations," Radio Science **51**, 1312–1321 (2016)

[110] A. Alù, A. Salandrino, and N. Engheta, "Negative effective permeability and left-handed materials at optical frequencies," Opt. Express **14**, 1557–1567 (2006)

[111] C. R. Simovski and S. A. Tretyakov, "Model of isotropic resonant magnetism in the visible range based on core-shell clusters," Phys. Rev. B **79**, 045111 (2009)

[112] F. Monticone and A. Alù, "The quest for optical magnetism: from split-ring resonators to plasmonic nanoparticles and nanoclusters," J. Mater. Chem. C **2**, 9059–9072 (2014)

[113] C. Menzel, E. Hebestreit, R. Alaee, M. Albooyeh, S. Mühlig, S. Burger, C. Rockstuhl, C. Simovski, S. Tretyakov, F. Lederer, and T. Pertsch, "Extreme coupling: A route towards local magnetic metamaterials," Phys. Rev. B **89**, 155125 (2014)

[114] M. A. Shapiro, G. Shvets, J. R. Sirigiri, and R. J. Temkin, "Spatial dispersion in metamaterials with negative dielectric permittivity and its effect on surface waves," Opt. Lett. **31**, 2051–2053 (2006)

[115] V. Yannopapas, "Non-local optical response of two-dimensional arrays of metallic nanoparticles," Journal of Physics: Condensed Matter **20**, 325211 (2008)

[116] A. V. Chebykin, A. A. Orlov, C. R. Simovski, Y. S. Kivshar, and P. A. Belov, "Nonlocal effective parameters of multilayered metal-dielectric metamaterials," Phys. Rev. B **86**, 115420 (2012)

[117] R.-L. Chern, "Spatial dispersion and nonlocal effective permittivity for periodic layered metamaterials," Opt. Express **21**, 16514–16527 (2013)

[118] K. Im, J.-H. Kang, and Q.-H. Park, "Universal impedance matching and the perfect transmission of white light," Nature Photonics **12**, 143–149 (2018)

[119] S. Horsley, "Non-locality prevents reflection," Nature Photonics **12**, 127–128 (2018)

[120] D. J. Cho, F. Wang, X. Zhang, and Y. R. Shen, "Contribution of the electric quadrupole resonance in optical metamaterials," Phys. Rev. B **78**, 121101 (2008)

[121] C. A. Dirdal, H. O. Hågenvik, H. A. Haave, and J. Skaar, "Higher order multipoles in metamaterial homogenization," IEEE Transactions on Antennas and Propagation **66**, 6403–6407 (2018)

[122] J. Skaar, H. O. Hågenvik, and C. A. Dirdal, "Four definitions of magnetic permeability for periodic metamaterials," Phys. Rev. B **99**, 064407 (Feb 2019)

[123] M. G. Silveirinha, "Nonlocal homogenization theory of structured materials," in *Metamaterials Handbook: Theory and phenomena of metamaterials*, edited by Filippo Capolino (CRC Press, London, 2009) Chap. 10

[124] A. P. Vinogradov and A. V. Aivazyan, "Scaling theory for homogenization of the Maxwell equations," Phys. Rev. E **60**, 987–993 (1999)

[125] V. A. Markel, "On the current-driven model in the classical electrodynamics of continuous media," Journal of Physics: Condensed Matter **22**, 485401 (2010)

[126] V. A. Markel and I. Tsukerman, "Current-driven homogenization and effective medium parameters for finite samples," Phys. Rev. B **88**, 125131 (2013)

[127] M. G Silveirinha, "Boundary conditions for quadrupolar metamaterials," New Journal of Physics **16**, 083042 (2014)

[128] A. P. Vinogradov, "On the form of constitutive equations in electrodynamics," Physics-Uspekhi **45**, 331 (2002)

[129] J. van Bladel, *Electromagnetic Fields* (IEEE Press, Hoobken, NJ, 2007)

[130] J. Petschulat, C. Menzel, A. Chipouline, C. Rockstuhl, A. Tünnermann, F. Lederer, and T. Pertsch, "Multipole approach to metamaterials," Phys. Rev. A **78**, 043811 (2008)

[131] C. Simovski and S. Tretyakov, "Material parameters and field energy in reciprocal composite media," in *Metamaterials Handbook: Theory and Phenomena of Metamaterials*, edited by Filippo Capolino (CRC Press, London, 2009) Chap. 2

[132] R. E. Raab, "Magnetic multipole moments," Molecular Physics **29**, 1323–1331 (1975)

[133] E. B. Graham, J. Pierrus, and R. E. Raab, "Multipole moments and Maxwell's equations," Journal of Physics B: Atomic, Molecular and Optical Physics **25**, 4673 (1992)

[134] A. Chipouline, C. Simovski, and S. Tretyakov, "Basics of averaging of the Maxwell equations for bulk materials," Metamaterials **6**, 77 – 120 (2012)

[135] E. Pshenay-Severin, A. Chipouline, J. Petschulat, U. Hübner, A. Tünnermann, and T. Pertsch, "Optical properties of metamaterials based on asymmetric double-wire structures," Opt. Express **19**, 6269–6283 (2011)

[136] A. Yaghjian, M. Silveirinha, A. Askarpour, and A. Alù, "Electric quadrupolarizability of a source-driven dielectric sphere," Progress In Electromagnetics Research B **63**, 95–106 (2015)

[137] J. D. Joannopoulos, S. G. Johnson, S. N. Winn, and R. D. Meade, *Photonic Crystals: Molding the flow of light, 2nd ed.* (Princeton University Press, 2008)

[138] S. I. Pekar, "Theory of electromagnetic waves in a crystal with excitons," Journal of Physics and Chemistry of Solids **5**, 11 – 22 (1958)

[139] V.L. Ginzburg, "Electromagnetic waves in isotropic and crystalline media characterized by dielectric permittivity with spatial dispersion," JETP Lett. **7**, 1096–1103 (1958)

[140] S. I. Pekar, "On the theory of absorption and dispersion of light in crystals," Soviet Physics JEPT **9**, 785–796 (1958)

[141] V. M. Agranovich, Y. N. Gartstein, and A. A. Zakhidov, "Negative refraction in gyrotropic media," Phys. Rev. B **73**, 045114 (2006)

[142] D. C. Langreth, "Macroscopic approach to the theory of reflectivity," Phys. Rev. B **39**, 10020–10027 (1989)

[143] A. D. Yaghjian, "Extreme electromagnetic boundary conditions and their manifestation at the inner surfaces of spherical and cylindrical cloaks," Metamaterials **4**, 70 – 76 (2010), Metamaterials-2009 Congress in London

[144] M. G. Silveirinha and C. A. Fernandes, "Transverse-average field approach for the characterization of thin metamaterial slabs," Phys. Rev. E **75**, 036613 (2007)

Paper I

Fourier theory of linear gain media

Published in Physical Review A **91**, 043826 (2015)

PHYSICAL REVIEW A **91**, 043826 (2015)

Fourier theory of linear gain media

Hans Olaf Hågenvik, Markus E. Malema, and Johannes Skaar*
Department of Electronics and Telecommunications, Norwegian University of Science and Technology, NO-7491 Trondheim, Norway
(Received 1 July 2014; published 15 April 2015)

The analysis of wave propagation in linear, passive media is usually done by considering a single real frequency (the monochromatic limit) and also often a single plane-wave component (plane-wave limit). For gain media, we demonstrate that these two limits generally do not commute; for example, one order may lead to a diverging field, while the other order leads to a finite field. Moreover, the plane-wave limit may be dependent on whether it is realized with a finite-support excitation or Gaussian excitation, eventually of infinite widths. We consider wave propagation in gain media by a Fourier-Laplace integral in space and time, and demonstrate how the correct monochromatic limit or plane-wave limit can be taken, by deforming the integration surface in complex frequency–complex wave-number space. We also give the most general criterion for absolute instabilities. The general theory is applied in several cases, and is used to predict media with novel properties. In particular, we show the existence of isotropic media which in principle exhibit simultaneous refraction, meaning that they refract positively and negatively at the same time.

DOI: 10.1103/PhysRevA.91.043826 PACS number(s): 42.70.−a, 81.05.Xj, 42.25.Bs, 41.20.−q

I. INTRODUCTION

Fourier theory makes it possible to consider single frequencies and plane-wave components separately, in describing electromagnetic wave propagation in linear, passive media. This leads to huge simplification in analysis and interpretation, especially for dispersive (and/or spatially dispersive) media. Nevertheless, we must have in mind that real physics happens in the time-spatial domain, not in frequency-wave-number space; the monochromatic and plane-wave limits can never be realized in practice. The monochromatic limit is approached by turning on the excitation at some time $t = 0$ [1], and waiting a sufficiently long time until the transients have died out. The plane-wave limit is approached by letting the width of the excitation be sufficiently large.

For active media (gain media), it is clearly of large interest to use the same Fourier theory, by decomposing the field into frequency components and/or plane waves. There are, however, a number of obstacles. The most obvious one is that active media are inherently nonlinear due to gain saturation [2]. In practice, this can be dealt with by verifying that the magnitude of the solution is less than the threshold for gain saturation. If it is not, then the excitation must be reduced accordingly, or the solution must be rejected. If there are divergences associated with the linear solution, the solution must be rejected in any case.

Another problem is that the Fourier transform does not necessarily exist. A remedy is to use the Laplace transform, decomposing the time-domain fields into exponentially increasing functions $\exp(-i\omega t)$ for $\mathrm{Im}\,\omega > 0$ (see Sec. II). Once the solution has been found, it can often be continuated towards real frequencies, enabling simpler interpretation (Sec. III). One may argue that the Fourier transform should be sufficient for the relevant situations since diverging solutions must be rejected anyway. However, this strategy is dangerous, as imposing Fourier transform analysis may give the impression of false, stable solutions.

An extensively discussed problem in the context of active media is the determination of the sign of the longitudinal wave number k_z. This problem is far from trivial, even, e.g., in the context of total internal reflection from a weakly amplifying medium [3–6]. More recently, the problem has been discussed in the context of the wave vector or refractive index of more advanced active media including active metamaterials [7–10].

We are not going to focus on this problem here, as it now seems to be agreed that the sign of the longitudinal wave number must be determined by ensuring it is analytic in some upper half-plane of complex frequency, and such that $k_z \to +\omega/c$ for $\omega \to \infty$ [8–12]. Here, ω is the (possibly complex) frequency and c the vacuum light velocity. However, we will take the analysis one important step further: by considering a double Fourier-Laplace transform with respect to space and time. Clearly, for realistic situations, the fields can neither have infinite durations nor infinite widths. In addition to turning the field excitations on at $t = 0$, it turns out to be crucial to let them have finite widths, to see how the medium behaves in practice. Indeed, even though a particular medium does not show absolute instabilities for plane-wave excitations, it can support absolute instabilities in the presence of other excitations.

Once the general theory governing causal finite beam propagation has been discussed, it is of interest to consider the monochromatic limit and plane-wave limit. A number of peculiar but interesting results arise. First of all, the monochromatic and plane-wave limits do not commute in general. For very common situations with conventional gain media, one order leads to finite fields, while the other order leads to infinite fields. Second of all, the plane-wave limit may depend on the way it is taken, if it is realized using a finite-support excitation or a Gaussian excitation, eventually of infinite widths. Our analysis leads to a better understanding of the nontrivialities associated with earlier, monochromatic, and plane-wave analyses of active media. It also can be used to predict new classes of active media, with novel responses. For example, we predict the presence of isotropic media which exhibit simultaneous refraction, i.e., both positive and negative refraction simultaneously. While this is a novel

*johannes.skaar@ntnu.no

and surprising response, it may be argued that the required gain is unrealistically high, and makes both realization and time-domain simulations challenging, at least for the specific media proposed here.

Previously, Kolokolov [4] and Grepstad and Skaar [6] have treated the problem of Fourier-Laplace transform analysis of active media. However, Kolokolov only considered the special case with weak or no dispersion. Dispersion has important consequences for the theory, as it turns out to fundamentally change the method of deformation in the complex frequency–wave-number space. The dispersion, possibly engineered by metamaterials, may lead to new classes of active media, as shown by the different possible behaviors in frequency–wave-number space. Grepstad and Skaar did not perform a complete analysis since they did not consider the deformation in frequency–wave-number space, including the monochromatic limit for finite beams.

The article is structured as follows. In Sec. II, we state the problem and discuss the assumptions in detail, before analyzing the fields using the Laplace transform (in time) and Fourier transform (in space). In Sec. III, we discuss how we may approach real frequencies for media without absolute instabilities. This happens at the expense of deforming the integration path in the complex wave-number (k_x) space. In Sec. IV, we discuss the plane-wave limit, and the interpretation of divergences and noncommutativity. The theory is applied to the understanding of existing media and novel media in Sec. V. In particular, we show the presence of simultaneous refraction, before concluding in Sec. VI.

II. LAPLACE AND FOURIER TRANSFORM ANALYSIS

We restrict the analysis to linear, time-shift invariant, isotropic, homogeneous media without spatial dispersion. Moreover, we assume the following asymptotic behavior for the product of relative permittivity ϵ and relative permeability μ, as $\omega \to \infty$ [13]: $\epsilon(\omega)\mu(\omega) = 1 + O(\omega^{-2})$. Finally, we assume that the medium does not support superexponential instabilities [14], meaning that any field solution should not grow faster with time than an exponential.

In the analysis we consider an infinite or semi-infinite medium. Considering infinite media helps us understand the electromagnetic response given solely by the medium's properties; effects related to interactions with surrounding media have been ruled out. Of course, there are no infinite gain media in practice. However, as long as the smallest distance from an observation point to the boundary of the medium is larger than $ct_{\max}$, where $t_{\max}$ is the maximum duration of the experiment, the size does not matter and we may as well assume it is infinite. To approach steady state (or the monochromatic limit) we will later require $t_{\max}$ to be large. Then, we must have in mind that the dimensions of the gain medium must be accordingly large.

We will assume that the medium is dark for $t \leqslant 0$. This assumption needs some clarification. To establish the active medium, an energy pump must be turned on before $t = 0$. When the system does not support instabilities, we can imagine that the pump was turned on a long time before $t = 0$, such that any transients have died out. If there are instabilities, however, any disturbance will blow up with time. We could assume that the pump is turned on slowly before $t = 0$, sufficiently smooth such that no significant transients are generated as a result of the pump, but sufficiently fast such that the (small) transients do not grow too much before $t = 0$. We do not consider the existence of such a tradeoff further; we rather demand that any transients from the pump or from other perturbations or fluctuations in the system must be included into the analysis. This is done by including them into the excitation of the system, to be defined in the following.

It is also in order to comment on the linearity assumptions in some detail. The amplitude in any practical medium will be limited by nonlinear effects such as gain saturation. When we refer to "diverging fields," or "instabilities," it strictly means that the fields grow until they are limited by gain saturation. Clearly, in such cases the linear analysis is only accurate for a limited duration. In the absence of instabilities, the analysis is clearly accurate for all times, provided the excitations are sufficiently weak.

For simplicity, we limit the discussion to propagation in two dimensions x and z and transversal electric (TE) fields. Let $\mathcal{E}(x,z,t)\hat{\mathbf{y}}$ be the physical electric field, pointing in the y direction $\hat{\mathbf{y}}$. Since the medium is active, the field may diverge with time t. We have limited our attention to active media and sources that lead to fields growing at most exponentially. Moreover, we assume that the electric field is square integrable (finite energy) with respect to x (for the complete assumptions, see Appendix B). The electric field is Laplace transformable:

$$E(x,z,\omega) = \int_0^\infty \mathcal{E}(x,z,t)\exp(i\omega t)dt \tag{1}$$

for $\operatorname{Im}\omega > \gamma$, where γ is a sufficiently large positive number characterizing the maximum growth of the field. Furthermore, $E(x,z,\omega)$ is Fourier transformed wrt x, to obtain the plane-wave spectrum

$$E(k_x,z,\omega) = \int_{-\infty}^\infty E(x,z,\omega)\exp(-ik_x x)dx. \tag{2}$$

The inverse transform can be written

$$\begin{aligned}(2\pi)^2&\mathcal{E}(x,z,t)\\ &= \int_{i\gamma-\infty}^{i\gamma+\infty}\int_{-\infty}^{\infty} E(k_x,z,\omega)\exp(ik_x x - i\omega t)dk_x d\omega\\ &= \int_{-\infty}^{\infty}\int_{i\gamma-\infty}^{i\gamma+\infty} E(k_x,z,\omega)\exp(ik_x x - i\omega t)d\omega\, dk_x,\end{aligned} \tag{3}$$

where, in the last equality, we have interchanged the order of integration (see Appendix B).

We consider a source in the plane $z = 0$ (Fig. 1) infinitely thin, but possibly of infinite width. In general, we may have sources everywhere; in that case, we would have to superpose the fields resulting from the different sources. For $z \neq 0$, Maxwell's equations mean that $(d^2/dz^2 - k_x^2 + \epsilon\mu\omega^2/c^2)E(k_x,z,\omega) = 0$. Furthermore, the transversal (x component) of the magnetic field is given by $-i\omega\mu\mu_0 H(k_x,z,\omega) = dE(k_x,z,\omega)/dz$, where μ_0 is the

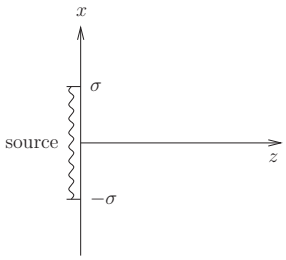

FIG. 1. An excitation is located at $z = 0$ in a homogeneous medium. In the figure, the special case with finite width 2σ is shown.

permeability in vacuum. Hence, we can express

$$E(k_x,z,\omega) = A(k_x,\omega)e^{ik_z z} + B(k_x,\omega)e^{-ik_z z}, \tag{4a}$$

$$H(k_x,z,\omega) = -\frac{k_z}{\omega\mu\mu_0}[A(k_x,\omega)e^{ik_z z} - B(k_x,\omega)e^{-ik_z z}] \tag{4b}$$

for $z < 0$, and

$$E(k_x,z,\omega) = C(k_x,\omega)e^{ik_z z} + D(k_x,\omega)e^{-ik_z z}, \tag{5a}$$

$$H(k_x,z,\omega) = -\frac{k_z}{\omega\mu\mu_0}[C(k_x,\omega)e^{ik_z z} - D(k_x,\omega)e^{-ik_z z}] \tag{5b}$$

for $z > 0$. Here,

$$k_z^2 = \epsilon\mu\frac{\omega^2}{c^2} - k_x^2. \tag{6}$$

The four functions $A(k_x,\omega)$, $B(k_x,\omega)$, $C(k_x,\omega)$, and $D(k_x,\omega)$ are connected by the electromagnetic boundary conditions, which in turn are dependent on the source. For a current source, $E(k_x,z,\omega)$ is continuous across the source plane, while $H(k_x,0^+,\omega) - H(k_x,0^-,\omega) = J(k_x,\omega)$, where $J(k_x,\omega)$ is the (Fourier-Laplace transformed) surface current source. With reflection symmetry about the plane $z = 0$, this means that

$$A = D, \tag{7a}$$

$$B = C, \tag{7b}$$

$$\frac{2k_z}{\omega\mu\mu_0}(A - B) = J(k_x,\omega). \tag{7c}$$

Clearly, both unknown functions A and B cannot be found from (7). Moreover, since the medium potentially is active, we cannot use principles like requiring the source to do positive work, or field decay as $z \to \infty$. We must invoke the principle of causality in its most fundamental form.

First, we note that the sign of k_z can be chosen arbitrarily in (4) and (5); a change of sign means only that the functions C and D (and A and B) are interchanged. Since $\epsilon(\omega)$ and $\mu(\omega)$ are analytic for $\mathrm{Im}\,\omega > \gamma$, and tend to unity as $\omega \to \infty$ there, we choose the sign such that for a fixed k_x,

$$k_z(k_x,\omega) \text{ is analytic for } \mathrm{Im}\,\omega > \gamma, \text{ and}$$
$$k_z(k_x,\omega) \to +\omega/c \text{ as } \omega \to \infty \text{ in the region } \mathrm{Im}\,\omega > \gamma. \tag{8}$$

Assuming that the medium and the source are dark for $t < 0$, the fields as described by (5) are causal, and we can use a version of Titchmarsh theorem for diverging functions (Appendix C) to prove that in (4) and (5), we have

$$A = D = 0, \tag{9a}$$

$$B = C = -\frac{\mu\mu_0\omega}{2k_z}J(k_x,\omega). \tag{9b}$$

Moreover, in Appendix A we prove that the function $k_z(k_x,\omega)$ is zero free in a region $\mathrm{Im}\,\omega > \gamma$; thus, B is analytic there.[1]

We now consider the usual situation described by the Fresnel equations, where we have different media on each side of the plane $z = 0$, and there is no source at $z = 0$ but rather somewhere in the medium on the left-hand side ($z < 0$). Clearly, we can use the identical causality argument on the right-hand side ($z > 0$) to obtain (8) and $D = 0$. The electromagnetic boundary conditions $E(k_x,0^+,\omega) = E(k_x,0^-,\omega)$ and $H(k_x,0^+,\omega) = H(k_x,0^-,\omega)$ then give the reflection and transmission coefficients

$$\frac{B}{A} = \frac{\mu_2 k_{1z} - \mu_1 k_{2z}}{\mu_2 k_{1z} + \mu_1 k_{2z}}, \tag{10a}$$

$$\frac{C}{A} = \frac{2\mu_2 k_{1z}}{\mu_2 k_{1z} + \mu_1 k_{2z}}, \tag{10b}$$

where $k_{iz}^2 = \epsilon_i\mu_i\omega^2/c^2 - k_x^2$. Here, subscripts 1 and 2 stand for the medium to the left and right, respectively. Throughout this paper, we will for simplicity assume that medium 1 is vacuum or a passive medium.

We will consider sources in the product form $u(x)v(t)$, with transform $U(k_x)V(\omega)$. For the situation with a current source plane, we set $J(k_x,\omega) = -U(k_x)V(\omega)/c\mu_0$, and for the situation with an incident wave, we set $A(k_x,\omega) = U(k_x)V(\omega)$. For later use, we sum up by writing the electric field solutions for $z > 0$ for the current source plane and the Fresnel situation, respectively:

$$E(k_x,z,\omega) = \frac{\mu\omega e^{ik_z z}}{2k_z c}U(k_x)V(\omega), \tag{11a}$$

$$E(k_x,z,\omega) = \frac{2\mu_2 k_{1z}e^{ik_{2z}z}}{\mu_2 k_{1z} + \mu_1 k_{2z}}U(k_x)V(\omega). \tag{11b}$$

Here, k_z is given by (6) and (8). It is important to note that these results have been derived for $\mathrm{Im}\,\omega > \gamma$. In Sec. III, we will consider the possibility of continuating the solutions towards real frequencies.

III. TOWARDS REAL FREQUENCIES

To facilitate interpretation and computation, it is useful to examine if we can move the inverse Laplace transform contour (Bromwich path) in (3) down to the real ω axis, such that it describes an inverse Fourier transform. This is

[1]If we had chosen the opposite sign for k_z in (8), we would have obtained $B = C = 0$. If we had chosen the sign in another, arbitrary way, we would have obtained $A = D = 0$ for some frequencies, and $B = C = 0$ else. Such choices are inconvenient (but perfectly valid) as k_z and the four functions A, B, C, and D get nonanalytic.

desirable, as steady-state harmonic excitations and solutions are convenient to interpret physically. For the active media and systems where this is possible, we have only convective instabilities [15,16]: Then, nondiverging excitations lead to nondiverging fields for every fixed point (x,z). This means that any growing wave must be convected away. On the other hand, if the Bromwich path cannot be moved down to the real axis due to singularities or cuts, the transform can be described as an inverse Fourier transform plus integrals around the nonanalytic points. Since the latter integrals diverge with time, we have absolute instabilities, meaning that the fields diverge even at fixed points in space.

For a wide range of active media of interest, it turns out to be possible to move the Bromwich path in (3) down to the real axis, at the expense of deforming the integration path in the k_x domain [16]. This is what we will consider in the following. The clue here is to realize that the integrand is analytic in both k_x and ω, so integration paths can be deformed until they reach singularities. To this end, we assume that $\epsilon\mu$ does not have singularities or zeros for $\mathrm{Im}\,\omega \geqslant 0$; situations with zeros in the upper half-plane will be discussed later. Under these conditions, $\sqrt{\epsilon\mu}$ is analytic and zero free for $\mathrm{Im}\,\omega \geqslant 0$. We consider the evaluation of the physical field in the spatial and time domain, according to (3), but along a possibly deformed surface Γ in the (k_x,ω) domain:

$$(2\pi)^2\mathcal{E}(x,z,t)=\int_\Gamma E(k_x,z,\omega)\exp(ik_x x - i\omega t)dk_x d\omega. \quad (12)$$

Here, $E(k_x,z,\omega)$ is given by (11). Apparently, the integrand is analytic in both k_x and ω, except at the branch cuts arising from the square root $k_z=\sqrt{\epsilon\mu\omega^2/c^2-k_x^2}$, and also if $k_z=0$ for the case (11a), or if $\mu_2 k_{1z}+\mu_1 k_{2z}=0$ for the case (11b). The last possibility will be ignored in the following; we simply assume that two involved media are chosen such that these singularities do not disturb the deformation of Γ. Examples will be given later. From the theory below it will also become clear how to generalize to account for such singularities.

Consider Figs. 2(a) and 2(b), showing the original integration paths in the ω and k_x domains. For all ω in the indicated domain D_ω, the branch points of k_z, i.e., $k_x=\pm\sqrt{\epsilon\mu}\omega/c$, are located in the domain D_{k_x}. Now, consider the short piece of the integration path that lies in D_ω. For these ω values, the idea is to deform the corresponding k_x integration path, as shown in Fig. 2(c). This can safely be done since $k_z(k_x,\omega)$ and therefore $E(k_x,z,\omega)$ are analytic wrt k_x away from the branch cuts.

The next step is to interchange the order of integration. For each k_x in the path in Fig. 3(b), we can deform the short piece of the ω path, obtaining the path in Fig. 3(a). Repeating the procedure for two neighboring pieces of the ω-integration curve, we obtain the situation in Fig. 4, generally with two different integration curves in the k_x domain. In simple situations such as the one in the figure, we could use a single, common integration curve in the k_x domain for both pieces in the ω domain. In general, to get rid of the vertical integration curves between the two domains in Fig. 4(a), we must require the existence of a common integration curve in the k_x domain detouring the interface between the neighboring domains [Fig. 4(c)]. If this is always the case, we can continue the deformation in the ω domain until the integration curve

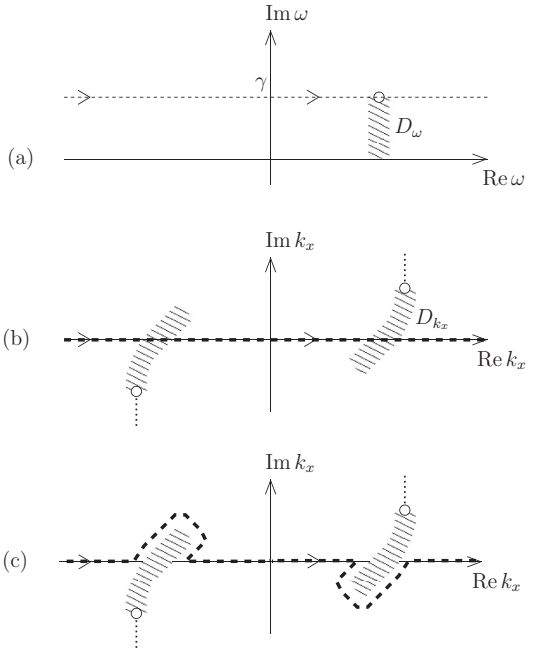

FIG. 2. The dashed lines correspond to the integration paths in (3): (a) ω domain; (b) k_x domain; and (c) deformed path in the k_x domain for the ω indicated by a circle in (a). The domain D_{k_x} corresponds to the set of values $k_x=\pm\sqrt{\epsilon\mu}\omega/c$ for $\omega\in D_\omega$. The open circles in the k_x plane correspond to the open circle in the ω plane. The dotted vertical lines indicate branch cuts for $k_z(k_x,\omega)$ for the particular ω as indicated by the open circle. We proved in Appendix A that $k_z(k_x,\omega)$ is analytic wrt k_x, for $\mathrm{Im}\,\omega=\gamma$ and real k_x; thus, the branch cuts must avoid the real k_x axis. In the figure, we take them to be vertical, starting at the circles.

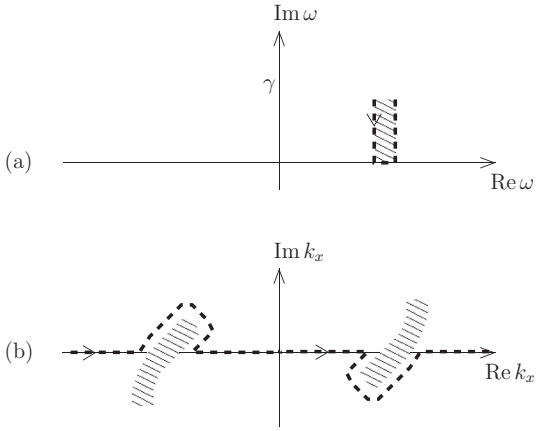

FIG. 3. Deformation in the ω domain. For each k_x in the path in (b), the integration path in D_ω can be deformed (a).

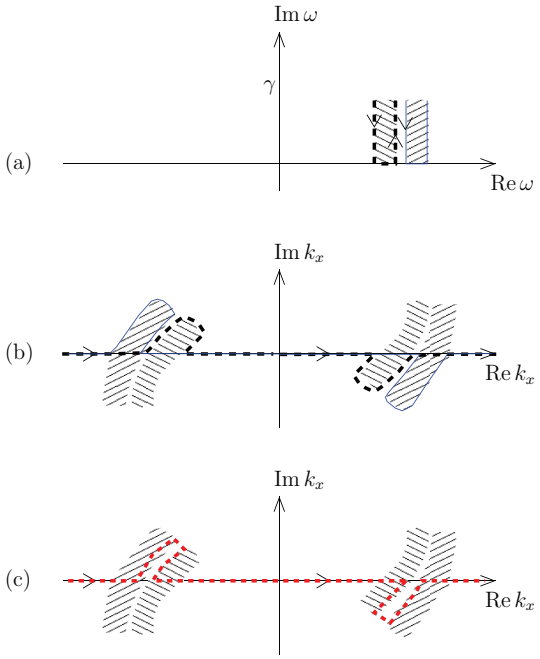

FIG. 4. (Color online) Deformation of two neighboring pieces of the ω-integration curve (dashed black and solid blue lines) (a) and the associated k_x-integration curves (b). For ω values along the vertical integration curves between the neighboring domains in (a), one can use a common k_x-integration curve (c).

coincides with the real axis:

$$\mathcal{E}(x,z,t) = \frac{1}{2\pi}\int_{-\infty}^{\infty} E(x,z,\omega)\exp(-i\omega t)d\omega, \tag{13}$$

where

$$E(x,z,\omega) = \frac{1}{2\pi}\int_{\kappa(\omega)} E(k_x,z,\omega)\exp(ik_x x)dk_x. \tag{14}$$

Here, $\kappa(\omega)$ is the deformed path in the k_x domain, for each ω. Since $\mathrm{Im}\,\omega = 0$ in (13), the resulting field will not diverge with time. Thus, in these situations, there are no absolute instabilities, and (14) can be interpreted as the usual frequency-domain field for real ω. The possible appearance of complex k_x's in the integration path $\kappa(\omega)$ means that the field may grow with x.

We have required the existence of a common k_x integration curve for any two neighboring ω's. To this end, consider the trajectories of k_z's branch points, $k_x = \pm\sqrt{\epsilon\mu}\omega/c$, as we reduce $\mathrm{Im}\,\omega$ from γ to zero. It is necessary that for two neighboring values of $\mathrm{Re}\,\omega$, these two trajectories will become arbitrarily close as the two $\mathrm{Re}\,\omega$'s approach each other. A sufficient condition for this is that $\sqrt{\epsilon\mu}$ is analytic for $\mathrm{Im}\,\omega \geqslant 0$.

We have also required that $\epsilon\mu$ be zero free for $\mathrm{Im}\,\omega \geqslant 0$. While even order zeros give analytic square root, they induce another problem: At the zero the two branch points in the k_x domain coincide so the integration curve gets "stuck."

The frequency-domain field $E(x,z,\omega)$ is related to the physical, time-domain field in the so-called monochromatic limit. From (13),

$$\mathcal{E}(x,z,t) = \frac{1}{2\pi}\int_{-\infty}^{\infty}\frac{E(x,z,\omega)}{V(\omega)}V(\omega)\exp(-i\omega t)d\omega, \tag{15}$$

where $E(x,z,\omega)/V(\omega)$ is the transfer function from the excitation $V(\omega)$ to the resulting field $E(x,z,\omega)$, as given by (11). Note that $V(\omega)$ is a factor in $E(x,z,\omega)$, so the transfer function is independent of $V(\omega)$. We can, for example, take a unit-step modulated complex exponential as the excitation:

$$v(t) = H(t)\exp(-i\omega_1 t), \quad H(t) = \begin{cases} 0, & t < 0 \\ 1, & t > 0 \end{cases} \tag{16}$$

with Laplace transform

$$V(\omega) = \frac{i}{\omega - \omega_1}. \tag{17}$$

The inverse transform (15) can be found with the residue theorem by closing the contour by a large semicircle in the lower half-plane:

$$\mathcal{E}(x,z,t) = \left[\frac{E(x,z,\omega)}{V(\omega)}\exp(-i\omega t)\right]_{\omega=\omega_1} + \text{transients}(t). \tag{18}$$

Here, the term transients(t) is a result of the integration around all singularities and cuts in the lower half-plane, and will decay exponentially. For later use, we define the monochromatic limit $\lim_{\omega_1}\mathcal{E}(x,z,t)$ as the field when the excitation is given by (16), and for sufficiently large t such that the transients can be ignored:

$$\lim_{\omega_1}\mathcal{E}(x,z,t) = \frac{E(x,z,\omega_1)}{V(\omega_1)}\exp(-i\omega_1 t), \tag{19}$$

valid when $\epsilon\mu$ is analytic and zero free for $\mathrm{Im}\,\omega \geqslant 0$. Even though the monochromatic limit exists in principle, in some situations (media with large gain and large x or z) the transients may be extremely strong, which means it may take a very long time before they have died out.

We now consider the more complicated situation where $\epsilon\mu$ is not analytic or zero free everywhere in the upper half-plane $\mathrm{Im}\,\omega > 0$. For concreteness, we assume $\epsilon\mu$ has two simple zeros but is analytic otherwise. Then, $\sqrt{\epsilon\mu}$ has branch cuts, which we take to be vertical towards $-i\infty$. Since $\sqrt{\epsilon\mu}$ is analytic everywhere in the upper half-plane except at the branch cuts, we can use the procedure above to deform the integration paths, leading to the ω-integration curve depicted in Fig. 5(a). It is natural to try to deform also the remaining detours to reach the real ω axis everywhere. To this end, we let $\mathrm{Im}\,\omega$ be reduced from γ to zero, on the left-hand side and right-hand side of $\sqrt{\epsilon\mu}$'s branch cut [Fig. 5(b)]. The corresponding trajectories of $k_x = \pm\sqrt{\epsilon\mu}\omega/c$ are shown in Figs. 5(c) and 5(d), respectively. Apparently, the result of the integration in Fig. 5(c) differs from that of Fig. 5(d), so the integrations up and down in Fig. 5(a) generally do not cancel. As a result, the detours cannot be omitted. The necessary presence of complex frequencies $\exp(-i\omega t)$ with

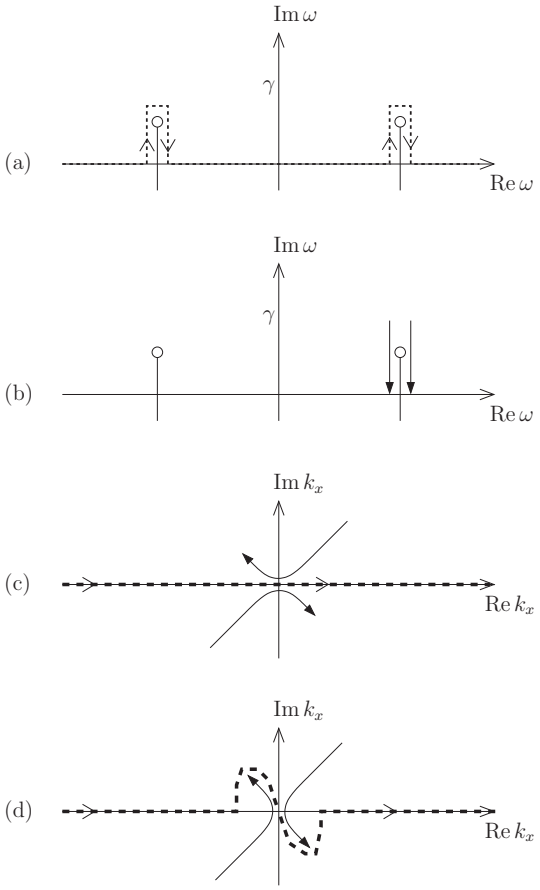

FIG. 5. Deformed integration paths (dashed line) when $\sqrt{\epsilon\mu}$ has branch cuts in the upper half-plane. The branch points of $\sqrt{\epsilon\mu}$ are shown by open circles in (a); the cuts go vertically towards $-i\infty$. As $\mathrm{Im}\,\omega$ is reduced from γ to zero along the left and right arrows in (b), the corresponding trajectories of $k_x = \pm\sqrt{\epsilon\mu}\omega/c$ are shown by solid lines in (c) and (d), respectively.

$\mathrm{Im}\,\omega > 0$ means that the field will diverge with time, even at a fixed point in space. This means that the field cannot be interpreted at real frequencies as in (18); we have an absolute instability.

IV. PLANE-WAVE LIMIT

We have seen that when there are no absolute instabilities, it is possible to move the inverse Laplace transform path down to the real axis, enabling interpretation of the fields (4) and (5) for real frequencies. However, considering active media, this has come at a price: The integration curve in k_x must be deformed to include complex values of k_x. As will be demonstrated shortly, this means that it is not necessarily possible to approach the plane-wave limit any longer.

Consider an excitation in the form $u(x)v(t)$, with transform $U(k_x)V(\omega)$. The function $v(t)$ could be given by (16), while $u(x)$ could be, e.g., one of the following alternatives:

$$u_1(x) = \mathrm{beam}(x/\sigma)\exp(iK_x x), \tag{20a}$$

$$u_2(x) = \exp(-x^2/2\sigma^2)\exp(iK_x x). \tag{20b}$$

Here, $\mathrm{beam}(x/\sigma)$ stands for a function which vanishes for $|x| > \sigma$, is smooth for $|x| < \sigma$, and $\mathrm{beam}(0) = 1$. Both alternatives represent a beam of thickness $\sim\sigma$ and a bundle of k_x's around the central transversal wave number K_x. The wave-number spectra of the excitations are given by

$$U_1(k_x) = \sigma\,\mathrm{Beam}[\sigma(k_x - K_x)], \tag{21a}$$

$$U_2(k_x) = \sqrt{2\pi}\sigma\exp[-\sigma^2(k_x - K_x)^2/2]. \tag{21b}$$

Here, $\mathrm{Beam}(k_x)$ is the Fourier transform of $\mathrm{beam}(x)$. Both spectra $U_1(k_x)$ and $U_2(k_x)$ are entire functions in k_x. For real k_x and K_x both functions can be thought of as $2\pi\delta(k_x - K_x)$ in the limit $\sigma \to \infty$. However, the two of them are fundamentally different in the sense that the first goes slowly to zero compared to the second. Indeed, if the mth derivative of $\mathrm{beam}(x)$ is nonzero at the endpoints, while the lower-order derivatives vanish, the asymptotic behavior of $U_1(k_x)$ for large $|k_x|$ is

$$|U_1(k_x)| \sim \frac{\exp(|\mathrm{Im}\,k_x|\sigma)}{|k_x|^{m+1}\sigma^m}, \tag{22}$$

as can be proved using integration by parts. A similar result is valid for smooth functions with support $[-\sigma,\sigma]$ (so-called bump functions), except that the decay along the real k_x axis is faster than 1/polynomial and slower than an exponential.

We will now consider $\lim_{\sigma\to\infty}\lim_{\omega_1}\mathcal{E}(x,z,t)$. This limit can be realized as follows. We pick an excitation width σ and perform the experiment, waiting a sufficiently long time such that the electric field has reached the monochromatic limit. Next, we pick a larger σ and repeat the experiment, waiting a sufficiently long time (possibly longer than the first time) until the field has reached the monochromatic limit. After repeating the experiment several times, with increasing σ, the field will tend to $\lim_{\sigma\to\infty}\lim_{\omega_1}\mathcal{E}(x,z,t)$.

The monochromatic limit is given by (19), so we need to consider the limit $\sigma \to \infty$ in (14), expressed at the real excitation frequency ω_1. To this end, we have assumed that the monochromatic limit exists (no absolute instabilities), i.e., $\epsilon\mu$ has no poles or zeros in the upper half-plane $\mathrm{Im}\,\omega \geqslant 0$. The integration path $\kappa(\omega_1)$ in the k_x plane, such as that in Fig. 3(b), involves complex k_x. Surprisingly, now the limit $\sigma \to \infty$ does not necessarily exist, as $U_1(k_x)$ diverges for complex k_x. In fact, this will always be the case in practice since the excitation necessarily must have finite support to be realizable.

However, from a theoretical perspective it is quite common to consider Gaussian beams or excitations, so it is interesting to consider the possibility $U_2(k_x)$. Surprisingly, even though the plane-wave limit $\sigma \to \infty$ did not exist when using $U_1(k_x)$, it may exist when using $U_2(k_x)$ since the Gaussian tends to zero provided $|\mathrm{Im}\,k_x| < |\mathrm{Re}\,k_x - K_x|$. Thus, when the detours of the k_x-integration curve are not too far away from the real axis, or too close to the excitation wave number K_x, we can take the plane-wave limit using a Gaussian excitation, but not

a finite-support excitation. When the limit exists, we can write

$$E(x,z,\omega_1) = \frac{\tilde{E}(K_x,z,\omega_1)}{U(K_x)} \exp(iK_x x) \tag{23}$$

for some function $\tilde{E}(K_x,z,\omega_1)$, expressing the field with a single wave number K_x. For most media, the part of the integration in (14) along the real axis is one way, which means that $\tilde{E}(K_x,z,\omega_1) = E(K_x,z,\omega_1)$. For certain, very special media, as we will see in Sec. V E, the integration along part of the real axis will give rise to one more term in $\tilde{E}(K_x,z,\omega_1)$. Equation (23) means that the physical time-domain field in the monochromatic limit will tend to

$$\lim_{\sigma\to\infty} \lim_{\omega_1} \mathcal{E}(x,z,t) = \frac{\tilde{E}(K_x,z,\omega_1)}{U(K_x)V(\omega_1)} \exp(iK_x x - i\omega_1 t), \tag{24}$$

as the width of the Gaussian tends to infinity.

The peculiar divergence discussed above can be interpreted as follows. For certain frequencies ω and wave numbers $\pm k_x$, the longitudinal wave number k_z becomes zero. These modes correspond to side waves, which propagate in the $\pm x$ direction. If the medium is gainy, and the excitation extends over all x's, the field at an observation point x may diverge since the side waves propagate an unlimited distance before reaching the point. For the finite-support excitation $u_1(x)$, as σ increases, side waves will have the chance to propagate a larger distance before reaching the observation point; thus, we expect an exponential growth. At the same time, the excitation $U_1(k_x)$ at the particular k_x associated with the side wave becomes weaker, but only as $\propto\sigma^{-m}$. For the Gaussian excitation $u_2(x)$, an increased σ will again give rise to an exponential growth as a result of the increased distance; however, the excitation itself at the particular k_x associated with the side wave may be much weaker due to the factor $\exp[-\sigma^2(k_x - K_x)^2/2]$.

We now consider $\lim_{\omega_1}\lim_{\sigma\to\infty}\mathcal{E}(x,z,t)$. This order of limits is more difficult to realize that the opposite order, but can be approached by measuring the time response $\mathcal{E}(x,z,t)$ for a fixed-time interval, repeating the experiment for increasing σ. After convergence, the time interval is shifted to later times, and the series of experiments is repeated, etc.

Mathematically, $\lim_{\omega_1}\lim_{\sigma\to\infty}\mathcal{E}(x,z,t)$ is found most easily by taking the limit $\sigma\to\infty$ in (3). Since only real k_x's are involved in the integral, the limit $\sigma\to\infty$ always exists, which leads to

$$\lim_{\sigma\to\infty} \mathcal{E}(x,z,t) = \frac{1}{2\pi}\int_{i\gamma-\infty}^{i\gamma+\infty} \frac{E(K_x,z,\omega)}{U(K_x)} \exp(iK_x x - i\omega t)d\omega. \tag{25}$$

Equation (25) has the disadvantage that it is expressed using complex frequencies. We would like to be able to set $\gamma = 0$ in (25) for interpretation at real frequencies. If the integrand is analytic for $\mathrm{Im}\,\omega \geqslant 0$, we can move the integration path to the real axis. However, as we will see in the following, this is not always the case, not even for media with analytic and zero free $\epsilon\mu$ for $\mathrm{Im}\,\omega \geqslant 0$. Since K_x is fixed, we must require that $\sqrt{\epsilon\mu\omega^2/c^2 - K_x^2}$ is analytic in the upper half-plane $\mathrm{Im}\,\omega \geqslant 0$ to avoid absolute instabilities. Although this can happen, it is not very common; for $K_x \neq 0$ it is not even the case for conventional, weak gain media [6,9]: For such media, there is a branch point slightly above the real ω axis, corresponding to a side wave with $K_z = 0$. For plane-wave excitations, this side wave propagates an infinite distance along the x axis, thus picking up an infinite amount of gain.

This type of absolute instability is somewhat artificial since it is induced by an excitation of infinite width. For the case with finite σ we have seen that the instability is only convective, as long as the medium has analytic and zero free $\epsilon\mu$ for $\mathrm{Im}\,\omega \geqslant 0$. This makes sense intuitively since, for finite σ, the side wave has only propagated a finite distance from the excitation to a fixed observation point.

In other words, if $\epsilon\mu$ is analytic and zero free for $\mathrm{Im}\,\omega \geqslant 0$, but $\sqrt{\epsilon\mu\omega^2/c^2 - K_x^2}$ is not analytic there (which is the case, e.g., for a weak inverted Lorentzian and $K_x \neq 0$),

$$\lim_{\omega_1} \mathcal{E}(x,z,t) = \text{finite} \tag{26}$$

for any finite σ, while

$$\lim_{\omega_1}\lim_{\sigma\to\infty} \mathcal{E}(x,z,t) = \infty. \tag{27}$$

However,

$$\lim_{\sigma\to\infty}\lim_{\omega_1} \mathcal{E}(x,z,t), \tag{28}$$

on the other hand, is dependent on the manner in which the plane-wave limit is taken. If it is taken using an excitation $U_1(k_x)$ of finite support, it is infinite, but if it is taken using a Gaussian $U_2(k_x)$, it is finite provided $|\mathrm{Im}\,k_x| < |\mathrm{Re}\,k_x - K_x|$ along the integration detour. The Gaussian excitation $u_2(x)$ is somewhat unphysical, as it requires an infinitely wide source even for finite σ. Even though the Gaussian excitation is unphysical, the fact that it makes it possible to take the plane-wave limit is interesting. It tells us that the growing side waves in a gain medium may be reduced by making the source sufficiently smooth, and will disappear in the limit of a perfect Gaussian.

Remarkably, and less intuitively, for certain media with absolute instabilities for finite σ (meaning that $\epsilon\mu$ is not analytic and zero free everywhere in the upper half-plane), it is possible to eliminate the absolute instabilities by letting $\sigma\to\infty$. Indeed, if $\sqrt{\epsilon\mu\omega^2/c^2 - K_x^2}$ is analytic for $\mathrm{Im}\,\omega > 0$ while $\epsilon\mu$ is not analytic and zero free,

$$\lim_{\omega_1} \mathcal{E}(x,z,t) = \infty \tag{29}$$

for any σ, while

$$\lim_{\omega_1}\lim_{\sigma\to\infty} \mathcal{E}(x,z,t) = \text{finite}. \tag{30}$$

For example, this happens for media for which $\epsilon\mu\omega^2/c^2 - K_x^2$ has no zeros in the upper half-plane $\mathrm{Im}\,\omega > 0$, while $\epsilon\mu$ has two simple zeros there. Such a medium is suggested in Ref. [6]. Equations (29) and (30) can be interpreted as follows. Consider the field $\mathcal{E}(x,z,t)$ when σ and t are finite. As σ is made larger, the unstable mode with $k_z = 0$ is excited more weakly. Thus, a larger t can be tolerated before $\mathcal{E}(x,z,t)$ gets large. If $\sigma\to\infty$ first, we can let t be infinite as well, without getting an infinite field. Thus, the monochromatic limit exists.

We conclude this section by noting that the monochromatic and plane-wave limits are far from trivial in gain media. Although it can be argued that these limits are unphysical, since infinite experiment durations or infinite beam

thicknesses cannot exist, they provide valuable intuition for experiments with wide beam excitations or long duration. Apparently, different results may be obtained dependent on the wideness of the excitation and the duration of the experiment.

V. MEDIA

The general method from the previous sections is now applied to analyze a wide range of media of interest, starting with simple passive and active media, and ending with novel classes of active media.

A. Passive media

Passive media are simple to analyze, due to the absence of instabilities. Fourier analysis is therefore sufficient, and the Fourier components wrt k_x and ω can be interpreted straightforwardly. Although these facts are well known, it is useful to demonstrate the formalism before moving on to more complex cases.

A passive medium has $\mathrm{Im}\,\epsilon(\omega) > 0$, $\mathrm{Im}\,\mu(\omega) > 0$, and $\mathrm{Im}\,n(\omega) > 0$ for $\omega > 0$. Here, $n(\omega) = \sqrt{\epsilon\mu}$ is the refractive index, which is analytic in the upper half-plane [17]. Due to odd symmetry of these functions, $\mathrm{Im}\,n\omega/c \geqslant 0$ for all real ω. Since $\mathrm{Im}\,n\omega/c$ is a harmonic function [18], it takes its minimum on the real axis; thus, $\mathrm{Im}\,n\omega/c \geqslant 0$ in the closed upper half-plane. It follows that k_z's branch points, $k_x = \pm n\omega/c$, do not cross the real k_x axis as we reduce $\mathrm{Im}\,\omega$ towards zero. In Fig. 6, we show two different possibilities; a passive medium which will turn out to show positive refraction (b), and a passive medium with negative refraction (c). Clearly, in both cases we can integrate along the real ω and k_x axes, and the monochromatic and plane-wave limits may be taken, leading to fields with frequency ω_1 and wave number K_x. The resulting K_z shows the behavior of the wave in the medium.

We can find the sign of K_z by tracing $\arg k_z$ as k_x decreases from $+\infty$ to K_x. For $k_x \to +\infty$, $k_z \to +ik_x$ (see Appendix A). As k_x decreases, consider $k_z^2 = \epsilon(\omega_1)\mu(\omega_1)\omega_1^2/c^2 - k_x^2$, with the two zeros shown by the solid arrow ends in Figs. 6(b) and 6(c). Now, k_z^2 picks up phase from the two zeros, but very little if k_x is in the regime far away from the zeros. Since $k_z(k_x,\omega)$ is continuous in k_x away from the branch cuts, it follows that $K_z = k_z(K_x,\omega_1) \approx iK_x$ in the regime far to the right of the zeros, corresponding to an evanescent behavior in the total internal reflection regime of large K_x. So far, we have not invoked the properties of the medium; in other words, the result is valid for all media and situations where the monochromatic and plane-wave limits exist.

As K_x becomes smaller, we must consider the two passive media separately. For the positive refractive medium [Fig. 6(b)], since the right-hand zero is above the real k_x axis, as we pass it on the way from large k_x to small k_x, the phase $\arg k_z^2$ reduces from π through $\pi/2$ towards $\arg\{\epsilon(\omega_1)\mu(\omega_1)\}$. Again, since $k_z(k_x,\omega)$ is continuous in k_x away from the branch cuts, it follows that $\arg k_z(k_x,\omega_1)$ goes from $\pi/2$ through $\pi/4$ towards the small number $\arg\{\epsilon(\omega_1)\mu(\omega_1)\}/2$. Thus, as expected, we obtain a damped, propagating wave with wave vector directed away from the source.

For the negative refractive medium [Fig. 6(c)], the right-hand zero is below the real k_x axis. Thus, we find that $\arg k_z^2$ increases from π to almost 2π, and therefore, $\arg k_z$ increases from $\pi/2$ to almost π. In other words, K_z will be close to a negative number (negative refraction) in the regime of small K_x.

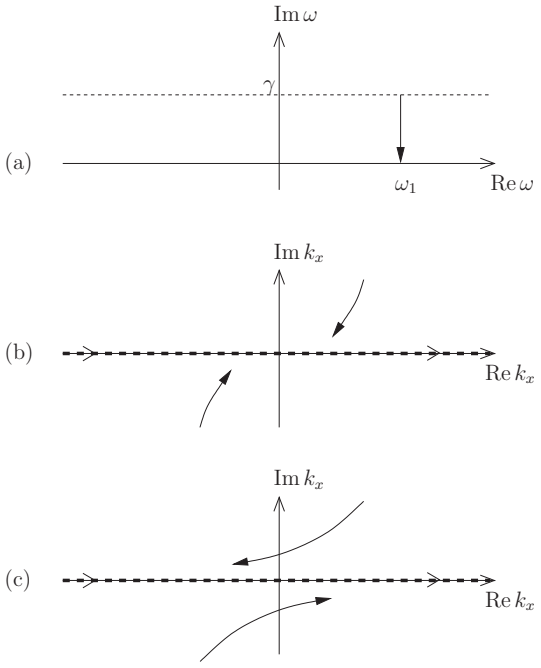

FIG. 6. As $\mathrm{Im}\,\omega$ is reduced from γ to zero (a), k_z's branch points, $k_x = \pm\sqrt{\epsilon\mu}\omega/c$, moves along the trajectories in (b) for a passive, positive refractive medium, and (c) for a passive, negative refractive medium.

B. Weak gain medium

We now consider a weak gain medium, or conventional gain medium, with $|\mathrm{Im}\,\epsilon| \ll 1$ and $|\mathrm{Im}\,\mu| \ll 1$ for all frequencies, and weak dispersion. For example, we can consider a nonmagnetic medium with $\epsilon(\omega) = 1 + \chi(\omega)$, where $\mathrm{Im}\,\chi(\omega)$ is negative at the observation frequency, and $|\chi(\omega)| \ll 1$ for all ω. When we reduce $\mathrm{Im}\,\omega$ as in Fig. 7(a), the branch points $k_x = \pm\sqrt{\epsilon\mu}\omega/c$ move according to Fig. 7(b). Thus, to be able to express the integral (12) with real frequencies ω, it is necessary to deform the k_x integration with detours. These detours are result of the fact that the system supports amplifying side waves with $k_x = \pm\sqrt{\epsilon\mu}\omega/c$.

Having taken the monochromatic limit, we consider the possibility of approaching plane waves. According to the discussion in Sec. IV, the limit $\sigma \to \infty$ does not exist when using excitation profiles of finite support; then, the side waves will diverge. However, for the Gaussian excitation profile $u_2(x)$, and provided $|\mathrm{Im}\,\sqrt{\epsilon\mu}\omega_1/c| < |\mathrm{Re}\,\sqrt{\epsilon\mu}\omega_1/c - K_x|$, we can take the plane-wave limit since then the side waves are very weakly excited. By tracing $\arg k_z$ as k_x is reduced from ∞ (as in Sec. V A), we still obtain $K_z \approx iK_x$ in the total internal refraction regime of large K_x. Thus, the

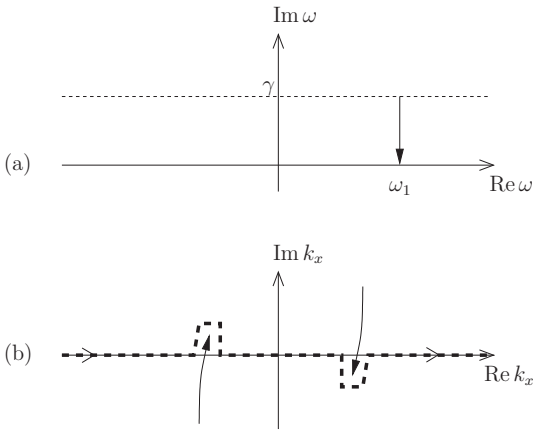

FIG. 7. As $\mathrm{Im}\,\omega$ is reduced from γ to zero (a), k_z's branch points $k_x = \pm\sqrt{\epsilon\mu}\omega/c$ move along the trajectories in (b) for a weak gain medium. The integration path in the k_x domain must detour around these branch points.

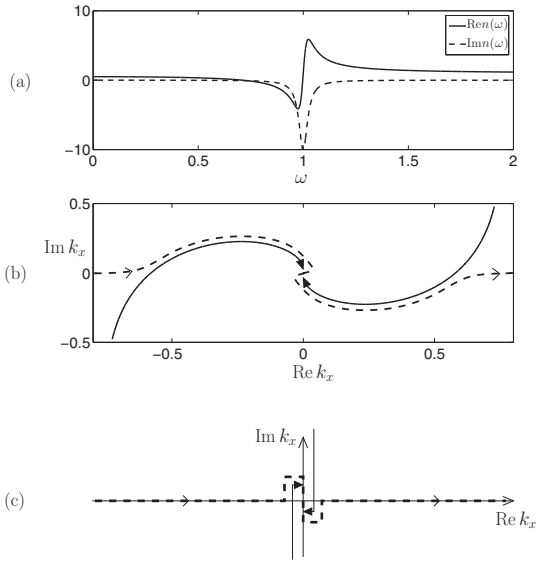

FIG. 8. Plot (a) shows $n(\omega)$ as given by (31). Plot (b) shows the trajectories of k_z's branch points, $k_x = \pm n(\omega)\omega/c$, as $\mathrm{Im}\,\omega$ is reduced from γ to zero, and $\mathrm{Re}\,\omega = \omega_1$. The values for $\omega = \omega_1$ are shown with solid arrows. The branch cuts in the k_x domain, for $\omega = \omega_1$, can be taken along the trajectories (b, solid lines); however, it is convenient to use analytic continuation to deform them into the solid lines shown in (c). The integration path in the k_x domain (dashed line) must detour around the branch cuts.

behavior remains approximately evanescent there, in agreement with earlier predictions [4] and finite-difference time-domain (FDTD) simulations [5]. FDTD simulations solve Maxwell's equations directly in the time domain, and thus provide an independent verification of the theory. For small K_x, since we have passed the zero from below, we get $\arg K_z \approx \arg\{\epsilon(\omega_1)\mu(\omega_1)\}/2$. This represents a weakly amplified wave, a result that is well documented with numerous experiments and simulations.

As an alternative, we can take the plane-wave limit while keeping the Bromwich integration path at $\mathrm{Im}\,\omega = \gamma$, leading to a single wave number K_x. Then, we can deform the Bromwich path towards the real axis; however, there will be branch points close to $\omega = K_x c$, above the real axis. This means that the system supports absolute instabilities, and that the real frequencies are not meaningful in general. The absolute instabilities are again a result of diverging side waves, being excited infinitely far away from the observation point. However, as shown in Ref. [6], as long as the excitation frequency ω_1 is far away from $K_x c$, we can interpret the field as "quasimonochromatic" up to a certain time, where the diverging side waves start to dominate.

C. Nonmagnetic negative index medium

If the permittivity and permeability from the negative index medium in Sec. V A are denoted ϵ_p and μ_p, we let the permittivity of an active, nonmagnetic medium be $\epsilon = \epsilon_\mathrm{p}\mu_\mathrm{p}$. Clearly, the behavior of the branch points and the integration paths becomes identical to that in Fig. 6(c), and we get a negative refractive index at the frequency shown in the figure. This type of media was suggested in Ref. [7] and analyzed in Ref. [8]. When a plane wave is normally incident from vacuum, a backward wave is excited in the medium, drawing energy from the medium and propagating energy towards the interface [8]. However, note that both the phase velocity and the Poynting vector point backwards, so the medium is fundamentally different from left-handed negative index media.

The fact that this type of media exhibits negative refraction has also been independently verified through time-domain simulations, e.g., in Ref. [10].

D. Antievanescent medium

Having analyzed previously known media with the ω- and k_x-integration formalism, we now consider how the formalism can be used to predict novel classes of media. As we reduce $\mathrm{Im}\,\omega$ from γ to zero, the trajectories of k_z's branch points may be more complicated than in the previous examples.

Consider a medium with refractive index

$$n(\omega) = 1 - \frac{F\omega_0^2}{\omega_0^2 - \omega^2 - i\Gamma\omega}, \tag{31}$$

and $F > 0$ [see Fig. 8(a)]. This refractive index can be obtained, e.g., by letting $\epsilon(\omega) = \mu(\omega) = n(\omega)$. Such Lorentzian resonances can be realized in metamaterials; however, there are challenges associated with high gain (see Sec. V E). The same refractive index can be obtained by setting $\epsilon(\omega) = [n(\omega)]^2$ and $\mu = 1$. In the following, we will for simplicity consider this nonmagnetic realization.

Provided $F < 1$, the zeros of $\epsilon(\omega)$ are located in the lower half-plane, so the medium does not support absolute

instabilities. Hence, we may consider the monochromatic limit. We take $F = 0.5$ and $\Gamma = 0.05\omega_0$, and consider the observation frequency $\omega_1 = 0.71\omega_0$, for which $\mathrm{Re}\, n(\omega_1) = 0$ and $\mathrm{Im}\, n(\omega_1) = -i0.072$.

The trajectories of k_z's branch points $k_x = \pm n(\omega)\omega/c$, as $\mathrm{Im}\,\omega$ is reduced from γ to 0 while $\mathrm{Re}\,\omega = \omega_1$, are shown in Fig. 8(b). For $\omega = \omega_1$ we can take the branch cuts along the solid lines in Fig. 8(c), and the integration path along the dashed line. We let the two branch cuts approach each other. Considering an incident wave from vacuum, we find with the help of (11b) and (14)

$$2\pi \frac{E(x,z,\omega_1)}{V(\omega_1)} = \int_{-\infty}^{\infty} U(k_x) \frac{2k_{1z} e^{ik_{2z}z}}{k_{1z}+k_{2z}} e^{ik_x x} dk_x + \int_{-k_b}^{k_b} U(k_x) \left(\frac{2k_{1z} e^{ik_{2z}z}}{k_{1z}+k_{2z}} - \frac{2k_{1z} e^{-ik_{2z}z}}{k_{1z}-k_{2z}} \right) e^{ik_x x} dk_x. \tag{32}$$

Here, the integration $\int_{-k_b}^{k_b}$ is along a vertical path from the lower to the upper branch point [indicated with solid arrows in Fig. 8(c)], immediately to the right of the branch cuts.

To interpret (32), we note that $k_{2z}^2 = n^2(\omega_1)\omega_1^2/c^2 - k_x^2$ is negative for real k_x and also along the vertical integration paths in Fig. 8(c). Since $k_{2z} \to +ik_x$ for $k_x \to +\infty$, k_{2z} must be positive imaginary for real k_x away from the branch cuts. Along the imaginary axis, however, k_{2z} becomes negative imaginary, due to the presence of the right-hand branch cut. We choose an excitation $U(k_x) = U_1(k_x)$, with $K_x = 0$ (normal incidence). Clearly, the plane-wave limit does not exist, as the second integral in (32) involves complex k_x's for which $U_1(k_x)$ diverges as $\sigma \to \infty$. For a finite, though large σ, the field is dominated by the second integral in (32). As a result of the two terms of the second integral, the field contains a superposition of modes with both signs of k_z: evanescent ($\mathrm{Im}\, k_z > 0$) and antievanescent ($\mathrm{Im}\, k_z < 0$).

The situation is different if we take the plane-wave limit before the monochromatic limit. If we still assume $K_x = 0$, we have $K_{2z} = +n(\omega)\omega/c$. Both limits exist, and we end up with the monochromatic field amplitude

$$\mathcal{E}(x,z,t) = \frac{2K_{1z}}{K_{1z}+K_{2z}} e^{iK_x x + iK_{2z}z - i\omega_1 t}. \tag{33}$$

For the medium in this example, $n(\omega)$ is negative imaginary at the observation frequency $\omega = \omega_1$. Thus, we have an antievanescent behavior.

In other words, let the beam width σ be fixed and finite. Then, after sufficiently long time, the field will be a superposition of evanescent and antievanescent modes. On the other hand, for $\sigma \to \infty$, and after a long time the field will be purely antievanescent.

E. Simultaneous refractive index medium

In the previous example, we observed that the evanescent and antievanescent modes were excited simultaneously. We will now demonstrate a remarkable result: that there exist isotropic media exhibiting positive and negative refraction simultaneously.

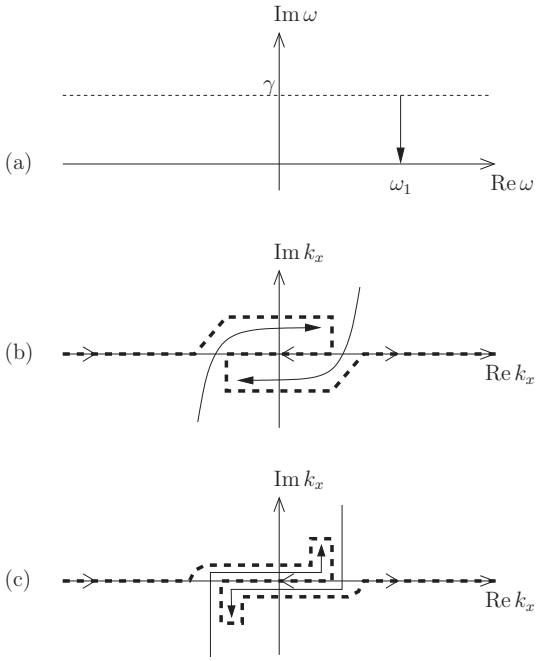

FIG. 9. As $\mathrm{Im}\,\omega$ is reduced from γ to zero (a), k_z's branch points $k_x = \pm\sqrt{\epsilon\mu}\,\omega/c$ move along the trajectories (b). By deforming branch cuts and integration paths, we get situation (c). In (b) the branch cuts are taken to be along the trajectories, while in (c) they are deformed into the solid lines.

Consider the example in Fig. 9. As ω approaches the real axis, the branch point in the first quadrant moves via the fourth to the third quadrant. The integration path therefore becomes zigzag. We consider an incident wave from a passive medium (medium 1) to the medium under investigation (medium 2), and calculate the transmitted field using (11b). Using the integration path in Fig. 9(c), this leads to

$$2\pi \frac{E(x,z,\omega_1)}{V(\omega_1)} = \left(\int_{-\infty}^{-k_b} + \int_{k_b}^{\infty} \right) U(k_x) \frac{2\mu_2 k_{1z} e^{ik_{2z}z}}{\mu_2 k_{1z} + \mu_1 k_{2z}} e^{ik_x x} dk_x + \int_{-k_b}^{k_b} U(k_x) \left(\frac{4\mu_2 k_{1z} e^{ik_{2z}z}}{\mu_2 k_{1z} + \mu_1 k_{2z}} - \frac{2\mu_2 k_{1z} e^{-ik_{2z}z}}{\mu_2 k_{1z} - \mu_1 k_{2z}} \right) e^{ik_x x} dk_x + \int_{\text{vertical detours}} U(k_x) \frac{2\mu_2 k_{1z} e^{ik_{2z}z}}{\mu_2 k_{1z} + \mu_1 k_{2z}} e^{ik_x x} dk_x. \tag{34}$$

In (34), k_b is the real part of the branch point in the first quadrant, and the last integral represents all vertical integration paths in Fig. 9(c), letting the up-and-down paths around a branch cut be infinitely close to each other. In the third line of (34), k_{2z} is the value along the upper integration path, above both branch cuts.

Considering the observation frequency ω_1 (monochromatic limit), we now take the plane-wave limit $\sigma \to \infty$. Using the Gaussian excitation $U_2(k_x)$, the limit exists provided $|\mathrm{Im}\, k_x| < |\mathrm{Re}\, k_x - K_x|$ on the integration path. Assuming $-k_\mathrm{b} < K_x < k_\mathrm{b}$, we end up with

$$\mathcal{E}(x,z,t) = \left(\frac{4\mu_2 K_{1z} e^{iK_{2z}z}}{\mu_2 K_{1z} + \mu_1 K_{2z}} - \frac{2\mu_2 K_{1z} e^{-iK_{2z}z}}{\mu_2 K_{1z} - \mu_1 K_{2z}} \right) e^{iK_x x - i\omega_1 t}. \tag{35}$$

With an excitation $u_1(x)$ of finite support, the limit would not exist; however, for bounded x and z we may come as close as we wish to the field (35) by ensuring that the medium has branch points sufficiently close to the real k_x axis.

On the other hand, by taking the limit $\sigma \to \infty$ without taking the monochromatic limit, we get

$$\mathcal{E}(x,z,t) = \frac{1}{2\pi} \int_{i\gamma-\infty}^{i\gamma+\infty} V(\omega) \frac{2\mu_2 K_{1z}}{\mu_2 K_{1z} + \mu_1 K_{2z}} \times \exp(iK_x x + iK_{2z} z - i\omega t) d\omega. \tag{36}$$

However, moving the integration path down to the real ω axis requires K_{2z} to be analytic for $\mathrm{Im}\, \omega \geqslant 0$. Even for weak gain media, this will not be the case [6], except for the special case $K_x = 0$.

If $K_x = 0$, and both $\sqrt{\epsilon\mu}$ and the Fresnel transmission coefficient are analytic for $\mathrm{Im}\, \omega > 0$, the integration path can in fact be moved down to the real ω axis. In the monochromatic limit, we then get

$$\mathcal{E}(x,z,t) = \frac{2\mu_2 K_{1z}}{\mu_2 K_{1z} + \mu_1 K_{2z}} e^{iK_x x + iK_{2z} z - i\omega_1 t}, \tag{37}$$

with $K_{2z} = +n(\omega_1)\omega_1/c$. This differs from (35), and once again the two orders of the monochromatic and plane-wave limits yield different results.

In other words, consider the case $K_x = 0$, for a sufficiently large, but finite σ. In the monochromatic limit $t \to \infty$, the field will then be approximately given by (35), i.e., a superposition of waves with wave number $+K_{2z}$ and $-K_{2z}$ in the z direction. However, if $\sigma \to \infty$ first, the monochromatic limit leads to a plane wave propagating in the z direction, with wave number $+K_{2z}$. From this, it is understood that simultaneous refraction is a two-dimensional effect. In the case of a finite σ there will always be oblique waves with $k_x \neq 0$ excited, no matter how large σ is. After a sufficiently long time t these oblique waves will somehow establish waves along the z direction with both signs for K_{2z}. However, if $\sigma \to \infty$ is taken first, there will be no oblique waves excited. The simultaneous refracting waves can thus not be established. This latter situation is one dimensional, as the excitation $u_2(x)$ is constant for all x, and $K_x = 0$.

Trajectories for k_z's branch points, similar to those in Fig. 9(b), can be achieved using a medium with the same refractive index (31) as in the previous example, but at a slightly higher observation frequency $\omega_1 = 0.853\omega_0$. At this frequency, and for sufficiently small $|K_x|$, we have $|\mathrm{Im}\, k_x| < |\mathrm{Re}\, k_x - K_x|$ on the integration path [Fig. 9(c)]. Then, the limit $\sigma \to \infty$ exists, and we end up with the field (35) for the Fresnel situation, and a similar result for the current source in the plane $z = 0$ (then the transmission coefficients $\frac{2\mu_2 K_{1z}}{\mu_2 K_{1z} \pm \mu_1 K_{2z}}$ are replaced by $\pm\mu\omega_1/2K_z c$).

The time-domain response of a medium with $\epsilon(\omega) = \mu(\omega) = n(\omega)$, where the refractive index $n(\omega)$ is given by (31), was simulated using the FDTD method [19] for Lorentzian media [20]. In the simulation, the situation with a current source in $z = 0$ was implemented. For $K_x = 0$, $\omega_1 = 0.853\omega_0$, and a finite, but large σ, the field should describe a partially standing wave consisting of traveling waves with both signs of K_z, after sufficiently long time. It turns out, however, that the time it takes to reach the monochromatic limit is much longer than what is possible to simulate.

The simulations show that the fields grow rapidly as they propagate, both in the x and z directions. This rapid growth is explained as follows. Since the excitation vanishes for $t < 0$, it will contain other frequencies than just the observation frequency. Even though the frequency spectrum has a large peak at ω_1, the frequencies around resonance ω_0 will dominate for a very long time, due to extremely high gain there. Indeed, $n(\omega_0) = 1 - 10i$, so at resonance the forward propagating wave will grow as $\exp(20\pi z/\lambda)$, where λ is the vacuum wavelength, as it propagates in the z direction. Also, the side waves, with $k_x = \pm n(\omega_0)\omega_0/c$, will grow at this rate in the $\pm x$ direction. Since $|\mathrm{Im}\, k_x| > |\mathrm{Re}\, k_x|$ these side waves will be strongly excited. For $t \to \infty$, the excitation only contains ω_1, and the field should eventually describe simultaneous refraction. However, as can be verified using frequency-domain simulations, the transients are extremely strong so it takes a very long time for them to die out.

Due to numerical errors, artificial reflections may happen during FDTD if the fields become extremely large. If such artificial reflections occur before the monochromatic limit is reached, the simulation will never be able to reveal simultaneous refraction: waves may be reflected back and forth, being amplified as they propagate, and the solution will eventually grow with time even at fixed points in space.

Nistad and Skaar showed that negative refraction can occur at a single observation frequency ω_1, with arbitrarily low loss for all frequencies, if there is a steep drop in $\mathrm{Im}\, n(\omega)$ just below ω_1 [14]. It is similarly possible to achieve a negative refractive index $n = \sqrt{\epsilon\mu}$ at arbitrarily low gain through a steep drop in $\mathrm{Im}\, n(\omega)$ just above the observation frequency. For such a medium, the trajectories of k_z's branch points will in fact be similar to those in Fig. 9(b) for the frequencies where $n(\omega) < 0$. One such medium, where the maximum gain was reduced to $\mathrm{Im}\, n(\omega) = -2$, was simulated, but artificial reflections destroy the validity of the simulation solution before the transients die out. For FDTD simulations to be able to reveal simultaneous refraction, media with a significantly lower gain, while having branch point trajectories as in Fig. 9(b), must be found.

VI. DISCUSSION AND CONCLUSION

Wave propagation in gain media has been considered by a Fourier-Laplace integral in space and time. How the correct monochromatic and plane-wave limits can be taken is demonstrated by deforming the integration surface in complex frequency–wave-number space. In some cases, it is possible to deform the inverse Laplace transform contour down to the

real ω axis, at the expense of deforming the inverse Fourier k_x-integration path. For active media where this can be done, the path will contain complex k_x, representing amplified waves as they propagate in the x direction. If such a deformation is not possible, the inverse Laplace transform will contain complex frequencies, and the field will therefore grow exponentially with time, even at a fixed point in space: there is an absolute instability.

It is shown that the monochromatic and plane-wave limits generally do not commute; for example, one order may lead to a diverging field, while the other order leads to a finite field. The plane-wave limit may be dependent on whether it is realized by a Gaussian excitation or a finite-support excitation, eventually of infinite width. This is because amplifying side waves are less excited by the Gaussian excitation.

The general path deformation theory is applied to analyze familiar passive and active media, and to predict media with novel properties. In particular, it is shown that certain gain media may be simultaneous refracting, i.e., they refract positively and negatively at the same time. It is argued that this is a two-dimensional effect, i.e., it will not occur if an infinitely wide source produces a wave propagating only in the z direction. The monochromatic plane-wave response of these media generally depends on which of the limits is taken first, or the width of the source relative to the duration of the experiment as both of these parameters tend to infinity.

An example of a simultaneous refracting medium is given. For a large, but finite width of the source, this medium is, in principle, simultaneous refracting after a sufficiently long time, i.e., in the monochromatic limit. In attempt to visualize the effect, and to independently verify the theory, time-domain simulations of this medium were performed. However, the simulations were not able to visualize the effect, as the monochromatic limit never was reached. The suggested medium has a very large gain at resonance, so frequencies of the transients close to resonance will be strongly amplified as they propagate into the medium. Due to the occurrence of artificial reflections before these transients die out, simultaneous refraction is therefore not seen in the simulations. Similar stability problems are expected for experimental realizations. It should therefore be investigated if simultaneous refracting media with significantly less gain exist.

APPENDIX A: PROPERTIES OF $k_z(k_x,\omega)$

We here consider the properties of the function $k_z(k_x,\omega)$ along the real k_x axis, and in a region $\mathrm{Im}\,\omega > \gamma$. The function is defined by (6) and (8). We prove that $k_z(k_x,\omega)$ is zero free and analytic in both arguments. Moreover, $k_z \to +\omega/c$ for $\omega \to \infty$ and fixed k_x, and $k_z \to +ik_x$ for $k_x \to +\infty$ and fixed ω. Initially, we require γ to be large, such that $\epsilon\mu$ is close to unity in the region. In Sec. III, we use analytic continuation to make use of the results in a larger region (i.e., reduce γ).

First, we consider the zeros of $k_z(k_x,\omega)$, given by $k_x = \pm\sqrt{\epsilon\mu}\omega/c$ (see Fig. 10). None of these is located at real k_x since ω is complex in the region $\mathrm{Im}\,\omega > \gamma$ and $\epsilon\mu$ is close to unity there: Consider first a region characterized by a bounded $\mathrm{Re}\,\omega$. If a zero existed for positive k_x, we could just increase γ (and therefore $\mathrm{Im}\,\omega$) such that $\sqrt{\epsilon\mu}$ gets closer to unity

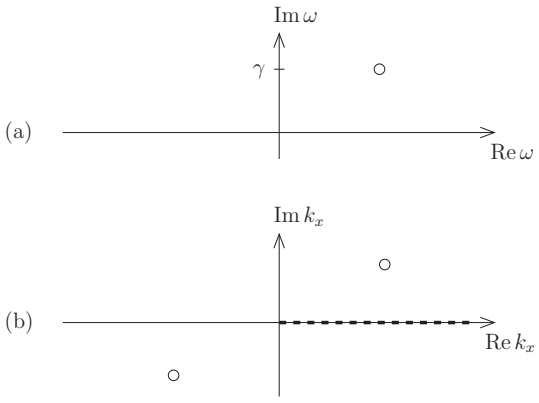

FIG. 10. For a fixed ω, with $\mathrm{Im}\,\omega > \gamma$ and $\mathrm{Re}\,\omega > 0$ [indicated by an open circle in the complex ω plane (a)], the zeros of $k_z^2 = \epsilon\mu\omega^2/c^2 - k_x^2$ are shown in the complex k_x plane (b). For large $\mathrm{Im}\,\omega$, the zeros $k_x = \pm\sqrt{\epsilon\mu}\omega/c$ are located away from the real axis.

and $\arg\omega$ increases; then the zero would move away from the real k_x axis. Next, consider $\mathrm{Re}\,\omega \to \infty$. Since $\sqrt{\epsilon\mu} = 1 + O(\omega^{-2})$, the zeros are located at $k_x = \pm\omega/c + O(\omega^{-1})$. Thus, $k_z(k_x,\omega)$ has no zeros approaching the real k_x axis as $\mathrm{Re}\,\omega \to \infty$.

Second, we argue that $k_z(k_x,\omega)$ is analytic in both arguments. The analyticity in ω has already been established (8), and the analyticity in k_x is immediate from (6) provided there are no sign changes. Indeed, such sign changes are impossible: If $k_z(k_x,\omega)$ were discontinuous in k_x, we could find a (k_x,ω) and a tiny δ such that $k_z(k_x+\delta,\omega) \approx -k_z(k_x,\omega)$. This leads to a contradiction since $k_z(k_x,\omega)$ is zero free and continuous in ω in the region $\mathrm{Im}\,\omega > \gamma$, and $k_z(k_x+\delta,\omega) \to k_z(k_x,\omega)$ as $\omega \to \infty$ there.

It is interesting to examine the behavior of k_z in the limit of large k_x. The sign of k_z for active media in the total internal reflection regime has been discussed extensively in previous literature [3,4,6]. For $k_x = 0$, we have $k_z \approx \omega/c$ in the region $\mathrm{Im}\,\omega > \gamma$. As k_x increases along the dashed line in Fig. 10, the complex argument of k_z^2 increases according to the zero configuration in the figure. Since k_z is a continuous function of k_x it follows that as $k_x \to +\infty$, $k_z \to +ik_x$. This seems to predict an evanescent behavior in the total internal reflection regime of large k_x; however, it is important to remember that we only have considered the complex frequencies with $\mathrm{Im}\,\omega > \gamma$. Interpretation at real frequencies is possible under certain circumstances (Sec. V B) [4,6]; however, for conventional, weak gain media it turns out to be an instability associated with amplified side waves.

APPENDIX B: EXISTENCE OF TRANSFORMS AND INTERCHANGING THE ORDER OF INTEGRATION

Here, we establish the existence of the involved transforms in solving Maxwell's equations, and argue that their order can be interchanged. To establish the existence, we must make assumptions on the electric and magnetic fields, and

their derivatives wrt x, z, and t. These assumptions enable formulating electromagnetics in the (k_x,ω) domain by the $\mathcal{L}^2$ theory of Fourier transforms, to obtain the solutions (11). Finally, we verify that the solutions are consistent with the initial assumptions, making a self-consistent theory.

To limit the amount of writing, we will only consider the electric field $\mathcal{E}(x,z,t)$ here; the other functions can be treated similarly with some small complications from derivatives. We will only consider the solution (11a); the other solution (11b) can be treated similarly. With respect to x the function $\mathcal{E}(x,z,t)$ is assumed to be in the Hilbert space $\mathcal{L}^2$ of square integrable functions. With respect to t, $\mathcal{E}(x,z,t)\exp(-\gamma t)$ is assumed to be in $\mathcal{L}^2$, for a sufficiently large, positive γ. Defining

$$E(x,z,\omega) = \int_0^\infty \mathcal{E}(x,z,t)\exp(i\omega t)dt, \tag{B1a}$$

$$E(k_x,z,t) = \int_{-\infty}^\infty \mathcal{E}(x,z,t)\exp(-ik_x x)dx, \tag{B1b}$$

we assume that $E(x,z,\omega)$ is in $\mathcal{L}^2$ wrt x for $\operatorname{Im}\omega = \gamma$, and $E(k_x,z,t)\exp(-\gamma t)$ is in $\mathcal{L}^2$ wrt t for real k_x. This means that we can Fourier transform $E(x,z,\omega)$ wrt x, or Laplace transform $E(k_x,z,t)$. By solving Maxwell's equation in the resulting transform domain (ω,k_x) we obtain (11a). Our job now is to verify all assumptions, after inverse transformation of (11a).

To this end, we assume that the source $u(x)v(t)$ is sufficiently smooth such that

$$U(k_x)k_x^p \in \mathcal{L}^1 \cap \mathcal{L}^2, \tag{B2a}$$

$$V(\omega)\omega^p \in \mathcal{L}^1 \cap \mathcal{L}^2 \tag{B2b}$$

for $p = 0$, 1, and 2. That a function of ω is in $\mathcal{L}^1 \cap \mathcal{L}^2$, such as, e.g., $V(\omega)$, is to be interpreted as $V(\omega' + i\gamma) \in \mathcal{L}^1 \cap \mathcal{L}^2$ viewed as a function of the real variable ω'.

Consider the factor $\mu\exp(ik_z z)/k_z$ in (11a). A little thought shows that this factor is bounded along the integration surface $(-\infty,\infty)\times(i\gamma-\infty, i\gamma+\infty)$ in the (k_x,ω) space. Thus, $E(k_x,z,\omega) \in \mathcal{L}^1$ wrt (k_x,ω), so with the help of Fubini's theorem we can express $\mathcal{E}(x,z,t)$ with inverse transforms of either order (3).

By taking only one of the inverse transforms in (3), we can write

$$E(x,z,\omega) = \frac{1}{2\pi}\int_{-\infty}^\infty E(k_x,z,\omega)e^{ik_x x}dk_x, \tag{B3a}$$

$$E(k_x,z,t) = \frac{1}{2\pi}\int_{i\gamma-\infty}^{i\gamma+\infty} E(k_x,z,\omega)e^{-i\omega t}d\omega. \tag{B3b}$$

Clearly, $E(k_x,z,\omega) \in \mathcal{L}^2$ both wrt k_x and ω, so the functions $E(x,z,\omega)$ and $E(k_x,z,t)\exp(-\gamma t)$ are in $\mathcal{L}^2$ wrt x and t, respectively.

Substituting (11a) into (B3) we obtain

$$E(x,z,\omega) = \frac{\mu V(\omega)\omega}{4\pi c}\int_{-\infty}^\infty \frac{e^{ik_z z}}{k_z}U(k_x)e^{ik_x x}dk_x, \tag{B4a}$$

$$E(k_x,z,t) = \frac{U(k_x)}{4\pi c}\int_{i\gamma-\infty}^{i\gamma+\infty} \frac{\mu e^{ik_z z}}{k_z}V(\omega)\omega e^{-i\omega t}d\omega. \tag{B4b}$$

Since the integrals in (B4a) and (B4b) are bounded wrt ω and k_x, respectively, it follows that $E(x,z,\omega)$ and $E(k_x,z,t)$ are in $\mathcal{L}^2$ wrt ω and k_x. After the final inverse transforms, we therefore obtain a function $\mathcal{E}(x,z,t)$ for which $\mathcal{E}(x,z,t)\exp(-\gamma t) \in \mathcal{L}^2$ wrt t and x.

We have assumed that the excitation $u(x)v(t)$ is sufficiently smooth, such that $U(k_x)$ and $V(\omega)$ tend to zero sufficiently quickly (B2). Considering the source $U_2(k_x)$, as given by (21), this is automatically satisfied. For $U_1(k_x)$, the condition will be satisfied if $u_1(x)$ is three times differentiable at its endpoints, as evident from (22). For $V(\omega)$, as given by (17), the condition will not be satisfied; however, this can be fixed by slightly smoothening the onset of $v(t)$ such that it is three times differentiable. This makes (17) valid for arbitrarily large ω, before it starts to decay faster. Defining $\tilde{v}(t)$ as the smoothened excitation, $\tilde{v}(t) - v(t)$ has finite support. Thus, $\tilde{V}(\omega) - V(\omega)$ is an entire function, which means that the smoothening does not affect the electric field solution in the monochromatic limit.

The reason for doing this analysis in a more rigorous way than is common in the physics literature is the appearance of unusual phenomena and the need to go back to first principles when considering gain media. Nevertheless, this Appendix shows that the conditions for existence of the transforms are similar for active and passive media; the only difference is that the Fourier transform in time (for passive media) must be replaced with the Laplace transform (for active media).

APPENDIX C: CAUSALITY AND THE TITCHMARSH THEOREM FOR DIVERGING FUNCTIONS

To prove the causality result (9) from the choice (8), we employ the Titchmarsh theorem [17,21], formulated for exponentially diverging functions.

Let $f(t)$ be a causal function

$$f(t) = 0 \quad \text{for} \quad t < 0, \tag{C1}$$

such that $f(t)\exp(-\gamma t)$ is square integrable for some real γ. Consider the Laplace transform of $f(t)$:

$$F(\omega) = \int_0^\infty f(t)\exp(i\omega t)dt. \tag{C2}$$

Then,

$$F(\omega) \text{ is analytic for } \operatorname{Im}\omega > \gamma, \tag{C3}$$

and there is a uniform bound K such that

$$\int_{-\infty}^\infty |F(\omega' + i\gamma')|^2 d\omega' \leqslant K < \infty \quad \text{for all } \gamma' \geqslant \gamma. \tag{C4}$$

The converse result is also true: Let a function $F(\omega)$ be analytic for $\operatorname{Im}\omega > \gamma$ and satisfy (C4) for some K. Then, the inverse Laplace transform

$$f(t) = \frac{1}{2\pi}\int_{i\gamma-\infty}^{i\gamma+\infty} F(\omega)\exp(-i\omega t)d\omega \tag{C5}$$

satisfies (C1) and $f(t)\exp(-\gamma t)$ is square integrable. The proof is immediate from the Titchmarsh theorem by considering the function $f(t)\exp(-\gamma t)$ and its Laplace (or Fourier) transform $F(\omega' + i\gamma)$.

Returning to the electric and magnetic fields for $z > 0$, as expressed by (5), we know that the corresponding time-domain fields are causal (C1). Thus, the fields satisfy (C3) and (C4). This means that $C(k_x,\omega)e^{ik_z z}$ and $D(k_x,\omega)e^{-ik_z z}$, separately, satisfy these conditions. From the initial value theorem and the fact that $k_z c = \omega + O(\omega^{-1})$, it is intuitively clear that the factor $e^{-ik_z z}$ shifts the beginning of the associated time-domain response to earlier times by an amount z/c. Thus, $D(k_x,\omega)e^{-ik_z z}$ can only be compatible with causality for all $z > 0$ if $D(k_x,\omega) \equiv 0$. A rigorous argument goes as follows (here, we suppress the k_x dependence for clarity): Since $D(\omega)\exp(-ik_z z)$ is required to satisfy (C4) for all z, and since $k_z c = \omega + O(\omega^{-1})$, we have for sufficiently large γ

$$\int_{-\infty}^{\infty} |D(\omega' + i\gamma)|^2 d\omega' \leqslant 2K(z)\exp(-2\gamma z/c). \tag{C6}$$

Here, $K(z)$ is independent of γ. If $d(t)$ is the inverse Laplace transform of $D(\omega)$, then $d(t)\exp(-\gamma t)$ is the inverse Laplace transform of $D(\omega + i\gamma)$. Thus, from Parseval's relation, $\int_0^\infty |d(t)|^2 \exp(-2\gamma t)dt = \frac{1}{2\pi}\int_{-\infty}^{\infty} |D(\omega' + i\gamma)|^2 d\omega'$. Combination with (C6) yields

$$\begin{aligned}\int_0^T |d(t)|^2 dt &\leqslant \exp(2\gamma T)\int_0^T |d(t)|^2 \exp(-2\gamma t)dt \\ &\leqslant \exp(2\gamma T)\int_0^\infty |d(t)|^2 \exp(-2\gamma t)dt \\ &\leqslant \frac{K(z)}{\pi}\exp[-2\gamma(z/c - T)]\end{aligned} \tag{C7}$$

valid for any z and T, and for sufficiently large γ. Letting $z/c > T$, it is apparent that we can make the right-hand side as small as we wish, by letting γ be sufficiently large. Since T was arbitrary, $d(t)$ vanishes almost everywhere.

[1] L. Brillouin, *Wave Propagation and Group Velocity* (Academic, New York, 1960).

[2] B. E. Saleh and M. C. Teich, *Fundamentals of Photonics,* 2nd ed. (Wiley, Hoboken, NJ, 2007).

[3] C. J. Koester, IEEE J. Quantum Electron. **2**, 580 (1966); G. N. Romanov and S. S. Shakhidzhanov, Pis'ma Zh. Eksp. Teor. Fiz. **16**, 298 (1972) [JETP Lett. **16**, 209 (1972)]; B. Y. Kogan, V. M. Volkov, and S. A. Lebedev, Pis'ma Zh. Eksp. Teor. Fiz. **16**, 144 (1972) [JETP Lett. **16**, 100 (1972)]; S. A. Lebedev, V. M. Volkov, and B. Y. Kogan, Opt. Spektrosk. **35**, 976 (1973) [Opt. Spectrosc. (USSR) **35**, 565 (1973)]; A. A. Kolokolov, Pis'ma Zh. Eksp. Teor. Fiz. **21**, 660 (1975) [JETP Lett. **21**, 312 (1975)]; P. R. Callary and C. K. Carniglia, J. Opt. Soc. Am. **66**, 775 (1976); W. Lukosz and P. P. Herrmann, Opt. Commun. **17**, 192 (1976); R. F. Cybulski and C. K. Carniglia, J. Opt. Soc. Am. **67**, 1620 (1977); R. F. Cybulski and M. P. Silverman, *ibid.* **73**, 1732 (1983); M. P. Silverman and R. F. Cybulski, *ibid.* **73**, 1739 (1983); A. A. Kolokolov, Radiotekh. Elektron. **43**, 901 (1998) [J. Commun. Technol. Electron. **43**, 837 (1998)]; J. Fan, A. Dogariu, and L. J. Wang, Opt. Express **11**, 299 (2003); A. Siegman, Opt. Photonics News **21**, 38 (2010).

[4] A. A. Kolokolov, Phys. Usp. **42**, 931 (1999).

[5] K. J. Willis, J. B. Schneider, and S. C. Hagness, Opt. Express **16**, 1903 (2008).

[6] J. O. Grepstad and J. Skaar, Opt. Express **19**, 21404 (2011).

[7] Y.-F. Chen, P. Fischer, and F. W. Wise, Phys. Rev. Lett. **95**, 067402 (2005); T. G. Mackay and A. Lakhtakia, *ibid.* **96**, 159701 (2006); S. A. Ramakrishna, *ibid.* **98**, 059701 (2007); Y.-F. Chen, P. Fischer, and F. W. Wise, *ibid.* **96**, 159702 (2006); **98**, 059702 (2007); S. A. Ramakrishna and O. J. F. Martin, Opt. Lett. **30**, 2626 (2005); V. U. Nazarov and Y.-C. Chang, *ibid.* **32**, 2939 (2007); M. Perez-Molina and L. Carretero, *ibid.* **33**, 1828 (2008); V. U. Nazarov and Y.-C. Chang, *ibid.* **33**, 1829 (2008).

[8] J. Skaar, Phys. Rev. E **73**, 026605 (2006).

[9] J. Skaar, Opt. Lett. **31**, 3372 (2006).

[10] J. B. Geddes III T. G. Mackay, and A. Lakhtakia, Opt. Commun. **280**, 120 (2007).

[11] M. Premaratne and G. P. Agrawal, *Light Propagation in Gain Media* (Cambridge University Press, Cambridge, UK, 2011).

[12] S. A. Afanas'ev, D. G. Sannikov, and D. I. Sementsov, J. Commun. Technol. Electron. **58**, 1 (2013).

[13] L. D. Landau and E. M. Lifshitz, *Electrodynamics of Continuous Media* (Pergamon, New York, 1960), Chap. 9.

[14] B. Nistad and J. Skaar, Phys. Rev. E **78**, 036603 (2008).

[15] P. A. Sturrock, Phys. Rev. **112**, 1488 (1958).

[16] R. J. Briggs, *Electron-Stream Interactions with Plasmas* (MIT Press, Boston, 1964).

[17] H. M. Nussenzveig, *Causality and Dispersion Relations* (Academic, New York, 1972), Chap. 1.

[18] L. V. Ahlfors, *Complex Analysis* (McGraw-Hill, New York, 1979).

[19] K. S. Yee, IEEE Trans. Antennas Propag. **14**, 302 (1966).

[20] D. Kelley and R. Luebbers, IEEE Trans. Antennas Propag. **44**, 792 (1996).

[21] E. C. Titchmarsh, *Introduction to the Theory of Fourier Integrals* (Oxford University Press, Oxford, 1948), Chap. 5.

Paper II

Fourier-Laplace analysis and instabilities of a gainy slab

Published in Journal of the Optical Society of America B **32**, 1947-1953 (2015)

Paper III

Dielectric media considered as vacuum with sources

Published in American Journal of Physics **85**, 830 (2017)

Dielectric media considered as vacuum with sources

Hans Olaf Hågenvik and Kjell Bløtekjær
Department of Electronic Systems, NTNU–Norwegian University of Science and Technology, NO-7491 Trondheim, Norway

Johannes Skaar
Department of Electronic Systems, NTNU–Norwegian University of Science and Technology, NO-7491 Trondheim, Norway and Department of Technology Systems, University of Oslo, P.O. Box 70, NO-2027 Kjeller, Norway

(Received 14 March 2017; accepted 6 September 2017)

Conventional textbook treatments on electromagnetic wave propagation consider the induced charge and current densities as "bound" and therefore absorb them into a refractive index. In principle, it must also be possible to treat the medium as vacuum but with explicit charge and current densities, thus giving a more direct, physical description. However, since the induced waves propagate in vacuum in this picture, it is not straightforward to reconcile that the wavelength becomes different compared to that in vacuum. We provide an explanation for this phenomenon, including associated time-domain simulations. As an extra bonus, the results turn out to illuminate the behavior of metamaterials.
[http://dx.doi.org/10.1119/1.5003810]

I. INTRODUCTION

Electromagnetic fields in a medium are governed by Maxwell's equations

$$\nabla \cdot \mathbf{D} = \rho_{\text{free}}, \tag{1a}$$

$$\nabla \cdot \mathbf{B} = 0, \tag{1b}$$

$$\nabla \times \mathbf{E} = i\omega \mathbf{B}, \tag{1c}$$

$$\nabla \times \mathbf{H} = -i\omega \mathbf{D} + \mathbf{J}_{\text{free}}. \tag{1d}$$

Here, we have assumed harmonic time dependence $e^{-i\omega t}$. The two equations containing the auxiliary fields $\mathbf{D}$ and $\mathbf{H}$ are, however, not unique. Their forms are dependent on which charges are considered as "bound" and which are "free." Taking a source-free dielectric medium as an example, the charge and current densities are conventionally considered as bound and therefore described by the polarization density $\mathbf{P}$. In this way, the charges and currents do not bother us; they are simply taken into account by using a (possibly complex) permittivity ϵ. In this picture, the two equations read

$$\nabla \cdot \epsilon \mathbf{E} = 0, \tag{2a}$$

$$\mu_0^{-1} \nabla \times \mathbf{B} = -i\omega \epsilon \mathbf{E}. \tag{2b}$$

But there is another possibility. The medium can be considered as vacuum, with charge and current densities described explicitly. In this picture, the previous equations become

$$\nabla \cdot \epsilon_0 \mathbf{E} = \rho, \tag{3a}$$

$$\mu_0^{-1} \nabla \times \mathbf{B} = -i\omega \epsilon_0 \mathbf{E} + \mathbf{J}. \tag{3b}$$

If we write $\epsilon \mathbf{E} = \epsilon_0 \mathbf{E} + \mathbf{P}$ in Eq. (2), we find the connection between the two pictures

$$\mathbf{J} = -i\omega \mathbf{P}, \tag{4a}$$

$$\rho = -\nabla \cdot \mathbf{P}. \tag{4b}$$

In this note, we would like to use the two pictures to solve Maxwell's equations in a dielectric slab. As we know from basic physics, the phase velocity and wavelength in the medium will be different from the values in vacuum.[1–3] In the first picture, this is shown straightforwardly in terms of a refractive index different from unity. In the second picture, however, it is less straightforward to realize that the phase velocity and wavelength are changed compared to the situation in vacuum. After all, in this picture the medium is considered as vacuum, with additional current and charge densities that can be viewed as sources. One would think that a superposition of waves with vacuum wavelength will result in the same vacuum wavelength.

It is worth mentioning that the second picture does not describe any new physical effects compared to the first picture. While the mathematical reason for the altered wavelength is clear in the first picture (Sec. II), the physical reason will become more transparent in the second (Sec. III). The fact that the induced field exactly cancels the incident field is known as the Ewald-Oseen extinction theorem.[4–6]

When considering wave propagation in dielectric media, it is usually most practical to consider the induced charges and currents as bound. The simplicity of the explanation of the altered wavelength and phase velocity in terms of a different refractive index is definitely appealing compared to the more complicated, but perhaps more illuminating, explanation in the second picture. However, in some circumstances, it is natural to consider induced currents as free, e.g., the induced current in a coil of wire due to a time varying magnetic field.

Whether induced currents should be characterized as free or bound is a relevant question within the research field of metamaterials. By designing structures with characteristic size small compared to the wavelength of the electromagnetic radiation, one may control the induced currents to obtain electromagnetic responses not available in natural materials. The superposition of fields produced by the induced currents in the designed structures gives effective permittivity ϵ_{eff} and permeability μ_{eff}.

As an example, consider a metamaterial consisting of periodically arranged, parallel, thin metallic wires surrounded by

vacuum.[7] For large wavelengths compared to the lattice constant, the metamaterial can be viewed as a continuous plasma with negative effective permittivity. This description corresponds to picture 1, since the currents in the wires are absorbed into an effective permittivity. For sufficiently small wavelengths, it makes little sense to describe the structure using an effective permittivity; it is more practical to describe the currents in the wires explicitly (picture 2). In an intermediate range of wavelengths, the medium can be described with an effective permittivity, however, with spatial dispersion. In this range, both pictures can be useful, dependent on the particular application.

We will consider a simple metamaterial example: 1D propagation through a periodic, layered structure[8] of alternating permittivities ϵ_1 and ϵ_2. The effective permittivity becomes a weighted average of the two permittivities

$$\epsilon_{\text{eff}} = \frac{\epsilon_1 d_1 + \epsilon_2 d_2}{d_1 + d_2}, \tag{5}$$

with d_1 and d_2 being the thicknesses of the two alternating layers. Such a metamaterial structure is used to visualize the second picture through simulations in Sec. IV.

This paper is intended for teachers and students in undergraduate physics who are familiar with basic electromagnetic fields and waves. In particular, the discussion illuminates the freedom in Maxwell's equations when it comes to whether charges and currents are considered as free or bound, thus providing a connection between undergraduate physics education and modern metamaterial research.

II. BOUND CHARGES AND CURRENTS

We consider a dielectric slab, located in the region $0 < z < a$, with vacuum elsewhere, as shown in Fig. 1. The dielectric medium is assumed to be linear, isotropic, and homogeneous. A plane wave is normally incident from a source located at $z = -\infty$. From Maxwell's equations, we can derive Helmholtz' equation

$$E''(z) + \beta^2 E(z) = 0, \tag{6}$$

with the following field solution in the dielectric medium:

$$E(z) = Ae^{i\beta z} + Be^{-i\beta z}. \tag{7}$$

Here, $\beta = kn$, $n = \sqrt{\epsilon_r}$ is the refractive index, $\epsilon_r = \epsilon/\epsilon_0$ is the relative permittivity, $k = \omega/c$ is the vacuum wavenumber, and c is the vacuum light velocity. From Eq. (7), we find that the wavelength in the medium is $2\pi/\beta = (2\pi/k)/n = \lambda/n$, and the phase velocity is c/n. Here, $\lambda = 2\pi/k$ is the vacuum wavelength. The constants A and B can be determined from a, ϵ, and the source by using the electromagnetic boundary conditions, i.e., that the electric and magnetic fields must be continuous at $z = 0$ and $z = a$.

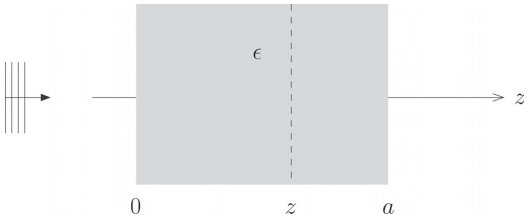

Fig. 1. A dielectric slab located in the region $0 < z < a$. A plane wave is incident from $z = -\infty$.

III. FREE CHARGES AND CURRENTS

We would like to explain the result in Sec. II by considering the medium as charges and currents situated in a vacuum. In each plane $z = z'$ in the material, there is a current density $J(z')$, while the charge density is zero, according to Eq. (4). The current density can be viewed as a source, distributed over the volume of the slab. The current generates a varying magnetic field and therefore also an electric field. By solving Maxwell's equations for a current source plane with surface current density $J(z')\mathrm{d}z'$ in vacuum, we obtain the field

$$\mathrm{d}E_J(z, z') = \begin{cases} -\frac{\eta}{2} J(z') e^{ik(z-z')} \mathrm{d}z' & \text{for } z > z', \\ -\frac{\eta}{2} J(z') e^{-ik(z-z')} \mathrm{d}z' & \text{for } z < z', \end{cases} \tag{8}$$

where $\eta = \sqrt{\mu_0/\epsilon_0}$ is the wave impedance in vacuum (see Appendix A or, e.g., Ref. 9). In the observation plane z, the total electric field will be a superposition of the field from all current planes, in addition to the direct field $E_s(z)$ from the source. If we let $0 < z < a$, we find

$$\begin{aligned} E(z) = E_s(z) &- \frac{\eta}{2} \int_0^z J(z') e^{ik(z-z')} \mathrm{d}z' \\ &- \frac{\eta}{2} \int_z^a J(z') e^{ik(z'-z)} \mathrm{d}z'. \end{aligned} \tag{9}$$

To proceed, we need to know the connection between the electric field and the resulting current. Assuming $J = -i\omega\epsilon_0\chi E$ for a susceptibility χ,

$$\begin{aligned} E(z) = E_s(z) &+ \xi e^{ikz} \int_0^z E(z') e^{-ikz'} \mathrm{d}z' \\ &+ \xi e^{-ikz} \int_z^a E(z') e^{ikz'} \mathrm{d}z', \end{aligned} \tag{10}$$

where $\xi = i\omega\epsilon_0\chi\eta/2 = ik\chi/2$. This integral equation expresses the total electric field as a sum of the source field and the induced field from the currents in the medium.

To solve the integral equation, we differentiate Eq. (10) twice and then substitute the original equation to eliminate the integrals. Taking the source to be $E_s(z) = e^{ikz}$, the result is

$$E''(z) + \beta^2 E(z) = 0, \tag{11}$$

where β now is defined by

$$\beta^2 = k^2(1 - 2i\xi/k) = k^2(1 + \chi). \tag{12}$$

To find the correspondence between the two pictures, we need that $\epsilon_r = 1 + \chi$, which is recognized as the usual connection between susceptibility and permittivity.[1,2]

The general solution to Eq. (11) is given by Eq. (7). The constants A and B cannot be determined from boundary conditions as in Sec. II, since now there is vacuum everywhere. However, they can be determined by Eq. (10) directly. Substituting Eq. (7) back into Eq. (10) gives

$$
\begin{aligned}
E(z) &= Ae^{i\beta z} + Be^{-i\beta z} \\
&= e^{ikz} + \xi Ae^{ikz}\int_0^z e^{i\beta z' - ikz'}\,\mathrm{d}z' \\
&\quad + \xi Be^{ikz}\int_0^z e^{-i\beta z' - ikz'}\,\mathrm{d}z' \\
&\quad + \xi Ae^{-ikz}\int_z^a e^{i\beta z' + ikz'}\,\mathrm{d}z' \\
&\quad + \xi Be^{-ikz}\int_z^a e^{-i\beta z' + ikz'}\,\mathrm{d}z'. \qquad (13)
\end{aligned}
$$

By calculating the integrals, one finds that the coefficients of the resulting $e^{\pm i\beta z}$ terms balance on each side of the equation. Once these terms are removed, A and B are found so as to make the remaining $e^{\pm ikz}$ terms exactly cancel. In particular, it then turns out that the z-dependence of the integral terms cancels the e^{ikz} dependence of the source.

The reason for the $e^{\pm i\beta z}$ dependence in the medium, rather than $e^{\pm ikz}$, can be explained intuitively as follows. First, let the observation plane z be outside the slab, i.e., $z > a$. Rather than Eq. (10), we would then have

$$
E(z) = E_s(z) + \xi e^{ikz}\int_0^a E(z')e^{-ikz'}\,\mathrm{d}z', \qquad (14)
$$

since now the observation plane is located to the right of all current sources ($z > z'$). Similarly, for $z < 0$ we have

$$
E(z) = E_s(z) + \xi e^{-ikz}\int_0^a E(z')e^{ikz'}\,\mathrm{d}z'. \qquad (15)
$$

Clearly, all sources (or induced currents) generate waves of the form $e^{\pm ikz}$, which, after superposition, also can be written in this form.

Returning to an observation plane inside the slab, we must use Eq. (10). As we move the observation plane to the right, a different set of sources will contribute to the forward-propagating wave, as seen by the upper limit z in the first integral. What this means is that the z-dependence is not only a result of the z-dependence of each wave separately but also a result of the fact that the set of contributing sources to the left of the observation plane is dependent on the position of the observation plane.

This provides a different perspective compared to the analysis by James and Griffiths,[3] who viewed the response of the dielectric medium as a perturbation expansion—the vacuum electric field induces a polarization, which induces a field, which in turn induces another polarization, etc. While such a perturbation series converges to a wave with reduced speed c/n, the analysis is somewhat complicated and does not explain the physical mechanism for the altered wavelength in terms of z-dependent sets of sources.

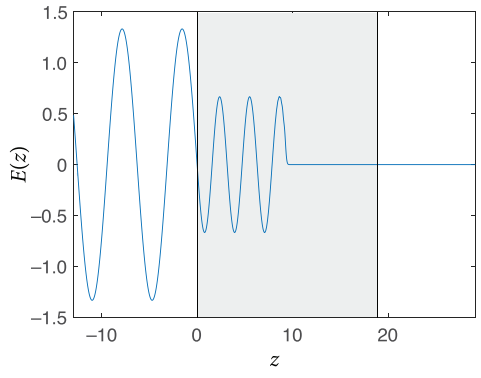

Fig. 2. A plane wave is incident from a source located at $z = -\infty$ propagating through a dielectric slab with constant permittivity $\epsilon_r = 4$ (enhanced online) [URL: http://dx.doi.org/10.1119/1.5003810.1].

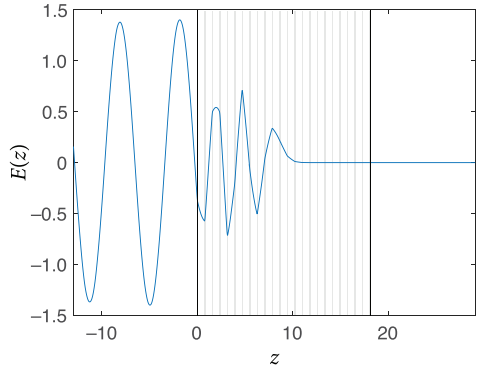

Fig. 3. A plane wave is incident from a source located at $z = -\infty$ propagating through a metamaterial slab with $\epsilon_{\text{eff}} = 4$. The slab is a layered structure where a high-index medium with $\epsilon_2 = 31$ fills 10% of the slab volume; the remaining layers consist of vacuum with $\epsilon_1 = 1$ (enhanced online) [URL: http://dx.doi.org/10.1119/1.5003810.2].

IV. FINITE TIME DOMAIN SIMULATIONS

Figures 2 and 3 show the resulting electric field of an electromagnetic wave propagating through a slab. We have used Finite Difference Time Domain (FDTD) simulations[10–12] of the conventional Maxwell equations in a dielectric medium, i.e., the time-domain counterparts of Eqs. (1b), (1c), and (2). Outside the slab there is vacuum. In both simulations, normalized units have been used. The source produces a wave with frequency $\omega = 1$ approaching the slab from the left. The speed of light in vacuum is taken to be $c = 1$. Using these units, the vacuum wavelength at $\omega = 1$ is $\lambda = 2\pi$.

In Fig. 2, the slab consists of a dielectric medium with $\epsilon_r = 4$, which gives a refractive index $n = \sqrt{\epsilon_r} = 2$. The wave propagates at the speed $c/2$, and the wavelength inside the slab is $\lambda/2$, in agreement with the first picture described in Sec. II.

In Fig. 3, the slab is a composite medium or metamaterial. The layered structure consists of a high-index medium ($\epsilon_2 = 31$) which fills 10% of the slab volume. Between the high-index layers, there is vacuum ($\epsilon_1 = 1$). According to Eq. (5), the homogenized, effective permittivity is $\epsilon_{\text{eff}} = 4$. The high-index layers are distributed evenly throughout the slab, with a separation distance such that there are approximately four unit cells over one effective wavelength. In other words, we have essentially compressed the induced currents in the homogeneous slab into thin current sheets surrounded by vacuum.

In some sense, Fig. 3 therefore visualizes the second picture described in Sec. III—the total electric field is a superposition of the source field and the fields produced by induced currents in all high-index layers. When viewing the field in Fig. 3 in detail, one finds that the variation with z in the vacuum layers is slow, corresponding to waves in a vacuum, while the variation in the high-index layers is rapid.

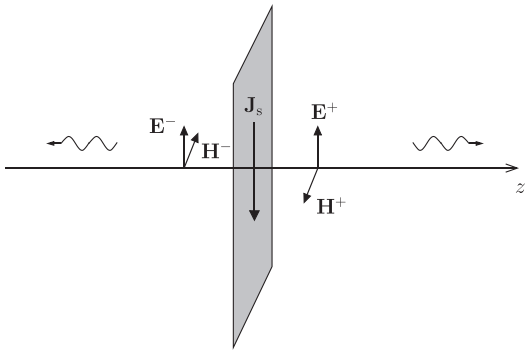

Fig. 4. A uniform surface current source $\mathbf{J}_s$ is located in the plane $z=0$. A harmonic time dependence $e^{-i\omega t}$ is assumed.

However, the resulting wave, if the small features are washed out, is approximately as in Fig. 2. In the present simulation, the parameters were chosen such that the nonideal effects are visible so that one sees the behavior in the different layers. A more homogeneous solution could be obtained by spreading the high-index layers out, i.e., by having more units cells per wavelength.

V. CONCLUSION

We have described propagation through a dielectric slab using two different pictures. The first picture, which is the conventional one, regards the induced charges and currents as bound, conveniently absorbing them into a relative permittivity ϵ_r. The fact that the wavelength and phase velocity of the electromagnetic wave are different in the medium compared to the situation in vacuum is explained in terms of a refractive index $n=\sqrt{\epsilon_r}$.

In the second picture, the medium is instead considered as vacuum with source charge and current densities. A superposition of waves from sources in vacuum seems to imply a wavelength equal to the vacuum wavelength. However, by examining the superposition in detail, we find that the altered wavelength and propagation speed are a result of the fact that the set of sources to the left and right of an observation plane z depends on z. Although the calculations become more complicated, this picture provides useful physical insights.

Figures and animations of the resulting electric field from FDTD simulations are provided to visualize the two descriptions. The second picture, together with the simulation of the metamaterial slab, may also be useful when it comes to understanding the homogenized, effective parameters of metamaterials.

APPENDIX: FIELD FROM A UNIFORM SURFACE CURRENT SOURCE

Let a uniform surface current source $\mathbf{J}_s$ be located in the plane $z=0$ and surrounded by vacuum (see Fig. 4). We want to determine the electric field everywhere. In the region $z>0$, the electric field solution to Helmholtz' equation must be of the type $\mathbf{E}^+e^{ikz}$, while in the region $z<0$ we must have a field $\mathbf{E}^-e^{-ikz}$. From reflection symmetry about the plane $z=0$, we must have $\mathbf{E}^-=\mathbf{E}^+$. We choose the coordinate system such that $\mathbf{E}^+=E^+\hat{\mathbf{x}}$. From Faraday's law, this gives a magnetic field

$$\mathbf{H}^+=\frac{1}{i\omega\mu_0}\nabla\times\mathbf{E}^+=\frac{kE^+}{\omega\mu_0}\hat{\mathbf{y}}=\frac{E^+}{\eta}\hat{\mathbf{y}}, \tag{A1}$$

and similarly we find $\mathbf{H}^-=-\mathbf{H}^+$. Now, we apply the Maxwell boundary condition

$$\mathbf{H}^+-\mathbf{H}^-=\mathbf{J}_s\times\hat{\mathbf{z}} \tag{A2}$$

to determine the constant $\mathbf{E}^+$. This gives $\mathbf{E}^+=-(\eta/2)\mathbf{J}_s$ and therefore

$$\mathbf{E}(z)=\begin{cases}-\dfrac{\eta}{2}\mathbf{J}_s e^{ikz} & \text{for } z>0,\\ -\dfrac{\eta}{2}\mathbf{J}_s e^{-ikz} & \text{for } z<0.\end{cases} \tag{A3}$$

[1]L. D. Landau, E. M. Lifshitz, and L. P. Pitaevskii, *Electrodynamics of Continuous Media* (Pergamon Press, Oxford, 1984).
[2]J. D. Jackson, *Classical Electrodynamics* (Wiley, New Jersey, 1999).
[3]M. B. James and D. J. Griffiths, "Why the speed of light is reduced in a transparent medium," Am. J. Phys. **60**, 309–313 (1992).
[4]M. Born and E. Wolf, *Principles of Optics*, 7th ed. (Cambridge U.P., Cambridge, 1999), Chap. 2.4.2.
[5]H. Fearn, D. F. V. James, and P. W. Milonni, "Microscopic approach to reflection, transmission, and the Ewald-Oseen extinction theorem," Am. J. Phys. **64**, 986–995 (1996).
[6]V. C. Ballenegger and T. A. Weber, "The Ewald-Oseen extinction theorem and extinction lengths," Am. J. Phys. **67**, 599–605 (1999).
[7]J. B. Pendry, A. J. Holden, D. J. Robbins, and W. J. Stewart, "Low frequency plasmons in thin-wire structures," J. Phys.: Condens. Matter **10**, 4785–4809 (1998).
[8]B. E. A. Saleh and M. C. Teich, *Fundamentals of Photonics* (Wiley, New Jersey, 2007).
[9]D. M. Pozar, *Microwave Engineering* (Wiley, New Jersey, 2012).
[10]K. S. Yee, "Numerical solution of initial boundary value problems involving Maxwell's equations in isotropic media," IEEE Trans. Antennas Propag. **14**, 302–307 (1966).
[11]K. S. Kunz and R. J. Luebbers, *The Finite Difference Time Domain Method for Electromagnetics* (CRC Press, New York, 1993).
[12]J. B. Schneider, Understanding the Finite-Difference Time-Domain Method, 2010 can be determined at <http://www.eecs.wsu.edu/~schneidj/ufdtd/ufdtd.pdf>.

Paper IV

Higher order multipoles in metamaterial homogenization

Published in IEEE Trans. Antennas Propag. **66**, 11 (2018)

Paper V

Four definitions of magnetic permeability for periodic metamaterials

Published in Physical Review B **99**, 064407 (2019)

Four definitions of magnetic permeability for periodic metamaterials

Johannes Skaar,[1,*] Hans Olaf Hågenvik,[2] and Christopher A. Dirdal[3]
[1]*Department of Technology Systems, University of Oslo, P. O. Box 70, NO-2027 Kjeller, Norway*
[2]*Department of Electronic Systems, NTNU—Norwegian University of Science and Technology, NO-7491 Trondheim, Norway*
[3]*SINTEF Digital, Microsystems and Nanotechnology, NO-0373 Oslo, Norway*

(Received 19 October 2018; published 7 February 2019)

We state and compare four different definitions of magnetic permeability for periodic, artificial media, or metamaterials. The connections among them, and properties in general, are discussed in detail, including causality, passivity, symmetry, asymptotic behavior, and origin dependence. The analysis is limited to metamaterials made from linear and nonmagnetic constituents.

DOI: 10.1103/PhysRevB.99.064407

I. INTRODUCTION

In their famous textbook [1], Landau and Lifshitz argue that magnetic permeability ceases to have any physical meaning at relatively low frequencies and above. The basis of their argument is that for high frequencies, the electric polarization current may become comparable or even larger than the current from the microscopic magnetization, contributing to the magnetic moment of the sample. The microscopic magnetization cannot therefore be interpreted as the total magnetic moment density.

For metamaterials, such as the split-ring resonator medium proposed by Pendry [2], the induced current in the inclusions is actually the main source of magnetism. By defining a macroscopic magnetization vector to describe a given part of the induced current, we obtain a definition of magnetic permeability which in principle can be used for all frequencies. However, this raises several questions. First, how should the induced current be decomposed into a magnetization term, electric polarization term, and possibly other terms? Second, will the resulting permeability have the "conventional" properties that we expect for a permeability?

We limit the discussion to periodic media. Clearly, there is an infinite number of possibilities to decompose the induced current [1,3–9]; any transversal part of the induced current can be described both as a time-dependent, electric polarization term and a magnetization term. We will consider four possibilities: In the so-called Landau-Lifshitz formulation (Sec. III A), all induced current is described by the electric polarization vector and therefore permittivity. Another natural and well-known possibility is to define the magnetization as the magnetic moment density of the sample, using a fixed origin in each unit cell (Sec. III B). A variant of this approach was proposed by Yaghjian, Alù, and Silveirinha [8], using a decomposition of induced current in Vinogradov and Aivazyan [3] (Sec. III C). A final possibility is to define the permeability to include "as much as possible" of the second-order spatial dispersion of the Landau-Lifshitz permittivity. This approach was used by Landau, Lifshitz, and Pitaevskii [1] and Silveirinha [5] and is generalized here (Sec. III D). The method used to construct other decompositions will be described briefly in Sec. III E.

Dependent on the particular decomposition, the resulting permeability gets more or less nonlocal (or dependent on wave number $\mathbf{k}$). However, at least for metamaterials which mimic natural magnetism, we expect that all four permeabilities coincide for low frequencies and that they are local there. Nevertheless, to obtain a sufficiently large response, metamaterials are often used for relatively large frequencies where the lattice constant is comparable to the wavelength. In this region the permeabilities may differ (Sec. IV).

In Secs. III and IV we will compare the different permeabilities and discuss their properties, including causality/analyticity, passivity, symmetry, asymptotic behavior, and origin dependence. While some of these properties have been established previously, at least for certain permeabilities or with limited generality, the complete list, with associated proofs, is new, to the best of our knowledge. In particular, we develop a rigorous framework where the source is treated as the proper input to the system and obtain analyticity and invertibility for the tensor response function and the Landau-Lifshitz permittivity tensor. This framework turns out to be useful to establish that all inverse permeabilities are causal (only one of them were known to be causal from Ref. [8]). Furthermore, we determine the asymptotic behavior of the permeabilities. We also find analytically and numerically that all permeabilities may be different even for small ka, where a is the lattice constant. This may appear surprising when comparing the definitions of magnetization in Secs. III B and III C. Finally, a novel feature about the formulations is that even for nongyrotropic media, the magnetizations are allowed to depend on the longitudinal electric field. This is necessary to obtain a general treatment valid in the absence of symmetries.

Before reviewing the homogenization procedure, we will make a couple of definitions. The analysis happens in the frequency domain. The fields and parameters are clearly dependent on frequency in general; however, for simplicity in notation, we will usually not write this dependence explicitly. We use the standard notations $O(k^n)$ and $\Theta(k^n)$ for the asymptotic behavior near zero or infinity; $O(k^n)$ is used for

*johannes.skaar@its.uio.no

expressions that are less than or equal to Ck^n (C sufficiently large constant), while $\Theta(k^n)$ means expressions that tends to Ck^n for some constant C.

A time-domain function or distribution $f(t)$ is said to be *causal* if it vanishes for $t < 0$. A frequency-domain function $f(\omega)$ is said to be *causal* if

(i) $f(\omega)$ is analytic in an upper half-plane $\mathrm{Im}\,\omega > \gamma$, where γ is some real constant;

(ii) $f(\omega) = O(|\omega|^n)$ as $\omega \to \infty$ in this half-plane, for some integer n.

This definition makes sense because of the following result from the theory of Laplace transforms [10]: Any function $f(\omega)$ satisfying (i) and (ii) above can be represented as a Laplace transform of a causal time-domain function or distribution $f(t)$, setting the Laplace variable $s = -i\omega$.

II. HOMOGENIZATION

We consider a cubic periodic metamaterial. The metamaterial inclusions are assumed to be linear, nonmagnetic, passive, and time-shift invariant. The microscopic, complex, relative permittivity in a unit cell will be denoted $\varepsilon(\mathbf{r})$. The permittivity and permeability in vacuum are ϵ_0 and μ_0, respectively, and the vacuum light velocity is $c = 1/\sqrt{\epsilon_0\mu_0}$. Angular frequency is denoted ω. The microscopic Maxwell curl equations in the frequency domain are

$$\nabla \times \mathbf{e}(\mathbf{r}) = i\omega \mathbf{b}(\mathbf{r}), \tag{1a}$$

$$\frac{1}{\mu_0}\nabla \times \mathbf{b}(\mathbf{r}) = -i\omega\epsilon_0 \mathbf{e}(\mathbf{r}) + \mathbf{j}(\mathbf{r}) + \mathbf{j}_{\mathrm{ext}}(\mathbf{r}), \tag{1b}$$

with time dependence convention $\exp(-i\omega t)$. Here $\mathbf{j}(\mathbf{r})$ is the induced current density, which includes the "bound" current due to time-dependent, electric polarization density. Moreover, $\mathbf{j}_{\mathrm{ext}}(\mathbf{r})$ represents an external source current density, which can be expressed by an inverse Fourier transform

$$\mathbf{j}_{\mathrm{ext}}(\mathbf{r}) = \frac{1}{(2\pi)^3}\int \mathbf{J}_{\mathrm{ext}}(\mathbf{k}) e^{i\mathbf{k}\cdot\mathbf{r}} d^3k. \tag{2}$$

To probe the metamaterial in the appropriate regime, it is natural to assume that the source is slowly varying over a unit cell size a, so that essentially only k values with $ka \ll 1$ contribute in the integral. However, this assumption is only necessary if we want our macroscopic fields to be true spatial averages [see the paragraph with Eqs. (8) and (9)].

It is convenient to consider each spatial Fourier component in (2) separately to enable the use of Floquet theory. Rather than (2), we will therefore use a source[1]

$$\mathbf{j}_{\mathrm{ext}}(\mathbf{r}) = \mathbf{J}_{\mathrm{ext}}(\mathbf{k}) e^{i\mathbf{k}\cdot\mathbf{r}}. \tag{3}$$

Then Floquet theory ensures that the fields can be written in the forms

$$\mathbf{e}(\mathbf{r}) = \mathbf{u}_{\mathbf{e}}(\mathbf{r},\mathbf{k}) e^{i\mathbf{k}\cdot\mathbf{r}}, \tag{4a}$$

$$\mathbf{b}(\mathbf{r}) = \mathbf{u}_{\mathbf{b}}(\mathbf{r},\mathbf{k}) e^{i\mathbf{k}\cdot\mathbf{r}}, \tag{4b}$$

$$\mathbf{j}(\mathbf{r}) = \mathbf{u}_{\mathbf{j}}(\mathbf{r},\mathbf{k}) e^{i\mathbf{k}\cdot\mathbf{r}}, \tag{4c}$$

[1]The dimension of $\mathbf{J}_{\mathrm{ext}}(\mathbf{k})$ in (3) has an extra m^{-3}.

where $\mathbf{u}_{\mathbf{e}}(\mathbf{r},\mathbf{k})$, $\mathbf{u}_{\mathbf{b}}(\mathbf{r},\mathbf{k})$, and $\mathbf{u}_{\mathbf{j}}(\mathbf{r},\mathbf{k})$ are periodic functions with periods equal to those of the material. Thus we can write

$$\mathbf{u}_{\mathbf{e}}(\mathbf{r},\mathbf{k}) = \sum_{lmn} \mathbf{E}_{lmn}(\mathbf{k}) e^{i\mathbf{b}_{lmn}\cdot\mathbf{r}}, \tag{5}$$

where $\mathbf{b}_{lmn}$'s are the reciprocal lattice vectors. In other words, the resulting field $\mathbf{e}(\mathbf{r})$ contains a discrete Fourier spectrum, with a fundamental component

$$\mathbf{E}(\mathbf{k}) \equiv \mathbf{E}_{000}(\mathbf{k}). \tag{6}$$

This component is the zeroth Fourier coefficient of the periodic function $\mathbf{u}_{\mathbf{e}}(\mathbf{r},\mathbf{k})$:

$$\mathbf{E}(\mathbf{k}) = \frac{1}{V}\int_V \mathbf{u}_{\mathbf{e}}(\mathbf{r},\mathbf{k}) d^3r = \frac{1}{V}\int_V \mathbf{e}(\mathbf{r}) e^{-i\mathbf{k}\cdot\mathbf{r}} d^3r, \tag{7a}$$

where V denotes the volume of a unit cell. Note that (7a) is not a Fourier transform, as $\mathbf{e}(\mathbf{r})$ is dependent on $\mathbf{k}$. Similarly, we have

$$\mathbf{B}(\mathbf{k}) = \frac{1}{V}\int_V \mathbf{u}_{\mathbf{b}}(\mathbf{r},\mathbf{k}) d^3r = \frac{1}{V}\int_V \mathbf{b}(\mathbf{r}) e^{-i\mathbf{k}\cdot\mathbf{r}} d^3r, \tag{7b}$$

$$\mathbf{J}(\mathbf{k}) = \frac{1}{V}\int_V \mathbf{u}_{\mathbf{j}}(\mathbf{r},\mathbf{k}) d^3r = \frac{1}{V}\int_V \mathbf{j}(\mathbf{r}) e^{-i\mathbf{k}\cdot\mathbf{r}} d^3r. \tag{7c}$$

As in Refs. [5,7,8], we define the macroscopic field associated with the single-Fourier-component source as

$$\mathcal{E}(\mathbf{r}) = \mathbf{E}(\mathbf{k}) e^{i\mathbf{k}\cdot\mathbf{r}}, \tag{8a}$$

$$\mathcal{B}(\mathbf{r}) = \mathbf{B}(\mathbf{k}) e^{i\mathbf{k}\cdot\mathbf{r}}, \tag{8b}$$

$$\mathcal{J}(\mathbf{r}) = \mathbf{J}(\mathbf{k}) e^{i\mathbf{k}\cdot\mathbf{r}}. \tag{8c}$$

This definition, from the fundamental Floquet mode can in principle be used for all $\mathbf{k}$ and ω. Only when $ka \ll 1$ can we view the macroscopic fields as true spatial averages according to

$$\mathcal{E}(\mathbf{r}) = \int f(\mathbf{r}')\mathbf{e}(\mathbf{r}-\mathbf{r}') d^3r', \tag{9a}$$

$$\mathcal{B}(\mathbf{r}) = \int f(\mathbf{r}')\mathbf{b}(\mathbf{r}-\mathbf{r}') d^3r', \tag{9b}$$

$$\mathcal{J}(\mathbf{r}) = \int f(\mathbf{r}')\mathbf{j}(\mathbf{r}-\mathbf{r}') d^3r'. \tag{9c}$$

Here $f(\mathbf{r})$ is a test function whose Fourier transform is negligible outside the first Brillouin zone and normalized to unity for $\mathbf{k} = 0$. The equivalence of (9) and (8) under these conditions is established by Fourier transforming (9) [11].

Starting from the microscopic Maxwell equations (1), using (4) and (5), we can prove (see Appendix A for details):

$$i\mathbf{k} \times \mathbf{E}(\mathbf{k}) - i\omega \mathbf{B}(\mathbf{k}) = 0, \tag{10a}$$

$$\frac{1}{\mu_0} i\mathbf{k} \times \mathbf{B}(\mathbf{k}) + i\omega\epsilon_0 \mathbf{E}(\mathbf{k}) - \mathbf{J}(\mathbf{k}) = \mathbf{J}_{\mathrm{ext}}(\mathbf{k}). \tag{10b}$$

As will become clear in the next two paragraphs, Eqs. (10) should be viewed as the $\mathbf{k}$-space counterparts of Maxwell's equations for macroscopic fields $\mathcal{E}(\mathbf{r})$, $\mathcal{B}(\mathbf{r})$, and $\mathcal{J}(\mathbf{r})$. They are *not* the $\mathbf{k}$-space counterparts of the microscopic Maxwell equations.

In this work we will mostly use the single-Fourier-component source. However, we will now discuss the macroscopic field after superposition of the spatial Fourier components according to (2). Rather than (8a) we then have the macroscopic field

$$\boldsymbol{\mathcal{E}}(\mathbf{r}) = \frac{1}{(2\pi)^3}\int \mathbf{E}(\mathbf{k})e^{i\mathbf{k}\cdot\mathbf{r}}d^3k, \tag{11}$$

which is the inverse Fourier transform of the fundamental Floquet mode $\mathbf{E}(\mathbf{k})$. The macroscopic fields $\boldsymbol{\mathcal{B}}(\mathbf{r})$ and $\boldsymbol{\mathcal{J}}(\mathbf{r})$ are expressed similarly. It is important to note that $\boldsymbol{\mathcal{E}}(\mathbf{r}) \neq \mathbf{e}(\mathbf{r})$ in general. Even for wave-number spectra with $ka \ll 1$, the microscopic field $\mathbf{e}(\mathbf{r})$ may vary rapidly in the unit cell, as described by the periodic function (5). The operation (7a) picks only out the constant term in (5), and the inverse Fourier transform (11) is not able to restore the rapid variation.

By inverse Fourier transforming (10) we obtain the Maxwell equations for the macroscopic fields (or fundamental Floquet modes):

$$\nabla \times \boldsymbol{\mathcal{E}}(\mathbf{r}) - i\omega\boldsymbol{\mathcal{B}}(\mathbf{r}) = 0, \tag{12a}$$

$$\frac{1}{\mu_0}\nabla \times \boldsymbol{\mathcal{B}}(\mathbf{r}) + i\omega\epsilon_0\boldsymbol{\mathcal{E}}(\mathbf{r}) - \boldsymbol{\mathcal{J}}(\mathbf{r}) = \mathbf{j}_{\text{ext}}(\mathbf{r}). \tag{12b}$$

In principle, the Maxwell equations (10) and (12) are valid for all ω and any spectra of $\mathbf{k}$'s. In other words, although it is natural to assume that $ka \ll 1$ for the contributing modes, such that the macroscopic fields are true spatial averages, we may in principle use the macroscopic fields for the entire $\mathbf{k}$ and ω spectrum, as long as we recall their meaning as fundamental Floquet modes. A natural question then is if the macroscopic fields have any physical significance for arbitrary ka. Indeed, it turns out that they can be used to calculate the work done by the source in each unit cell, provided the wave-number spectrum is sufficiently narrow (Appendix B).

Note that in the presence of a source, ω and $\mathbf{k}$ are free parameters [5,7,8,12], resulting from the Fourier decomposition of the source with respect to t and $\mathbf{r}$. For example, the homogenized electric field is described in $(\omega, \mathbf{k})$ space by the quantity $\mathbf{E}(\mathbf{k})$, which is dependent on ω and $\mathbf{k}$ separately (the ω dependence is suppressed in the notation). For discussions on causality and asymptotic behavior we will hold $\mathbf{k}$ fixed and vary ω. This corresponds to considering the frequency (or temporal) dependence of a single spatial Fourier component of the source and the associated response. As seen below, this leads, e.g., to a causal Landau-Lifshitz permittivity [1,12].

III. INDUCED CURRENT

Now the big question is how to decompose the induced current density to obtain a macroscopic permittivity, permeability, and possibly other parameters. In the most convenient and conventional case, we can express

$$\mathbf{J}(\mathbf{k}) = -i\omega\mathbf{P}(\mathbf{k}) + i\mathbf{k}\times\mathbf{M}(\mathbf{k}), \tag{13a}$$

$$\mathbf{P}(\mathbf{k}) = \epsilon_0(\boldsymbol{\epsilon} - 1)\mathbf{E}(\mathbf{k}), \tag{13b}$$

$$\mathbf{M}(\mathbf{k}) = \mu_0^{-1}(1 - \boldsymbol{\mu}^{-1})\mathbf{B}(\mathbf{k}), \tag{13c}$$

for some relative permittivity and permeability tensors $\boldsymbol{\epsilon}$ and $\boldsymbol{\mu}$ independent of $\mathbf{k}$. Then we have a local description of the constitutive relations. By defining auxiliary fields

$$\mathbf{D}(\mathbf{k}) = \epsilon_0\mathbf{E}(\mathbf{k}) + \mathbf{P}(\mathbf{k}), \tag{14a}$$

$$\mathbf{H}(\mathbf{k}) = \mathbf{B}(\mathbf{k})/\mu_0 - \mathbf{M}(\mathbf{k}), \tag{14b}$$

Maxwell's equations (10) can be written

$$i\mathbf{k}\times\mathbf{E}(\mathbf{k}) - i\omega\mathbf{B}(\mathbf{k}) = 0, \tag{15a}$$

$$i\mathbf{k}\times\mathbf{H}(\mathbf{k}) + i\omega\mathbf{D}(\mathbf{k}) = \mathbf{J}_{\text{ext}}(\mathbf{k}). \tag{15b}$$

Transforming to the spatial domain,

$$\nabla\times\boldsymbol{\mathcal{E}}(\mathbf{r}) - i\omega\boldsymbol{\mathcal{B}}(\mathbf{r}) = 0, \tag{16a}$$

$$\nabla\times\boldsymbol{\mathcal{H}}(\mathbf{r}) + i\omega\boldsymbol{\mathcal{D}}(\mathbf{r}) = \mathbf{j}_{\text{ext}}(\mathbf{r}), \tag{16b}$$

with

$$\boldsymbol{\mathcal{D}}(\mathbf{r}) = \epsilon_0\boldsymbol{\mathcal{E}}(\mathbf{r}) + \boldsymbol{\mathcal{P}}(\mathbf{r}) = \epsilon_0\boldsymbol{\epsilon}\boldsymbol{\mathcal{E}}(\mathbf{r}), \tag{17a}$$

$$\boldsymbol{\mathcal{H}}(\mathbf{r}) = \boldsymbol{\mathcal{B}}(\mathbf{r})/\mu_0 - \boldsymbol{\mathcal{M}}(\mathbf{r}) = \mu_0^{-1}\boldsymbol{\mu}^{-1}\boldsymbol{\mathcal{B}}(\mathbf{r}), \tag{17b}$$

where $\boldsymbol{\mathcal{P}}(\mathbf{r})$ and $\boldsymbol{\mathcal{M}}(\mathbf{r})$ are the inverse Fourier transform of $\mathbf{P}(\mathbf{k})$ and $\mathbf{M}(\mathbf{k})$, respectively. The equation set (16) with (17) is a local description of the electromagnetic fields.

In general, it is not always possible to express the induced current exactly as in (13) with local constitutive parameters $\boldsymbol{\epsilon}$ and $\boldsymbol{\mu}$ (independent of $\mathbf{k}$). In Secs. III A–III D we will consider four possibilities of how to decompose the induced current. All decompositions have appeared in previous literature, although the one in Sec. III D has been generalized. In each subsection, we will discuss the properties of the different, resulting permeabilities. In Sec. III E we discuss how one can construct other decompositions and analyze their properties.

We want Maxwell equations in the forms (15) and (16) to be valid in all cases, however, with different expressions for the auxiliary fields $\mathbf{D}(\mathbf{k})$ and $\mathbf{H}(\mathbf{k})$. The strategy will be, first, to define a magnetization $\mathbf{M}(\mathbf{k})$ and then put

$$\mathbf{D}(\mathbf{k}) = \epsilon_0\mathbf{E}(\mathbf{k}) + \frac{\mathbf{J}(\mathbf{k}) - i\mathbf{k}\times\mathbf{M}(\mathbf{k})}{-i\omega}, \tag{18a}$$

$$\mathbf{H}(\mathbf{k}) = \mathbf{B}(\mathbf{k})/\mu_0 - \mathbf{M}(\mathbf{k}). \tag{18b}$$

Substituting (18) into (15), we recover (10).

From now on, we will omit the $\mathbf{k}$ dependence in the notation, i.e., we will, e.g., write $\mathbf{J}$ rather than $\mathbf{J}(\mathbf{k})$. An exception is the Landau-Lifshitz permittivity in Sec. III A, which always will be denoted $\boldsymbol{\epsilon}(\omega, \mathbf{k})$, i.e., with arguments. Note that the fundamental fields, i.e., $\mathbf{E}$, $\mathbf{B}$, $\mathbf{J}$, and $\mathbf{J}_{\text{ext}}$, are the same in all formulations. We will often, without loss of generality, orient the coordinate system such that $\mathbf{k}$ points in the $\hat{\mathbf{x}}$ direction, i.e., $\mathbf{k} = k\hat{\mathbf{x}}$.

A. Landau-Lifshitz (ll) formulation

In the Landau-Lifshitz formulation [1], we describe all induced current in terms of a electric polarization density $\mathbf{P}^{\text{ll}}$:

$$\mathbf{J} = -i\omega\mathbf{P}^{\text{ll}}. \tag{19}$$

This means that the magnetization is zero ($\mathbf{M}^{\text{ll}} = 0$), and the permeability is trivial, $\boldsymbol{\mu}_{\text{ll}} = \mathbf{I}$. The displacement vector is

$\mathbf{D}^{\text{II}} = \epsilon_0\mathbf{E} + \mathbf{P}^{\text{II}}$, or

$$\mathbf{D}^{\text{II}} = \epsilon_0\mathbf{E} - \mathbf{J}/i\omega. \tag{20}$$

In a linear medium, there is a linear constitutive relation between $\mathbf{D}^{\text{II}}$ and $\mathbf{E}$:

$$\mathbf{D}^{\text{II}} = \epsilon_0\boldsymbol{\epsilon}(\omega, \mathbf{k})\mathbf{E}. \tag{21}$$

This defines the Landau-Lifshitz permittivity $\boldsymbol{\epsilon}(\omega, \mathbf{k})$. We note that the constitutive relations are described in the form of a single parameter, $\boldsymbol{\epsilon}(\omega, \mathbf{k})$. Considering terms up to second order in k,

$$\epsilon_{ij}(\omega, \mathbf{k}) - \delta_{ij} = \chi_{ij} + \alpha_{ikj}k_k/\epsilon_0 + \beta_{iklj}k_k k_l c^2/\omega^2, \tag{22}$$

for some tensors χ_{ij}, α_{ikj}, and β_{iklj}, independent of $\mathbf{k}$. In (22) summation over repeated indices is implied. In the presence of strong spatial dispersion, where higher-order terms are not negligible, we let the $\beta_{iklj}k_k k_l c^2/\omega^2$ term absorb the remainder. For such media the β_{iklj} tensor gets dependent on $\mathbf{k}$.

Maxwell's equations (10) take the form

$$i\mathbf{k} \times \mathbf{E} - i\omega\mathbf{B} = 0, \tag{23a}$$

$$\frac{1}{\mu_0} i\mathbf{k} \times \mathbf{B} + i\omega\epsilon_0\boldsymbol{\epsilon}(\omega, \mathbf{k})\mathbf{E} = \mathbf{J}_{\text{ext}}. \tag{23b}$$

By eliminating $\mathbf{B}$, we obtain

$$\left[k^2\mathbf{I}_\perp - \frac{\omega^2}{c^2}\boldsymbol{\epsilon}(\omega, \mathbf{k})\right]\mathbf{E} = i\omega\mu_0\mathbf{J}_{\text{ext}}, \tag{24}$$

with $\mathbf{I}_\perp = \mathbf{I} - \mathbf{k}\mathbf{k}/k^2$, where $\mathbf{I}$ is the identity, or

$$\mathbf{I}_\perp = \begin{bmatrix} 0 & 0 & 0 \\ 0 & 1 & 0 \\ 0 & 0 & 1 \end{bmatrix}, \tag{25}$$

expressed in a coordinate system where $\mathbf{k} = k\hat{\mathbf{x}}$. The matrix in the brackets in (24) can be inverted (Appendix C) to obtain an input-output relation

$$\mathbf{E} = \mathbf{G}(\omega, \mathbf{k})\mathbf{J}_{\text{ext}}, \tag{26}$$

where $\mathbf{G}(\omega, \mathbf{k})$ is a (matrix) response function given by

$$\mathbf{G}(\omega, \mathbf{k})^{-1} = (i\omega\mu_0)^{-1}\left[k^2\mathbf{I}_\perp - \frac{\omega^2}{c^2}\boldsymbol{\epsilon}(\omega, \mathbf{k})\right]. \tag{27}$$

For an isotropic medium, the permittivity tensor can be written

$$\boldsymbol{\epsilon}(\omega, \mathbf{k}) = \begin{bmatrix} \epsilon_\parallel & 0 & 0 \\ 0 & \epsilon_\perp & 0 \\ 0 & 0 & \epsilon_\perp \end{bmatrix}, \tag{28}$$

for a longitudinal $\epsilon_\parallel$ and transversal $\epsilon_\perp$ permittivity, respectively. In this case the response function $\mathbf{G}(\omega, \mathbf{k})$ becomes $G(\omega, k) = 1/i\omega\epsilon_0\epsilon_\parallel$ or

$$G(\omega, k) = \frac{i\omega\mu_0}{k^2 - \frac{\omega^2}{c^2}\epsilon_\perp}, \tag{29}$$

dependent on the direction of the source $\mathbf{J}_{\text{ext}}$.

For each $\mathbf{k}$, we have, due to passivity and causality (Appendix C):

$$\mathbf{G}(\omega, \mathbf{k}) \text{ analytic for } \operatorname{Im}\omega > 0 \text{ and fixed } \mathbf{k}, \tag{30a}$$

$$-\mathbf{G}(\omega, \mathbf{k})^{-1} - \mathbf{G}(\omega, \mathbf{k})^{-1\dagger} \text{ positive definite}, \tag{30b}$$

$$\det \mathbf{G}(\omega, \mathbf{k}) \neq 0 \text{ for } \operatorname{Im}\omega > 0, \tag{30c}$$

$$\det \mathbf{G}(\omega, \mathbf{k})^{-1} \neq 0 \text{ for } \operatorname{Im}\omega > 0, \tag{30d}$$

$$\boldsymbol{\epsilon}(\omega, \mathbf{k}) \text{ analytic for } \operatorname{Im}\omega > 0 \text{ and fixed } \mathbf{k}, \tag{30e}$$

$$-i\omega[\boldsymbol{\epsilon}(\omega, \mathbf{k}) - \boldsymbol{\epsilon}(\omega, \mathbf{k})^\dagger] \text{ positive semidefinite}. \tag{30f}$$

Here † denotes Hermitian conjugate (transpose and complex conjugate). For (30f) we have assumed real ω and $\mathbf{k}$, as is the case for Fourier decomposition of the fields (Sec. II). If the Fourier integrals in ω and $\mathbf{k}$ are deformed into the complex plane, then the permittivity satisfies (C13) rather than (30f).

For reciprocal metamaterial inclusions, we have

$$\mathbf{G}^T(\omega, -\mathbf{k}) = \mathbf{G}(\omega, \mathbf{k}), \tag{31a}$$

$$\boldsymbol{\epsilon}^T(\omega, -\mathbf{k}) = \boldsymbol{\epsilon}(\omega, \mathbf{k}), \tag{31b}$$

where the superscript "T" denotes transpose. From (27) the two equations in (31) are equivalent. The symmetry relation (31b) is well known in the literature [1,12]; a proof can be found in Ref. [8].

For nongyrotropic media, we have $\boldsymbol{\epsilon}(\omega, -\mathbf{k}) = \boldsymbol{\epsilon}(\omega, \mathbf{k})$ [1,12]. This will be the case if there is a center of symmetry in the medium. Then the odd-order term in (22) vanishes,

$$\alpha_{ikj} = 0. \tag{32}$$

The asymptotic behavior of $\boldsymbol{\epsilon}(\omega, \mathbf{k})$ as $\omega \to \infty$ can be viewed in two different ways. In principle, for sufficiently large frequencies the permittivities of the inclusions and host medium tend to unity [1]; thus eventually $\boldsymbol{\epsilon}(\omega, \mathbf{k}) \to \mathbf{I}$. Nevertheless, in some cases it can be convenient to describe the asymptotic behavior as $\epsilon(\omega, \mathbf{k}) \to$ const, where the constant tensor limit can be different from identity. This may be the case, e.g., if the permittivities of the inclusions and the host medium are considered nondispersive in the frequency range of interest.

With either of these asymptotic behaviors, the tensors $\boldsymbol{\epsilon}(\omega, \mathbf{k})$, $\mathbf{G}(\omega, \mathbf{k})^{-1}$, and $\mathbf{G}(\omega, \mathbf{k})$ are causal functions. This follows from the definition of a causal function in Sec. I and (27) and (30).

B. Multipole decomposition

The traditional way to decompose the induced current is by multipole expansion [7,9,13]. Consider the unit cell that contains the origin. Using

$$\exp(-i\mathbf{k}\cdot\mathbf{r}) = 1 - i\mathbf{k}\cdot\mathbf{r} - (\mathbf{k}\cdot\mathbf{r})^2/2 + \Theta[(\mathbf{k}\cdot\mathbf{r})^3], \tag{33}$$

we obtain from (7c) to second order in k:

$$\mathbf{J} = \frac{1}{V}\int_V \mathbf{j}e^{-i\mathbf{k}\cdot\mathbf{r}}d^3r \tag{34}$$

$$= \frac{1}{V}\cdot\left[\int_V \mathbf{j}d^3r - i\mathbf{k}\cdot\int_V \mathbf{r}\mathbf{j}d^3r - \frac{1}{2}\int_V (\mathbf{k}\cdot\mathbf{r})^2\mathbf{j}d^3r\right]$$

$$\equiv -i\omega\mathbf{P} + i\mathbf{k}\times\mathbf{M} - \omega\mathbf{k}\cdot\mathbf{Q}/2 - i\omega\mathbf{R}, \tag{35}$$

where

$$\mathbf{P} = \frac{1}{-i\omega V}\int_V \mathbf{j} d^3r, \tag{36a}$$

$$\mathbf{M} = \frac{1}{2V}\int_V \mathbf{r}\times\mathbf{j} d^3r, \tag{36b}$$

$$\mathbf{Q} = \frac{1}{-i\omega V}\int_V (\mathbf{rj}+\mathbf{jr}) d^3r, \tag{36c}$$

$$\mathbf{R} = \frac{1}{2i\omega V}\int_V (\mathbf{k}\cdot\mathbf{r})^2\mathbf{j} d^3r. \tag{36d}$$

Here we have decomposed the tensor $\mathbf{rj}$ into its antisymmetric and symmetric parts,

$$\begin{aligned}\mathbf{k}\cdot\mathbf{rj} &= \mathbf{k}\cdot(\mathbf{rj}-\mathbf{jr})/2 + \mathbf{k}\cdot(\mathbf{rj}+\mathbf{jr})/2 \\ &= -\mathbf{k}\times\mathbf{r}\times\mathbf{j}/2 + \mathbf{k}\cdot(\mathbf{rj}+\mathbf{jr})/2.\end{aligned} \tag{37}$$

In addition to the polarization vector $\mathbf{P}$, magnetization vector $\mathbf{M}$, and quadrupole tensor $\mathbf{Q}$, the extra term $\mathbf{R}$ includes electric octupole and magnetic quadrupole. All these multipole terms are dependent on $\mathbf{k}$ although not explicitly specified.

A convenient feature of the multipole decomposition is that the terms have a clear physical interpretation. In particular, $\mathbf{M}$ quantifies the amount of circulating, induced currents. For example, if a 2D metamaterial unit cell consists of a cylinder inclusion with a circular symmetric current in the azimuthal direction, we obtain $\mathbf{P}=0$, $\mathbf{Q}=0$, and $\mathbf{R}=0$, while $\mathbf{M}$ is nonzero.

From $\mathbf{M}$ we define, as usual,

$$\mathbf{H} = \mathbf{B}/\mu_0 - \mathbf{M}. \tag{38}$$

The remaining terms in (35) go into the displacement vector, according to(18a)[2]:

$$\mathbf{D} = \epsilon_0\mathbf{E} + \mathbf{P} - i\mathbf{k}\cdot\mathbf{Q}/2 + \mathbf{R}. \tag{39}$$

In a linear medium, we can write the associated constitutive relations

$$P_i = \epsilon_0\chi_{ij}E_j + \xi_{ikj}k_kE_j + \eta_{ikl\,j}k_kk_lE_j/(\mu_0\omega^2), \tag{40a}$$

$$M_i = \omega\zeta_{ij}E_j + \nu_{il\,j}k_lE_j/(\mu_0\omega), \tag{40b}$$

$$Q_{ik} = 2i\sigma_{ikj}E_j + 2i\gamma_{ikl\,j}k_lE_j/(\mu_0\omega^2), \tag{40c}$$

$$R_i = \psi_{ikl\,j}k_kk_lE_j/(\mu_0\omega^2), \tag{40d}$$

for some tensors χ_{ij}, ξ_{ikj}, $\eta_{ikl\,j}$, σ_{ikj}, $\gamma_{ikl\,j}$, $\psi_{ikl\,j}$, and pseudotensors ζ_{ij} and $\nu_{il\,j}$. Treating the (pseudo-)tensors as Taylor coefficients independent of $\mathbf{k}$, we have included the necessary orders of k such that $\mathbf{J}$ is second order when substituting in (35). We can consider higher-order spatial dispersion by letting the highest-order term in (40) take care of the remainder. For example, in (40b) this will lead to a $\nu_{il\,j}$ which is dependent on $\mathbf{k}$.

From Faraday's law $\mathbf{B} = \mathbf{k}\times\mathbf{E}/\omega$, we note that any dependence on $\mathbf{B}$ is taken care of by the $\mathbf{k}$-dependent terms in (40). For later convenience we have included certain $\mathbf{k}$-independent quantities (such as $\mu_0\omega^2$) in the tensor elements. Magnetoelectric coupling is taken into account in terms of ξ_{ikj} and ζ_{ij}.

We are interested in the magnetization (40b). Choosing a coordinate system such that $\mathbf{k} = k\hat{\mathbf{x}}$, we can write

$$\begin{aligned}M_i &= \omega\zeta_{ij}E_j + k\nu_{i1\,j}E_j/(\mu_0\omega) \\ &= \omega\zeta_{ij}E_j + k\nu_{i11}E_1/(\mu_0\omega) + \mu_0^{-1}(1-\boldsymbol{\mu}^{-1})_{ij}B_j,\end{aligned} \tag{41}$$

with

$$1-\boldsymbol{\mu}^{-1} = \begin{bmatrix} -\nu_{213} & \nu_{212} \\ -\nu_{313} & \nu_{312}\end{bmatrix}. \tag{42}$$

Here $\boldsymbol{\mu}^{-1}$ is identified as an inverse permeability, resulting from the magnetization $\mathbf{M}$ defined as the averaged magnetic moment density (36b). Note that in the coordinate system where $\mathbf{k} = k\hat{\mathbf{x}}$, the inverse permeability is described as 2×2. The reason for this is that $\mathbf{B}$ is transversal (i.e., $B_1 = 0$) and that only the transversal part of $\mathbf{M}$ contributes to $\mathbf{J}$ by (35). In an arbitrary coordinate system, (42) can be written

$$(1-\boldsymbol{\mu}^{-1})_{im} = \varepsilon_{mkj}\frac{k_kk_l}{k^2}\nu_{il\,j}, \tag{43}$$

where ε_{mkj} is the Levi-Civita symbol. This means that $1-\boldsymbol{\mu}^{-1}$ is a tensor.

We will now compare the Landau-Lifshitz formulation and the multipole decomposition. By eliminating $\mathbf{D}$ from (20) and (21), and comparing with (35), we obtain

$$\epsilon_0\boldsymbol{\epsilon}(\omega,\mathbf{k})\mathbf{E} = \epsilon_0\mathbf{E} + \mathbf{P} - \mathbf{k}\times\mathbf{M}/\omega - i\mathbf{k}\cdot\mathbf{Q}/2 + \mathbf{R}. \tag{44}$$

Using the constitutive relations (40), this gives

$$\begin{aligned}&\epsilon_{ij}(\omega,\mathbf{k}) - \delta_{ij} \\ &\quad= \chi_{ij} + (\xi_{ikj} + \sigma_{ikj} - \varepsilon_{ikm}\zeta_{mj})k_k/\epsilon_0 \\ &\qquad + (\gamma_{ikl\,j} + \psi_{ikl\,j} + \eta_{ikl\,j} - \varepsilon_{ikm}\nu_{ml\,j})k_kk_lc^2/\omega^2.\end{aligned} \tag{45}$$

Comparing (22) and (45), and noting that $\beta_{ikl\,j}$, $\psi_{ikl\,j}$, and $\eta_{ikl\,j}$ can be taken to be symmetric in k and l, we have

$$\alpha_{ikj} = \xi_{ikj} + \sigma_{ikj} - \varepsilon_{ikm}\zeta_{mj}, \tag{46a}$$

$$\beta_{ikl\,j} = \psi_{ikl\,j} + \eta_{ikl\,j} + \frac{\gamma_{ikl\,j}+\gamma_{ilkj}}{2} - \frac{\varepsilon_{ikm}\nu_{ml\,j} + \varepsilon_{ilm}\nu_{mkj}}{2}. \tag{46b}$$

For nongyrotropic media, if there is a center of symmetry in the medium, then we can take the center of the unit cell to be the center of symmetry. For $\mathbf{k}=0$, from symmetry and (36), it follows that $\mathbf{M}=0$ and $\mathbf{Q}=0$. This means that $\zeta_{ij}=0$, $\sigma_{ikj}=0$, and from (32), $\xi_{ikj}=0$.

In other words, for nongyrotropic media, $\mathbf{M}$ and $\mathbf{Q}$ contain only first-order terms in k, which means that all terms in (35) except $\mathbf{P}$ are second order in k. This means that the electric octupole-magnetic quadrupole term $\mathbf{R}$ can be of the same order of magnitude as the magnetization and quadrupole terms [9]. Thus, when concerned with the magnetic response, the $\mathbf{R}$ term and $\mathbf{Q}$ should in general be taken into account in addition to $\mathbf{M}$.

Even when considering an asymptotic behavior of the microscopic permittivity $\varepsilon(\mathbf{r}) \to 1$ as $\omega\to\infty$, it turns out that

[2]Alternatively, the electric octupole–magnetic quadrupole term $\mathbf{R}$ could be split such that the magnetic quadrupole is included into (38).

for fixed $\mathbf{k}$, we have $\boldsymbol{\mu}^{-1} \not\to \mathbf{I}$ in general [14]. An asymptotic value different from identity does not violate causality, as $\boldsymbol{\mu}^{-1} \to \mathbf{I}$ is only required for eigenmode propagation where ω and $\mathbf{k}$ are connected. Even though the asymptotic behavior for fixed $\mathbf{k}$ may have limited direct physical importance, it has implications for the Kramers-Kronig relations, being formulated for fixed $\mathbf{k}$. The asymptotic behavior of $\boldsymbol{\mu}$ is found as follows. The asymptotic behavior of any microscopic permittivity is of the form [1]

$$\varepsilon(\mathbf{r}) = 1 - \frac{\omega_p^2(\mathbf{r})}{\omega^2} + O(\omega^{-3}), \tag{47}$$

where $\omega_p(\mathbf{r})$ is the plasma frequency. As $\omega \to \infty$ the fields will tend to those we would have if the metamaterial were replaced by vacuum. Thus we can write

$$\mathbf{e}(\mathbf{r}) = \mathbf{E}\exp(i\mathbf{k}\cdot\mathbf{r}) + \mathbf{f}(\mathbf{r}), \tag{48a}$$

$$\mathbf{j}(\mathbf{r}) = -i\omega\epsilon_0[\varepsilon(\mathbf{r}) - 1][\mathbf{E}\exp(i\mathbf{k}\cdot\mathbf{r}) + \mathbf{f}(\mathbf{r})], \tag{48b}$$

for some $\mathbf{f}(\mathbf{r})$, with

$$\mathbf{f}(\mathbf{r}) \to 0 \text{ as } \omega \to \infty. \tag{49}$$

Here we have assumed a source such that $\mathbf{E}$ is independent of ω for large frequencies (this condition can be removed). Having an expression for $\mathbf{j}(\mathbf{r})$, it is straightforward to obtain $\mathbf{M}$ by (36b):

$$\mathbf{M} = \frac{i\omega\epsilon_0}{2V}\mathbf{E} \times \int_V \mathbf{r}[\varepsilon(\mathbf{r}) - 1]e^{i\mathbf{k}\cdot\mathbf{r}}d^3r - \frac{i\omega\epsilon_0}{2V}\int \mathbf{r} \times \mathbf{f}(\mathbf{r})[\varepsilon(\mathbf{r}) - 1]d^3r. \tag{50}$$

According to (47) and (49), the last term in (50) tends to zero faster than ω^{-1}. Comparing with (40b), this means that the term will not contribute to $v_{il\,j}$ in the limit $\omega \to \infty$. The first term in (50) can be written

$$\frac{-i\epsilon_0}{2\omega V}\mathbf{E} \times \int_V \mathbf{r}\,\omega_p^2(\mathbf{r})e^{i\mathbf{k}\cdot\mathbf{r}}d^3r + O(\omega^{-2}). \tag{51}$$

The integral in (51) is clearly nonzero in general. Then (51) is $\Theta(\omega^{-1})$, which by (40b) means that $\boldsymbol{\nu} \not\to 0$. We therefore find that

$$1 - \boldsymbol{\mu}^{-1} = O(1) \text{ as } \omega \to \infty, \text{ for fixed } \mathbf{k}, \tag{52}$$

and, in general, $\boldsymbol{\mu}^{-1} \not\to \mathbf{I}$.

For diagonal $\boldsymbol{\mu}$ it is straightforward to find examples where $\operatorname{Im}\boldsymbol{\mu}$ is both positive and negative, depending on the frequency (see Sec. IV). This is not a violation of passivity; it is just an indication of the phase relationship between the magnetization and the macroscopic field in the unit cell. The fundamental passivity condition is only that the Landau-Lifshitz permittivity satisfies (30f).

We will now consider the causality and analyticity of the inverse permeability. Note that $\mathbf{E}$ is the same in all formulations, so we can use the Landau-Lifshitz formulation to express

$$\mathbf{E} = \mathbf{G}(\omega, \mathbf{k})\mathbf{J}_{\text{ext}}, \tag{53}$$

with a response function $\mathbf{G}(\omega, \mathbf{k})$, as in (26). According to (30c), $\mathbf{G}(\omega, \mathbf{k})$ is invertible in the upper half-plane $\operatorname{Im}\omega > 0$. Hence, we can choose $\mathbf{J}_{\text{ext}}$ such that only a single component of $\mathbf{E}$ is nonzero, say, E_j, and such that E_j is any analytic and causal function. The required $\mathbf{J}_{\text{ext}}$ is analytic in the upper half-plane from the analyticity of $\mathbf{G}(\omega, \mathbf{k})^{-1}$. Taking the asymptotic behavior of $\mathbf{G}^{-1}(\omega, \mathbf{k})$ as $\omega \to \infty$ into account, the required $\mathbf{J}_{\text{ext}}$ is realizable as a causal source.

We have from (41) that

$$M_i = \omega\zeta_{ij}E_j + k\nu_{i1j}E_j/(\mu_0\omega), \tag{54}$$

where now only a single component E_j is nonzero. Clearly, the microscopic, induced current $\mathbf{j}$ is causal, since it is causally related to the source. Thus M_i, as given by (36b), is causal. Putting $k = 0$ in (54), and remembering that E_j is any causal function, it follows that ζ_{ij} is analytic in the upper half-plane. By letting $k \neq 0$, we find that ν_{i1j} is analytic there, since M_i and $\omega\zeta_{ij}E_j$ are. From (42) we conclude that $\boldsymbol{\mu}^{-1}$ is analytic in the upper half-plane. Moreover, taking (52) into account, $\boldsymbol{\mu}^{-1}$ is causal. Writing $\boldsymbol{\mu}^{-1}(\omega, \mathbf{k}) \to \boldsymbol{\mu}^{-1}(\infty, \mathbf{k})$, we can establish Kramers-Kronig relations (C10) for $\boldsymbol{\chi}(\omega, \mathbf{k}) \equiv \boldsymbol{\mu}^{-1}(\omega, \mathbf{k}) - \boldsymbol{\mu}^{-1}(\infty, \mathbf{k})$ [15].

It is also possible to combine ζ_{ij} and μ_{ij}^{-1} into a single, inverse permeability tensor [8] and consider its causality. In a coordinate system where $\mathbf{k} = k\hat{\mathbf{x}}$, Faraday's law (10a) becomes $E_2 = B_3\omega/k$ and $E_3 = -B_2\omega/k$. We can then express (41) as

$$M_i = \omega\zeta_{i1}E_1 + k\nu_{i11}E_1/(\mu_0\omega) + \omega^2\zeta_{i2}B_3/k - \omega^2\zeta_{i3}B_2/k + \mu_0^{-1}(1 - \boldsymbol{\mu}^{-1})_{ij}B_j \tag{55}$$

or

$$M_i = \omega\zeta_{i1}E_1 + k\nu_{i11}E_1/(\mu_0\omega) + \mu_0^{-1}(1 - \tilde{\boldsymbol{\mu}}^{-1})_{ij}B_j \tag{56}$$

with the modified inverse permeability

$$\tilde{\boldsymbol{\mu}}^{-1} = \boldsymbol{\mu}^{-1} - \frac{\mu_0\omega^2}{k}\begin{bmatrix} -\zeta_{23} & \zeta_{22} \\ -\zeta_{33} & \zeta_{32} \end{bmatrix}. \tag{57}$$

In the two previous paragraphs we found that $\boldsymbol{\mu}^{-1}$ and ζ_{ij} are analytic in the upper half-plane; thus so is $\tilde{\boldsymbol{\mu}}^{-1}$.

It is interesting to note that all (pseudo-)tensor elements in (40) are analytic in the upper half-plane. This is seen as follows. First, recall from (53) and (30c) that the source can be chosen such that only a single component of the electric field, say, E_j, is nonzero and such that E_j is any analytic function. Also, P_i, M_i, Q_{ik}, and R_i are analytic, since they are given by the induced, microscopic current through (36). We now apply the general result in Appendix E to the expansions (40), with the result that all (pseudo-)tensor elements in (40) are analytic in the upper half-plane.

Finally, we note the well-known fact [16] that, in general, the multipole quantities are dependent on the choice of origin. We have assumed that the origin is inside the unit cell V, but we are free to move the origin inside the cell. Substituting $\mathbf{r} = \mathbf{r}' + \mathbf{r}_0$ in (34) and expanding the exponential $\exp(-i\mathbf{k}\cdot\mathbf{r}')$ give

$$\mathbf{J} = e^{-i\mathbf{k}\cdot\mathbf{r}_0}(-i\omega\mathbf{P} + i\mathbf{k} \times \mathbf{M}' - \omega\mathbf{k}\cdot\mathbf{Q}'/2 - i\omega\mathbf{R}'), \tag{58}$$

with

$$\mathbf{M}' = \frac{1}{2V}\int_V \mathbf{r}' \times \mathbf{j} d^3r, \tag{59a}$$

$$\mathbf{Q}' = \frac{1}{-i\omega V}\int_V (\mathbf{r}'\mathbf{j} + \mathbf{j}\mathbf{r}') d^3r, \tag{59b}$$

$$\mathbf{R}' = \frac{1}{2i\omega V}\int_V (\mathbf{k}\cdot\mathbf{r}')^2 \mathbf{j} d^3r. \tag{59c}$$

By changing $\mathbf{r}_0$, the different multipole quantities will change, however, such that the sum of contributions to the induced current [right-hand side of (58)] is constant. Since

$$\mathbf{M}' = \mathbf{M} + \frac{i\omega\mathbf{r}_0}{2} \times \mathbf{P}, \tag{60}$$

we have $\mathbf{M}' \approx \mathbf{M}$ when $\omega a P \ll M$.

Since the magnetization vector is dependent on the choice of origin, so is the resulting $\boldsymbol{\mu}$ in general. This dependence is not only a consequence of the difference between $\mathbf{M}'$ and $\mathbf{M}$ but also the exponential factor $\exp(-i\mathbf{k}\cdot\mathbf{r}_0) \approx 1 - i\mathbf{k}\cdot\mathbf{r}_0$ in (58). This factor will mix the $\Theta(1)$ and $\Theta(k)$ terms in (54) in the presence of magnetoelectric coupling ($\zeta_{ij} \neq 0$).

C. Vinogradov-Yaghjian (vy) decomposition

In Vinogradov and Aivazyan [3] the microscopic current is decomposed into three terms:

$$\mathbf{j} = -\mathbf{r}\,\nabla\cdot\mathbf{j} + \tfrac{1}{2}\nabla\times(\mathbf{r}\times\mathbf{j}) + \tfrac{1}{2}\nabla\cdot(\mathbf{r}\mathbf{j} + \mathbf{j}\mathbf{r}). \tag{61}$$

Equation (61) can be verified by straightforward calculation. The microscopic current satisfies continuity $\nabla\cdot\mathbf{j} = i\omega\varrho$, where ϱ is the microscopic induced charge density. Yaghjian, Alù, and Silveirinha [8] suggested to decompose the macroscopic induced current by substituting (61) into (7c), resulting in

$$\mathbf{J} = -i\omega\mathbf{P}^{\mathrm{vy}} + i\mathbf{k}\times\mathbf{M}^{\mathrm{vy}} + \omega\mathbf{k}\cdot\mathbf{Q}^{\mathrm{vy}}/2, \tag{62}$$

where

$$\mathbf{P}^{\mathrm{vy}} = \frac{1}{V}\int_V \varrho(\mathbf{r})\mathbf{r}e^{-i\mathbf{k}\cdot\mathbf{r}} d^3r, \tag{63a}$$

$$\mathbf{M}^{\mathrm{vy}} = \frac{1}{2V}\int_V \mathbf{r}\times\mathbf{j}(\mathbf{r})e^{-i\mathbf{k}\cdot\mathbf{r}} d^3r, \tag{63b}$$

$$\mathbf{Q}^{\mathrm{vy}} = -\frac{1}{i\omega V}\int_V (\mathbf{j}\mathbf{r} + \mathbf{r}\mathbf{j})e^{-i\mathbf{k}\cdot\mathbf{r}} d^3r. \tag{63c}$$

The integrals are over the unit cell containing the origin. To obtain (62) it is assumed that the boundaries of the unit cells lie in free space. Equation (62) is not a multipole expansion, due to the factor $\exp(-i\mathbf{k}\cdot\mathbf{r})$ in the integrands of (63). All induced current is described by the three terms in (62), as opposed to a multipole expansion with an infinite number of terms. Note that the sign of the "quadrupole" term $\omega\mathbf{k}\cdot\mathbf{Q}^{\mathrm{vy}}/2$ is opposite of that resulting from a conventional multipole expansion (35).

From the magnetization $\mathbf{M}^{\mathrm{vy}}$, we can define a permeability exactly as in Sec. III B. From a constitutive relation

$$M_i^{\mathrm{vy}} = \omega\zeta_{ij}^{\mathrm{vy}} E_j + \nu_{ilj}^{\mathrm{vy}} k_l E_j/(\mu_0\omega), \tag{64}$$

set

$$\left(1 - \boldsymbol{\mu}_{\mathrm{vy}}^{-1}\right)_{im} = \varepsilon_{mkj}\frac{k_k k_l}{k^2}\nu_{ilj}^{\mathrm{vy}} \tag{65}$$

or

$$1 - \boldsymbol{\mu}_{\mathrm{vy}}^{-1} = \begin{bmatrix} -\nu_{213}^{\mathrm{vy}} & \nu_{212}^{\mathrm{vy}} \\ -\nu_{313}^{\mathrm{vy}} & \nu_{312}^{\mathrm{vy}} \end{bmatrix} \tag{66}$$

in a coordinate system where $\mathbf{k} = k\hat{\mathbf{x}}$. (Alternatively, as in Ref. [8] and in (57), we can define a new permeability $\tilde{\boldsymbol{\mu}}_{\mathrm{vy}}$ by combining $\boldsymbol{\mu}_{\mathrm{vy}}$ and $\boldsymbol{\zeta}^{\mathrm{vy}}$ into a single tensor.)

The asymptotic behavior of $\boldsymbol{\mu}_{\mathrm{vy}}^{-1}$ turns out to be different from that of $\boldsymbol{\mu}^{-1}$ in Sec. III B. Substituting (48b) into (63b):

$$\mathbf{M}^{\mathrm{vy}} = \frac{i\omega\epsilon_0}{2V}\mathbf{E}\times\int_V \mathbf{r}[\varepsilon(\mathbf{r}) - 1]d^3r - \frac{i\omega\epsilon_0}{2V}\int \mathbf{r}\times\mathbf{f}(\mathbf{r})[\varepsilon(\mathbf{r}) - 1]e^{-i\mathbf{k}\cdot\mathbf{r}} d^3r. \tag{67}$$

The first integral is independent of $\mathbf{k}$ and therefore cannot contribute to the last term in (64). The second term in (67) tends to zero faster than ω^{-1} [see (47) and (49)] and leads to a ν_{ilj}^{vy} that tends to zero. We therefore find that

$$\boldsymbol{\mu}_{\mathrm{vy}}^{-1} \to \mathbf{I} \quad \text{as} \quad \omega \to \infty. \tag{68}$$

The definition of $\mathbf{M}^{\mathrm{vy}}$ in (63b) can be used to prove that $\boldsymbol{\mu}_{\mathrm{vy}}^{-1}$ is analytic in the upper half-plane $\mathrm{Im}\,\omega > 0$, using the exact same method as in Sec. III B. This result is already known from Ref. [8]. Taking (68) into account, we conclude that $\boldsymbol{\mu}_{\mathrm{vy}}^{-1}$ is causal for each, fixed $\mathbf{k}$.

The connection between the constitutive parameters for $\mathbf{P}^{\mathrm{vy}}$, $\mathbf{M}^{\mathrm{vy}}$, $\mathbf{Q}^{\mathrm{vy}}$, and the Landau-Lifshitz permittivity can be obtained directly from (45) by setting $\psi_{iklj} = 0$ (and adding superscripts "vy").

At first sight, the multipole quantities in (36) and in (63) seem to be quite similar; the difference is only a factor $\exp(-i\mathbf{k}\cdot\mathbf{r})$ in the integrands. The connection between the multipole quantities can be established by expanding the exponential (33). Note that since we are interested in magnetic effects, which are known to be a second-order $\Theta(k^2)$ effect in the Landau-Lifshitz permittivity, we include terms for the induced current up to order $\Theta(k^2)$. Expressing $i\omega\varrho = \nabla\cdot\mathbf{j}$ and using integration by parts, we obtain from (63a):

$$-i\omega\mathbf{P}^{\mathrm{vy}} = \frac{1}{V}\int_V \mathbf{j}e^{-i\mathbf{k}\cdot\mathbf{r}} d^3r - \frac{i\mathbf{k}\cdot}{V}\int_V \mathbf{j}\mathbf{r}e^{-i\mathbf{k}\cdot\mathbf{r}} d^3r. \tag{69}$$

Expanding the exponential we find to second order in k:

$$-i\omega\mathbf{P}^{\mathrm{vy}} = -i\omega\mathbf{P} - \omega\mathbf{k}\cdot\mathbf{Q} - i\omega\mathbf{R} - \frac{1}{V}\int_V (\mathbf{k}\cdot\mathbf{j})(\mathbf{k}\cdot\mathbf{r})\mathbf{r} d^3r. \tag{70}$$

Furthermore, we obtain

$$i\mathbf{k}\times\mathbf{M}^{\mathrm{vy}} = i\mathbf{k}\times\mathbf{M} + \frac{\mathbf{k}}{2V}\cdot\int_V (\mathbf{j}\mathbf{r} - \mathbf{r}\mathbf{j})(\mathbf{k}\cdot\mathbf{r}) d^3r \tag{71}$$

and

$$\omega\mathbf{k}\cdot\mathbf{Q}^{\mathrm{vy}} = \omega\mathbf{k}\cdot\mathbf{Q} + \frac{\mathbf{k}}{V}\cdot\int_V (\mathbf{j}\mathbf{r} + \mathbf{r}\mathbf{j})(\mathbf{k}\cdot\mathbf{r}) d^3r. \tag{72}$$

Equations (70)–(72) show the relation between the "dipole" and "quadrupole" terms in (62) compared to the usual ones.

For example, (71) shows that the difference $i\mathbf{k}\times(\mathbf{M}^{\mathrm{vy}}-\mathbf{M})$ is given by a magnetic quadrupole term.

Summing the contributions to the induced current, we obtain

$$\begin{aligned}&-i\omega\mathbf{P}^{\mathrm{vy}}+i\mathbf{k}\times\mathbf{M}^{\mathrm{vy}}+\omega\mathbf{k}\cdot\mathbf{Q}^{\mathrm{vy}}/2\\&\quad=-i\omega\mathbf{P}+i\mathbf{k}\times\mathbf{M}-\omega\mathbf{k}\cdot\mathbf{Q}/2-i\omega\mathbf{R}.\end{aligned}\tag{73}$$

Equation (73) could have been found directly by comparing (35) and (62).

One may think that $\mathbf{M}^{\mathrm{vy}}$ and $\mathbf{M}$, and the corresponding permeabilities, are equal in the limit $ka\to 0$, since then the $\exp(-i\mathbf{k}\cdot\mathbf{r})$ factor in the integrand in (63b) tends to unity. Surprisingly, this is, however, not true in general. As an example, consider a metamaterial with a center of symmetry in the unit cell, which is taken as the origin. We must have

$$\mathbf{j}(-\mathbf{r})=\mathbf{j}(\mathbf{r})\quad\text{when }\mathbf{k}\to 0,\tag{74}$$

which means that $\mathbf{M}\to 0$ as $\mathbf{k}\to 0$. In other words, $\mathbf{M}=O(k)$. This can also be realized from Faraday's law: When there is no magnetoelectric coupling, $\mathbf{M}$ is proportional to $\mathbf{B}$, i.e., $\mathbf{M}=\boldsymbol{\chi}\mathbf{B}=\boldsymbol{\chi}(\mathbf{k}\times\mathbf{E})/\omega=O(k)$ for some tensor $\boldsymbol{\chi}$. By expanding the exponential in the definition of $\mathbf{M}^{\mathrm{vy}}$ (63b), the connection between $\mathbf{M}^{\mathrm{vy}}$ and $\mathbf{M}$ can be written

$$\mathbf{M}^{\mathrm{vy}}=\mathbf{M}+\frac{-i}{2V}\int_V(\mathbf{k}\cdot\mathbf{r})\mathbf{r}\times\mathbf{j}(\mathbf{r})d^3r.\tag{75}$$

The factor $\mathbf{k}\cdot\mathbf{r}$ in the integrand destroys the odd inversion symmetry, so the integral does not vanish in general. Thus the integral is $\Theta(k)$ and may be equally important as $\mathbf{M}$ in the limit $ka\to 0$. Recall that the permeabilities are found from the $O(k)$ part of $\mathbf{M}^{\mathrm{vy}}$ and $\mathbf{M}$, respectively. In other words, even though both $\mathbf{M}^{\mathrm{vy}}$ and $\mathbf{M}$ tend to zero, the permeabilities derived from $\mathbf{M}^{\mathrm{vy}}$ and $\mathbf{M}$ may be different. The difference between the permeabilities will be explored numerically in Sec. IV.

Finally, we note that in general, the quantities $\mathbf{P}^{\mathrm{vy}}$, $\mathbf{M}^{\mathrm{vy}}$, and $\mathbf{Q}^{\mathrm{vy}}$ are dependent on the choice of origin inside the cell V. Since $\mathbf{M}^{\mathrm{vy}}$ may be origin dependent, so is the resulting permeability $\boldsymbol{\mu}_{\mathrm{vy}}$. From the definition (63b) it follows that the relative size of the origin dependence of $\mathbf{M}^{\mathrm{vy}}$ is negligible when $\omega aP^{\mathrm{ll}}\ll M^{\mathrm{vy}}$. Numerically, the origin dependence of $\boldsymbol{\mu}_{\mathrm{vy}}$ turns out to be minor, as discussed in Sec. IV.

D. Transversal-longitudinal (tl) decomposition

Starting from the Landau-Lifshitz permittivity, it is natural to use a strategy to put "as much as possible" of the $\mathbf{k}$-dependent induced current into the magnetization and therefore the permeability. The resulting permeability is a generalization of that in chapter XII of Landau and Lifshitz's textbook [1] and in Silveirinha [5].

The induced current can be divided into two parts:

$$\mathbf{J}=-i\omega\mathbf{P}^{\mathrm{tl}}+i\mathbf{k}\times\mathbf{M}^{\mathrm{tl}}.\tag{76}$$

In (76) the part which is independent of $\mathbf{k}$ is put into the first term $-i\omega\mathbf{P}^{\mathrm{tl}}$. Moreover, the $\mathbf{k}$-dependent part is divided into a longitudinal part (which is parallel to $\mathbf{k}$) and a transversal part. The longitudinal part is also absorbed by the $-i\omega\mathbf{P}^{\mathrm{tl}}$ term, while the transversal part is taken care of by the magnetization term $i\mathbf{k}\times\mathbf{M}^{\mathrm{tl}}$. In a coordinate system oriented such that $\mathbf{k}=k\hat{\mathbf{x}}$, we can write

$$\mathbf{J}=\big(-i\omega P_1^{\mathrm{tl}},-i\omega P_2^{\mathrm{tl}}-ikM_3^{\mathrm{tl}},-i\omega P_3^{\mathrm{tl}}+ikM_2^{\mathrm{tl}}\big),\tag{77}$$

where P_2^{tl} and P_3^{tl} are independent of $\mathbf{k}$. As in Sec. III B (41), we express

$$\begin{aligned}M_i^{\mathrm{tl}}&=\omega\zeta_{ij}^{\mathrm{tl}}E_j+k\nu_{i1j}^{\mathrm{tl}}E_j/(\mu_0\omega)\\&=\omega\zeta_{ij}^{\mathrm{tl}}E_j+\frac{k\nu_{i11}^{\mathrm{tl}}E_1}{\mu_0\omega}+\mu_0^{-1}\big(1-\boldsymbol{\mu}_{\mathrm{tl}}^{-1}\big)_{ij}B_j\\&=\omega\zeta_{ij}^{\mathrm{tl}}E_j+\frac{k\nu_{i11}^{\mathrm{tl}}E_1}{\mu_0\omega}+\frac{1}{\mu_0\omega}\big[\big(1-\boldsymbol{\mu}_{\mathrm{tl}}^{-1}\big)\mathbf{k}\times\mathbf{E}\big]_i\end{aligned}\tag{78}$$

for some ζ_{ij}^{tl}, ν_{ilk}^{tl}, and $\boldsymbol{\mu}_{\mathrm{tl}}$.

The induced current density can also be expressed

$$J_i=-i\omega\epsilon_0[\epsilon_{ij}(\omega,\mathbf{k})-\delta_{ij}]E_j,\tag{79}$$

$$=-i\omega\epsilon_0[\chi_{ij}+\alpha_{ikj}k_k/\epsilon_0+\beta_{iklj}k_kk_lc^2/\omega^2]E_j,\tag{80}$$

where we have substituted the Landau-Lifshitz permittivity (22). Equating the $O(k^2)$ part of (77) and the last term in (80), we obtain

$$1-\boldsymbol{\mu}_{\mathrm{tl}}^{-1}=\begin{bmatrix}\beta_{3113}&-\beta_{3112}\\-\beta_{2113}&\beta_{2112}\end{bmatrix}.\tag{81}$$

In an arbitrary coordinate system, the tensor (81) can be written

$$\big[1-\boldsymbol{\mu}_{\mathrm{tl}}^{-1}\big]_{mn}=\varepsilon_{mip}\varepsilon_{njq}\frac{k_kk_lk_pk_q}{k^4}\beta_{iklj}.\tag{82}$$

For strongly spatially dispersive media, we have let the last term in (80) contain the remainder [$\Theta(k^2)$ and higher order]. Then β_{iklj} and the resulting $\boldsymbol{\mu}_{\mathrm{tl}}$ become dependent on $\mathbf{k}$.

The symmetry (31b) means, according to (22), that $\beta_{iklj}(\mathbf{k})=\beta_{jkli}(-\mathbf{k})$. This means that

$$\boldsymbol{\mu}_{\mathrm{tl}}^T(-\mathbf{k})=\boldsymbol{\mu}_{\mathrm{tl}}(\mathbf{k}).\tag{83}$$

In particular, if we only consider terms of $\boldsymbol{\epsilon}(\omega,\mathbf{k})$ up to second order in k (weakly spatially dispersive media), then we have $\boldsymbol{\mu}_{\mathrm{tl}}^T=\boldsymbol{\mu}_{\mathrm{tl}}$.

As for the asymptotic behavior of $\boldsymbol{\mu}_{\mathrm{tl}}$ as $\omega\to\infty$, recall that the microscopic field tends to a plane wave in this limit, approximately unaffected by the structure. Using (7c) and (48), we find

$$\mathbf{J}=\frac{-i\omega\epsilon_0\mathbf{E}}{V}\int_V[\varepsilon(\mathbf{r})-1]d^3r+\Delta\mathbf{J},\tag{84}$$

where

$$\Delta\mathbf{J}=-\frac{i\omega\epsilon_0}{V}\int_V[\varepsilon(\mathbf{r})-1]\mathbf{f}(\mathbf{r})e^{-i\mathbf{k}\cdot\mathbf{r}}d^3r.\tag{85}$$

The asymptotic behavior of $\varepsilon(\mathbf{r})$ as $\omega\to\infty$ is of the form (47). From (49) it is clear that $\Delta\mathbf{J}\to 0$ faster than $\mathbf{J}$. By comparison to (79) the resulting Landau-Lifshitz permittivity becomes

$$\epsilon_{ij}(\omega,\mathbf{k})=\frac{\delta_{ij}}{V}\int_V\varepsilon(\mathbf{r})d^3r+F_{ij}(\omega,\mathbf{k}),\tag{86}$$

where $F_{ij}(\omega,\mathbf{k})$ tends to zero faster than ω^{-2}. The first term in (86) is independent of $\mathbf{k}$; thus it does not contribute to the

$\Theta(k^2)$ term of the Landau-Lifshitz permittivity (22). The term $F_{ij}(\omega, \mathbf{k})$ may contribute but gives a $\beta_{ikl\,j}$ that tends to zero as $\omega \to \infty$. In other words,

$$\boldsymbol{\mu}_{\rm tl}^{-1} \to \mathbf{I} \text{ when } \omega \to \infty. \tag{87}$$

Since $\beta_{ikl\,j}$ are the second-order coefficients of $\epsilon_{ij}(\omega, \mathbf{k})$, we can apply the general result in Appendix E to deduce that $\beta_{ikl\,j}$ and therefore $\boldsymbol{\mu}_{\rm tl}^{-1}$ are analytic in the upper half-plane. With (87) we conclude that $\boldsymbol{\mu}_{\rm tl}^{-1}$ is causal.

The relation between the permeability resulting from the magnetic moment density (Sec. III B) and that in (81) can be found by subtracting (81) and (42):

$$\boldsymbol{\mu}^{-1} - \boldsymbol{\mu}_{\rm tl}^{-1} = \begin{bmatrix} (\gamma+\psi+\eta)_{3113} & -(\gamma+\psi+\eta)_{3112} \\ -(\gamma+\psi+\eta)_{2113} & (\gamma+\psi+\eta)_{2112} \end{bmatrix}. \tag{88}$$

In other words, the difference is due to the electric quadrupole, magnetic quadrupole + electric octupole, and $\Theta(k^2)$ part of electric dipole. The difference $\boldsymbol{\mu}_{\rm vy}^{-1} - \boldsymbol{\mu}_{\rm tl}^{-1}$ can be expressed similarly as in (88), however, without the ψ tensor.

We have chosen, somewhat arbitrarily, to associate the entire $\Theta(k)$ term of the transversal current with the magnetization $\mathbf{M}^{\rm tl}$. The $\Theta(k)$ term could be associated with polarization $\mathbf{P}^{\rm tl}$ instead or shared between the two. This has, however, no influence on the permeability (81), being defined from the $O(k^2)$ term.

Since the permeability $\boldsymbol{\mu}_{\rm tl}$ is derived from the Landau-Lifshitz total permittivity $\boldsymbol{\epsilon}(\omega, \mathbf{k})$, which in turn is found from $\mathbf{J}$ and $\mathbf{E}$ with (7a) and (7c), it follows that $\boldsymbol{\mu}_{\rm tl}$ is not dependent on the choice of origin.

E. Other decompositions

Clearly, there are infinite number of ways to decompose the induced current, obtaining "**P**," "**M**," and possibly other "multipole" terms. The possible decompositions fall roughly into two categories. In the first category the magnetization vector is defined from an integral of the microscopic current. Examples include (36b) and (63b). The analyticity of the resulting inverse permeabilities, asymptotic behavior, and connection to the Landau-Lifshitz permittivity follow in the same way as in Sec. III B. In the second category the magnetization is defined from a certain division of the $O(k^2)$ part of the induced current by including any desired part of the $\beta_{ikl\,j}$ tensor in (22). Then the properties of the resulting $\boldsymbol{\mu}^{-1}$ can be explored along the lines in Sec. III D. Of course, not all such definitions lead to an analytic $\boldsymbol{\mu}^{-1}$; this must be ensured by carefully considering the frequency dependence of the division. Also, to ensure that $\boldsymbol{\mu}^{-1}$ is a tensor, the division of $\beta_{ikl\,j}$ must be possible to formulate in tensor form.

IV. NUMERICAL RESULTS

We will now consider some concrete examples of 2D metamaterials, using a finite-difference-frequency-domain numerical method [9,17]. The metamaterial unit cells, and the associated, inverse permeability element 33 (perpendicular to the unit cell figures) are shown in Figs. 1–4 for $k = 0$. For all examples except that in Fig. 1(b), we have used silver inclusions described by a Drude-Lorentz model with parameters from Ref. [18].

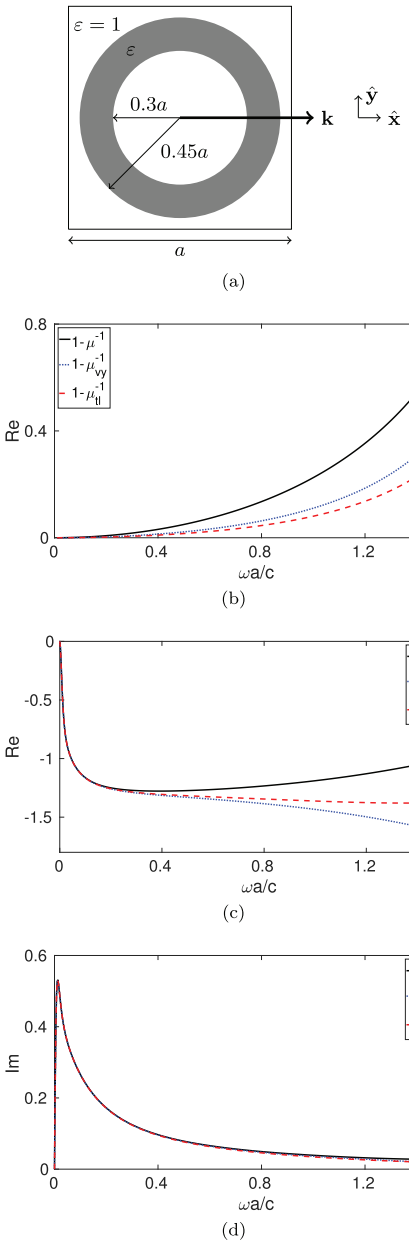

FIG. 1. (a) Unit cell with an annulus; (b) $1 -$ permeability^{-1} when the annulus is a lossless dielectric ($\varepsilon = 16$). Real (c) and imaginary (d) parts when the annulus is made from silver, $a = 1$ μm.

We observe that the different permeabilities are identical in the low-frequency limit. However, for the dielectric inclusions [Fig. 1(b)], the *relative* differences are relatively large and do not vanish in the low-frequency limit. For $\omega a/c > 0.6$,

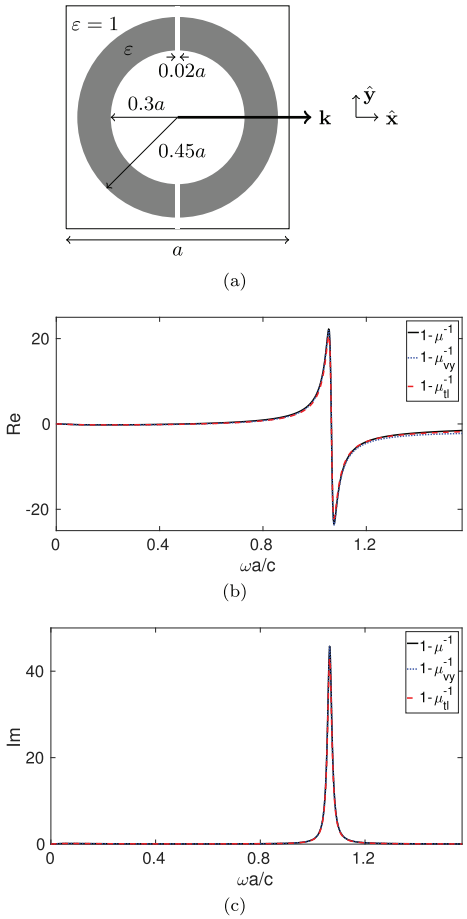

FIG. 2. (a) Unit cell with a split-ring resonator made from silver, $a = 1$ μm. Real (b) and imaginary (c) part of $1 -$ permeability^{-1}.

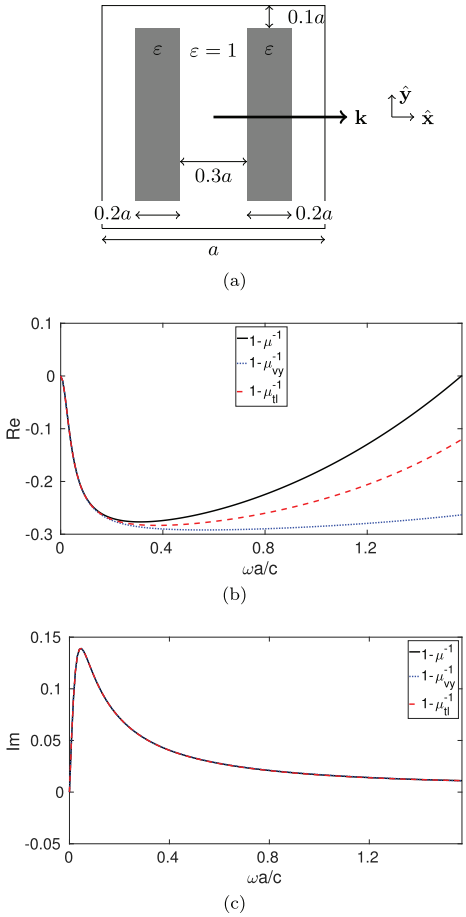

FIG. 3. (a) Unit cell with two bars made from silver, $a = 1$ μm. Real (b) and imaginary (c) part of $1 -$ permeability^{-1}.

corresponding to $a/\lambda > 0.1$ (λ is the vacuum wavelength), the differences between the permeabilities are quite visible for all examples except the split ring resonator medium (Fig. 2).

Note that although the definition of $\boldsymbol{\mu}_{\rm vy}$ is similar to that of $\boldsymbol{\mu}$, in the examples $\boldsymbol{\mu}_{\rm vy}$ is closer to $\boldsymbol{\mu}_{\rm tl}$ in magnitude.

In Fig. 4 we observe the origin dependence of the permeabilities. The permeability $\boldsymbol{\mu}_{\rm tl}$ is origin independent by definition, while $\boldsymbol{\mu}$ and $\boldsymbol{\mu}_{\rm vy}$ are dependent on the choice of origin. The origin dependence is, however, rather weak in the considered frequency range. In general, the origin dependence of $\boldsymbol{\mu}_{\rm vy}$ seems to be weaker than that of $\boldsymbol{\mu}$. In fact, for the examples in Figs. 1–3 the origin dependence of $\boldsymbol{\mu}_{\rm vy}$ turned out to be negligible (not shown).

In Fig. 4 we find that for larger frequencies, the imaginary parts of the three permeabilities can be negative. Clearly, the medium response must be highly nonlocal in this region; in the presence of spatial dispersion the condition for passivity is formulated in terms of the Landau-Lifshitz permittivity $\boldsymbol{\epsilon}(\omega, \mathbf{k})$ [see (C14)].

The causal properties of the inverse permeabilities $\boldsymbol{\mu}^{-1}$, $\boldsymbol{\mu}_{\rm vy}^{-1}$, and $\boldsymbol{\mu}_{\rm tl}^{-1}$, proven in Sec. III, have been verified numerically for the metamaterials in Figs. 1(a)–4(a) using a Lorentzian model for the microscopic permittivity. This is done by first computing the (3,3) elements of the inverse permeabilities over a large bandwidth (such that the asymptotic limit can be seen). Then the results are Fourier transformed and verified to be vanishing small for negative time.

Although the inverse permeabilities are causal, the permeabilities are generally not. This was noted for the $\boldsymbol{\mu}_{\rm vy}$ permeability in Ref. [19]. Note that the inverse permeability is the natural response quantity appearing when expressing $\mathbf{M}$ from the fundamental field $\mathbf{B}$ [or expressing $\mathbf{M}$ from the applied current density $\mathbf{J}_{\rm ext}$, using (54), (53), and (42)]. Therefore, the inverse permeability is causal. Proving that the permeability itself is causal, from the causality of the inverse permeability, is possible only in certain special cases [1,19]. For example, when the inverse permeability is scalar, and $\mathrm{Im}\,\mu^{-1}$ takes only negative values, the inverse permeability turns out to be zero free in the upper half-plane $\mathrm{Im}\,\omega > 0$.

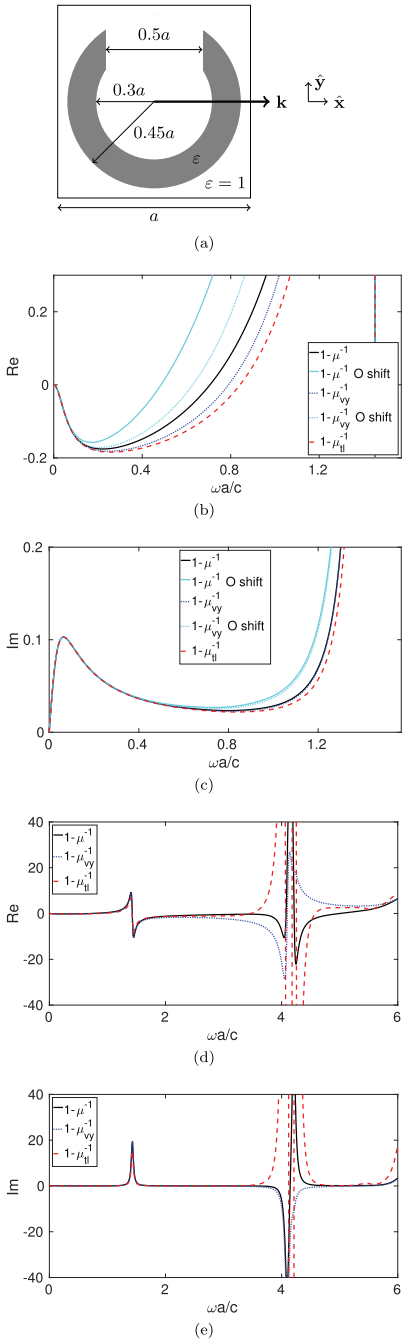

FIG. 4. (a) Unit cell with a "U" made from silver, $a = 1$ μm. Real (b) and imaginary (c) part of $1 -$ permeability^{-1}. Also shown are the results when the origin has been shifted from the center of the cell (0,0) to top right corner $(a/2, a/2)$. In (d) and (e) the results are plotted for higher frequencies, demonstrating that the imaginary parts can have either sign in this region. This does not mean violation of passivity but that the medium response is nonlocal.

Then the permeability becomes causal. Otherwise, as for the metamaterials in Figs. 1(a)–4(a), the permeabilities are noncausal despite the inverse permeabilities being causal.

V. DISCUSSION AND CONCLUSION

In conclusion we have considered four definitions of permeability for periodic metamaterials and their properties. The properties of the induced current decompositions and associated permeabilities are summed in Table I.

Having considered several different definitions of the magnetic permeability, it is natural to ask which is preferred. Of course there is no simple answer to this question. The Vinogradov-Yaghjian decomposition has the advantage of representing all induced current with only three terms. On the other hand, the conventional multipole decomposition has a clear physical interpretation; in particular, the permeability $\boldsymbol{\mu}$ is induced from the magnetic moment density $\mathbf{M}$. However, the asymptotic behavior for $\omega \to \infty$ and fixed $\mathbf{k}$ is not necessarily $\boldsymbol{\mu} \to \mathbf{I}$, and the origin dependence is generally larger than that of $\boldsymbol{\mu}_{\rm vy}$. The permeability $\boldsymbol{\mu}_{\rm tl}$ has a less direct physical interpretation compared to $\boldsymbol{\mu}$ but has the nice properties that it is independent of the choice of origin and symmetric. In addition it is appealing that it contains "as much as possible" of the $O(k^2)$ part of the Landau-Lifshitz permittivity.

For weakly spatially dispersive media where the higher-order $O(k^3)$ terms are ignored, all permeabilities are independent of k. For $\boldsymbol{\mu}$ and $\boldsymbol{\mu}_{\rm vy}$, higher-order terms are included by allowing ν_{ilj} in (40b) and (64) to be dependent on $\mathbf{k}$. For $\boldsymbol{\mu}_{\rm tl}$, higher-order terms are included by letting β_{iklj} in (22) be dependent on $\mathbf{k}$. In all these cases the highest-order term in the Taylor expansions absorbs the remainder, making the permeabilities dependent on $\mathbf{k}$ in a straightforward way. For strongly spatially dispersive media, this could perhaps be useful in certain cases where the magnetization part of the induced current dominates.

Despite the induced current being exactly represented by the expansion terms, neither of the permeabilities can alone describe the entire $\Theta(k^2)$ part of the Landau-Lifshitz permittivity. Therefore, even for weakly spatially dispersive media, we cannot always use one of the permeabilities in addition to a permittivity in Fresnel equations to describe reflection and transmission at an interface. When using the Fresnel equations, the errors will be dependent on the impact of the missed terms but also induced by the fact that the conventional boundary conditions are not necessarily valid for the fundamental Floquet mode fields [20]. In the multipole expansion, the missed terms are the $\Theta(k^2)$ part of $\mathbf{P}$, $\mathbf{Q}$, and $\mathbf{R}$. In the Vinogradov-Yaghjian decomposition, the missed terms are the $\Theta(k^2)$ part of $\mathbf{P}^{\rm vy}$ and $\mathbf{Q}^{\rm vy}$. In the transversal-longitudinal decomposition the missed term is the $\Theta(k^2)$ part of $\mathbf{P}^{\rm tl}$. Here we have assumed a nongyrotropic medium.

The semi-infinite case has been studied numerically in a separate work [20]. It was found that Fresnel equations with the three permeabilities in Secs. III B–III D give accurate results for 2D metamaterials which mimic natural magnetism in a frequency range with nontrivial magnetic response. The frequency range where the prediction of Fresnel's equation is accurate is where the three permeabilities are approximately equal. Considering the numerical examples in Sec. IV, we can

TABLE I. General properties of induced current expansions and associated permeabilities; i.g. = in general. For the Landau-Lifshitz formulation the permeability is trivial, and the table column displays the properties of the permittivity tensor $\boldsymbol{\epsilon}(\omega, \mathbf{k})$.

	III B Multipole	III C Vinogradov-Yaghjian	III D Transversal-longitudinal	III A Landau-Lifshitz, $\boldsymbol{\mu}_{\mathrm{ll}} = \mathbf{I}$
Number of $\mathbf{J}$ expansion terms	∞ ($\mathbf{P}$, $\mathbf{M}$, $\mathbf{Q}$, $\mathbf{R}$, ...)	3 ($\mathbf{P}^{\mathrm{vy}}$, $\mathbf{M}^{\mathrm{vy}}$, $\mathbf{Q}^{\mathrm{vy}}$)	2 ($\mathbf{P}^{\mathrm{tl}}$, $\mathbf{M}^{\mathrm{tl}}$)	1 ($\mathbf{P}^{\mathrm{ll}}$)
Causal, $\boldsymbol{\mu}^{-1}$ analytic for Im $\omega > 0$	Yes	Yes	Yes	$\mathbf{G}(\omega, \mathbf{k})$ causal
Causal, $\boldsymbol{\mu}$ analytic for Im $\omega > 0$	No (i.g.)	No (i.g.)	No (i.g.)	$\boldsymbol{\epsilon}(\omega, \mathbf{k})$ causal
For $\omega \to \infty$ and fixed $\mathbf{k}$	$\boldsymbol{\mu} \to$ const	$\boldsymbol{\mu}_{\mathrm{vy}} \to \mathbf{I}$	$\boldsymbol{\mu}_{\mathrm{tl}} \to \mathbf{I}$	$\boldsymbol{\epsilon}(\omega, \mathbf{k}) \to \mathbf{I}$
Sign of Im $\boldsymbol{\mu}$ (for diagonal $\boldsymbol{\mu}$)	Both (i.g.)	Both (i.g.)	Both (i.g.)	$\omega[\boldsymbol{\epsilon}(\omega, \mathbf{k}) - \boldsymbol{\epsilon}(\omega, \mathbf{k})^{\dagger}]$ pos.
Symmetry	–	–	$\boldsymbol{\mu}_{\mathrm{tl}}^{T}(-\mathbf{k}) = \boldsymbol{\mu}_{\mathrm{tl}}(\mathbf{k})$	$\boldsymbol{\epsilon}^{T}(\omega, -\mathbf{k}) = \boldsymbol{\epsilon}(\omega, \mathbf{k})$
Origin dependence	Yes (i.g.)	Yes (i.g.)	No	No

therefore expect that the permeabilities (except the trivial one in Sec. III A) are useful in Fresnel's equation in the range where they approximately coincide.

For media with strong electric quadrupole response, and/or higher-order multipoles, the basic Fresnel equation will not give an accurate prediction. The permeability can still be relevant, provided additional boundary conditions for the particular structure are found [21–25]. In these cases, a better alternative could perhaps be to calculate the reflection and transmission using exact mode matching techniques or even, e.g., finite-difference time-domain simulations.

It is natural to ask whether the permeabilities are useless in the frequency ranges where they cannot be used to predict the reflection from a semi-infinite structure. Although the permeabilities have limited use in these cases, it is convenient to have definitions which are valid for all frequencies. This makes it possible to apply Kramers-Kronig relations and other theoretical constraints which are formulated for the entire frequency range. Although the permeabilities lose their usual physical interpretation for sufficiently large frequencies, they are still physical in the sense that they are found from the physical, microscopic fields using the particular definition. For example, $\boldsymbol{\mu}$ in Sec. III B results from a magnetization $\mathbf{M}$ which quantifies the magnetic moment of the unit cell.

ACKNOWLEDGMENTS

The authors thank Arthur Yaghjian for constructive feedback and fruitful discussions.

APPENDIX A: DERIVING k-DOMAIN MAXWELL EQUATIONS FOR HOMOGENIZED FIELDS

Our starting point is the microscopic Maxwell equations:

$$\nabla \times \mathbf{e} = i\omega \mathbf{b}, \tag{A1a}$$

$$\frac{1}{\mu_0}\nabla \times \mathbf{b} = -i\omega\epsilon_0 \mathbf{e} + \mathbf{j}(\mathbf{r}) + \mathbf{J}_{\mathrm{ext}} e^{i\mathbf{k}\cdot\mathbf{r}}. \tag{A1b}$$

Since the structure is periodic, and the source is of the form $\mathbf{J}_{\mathrm{ext}} e^{i\mathbf{k}\cdot\mathbf{r}}$ with constant $\mathbf{J}_{\mathrm{ext}}$, all fields can be written in Floquet form. For example, $\mathbf{e} = \mathbf{u}_{\mathbf{e}} e^{i\mathbf{k}\cdot\mathbf{r}}$. Substituting into (A1) we obtain

$$\nabla \times \mathbf{u}_{\mathbf{e}} + i\mathbf{k} \times \mathbf{u}_{\mathbf{e}} = i\omega \mathbf{u}_{\mathbf{b}}, \tag{A2a}$$

$$\frac{1}{\mu_0}\nabla \times \mathbf{u}_{\mathbf{b}} + \frac{1}{\mu_0} i\mathbf{k} \times \mathbf{u}_{\mathbf{b}} = -i\omega\epsilon_0 \mathbf{u}_{\mathbf{e}} + \mathbf{u}_{\mathbf{j}} + \mathbf{J}_{\mathrm{ext}}. \tag{A2b}$$

Recall that the periodic $\mathbf{u}$ functions can be written in terms of their Fourier components, as in (5). Equations (A2) [and therefore (A1)] are satisfied if and only if the Fourier components of (A2) satisfy:

$$i(\mathbf{b}_{lmn} + \mathbf{k}) \times \mathbf{E}_{lmn} = i\omega \mathbf{B}_{lmn}, \tag{A3a}$$

$$\frac{1}{\mu_0} i(\mathbf{b}_{lmn} + \mathbf{k}) \times \mathbf{B}_{lmn} = -i\omega\epsilon_0 \mathbf{E}_{lmn} + \mathbf{J}_{lmn}, \tag{A3b}$$

for all l, m, n except $l = m = n = 0$, for which the set can be written

$$i\mathbf{k} \times \mathbf{E} = i\omega \mathbf{B}, \tag{A4a}$$

$$\frac{1}{\mu_0} i\mathbf{k} \times \mathbf{B} = -i\omega\epsilon_0 \mathbf{E} + \mathbf{J} + \mathbf{J}_{\mathrm{ext}}. \tag{A4b}$$

Equations (A4) are the Maxwell equations for the fundamental Floquet modes, which we have taken to be the macroscopic fields. Equations (A3) are the equations that the other Fourier components must satisfy.

The induced current $\mathbf{J}_{lmn}$ couples between sets with different indices. Defining $\sigma(\mathbf{r}) = -i\omega\epsilon_0[\varepsilon(\mathbf{r}) - 1]$, we have

$$\begin{aligned} \mathbf{J}_{lmn} &= \frac{1}{V}\int \mathbf{j}(\mathbf{r}) e^{-i\mathbf{k}\cdot\mathbf{r} - i\mathbf{b}_{lmn}\cdot\mathbf{r}} d^3 r \\ &= \frac{1}{V}\int \sigma(\mathbf{r})\mathbf{e}(\mathbf{r}) e^{-i\mathbf{k}\cdot\mathbf{r} - i\mathbf{b}_{lmn}\cdot\mathbf{r}} d^3 r \\ &= \sum_{l'm'n'} \mathbf{E}_{l'm'n'} \cdot \frac{1}{V}\int \sigma(\mathbf{r}) e^{i(\mathbf{b}_{l'm'n'} - \mathbf{b}_{lmn})\cdot\mathbf{r}} d^3 r \end{aligned} \tag{A5}$$

By eliminating $\mathbf{B}_{lmn}$ from (A3) and (A4), and using (A5), we obtain a linear equation set in the form

$$\sum_n A_{mn} E_n = J_{\mathrm{ext}} \delta_{m0}, \tag{A6}$$

where the matrix A_{mn} depends on ω, $\mathbf{k}$, and microscopic permittivity but not the fields. The three indices lmn and the index of the vector components have been combined into a single index n or m, and the coordinate system is oriented such that $\mathbf{J}_{\mathrm{ext}}$ is along one of the axes, corresponding to $m = 0$. The elements E_n of the new field vector contains the three components of each $\mathbf{E}_{lmn}$. From (A6) we note that all fields, e.g., $\mathbf{E}_{lmn}$ or $\mathbf{E}$, are proportional to J_{ext}.

APPENDIX B: MACROSCOPIC FIELDS FOR ARBITRARY *ka*

Here we will prove that the macroscopic fields (or fundamental Floquet mode fields) can be used to calculate the work done by the source in a unit cell, even for large wave numbers. Consider, first, a source with a single, spatial Fourier component, $\mathbf{j}_{\text{ext}}(\mathbf{r}) = \mathbf{J}_{\text{ext}}(\mathbf{k})e^{i\mathbf{k}\cdot\mathbf{r}}$. The work done by the source per unit volume and per unit time (after averaging over a period) is

$$p_{\text{ext}} = \tfrac{1}{2}\text{Re}\,\{\mathbf{j}_{\text{ext}} \cdot (-\mathbf{e}^*)\}, \tag{B1}$$

where $\mathbf{e}$ is the microscopic electric field. Substituting (3) and (4a) we find

$$p_{\text{ext}} = \tfrac{1}{2}\text{Re}\,\{\mathbf{J}_{\text{ext}} \cdot (-\mathbf{u}_{\mathbf{e}}^*)\}, \tag{B2}$$

which after averaging over a unit cell V [using (7a)] becomes

$$\langle p_{\text{ext}}\rangle = \tfrac{1}{2}\text{Re}\,\{\mathbf{J}_{\text{ext}} \cdot (-\mathbf{E}^*)\} \tag{B3}$$

or

$$\langle p_{\text{ext}}\rangle = \tfrac{1}{2}\text{Re}\,\{\mathbf{j}_{\text{ext}} \cdot (-\boldsymbol{\mathcal{E}}^*)\}. \tag{B4}$$

In other words, we can find the work from the macroscopic field $\boldsymbol{\mathcal{E}}$.

For a source in the form

$$\mathbf{j}_{\text{ext}}(\mathbf{r}) = \mathbf{j}_0(\mathbf{r})e^{i\mathbf{k}_0\cdot\mathbf{r}}, \tag{B5}$$

where $\mathbf{k}_0$ is any constant vector, and $\mathbf{j}_0(\mathbf{r}) \neq 0$, (B4) remains valid if the source contains a sufficiently narrow band of wave vectors around $\mathbf{k}_0$. This can be demonstrated by expressing the Fourier integrals of the source and the microscopic electric field and averaging (B1) over a unit cell. For more details on sources of finite sizes, see Appendix D.

APPENDIX C: CAUSALITY, PASSIVITY, AND KRAMERS-KRONIG RELATIONS

Here we will establish a framework for studying the analytic properties of the electromagnetic parameters and the implications of passivity [1,8,12,26,27]. If we use the Landau-Lifshitz formulation in which the medium is described solely by a permittivity $\boldsymbol{\epsilon}(\omega, \mathbf{k})$, then it has been stated that $\boldsymbol{\epsilon}(\omega, \mathbf{k})$ is an analytic function in the upper half-plane $\text{Im}\,\omega > 0$ for fixed $\mathbf{k}$, at least for sufficiently small k [1,12]. This follows by regarding the electric field as the excitation and the displacement field as the response. However, as pointed out in Ref. [26], such an argument is not compelling since the electric field includes the response of the medium. Here we will use the relation between the applied source and the resulting field to prove that for fixed, real $\mathbf{k}$, the Landau-Lifshitz permittivity tensor $\boldsymbol{\epsilon}(\omega, \mathbf{k})$ is analytic in the upper half-plane, even for anisotropic, bianisotropic, and spatially dispersive media. We will also provide the passivity condition.

Since the medium is assumed linear and time-shift invariant, the resulting macroscopic field $\mathbf{E}$ is related to the source $\mathbf{J}_{\text{ext}}$ by a linear relation

$$\mathbf{E} = \mathbf{G}(\omega, \mathbf{k})\mathbf{J}_{\text{ext}}, \tag{C1}$$

where $\mathbf{G}(\omega, \mathbf{k})$ is a (matrix) response function. For simplicity in notation we have suppressed the ω and $\mathbf{k}$ dependence of the fields. Recall that the medium is assumed to be causal and passive, so if the time-domain source current is any finite-duration pulse starting at $t = 0$, then the time-domain electric field vanishes for $t < 0$ and does not blow up as $t \to \infty$. It follows that

$$\mathbf{G}(\omega, \mathbf{k}) \text{ analytic for } \text{Im}\,\omega > 0 \text{ and fixed } \mathbf{k}. \tag{C2}$$

This applies to all elements of the matrix, since $\mathbf{J}_{\text{ext}}$ can be chosen to point in any direction.

Since the work done by the source must be non-negative, we must have $-\text{Re}\,\mathbf{J}_{\text{ext}}^* \cdot \mathbf{E} \geqslant 0$ [see (B3)], or

$$-\text{Re}\,\mathbf{J}_{\text{ext}}^\dagger \mathbf{G}(\omega, \mathbf{k})\mathbf{J}_{\text{ext}} \geqslant 0, \tag{C3}$$

for real frequencies. Here † stands for Hermitian conjugate, i.e., transpose and complex conjugate. We have argued for (C2) and (C3) using a single $\mathbf{k}$ source; however, as shown in Appendix D, they also follow when using a realistic source of finite size. Inequality (C3) is valid in the upper half-plane $\text{Im}\,\omega > 0$, as shown in Appendix D.

Define a function

$$f(\omega) = -\mathbf{J}_0^\dagger \mathbf{G}(\omega, \mathbf{k})\mathbf{J}_0, \tag{C4}$$

where $\mathbf{J}_0$ is an arbitrary but constant vector. We have just seen that $\text{Re}\,f(\omega) \geqslant 0$ for $\text{Im}\,\omega > 0$. In fact, since $f(\omega)$ is an analytic function, it must be that $\text{Re}\,f(\omega) > 0$ for $\text{Im}\,\omega > 0$: Assume $f(\omega) = 0$ somewhere in the upper half-plane. A zero of an analytic function is isolated, and in the vicinity of a zero, the function's complex argument takes all values from 0 to 2π. This would make $\text{Re}\,f(\omega) < 0$ somewhere around zero, which contradicts $\text{Re}\,f(\omega) \geqslant 0$.

We have proved that

$$-\text{Re}\,[\mathbf{J}_0^\dagger \mathbf{G}(\omega, \mathbf{k})\mathbf{J}_0] > 0 \text{ for } \text{Im}\,\omega > 0 \tag{C5}$$

for any constant $\mathbf{J}_0$. Thus $\mathbf{E} = \mathbf{G}(\omega, \mathbf{k})\mathbf{J}_{\text{ext}} \neq 0$ for any nonzero $\mathbf{J}_{\text{ext}}$ for $\text{Im}\,\omega > 0$. This means that

$$\det \mathbf{G}(\omega, \mathbf{k}) \neq 0 \quad \text{for } \text{Im}\,\omega > 0. \tag{C6}$$

In other words, for all ω in the upper half-plane, we can invert $\mathbf{G}(\omega, \mathbf{k})$ to obtain $\mathbf{G}(\omega, \mathbf{k})^{-1}$. Since $\mathbf{G}(\omega, \mathbf{k})$ is analytic, so is $\mathbf{G}(\omega, \mathbf{k})^{-1}$.

In the Landau-Lifshitz formulation, the Maxwell equations take the form

$$i\mathbf{k} \times \mathbf{E} - i\omega\mathbf{B} = 0, \tag{C7a}$$

$$\frac{1}{\mu_0} i\mathbf{k} \times \mathbf{B} + i\omega\epsilon_0 \boldsymbol{\epsilon}(\omega, \mathbf{k})\mathbf{E} = \mathbf{J}_{\text{ext}} \tag{C7b}$$

in the frequency–wave-number space. Combining them, we obtain

$$\left[k^2 \mathbf{I}_\perp - \frac{\omega^2}{c^2}\boldsymbol{\epsilon}(\omega, \mathbf{k})\right]\mathbf{E} = i\omega\mu_0 \mathbf{J}_{\text{ext}}, \tag{C8}$$

with $\mathbf{I}_\perp = \mathbf{I} - \mathbf{k}\mathbf{k}/k^2$ [or expressed by (25) in a coordinate system where $\mathbf{k} = k\hat{\mathbf{x}}$]. Comparing (C8) and $\mathbf{E} = \mathbf{G}(\omega, \mathbf{k})\mathbf{J}_{\text{ext}}$, we identify

$$\mathbf{G}(\omega, \mathbf{k})^{-1} = (i\omega\mu_0)^{-1}\left[k^2 \mathbf{I}_\perp - \frac{\omega^2}{c^2}\boldsymbol{\epsilon}(\omega, \mathbf{k})\right]. \tag{C9}$$

We have already proved that $\mathbf{G}(\omega,\mathbf{k})^{-1}$ is analytic in the upper half-plane $\mathrm{Im}\,\omega > 0$; thus so is $\boldsymbol{\epsilon}(\omega,\mathbf{k})$.

With an asymptotic behavior $\epsilon(\omega,\mathbf{k}) \to \boldsymbol{\epsilon}(\infty,\mathbf{k})$ as $\omega \to \infty$ and $\mathbf{k}$ is fixed, we can now state the Kramers-Kronig relations for $\boldsymbol{\chi}(\omega,\mathbf{k}) \equiv \boldsymbol{\epsilon}(\omega,\mathbf{k}) - \boldsymbol{\epsilon}(\infty,\mathbf{k})$:

$$\mathrm{Re}\,\boldsymbol{\chi}(\omega,\mathbf{k}) = \frac{2}{\pi}P\int_0^\infty \frac{\mathrm{Im}\,\boldsymbol{\chi}(\nu,\mathbf{k})\nu}{\nu^2-\omega^2}d\nu, \tag{C10a}$$

$$\mathrm{Im}\,\boldsymbol{\chi}(\omega,\mathbf{k}) = -\frac{2\omega}{\pi}P\int_0^\infty \frac{\mathrm{Re}\,\boldsymbol{\chi}(\nu,\mathbf{k})}{\nu^2-\omega^2}d\nu. \tag{C10b}$$

Here ω is real, and P denotes the Cauchy principal value. To obtain the Kramers-Kronig relations from the analyticity and the asymptotic behavior, we have used the Titchmarsh theorem [15]. To this end we have assumed that $\boldsymbol{\chi}(\omega,\mathbf{k}) \to 0$ sufficiently fast as $|\omega| \to \infty$, and that $\chi(\omega,\mathbf{k})$ does not have singularities for real frequencies.[3]

Substituting $\mathbf{J}_0 = \mathbf{G}(\omega,\mathbf{k})^{-1}\mathbf{E}_0$ in (C5) gives

$$-\mathrm{Re}\,[\mathbf{E}_0^\dagger \mathbf{G}(\omega,\mathbf{k})^{-1^\dagger}\mathbf{E}_0] > 0 \text{ for } \mathrm{Im}\,\omega > 0, \tag{C11}$$

valid for any vector $\mathbf{E}_0$. This can be written

$$-\mathbf{G}(\omega,\mathbf{k})^{-1} - \mathbf{G}(\omega,\mathbf{k})^{-1^\dagger} \text{ positive definite}, \tag{C12}$$

or, using (C9),

$$i\left[\omega\boldsymbol{\epsilon}(\omega,\mathbf{k}) - \frac{k^2c^2}{\omega}\mathbf{I}_\perp\right]^\dagger - i\left[\omega\boldsymbol{\epsilon}(\omega,\mathbf{k}) - \frac{k^2c^2}{\omega}\mathbf{I}_\perp\right] \text{ positive definite}. \tag{C13}$$

In principle, the passivity condition (C13) has been derived for $\mathrm{Im}\,\omega > 0$. By taking the limit $\mathrm{Im}\,\omega \to 0$, the passivity condition remains valid for all $\mathrm{Re}\,\omega$ where this limit exists, provided we relax "positive definite" to "positive semidefinite." When both ω and k are real, as is the case when they represent a Fourier component in time and space, the passivity condition becomes

$$-i\omega[\boldsymbol{\epsilon}(\omega,\mathbf{k}) - \boldsymbol{\epsilon}(\omega,\mathbf{k})^\dagger] \text{ positive semidefinite}. \tag{C14}$$

This reduces to the well-known condition $\mathrm{Im}\,\epsilon(\omega,\mathbf{k}) \geqslant 0$ for scalar permittivity and positive frequency.

APPENDIX D: SOURCE OF FINITE SIZE

In Appendix C we imagined a source with a single wave vector $\mathbf{k}$. This source is somewhat unphysical, since it is present everywhere. Here we will consider sources of finite size and rederive the causality and work results (C2) and (C3).

In this section we will write out the ω and $\mathbf{k}$ dependence explicitly. Let us consider a causal source in product form,

$$\mathbf{J}_{\mathrm{ext}}(\omega,\mathbf{k}) = F(\mathbf{k})\mathbf{W}(\omega). \tag{D1}$$

From (4a) and (5) the frequency-domain microscopic electric field is

$$\begin{aligned}\mathbf{e}(\omega,\mathbf{r}) &= \frac{1}{(2\pi)^3}\int \sum_{lmn} \mathbf{E}_{lmn}(\omega,\mathbf{k})e^{i\mathbf{b}_{lmn}\cdot\mathbf{r}+i\mathbf{k}\cdot\mathbf{r}}d^3k \\ &= \frac{1}{(2\pi)^3}\sum_{lmn}\int \mathbf{E}_{lmn}(\omega,\mathbf{k})e^{i\mathbf{b}_{lmn}\cdot\mathbf{r}+i\mathbf{k}\cdot\mathbf{r}}d^3k \\ &= \frac{1}{(2\pi)^3}\sum_{lmn}\int \mathbf{E}_{lmn}(\omega,\mathbf{k}'-\mathbf{b}_{lmn})e^{i\mathbf{k}'\cdot\mathbf{r}}d^3k' \\ &= \frac{1}{(2\pi)^3}\int \sum_{lmn} \mathbf{E}_{lmn}(\omega,\mathbf{k}-\mathbf{b}_{lmn})e^{i\mathbf{k}\cdot\mathbf{r}}d^3k,\end{aligned} \tag{D2}$$

where $\mathbf{E}_{lmn}(\omega,\mathbf{k})$ is proportional to $F(\mathbf{k})$. Since $\mathbf{e}(\omega,\mathbf{r})$ describes a causal field for all $\mathbf{r}$, we must have

$$\sum_{lmn}\mathbf{E}_{lmn}(\omega,\mathbf{k}-\mathbf{b}_{lmn}) \text{ causal, for fixed } \mathbf{k}. \tag{D3}$$

The source function $F(\mathbf{k})$ can be chosen such that

$$\begin{aligned}F(\mathbf{k}_0) &= 1 \text{ for } lmn = 000, \\ F(\mathbf{k}_0-\mathbf{b}_{lmn}) &= 0 \text{ for all } lmn \neq 000.\end{aligned} \tag{D4}$$

In other words, there is a peak at $\mathbf{k} = \mathbf{k}_0$ and zeros at $\mathbf{k} = \mathbf{k}_0 - \mathbf{b}_{lmn}$ for $lmn \neq 000$. This is achieved, e.g., if

$$F(\mathbf{k}) = \mathrm{sinc}^2[(k_x-k_{0x})a]\mathrm{sinc}^2[(k_y-k_{0y})a]\mathrm{sinc}^2[(k_z-k_{0z})a]. \tag{D5}$$

This source has a finite extent, as seen by inverse Fourier transforming (D5). By setting $\mathbf{k} = \mathbf{k}_0$, and considering (D3), we find that $\mathbf{E}(\omega,\mathbf{k}) \equiv \mathbf{E}_{000}(\omega,\mathbf{k})$ is causal.

We can write

$$\mathbf{E}(\omega,\mathbf{k}) = \mathbf{G}(\omega,\mathbf{k})\mathbf{J}_{\mathrm{ext}}(\omega,\mathbf{k}), \tag{D6}$$

where $\mathbf{G}(\omega,\mathbf{k})$ is a (tensor) response function. We choose a source with finite duration in the time domain. Since the medium is passive, the electric field does not blow up as $t \to \infty$. Since $\mathbf{J}_{\mathrm{ext}}(\omega,\mathbf{k})$ and $\mathbf{E}(\omega,\mathbf{k})$ are causal, it follows that they are analytic in the upper half-plane $\mathrm{Im}\,\omega > 0$. As $\mathbf{J}_{\mathrm{ext}}(\omega,\mathbf{k})$ is otherwise arbitrary, the response function $\mathbf{G}(\omega,\mathbf{k})$ must therefore be analytic for $\mathrm{Im}\,\omega > 0$ for each fixed $\mathbf{k}$ (C2).

The properties of $\mathbf{G}(\omega,\mathbf{k})$ in the upper half-plane can be further explored by considering sources with time dependence $\exp(\gamma t - i\omega' t)$ [28]:

$$\mathbf{j}_{\mathrm{ext}}(t,\mathbf{r}) = \mathrm{Re}\,[\mathbf{f}(\mathbf{r})u(t)e^{\gamma t - i\omega' t}]. \tag{D7}$$

Here $u(t)$ is the unit step function, $\gamma > 0$, and ω' is real. Taking $\mathbf{f}(\mathbf{r})$ to be real, this source can be expressed in frequency–wave-number space

$$\mathbf{J}_{\mathrm{ext}}(\omega,\mathbf{k}) = \mathbf{F}(\mathbf{k})W(\omega), \tag{D8}$$

where $\mathbf{F}(\mathbf{k})$ is the Fourier transform of $\mathbf{f}(\mathbf{r})$, and $W(\omega)$ is the Laplace transform of $e^{\gamma t}\cos(\omega' t)$, after setting the Laplace variable $s = -i\omega$.

At least for $t \gg 1/\gamma$, the transients can be ignored compared to the exponentially increasing field. Then the electric field will be of the form $\exp(\gamma t - i\omega' t)$, and the power density

[3] To establish Kramers-Kronig relations, the Titchmarsh theorem requires the function to be uniformly square integrable along a line in the upper half-plane, parallel to the real axis. The assumption is for example valid if the function vanishes as $1/|\omega|$ or faster, but, clearly, weaker conditions are possible. If the function has singularities on the real axis, then modified Kramers-Kronig relations can be derived [1].

$p_{\rm ext}(t) = -\mathbf{j}_{\rm ext}(t,\mathbf{r})\cdot\mathbf{e}(t,\mathbf{r})$ becomes

$$p_{\rm ext}(t) = -{\rm Re}\left[\frac{e^{\gamma t - i\omega' t}}{(2\pi)^3}\int \mathbf{F}(\mathbf{k})e^{i\mathbf{k}\cdot\mathbf{r}}d^3k\right] \cdot{\rm Re}\left[\frac{e^{\gamma t - i\omega' t}}{(2\pi)^3}\int\sum_{lmn}\tilde{\mathbf{E}}_{lmn}(\omega,\mathbf{k}-\mathbf{b}_{lmn})e^{i\mathbf{k}\cdot\mathbf{r}}d^3k\right]. \tag{D9}$$

Here $\tilde{\mathbf{E}}_{lmn}(\omega,\mathbf{k})$ is the same as $\mathbf{E}_{lmn}(\omega,\mathbf{k})$ except that the factor $W(\omega)$ has been removed and $\omega = \omega' + i\gamma$. Using ${\rm Re}\,\alpha = (\alpha+\alpha^*)/2$, and integrating the resulting expression over all space and from time t_0 to t_1, we find the total work in this time interval:

$$\begin{aligned} W_{\rm ext} &= \int_{t_0}^{t_1}\int p_{\rm ext}d^3r dt \\ &= -\frac{e^{2\gamma t_1}-e^{2\gamma t_0}}{4\gamma(2\pi)^3}{\rm Re}\int \mathbf{F}^*(\mathbf{k})\cdot\sum_{lmn}\tilde{\mathbf{E}}_{lmn}(\omega,\mathbf{k}-\mathbf{b}_{lmn})d^3k \\ &\quad + {\rm Re}\,[C(e^{2\gamma t_1 - 2i\omega' t_1} - e^{2\gamma t_0 - 2i\omega' t_0})], \end{aligned} \tag{D10}$$

where C is a complex-valued quantity which is independent of t_0 and t_1. Let $t_0 \gg 1/\gamma$. Since t_0 is finite, the source has only done a finite amount of work W_0 before t_0. Assuming the medium has no stored energy before $t = 0$, we must have $W_0 + W_{\rm ext} \geqslant 0$. For a sufficiently large t_1, but such that $Ce^{-2i\omega' t_1}$ is imaginary, we obtain the condition

$$-{\rm Re}\int \mathbf{F}^*(\mathbf{k})\cdot\sum_{lmn}\tilde{\mathbf{E}}_{lmn}(\omega,\mathbf{k}-\mathbf{b}_{lmn})d^3k \geqslant 0. \tag{D11}$$

Recall that $\tilde{\mathbf{E}}_{lmn}(\omega,\mathbf{k})$ is proportional to $F(\mathbf{k})$. Thus, by picking a source with a sufficiently narrow, effective band Δk around a fixed wave number $\mathbf{k}_0$ ($\Delta k a \ll 1$, which means that the source must cover several unit cells), we can make the terms with $lmn \neq 000$ arbitrarily small. Hence we must have

$$-{\rm Re}\int \mathbf{F}^*(\mathbf{k})\cdot\tilde{\mathbf{E}}(\omega,\mathbf{k})d^3k \geqslant 0. \tag{D12}$$

We now use (D6), which means $\tilde{\mathbf{E}}(\omega,\mathbf{k}) = \mathbf{G}(\omega,\mathbf{k})\mathbf{F}(\mathbf{k})$. Choosing a $\mathbf{F}(\mathbf{k})$ which is narrow banded in $\mathbf{k}$ compared to the variations in $\mathbf{G}(\omega,\mathbf{k})$, we obtain

$$-{\rm Re}\,\mathbf{J}_0^\dagger\mathbf{G}(\omega,\mathbf{k})\mathbf{J}_0 \geqslant 0 \tag{D13}$$

for all constant vectors $\mathbf{J}_0$.

APPENDIX E: ANALYTICITY OF TENSOR ELEMENTS

Suppose we have an expansion in the form

$$f(\omega,\mathbf{k}) = a(\omega) + b_i(\omega)k_i + c_{ij}(\omega)k_ik_j, \tag{E1}$$

where $a(\omega)$, $b_i(\omega)$, and $c_{ij}(\omega)$ are independent of $\mathbf{k}$. We take $c_{ij}(\omega)$ to be symmetric, as any antisymmetric part is irrelevant for the expansion. Let $f(\omega,\mathbf{k})$ be an analytic function of ω (in a given domain) for any fixed $\mathbf{k}$. We will prove that the coefficients $a(\omega)$, $b_i(\omega)$, and $c_{ij}(\omega)$ are analytic.

By putting $\mathbf{k} = 0$, we find that $a(\omega) = f(\omega,0)$ is analytic. Considering

$$f(\omega,\mathbf{k}) - f(\omega,-\mathbf{k}) = 2b_i(\omega)k_i, \tag{E2}$$

it follows that $b_i(\omega)$ is analytic. We now have that

$$c_{ij}(\omega)k_ik_j = f(\omega,\mathbf{k}) - a(\omega) - b_i(\omega)k_i \tag{E3}$$

is analytic. By letting $\mathbf{k}$ point in the $\hat{\mathbf{x}}$, $\hat{\mathbf{y}}$, or $\hat{\mathbf{z}}$ direction, we find that $c_{ii}(\omega)$ are analytic for any i. Finally we obtain, e.g., that c_{12} is analytic by letting $\mathbf{k} = k(\hat{\mathbf{x}}+\hat{\mathbf{y}})/\sqrt{2}$.

The argument can be extended to an infinite Taylor series, or a series with a remainder term, by noting that the partial derivatives $\partial f/\partial k_i$ and $\partial^2 f/\partial k_i\partial k_j$ are analytic. This follows by using the Cauchy-Riemann equations, assuming symmetry of second-order derivatives.

In particular, if the Landau-Lifshitz permittivity is expressed in the form

$$\epsilon_{ij}(\omega,\mathbf{k}) - \delta_{ij} = \chi_{ij} + \alpha_{ikj}k_k/\epsilon_0 + \beta_{iklj}k_kk_lc^2/\omega^2, \tag{E4}$$

then the analyticity of $\epsilon_{ij}(\omega,\mathbf{k})$ means that the tensors χ_{ij}, α_{ikj}, and β_{iklj} are analytic.

[1] L. D. Landau, E. M. Lifshitz, and L. P. Pitaevskii, *Electrodynamics of Continuous Media* (Pergamon Press, Oxford, 1984).

[2] J. B. Pendry, A. J. Holden, D. J. Robbins, and W. J. Stewart, IEEE Trans. Microw. Theor. Tech. **47**, 2075 (1999).

[3] A. P. Vinogradov and A. V. Aivazyan, Phys. Rev. E **60**, 987 (1999).

[4] A. P. Vinogradov, Phys. Usp. **45**, 331 (2002).

[5] M. G. Silveirinha, Phys. Rev. B **75**, 115104 (2007).

[6] C. Simovski and S. Tretyakov, in *Metamaterials Handbook: Theory and Phenomena of Metamaterials*, edited by F. Capolino (CRC Press, London, 2009), chap. 2.

[7] A. Alù, Phys. Rev. B **84**, 075153 (2011).

[8] A. D. Yaghjian, A. Alù, and M. G. Silveirinha, Photon. Nanostruct.: Fundam. Appl. **11**, 374 (2013).

[9] C. A. Dirdal, H. O. Hågenvik, H. A. Haave, and J. Skaar, IEEE Trans. Antennas Propag. **66**, 6403 (2018).

[10] G. Doetsch, *Introduction to the Theory and Application of the Laplace Transformation* (Springer Verlag, Berlin, 1974).

[11] M. G. Silveirinha, in *Metamaterials Handbook: Theory and Phenomena of Metamaterials*, edited by F. Capolino (CRC Press, London, 2009), chap. 10 .

[12] V. M. Agranovich and V. L. Ginzburg, *Crystal Optics with Spatial Dispersion, and Excitons* (Springer Verlag, Berlin, 1984).

[13] J. van Bladel, *Electromagnetic Fields* (IEEE Press, Hoboken, NJ, 2007).

[14] C. A. Dirdal and J. Skaar, Eur. Phys. J. B **91**, 131 (2018).

[15] E. C. Titchmarsh, *Introduction to the Theory of Fourier Integrals* (Oxford University Press, Oxford, 1948).

[16] R. E. Raab and O. L. de Lange, *Multipole Theory in Electromagnetism* (Oxford University Press, New York, 2005).

[17] J. T. Costa, M. G. Silveirinha, and S. I. Maslovski, Phys. Rev. B **80**, 235124 (2009).

[18] A. D. Rakić, A. B. Djurišić, J. M. Elazar, and M. L. Majewski, Appl. Opt. **37**, 5271 (1998).

[19] A. D. Yaghjian, A. Alù, and M. G. Silveirinha, Anisotropic representation for spatially dispersive periodic metamaterial arrays, in *Transformation Electromagnetics and Metamaterials:*

Fundamental Principles and Applications, edited by D. H. Werner and D.-H. Kwon (Springer London, London, 2014), pp. 395–457.
[20] H. O. Hågenvik and J. Skaar, arXiv:1812.05466.
[21] O. L. de Lange and R. E. Raab, J. Math. Phys. **54**, 093513 (2013).
[22] A. A. Golubkov and V. A. Makarov, Phys. Usp. **38**, 325 (1995).
[23] A. D. Yaghjian, Radio Sci. **49**, 1289 (2014).
[24] M. G. Silveirinha, New J. Phys. **16**, 083042 (2014).
[25] A. D. Yaghjian and M. G. Silveirinha, Radio Sci. **51**, 1312 (2016).
[26] O. V. Dolgov, D. A. Kirzhnits, and E. G. Maksimov, Rev. Mod. Phys. **53**, 81 (1981).
[27] A. Alù, A. D. Yaghjian, R. A. Shore, and M. G. Silveirinha, Phys. Rev. B **84**, 054305 (2011).
[28] O. Brune, Synthesis of a finite two-terminal network whose driving-point impedance is a prescribed function of frequency, Ph.D. thesis, Massachusetts Institute of Technology (1931).

Paper VI

Magnetic permeability in Fresnel's equation

Published in Journal of the Optical Society of America B **36**, 1386-1395 (2019)